FINAL THESIS OF THE MASTER IN INDUSTRIAL ENGINEERING

"PILE GROUPS UNDER HORIZONTAL LOADING: ANALYSIS METHODS REVIEW AND NUMERICAL SIMULATIONS UNDER STATIC AND DYNAMIC CONDITIONS"

STUDENT: JOSÉ EDUARDO MIRASOL CORBERÁN

PROFESSOR: QUINTILIO NAPOLEONI

ENGINEER ASSISTANT: GABRIELE PEPE

ACADEMIC YEAR 2017-2018

Me gustaría dedicar esta Tesis de Final de Máster a las dos únicas personas que fueron capaces de entender el verdadero esfuerzo desarrollado a lo largo de estos ocho años, sin el apoyo de las cuales, nada de esto hubiera sido posible. MIS PADRES.

En especial me gustaría dedicar esta Tesis de Final de Máster a una de las personas que más me ha marcado en la vida ayudándome a ser mejor persona, y que desgraciadamente nos ha dejado recientemente. Con cariño, a mi abuela, *JOSÉ FINA GARCÍA FORTEA*.

INDEX

1 Foreword

1.1 Deep pile's foundations

The foundations of a high number of the structures which can be found in the urban landscape such as bridges and civil and industrial buildings are based on piles. The deep foundations are required when the mechanical properties of the superficial layers of soil are poor, and it is necessary to reach deeper layers where the resistance of the soil is higher and capable of resisting the stresses induced by the structure into the soil by means of the foundation. The pile's foundations permit achieving those layers of soil with a higher stiffness like the rock's substrates where the piles can be supported without being produced big settlements. In these cases, the transmission of the loads to the soil is carried out by the tensions developed at the bottom surface of the piles. When there is not a stiff substrate on which sustain the foundation, the loads can be transmitted to the soil by means of the shear tensions that are developed on the lateral surface of the piles. In this case, the loads are transmitted to the soil gradually.

The deep foundations can be used in other circumstances: to face erosion phenomena at the bottom of the foundations disposed in presence of streams, in areas where are expected diggings next to the place where the foundations are located in, and to make front to phenomena of settlement in collapsible and swelling soils.

Figure 1-1 Examples of pile's foundations: the picture in the left side corresponds to a pile's wall placed in the city of Dresden (Germany); the picture in the right side corresponds to the pile's foundation of the bridge Zhou Jianhe (China).

The pile's foundations have been highly used along the mankind history to support big structures and to be able to transmit to the soil the loads induced by these. This kind of foundations have become in an ordinary practice in our days. The development of the technology has permitted the construction of more complex structures every time. The innovations in this field of the building engineering and the several techniques of construction, have permitted to increase the sizes of the piles, reaching high diameters and lengths for this sort of foundations. For example, the foundations of the oil platforms which are located in the ocean can achieve lengths higher than 100 meters and diameters bigger than 3 meters.

The pile's foundations work under combined loads due to the interaction effects with the structures placed on them. These forces can be decomposed in a vertical component, which is applied on the same direction as the gravitational force coinciding with the direction of the

3

pile's shafts, a horizontal component and a bending moment. As it has been mentioned, the function of the foundation is to transmit the loads from the structure placed on it to the soil, so that, the forces induced in the ground and those supported by the foundations are lower than the failure stresses, and the displacements in both directions, vertical and horizontal, are tolerable by the structures sustained by the foundations.

In general the most significant component of the forces is the vertical one. In these circumstances, the project criteria of the pile's foundations are related directly to the limit vertical loads of the piles, as well as the displacements in the vertical direction (settlements). It is not usual to find a project where the horizontal component of the forces results the limit project load. In these cases, the piles pertaining to a foundation are built according to a vertical axis, so that, the transmission of the loads to the soil is carried out by means of the shear stresses developed along the lateral surface of the piles and through the normal stresses which appear at the bottom (tip) of the piles. The vertical piles can also work under horizontal loads because of the shear stresses and the bending moments. Due to the fact that the horizontal components of the loads acting on a foundation are not zero, it is also necessary to verify the work and the failure conditions in this direction.

In some cases, the component of the horizontal loads acting on the pile's foundation cannot be low. It can suppose the main component of the forces, such as happens in the project of the supporting structures. These kind of forces can be also high in the case of the structures which support big loads due to the wind (bridges, skyscrapers), the waves of the sea (open ocean structures), those resulting from the river streams (bridges), those which appear in projects with big structural eccentricities and those cases in which a structure can receive the impact of a ship (the mole of a dock).

When the acting horizontal loads are particularly high, it is possible to build piles with an inclined axis. In these circumstances, a ratio of the horizontal loads can be absorbed by means of the normal force acting on the shaft of the pile, tensile and compressive stresses, depending on the inclination angle of the pile. When important vertical and horizontal loads coexist, the foundations can be constructed as a mixed pile foundation, which is constituted by piles with vertical and inclined axis. Because of the technological exigences, the inclination angle of the piles is limited to 45 degrees as maximum.
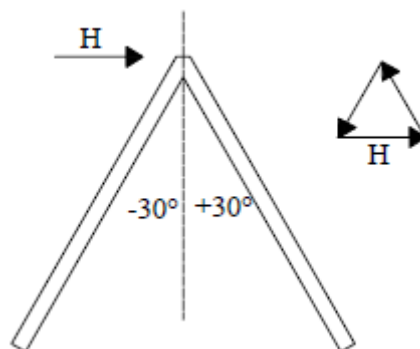
Figure 1-2 Scheme of the reactions of two piles inclined 30 degrees (G.LANDI).

1.2   Aims of the Master's Thesis

The aim of this Master's Thesis has been to study the behavior of deep foundations, composed by groups of piles, working under horizontal forces. It has been analyzed the main characteristics in the response of the single pile depending on some different factors.

Another of the goals of this Thesis has been to compare the models for the resistance of the soil proposed by BROMS (1946b) and BARTON (1942), and the different values of the limit horizontal forces which define the failure mechanisms of the piles, according to the equations proposed by BROMS (1946b) and particularizing them for the model of the soil's resistance suggested by BARTON (1982).

Afterwards, have been studied the differences between the answers observed in the single pile and in the group of piles, taking into account the different effects and phenomena of interaction between the piles of the group which cause that these responses are different. This theoretical base has been applied to two example cases.

Subsequently, another of the purposes of this Master's Thesis, has been to simulate a real case happened in the dock of Genova a few years ago, by means of a software of Finite Elements to evaluate the responses obtained by the numeric analysis and to determine the differences observed with regards to the results reached with the simplified models, also discussed in this Thesis and which have been applied to the same problem.

In the following point, is described the problem happened in the dock of Genova which is going to be approached in the fifth and sixth chapters of this Thesis.

1.3   The case of application: The pilot control tower of the dock of Genova

The 7th of May of 2013 at the 23:05 h, the cargo ship "Jolly Nero" pertaining to the company Messina, 239 meters in length and 30,5 meters in width, crash against the mole of the dock of Genova when it was trying to leave the dock with direction to the city of Naples. The control pilot tower of the dock of Genova was located near to the place where the collision was produced. As a consequence of the impact, were induced high stresses in the portion of soil where the foundation of the pilot tower was placed. These high stresses, induced in the foundation of the tower, resulted in huge displacements in its head, which gave place to the collapse of the pilot tower. Due to this incident, seven people died.

Figure 1-3 Effects of the impact of the cargo ship "Jolly Nero" against the mole of the Genova's dock.
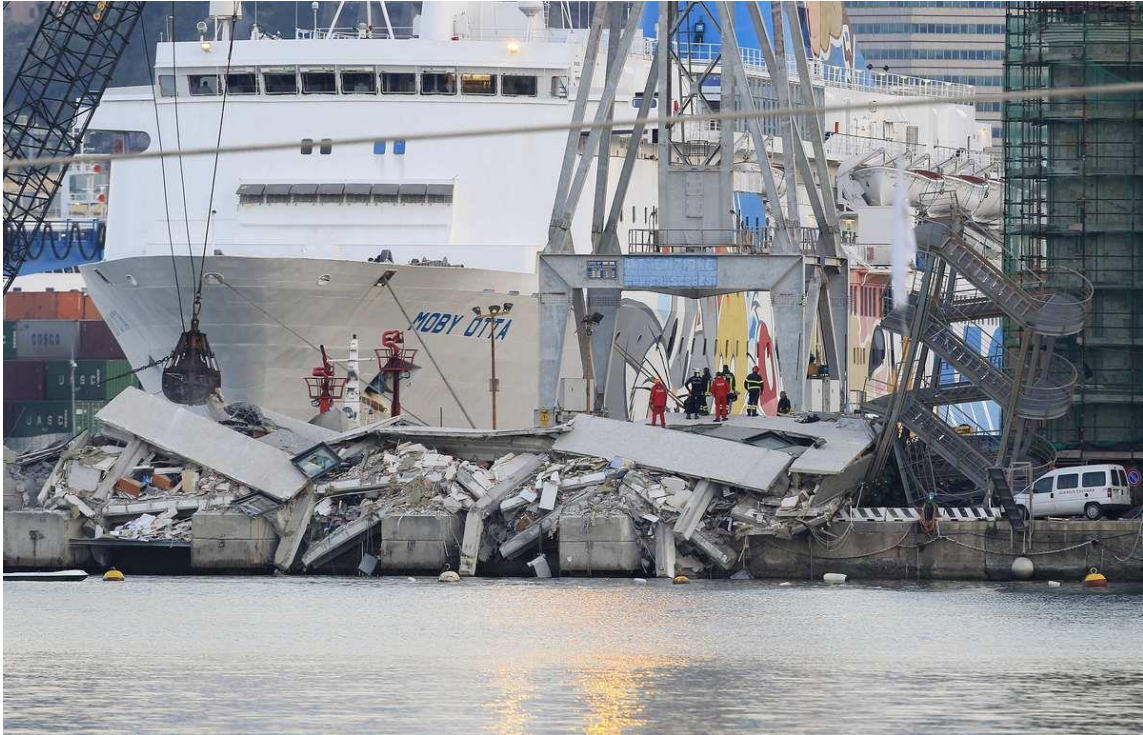
Figure 1-4 Effects of the impact of the cargo ship "Jolly Nero" against the mole of the Genova's dock.

Figure 1-5 Effects of the impact of the cargo ship "Jolly Nero" against the mole of the Genova's dock.

In this Master's Thesis have been developed two models to determine the displacements in the head of the new pilot tower of the Genova's dock, taking as reference the incident happened in the old pilot tower. In addition to this, are going to be studied two cases. In the first model developed, between the breakwater of the dock and the foundation of the pilot

tower, there is a concrete block whose displacements through the soil are not restrained due to the action of a pile's foundation placed under its bottom surface. Afterwards, it has been proposed a second model in which the concrete block contains the mentioned pile's foundation. This has been carried out to confront the different displacements achieved in head of the tower which are obtained from both models and to determine the improvement in the behavior of the system by adding the pile's foundation under the block.

The numerical models on which the analysis have been run, have been developed by means of the Finite Element software *PLAXIS* (Chapter 6).

To obtain more information about the incident in the dock of Genova, it can be clicked in the next link.

http://www.rtve.es/noticias/20130508/accidente-torre-control-puerto-genova-italia/658661.shtml

1.4   Summary of the Master's Thesis

As it has been mentioned above, the aim of this Master's Thesis is to study the response and the behavior experienced in pile's foundations working under horizontal forces.

In the second chapter of the Thesis, have been discussed the typical aspects of the response of a single pile working under horizontal loads and the factors which influence on this response, such as the modality of the load's application, the constraint conditions in the head of the piles, the technologies of implementation of the piles and how the geometry of the piles and the mechanical properties of the soil affect to the answer of the system. In addition to this, have been exposed the process to determine the limit load of a single pile when it is located in a granular and a cohesive soil. Afterwards, have been described the block failure mechanism and the response of the of the group of piles working under horizontal forces. At this point, it has been introduced the concept of the pile's efficiency, as well as the shadowing and the edge effects. Furthermore, have been studied the shape of the bending moment acting on the pile and the effect of the construction technology of the piles in the response of the system.

In the third chapter of the Thesis, have been discussed the failure mechanisms of the piles and the influence of the soil resistance on it, according to the models proposed by BROMS (1946b) and BARTON (1982) for the resistance of a granular soil. At this point, the equations proposed by BROMS (1946b) to determine the value of the limit horizontal forces which define the behavior of the single pile in a granular soil, have been particularized with the model of the soil's resistance suggested by BARTON (1982). Subsequently, both models have been confronted by representing the variation of the limit horizontal force in function of the yielding moment of the steel reinforcement of the piles for different values of the friction angle. It has been also studied the effect of the constraint conditions in the head of the single pile. This has been carried out by comparing, for each of the models of the soil's resistance, the values of the limit loads for a free-headed pile and for a restrained pile.

In the fourth chapter of this Master's Thesis, have been calculated the efficiencies, the horizontal forces and the displacements in the heads of the piles for two example cases corresponding to a group of piles 2 x 2 and 4 x 4 respectively. At this point, have been also determined the differences in the behavior of the piles pertaining to the different rows within the same group by plotting the relative displacements on their heads with regards to the displacements in the head of a pile whose efficiency is equal to the unit.

In the fifth chapter of the Thesis have been described the main features which have been taken into account to develop the FEM models on which have been run the analysis described in the sixth chapter of the Thesis, such as the determination of the impact force with which the cargo ship hit the mole of the Genova's dock and the stratigraphy and mechanical properties of the soil placed on the dock of Genova.

In the sixth chapter of this Master's Thesis, has been developed the Finite Element Analysis of the application case described in the previous point. Firstly, it has been made a brief description of some of the most significant features of the Finite Element Methods like the constitutive models and the determination of the critical step, which is very important to achieve trustable results from the calculation processes. Subsequently, it has been described the model of the Genova's dock developed with the Finite Element software PLAXIS, and have been presented and discussed the results of the four different analysis (two static, two dynamic) which have been carried out by means of this software with regards to the model described. Afterwards, for both cases of study proposed, that one corresponding to the real case and that one in which the concrete block contains a pile's foundation under its bottom surface, have been compared the displacements obtained with the static and dynamic analysis in different nodes of the model. Finally, to compare results obtained with regards to the numeric analysis with those achieved by the simplified models which have been described in the second and third chapters of this Thesis, have been calculated the displacements in the heads of the piles pertaining to the foundation of the concrete block which has been studied to determine improvement in the system's response with regards to the real situation happened in the dock of Genova.

In the seventh chapter, are presented the conclusions which have been obtained from the analysis developed along this Master's Thesis.

In the eighth chapter is listed the different bibliography which has been consulted to develop this Master's Thesis.

2 Theoretical Base Of The Thesis

2.1 Behavior of a single pile foundation under horizontal loads.

For a pile on a vertical shaft, with circular section, in a homogeneous soil. normal tensions acting on the lateral surface show an axisymmetric distribution, whose resultant force is equal to zero. When the pile is subjected to horizontal forces and/or to a bending moment, a translation is induced in the ground. The tension soil diagram, consequently, is modified; the normal stresses which the ground induces on the lateral surface of the pile increase and the soil tends to move away from it in a radial direction. Along the pile's edge, horizontal loads show normal and tangential tensions. The direction of the resultant force p [F/L] will be the same as the pile's displacement but the sense will be opposed.
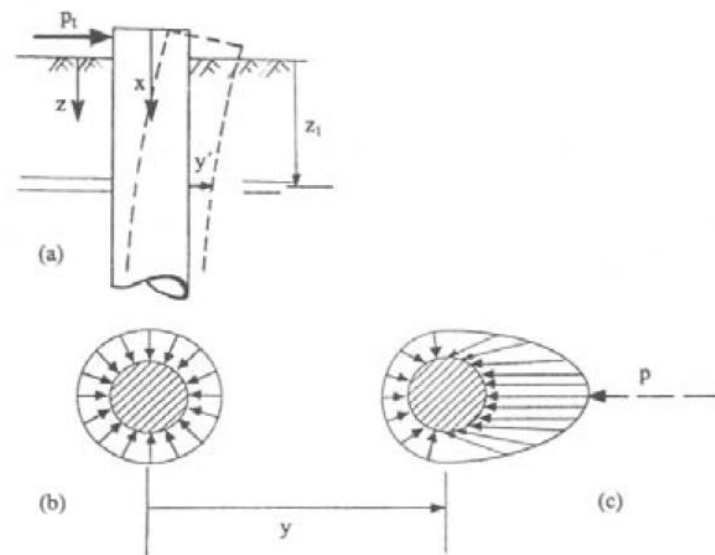
Figure 2-1. Pile-ground interaction (Landi, 2005).

On the one hand, at a certain load level, next to the surface of the ground, the soil behind the pile tends to split from it. On the other hand, the ground in front of the pile tends to collapse. Deeply the ground tends to slide, flowing along the edge of the pile, without a relative splitting on its back. According to the Ph. D. Thesis developed by G.LANDY (2005), it can be concluded that the response of the soil p depends on the reached displacement y of the pile and on the depth z.

Therefore, the vertical response of a pile under increasing horizontal loads, in term of the load-displacement curve, or in term of *load-maximum* bending moment, is not linear. In the next picture it is showed an example about the curves that correlate *load-displacement on the pile's head* and *load-maximum bending moment* acting along the pile's shaft.
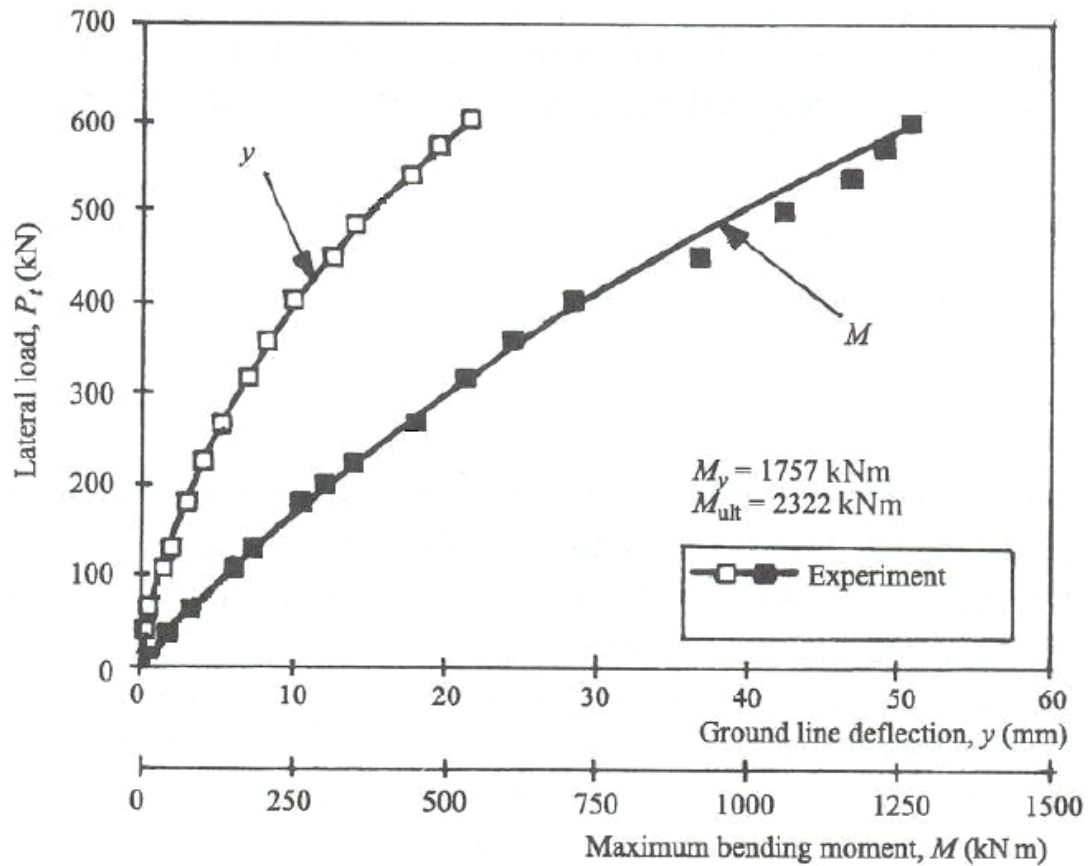
Figure 2-2 Experimental curves load-displacement and load-maximum bending moment (Reese et al., 1975).

2.2 Typical aspects of the response.

The biggest displacements of a pile under horizontal forces happen in the first meters of depth from the surface. In fact, it is rare to find big displacements of the pile in a depth higher than ten times the pile's diameter (FLEMING ET AL., 1985).

The depth at which the pile's displacements, the loads acting on them and the ground response can be considered irrelevant is known as *critical length* of the pile (RANDOLPH, 1981). The length of the pile is, in the most of the cases, greater than the critical length. If it is verified the last condition, the pile is defined as *flexible*. For this reason, the pile's length is not a significant parameter in terms of the global system response pile-ground when horizontal forces appear.

The value of the critical length depends on some of the parameters of the system. The first one, is the *relative stiffness* between the pile and the soil.

Due to the fact that the displacements of the pile take place near to the ground surface, the pile-ground system response under horizontal forces depends on the mechanic features of the soil next to the surface. For this reason it is very important to determine the characteristics of the soil in the first meters of depth. The position of the phreatic level and the individuation of a surface crust of over consolidation, are relevant factors in the determination of the ground response.

10

Another point which must be dealt with is the position of the maximum bending moment, that in the case of a pile with its head rotation blocked, it is located on the top the pile, and in the case in which the head pile can rotate free, this appears along its shaft. It must be told that in the second case, the maximum bending moment appears at a short depth from the surface. The depth at which the maximum bending moment takes places depends on the relative stiffness pile-ground.

The critical length and the depth of the section where the bending moment is maximum depend on the load's size. If this force increases, it will also enhance the critical length and the depth of the maximum bending moment. This behavior is showed in the following picture (G.LANDI, 2005).
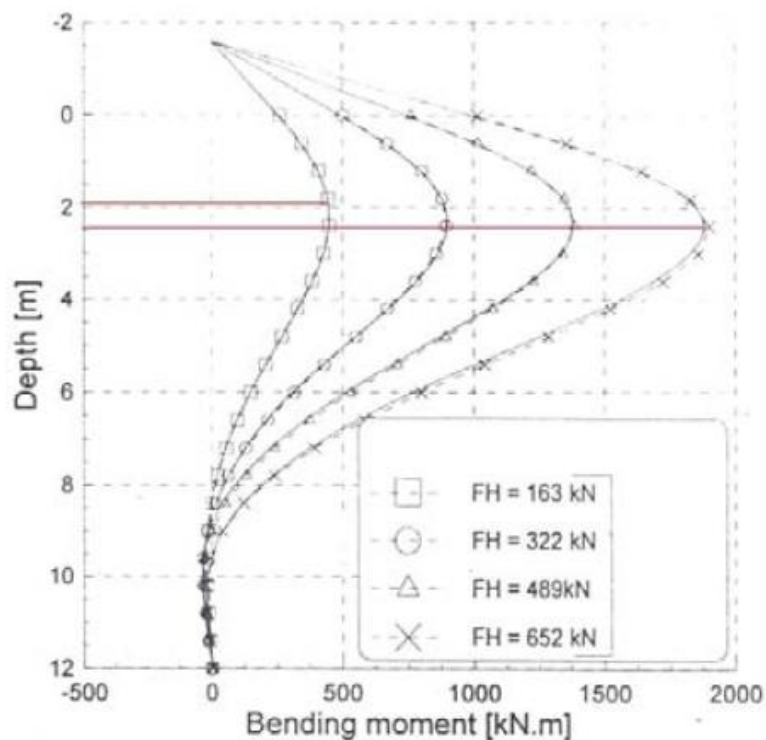
Figure 2-3 Progressive increasing of the section's depth where the bending moment is maximum, when raising the load (Remaud et al., 1998).

Regarding to the achievement of limit conditions, except cases in which the piles are very resistant or with a very high relative stiffness in regards to the ground, a pile under horizontal loads behaves like a *long pile* (BROMS, 1964a; 1964b). The collapse condition of the pile-ground system is achieved when a *plastic hinge* appears along the pile foundation (in case of free rotation of the head's pile), or when two plastic hinges show up, one on the top of the pile and another along the pile's shaft (pile head rotation restrained). In order to determine the limit value of the resistance of the pile-ground system under horizontal loads, is very important to know the yielding bending moment of the pile, which determines the formation of the plastic hinge.

In a project of pile foundations under horizontal forces is necessary to verify, according to similar modalities used to characterize the pile foundations under axial loads, that the pile-

ground system satisfies the minimum factor of safety towards the horizontal load limit state of failure. Furthermore, it must be guaranteed that the displacements on the pile's head are acceptable, based on the features of the structure placed over the foundation.. In both cases A correct prevision of the bending moment value that causes the appearance of the plastic hinge is very relevant.

2.3   Factors that influence the pile response.

The way a single pile works under horizontal loads depends on the characteristics of the soil, the variation of the resultant force *p* with the increasing pile displacement *y* and on the reference depth. However, the response of the system also depends on some other factors, which are the developed in the following.

- Modality of load application.
- Constraint conditions on pile's head.
- Technology of implementation of the piles.
- Pile features: geometry and mechanic properties.

INFLUENCE OF THE LOAD APPLICATION

Based on the Ph.D.. Thesis of G.LANDI (2005), there are different kind of loads: static, cyclic or dynamic. These load modalities try to reproduce the several situations in which the foundation will be involved during its life.

During the **static test**, the load is applied monotonically, by means of successive increments at short time intervals (short-term loading) or long intervals of time (sustained o maintained loading). In soils with thin size grains, a short-term loading refers to undrained conditions. Nevertheless, a sustained loading refers to drain conditions. An example of the evolution of the resultant force *p* when varying the pile's head displacement *y* is showed in the next picture taken from the Ph.D.. Thesis of G.LANDI (2005). During the first phase, it exists a linear relationship between the soil resistance and the pile deflection (until point a). In the second phase (stretch a – b), the relationship between these two parameters is not linear and tends to achieve an upper limit that is known as ultimate resistance p_{ult}. The reaction modulus of the soil (defined as $E_{py} = p/y \ [F/L^2]$), with regards to a pile loaded under horizontal forces, maintains itself constant for small values of the pile deflection *y*. When the deflection increases itself, it starts decreasing the soil modulus describing a curve as it is showed in the picture.
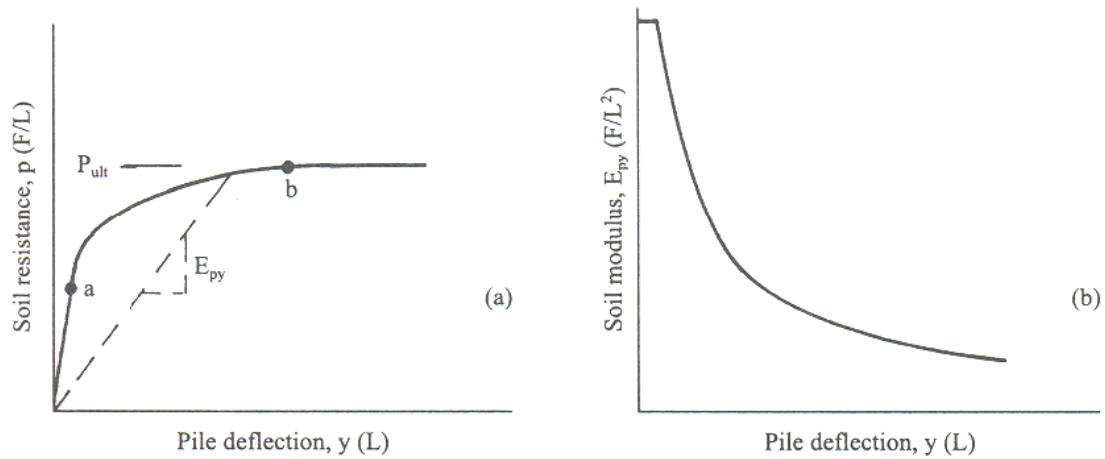
Figure 2-4 Variation of the resistance p and reaction modulus E_{py} of the soil during a static load test (Reese & Van Impe, 2001).

The soil response *p* also varies according to the referring depth *z*. In the next picture are showed some experimental *p – y* curves when varying the depth. These have been obtained by REESE ET AL. (1975) from static load tests on cylindrical piles (diameter 641 millimeters; 15,2 meters in length) in a ground consisting of over consolidated clay. From these curves, it is noticed that the initial values of the stiffness increases when the depth grows up, as well as the value of the least resistance.
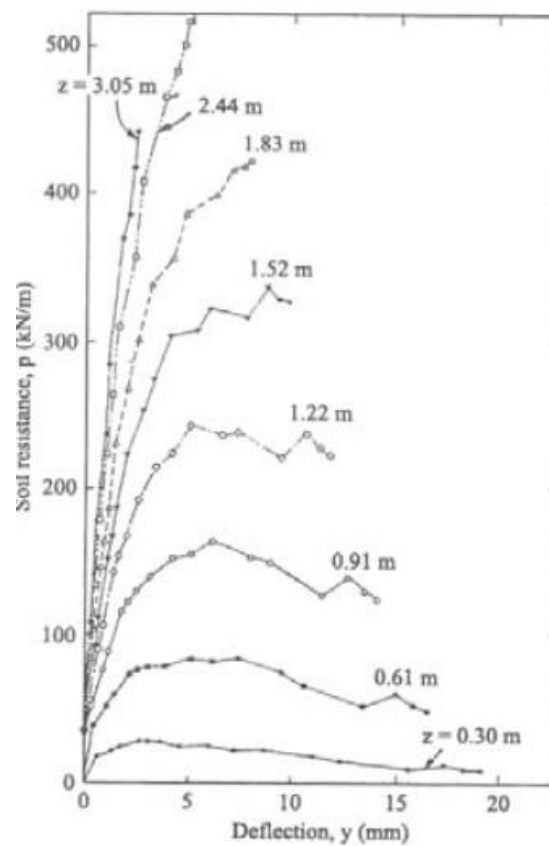

Figure 2-5 Experimental curves p – y: evolution when varying the depth (Reese et al., 1975).

13

The response obtained in a static test with loads applied for short periods or with loads kept constant for prolonged periods of time does not vary significantly if the soil in which is performed are granular or constituted by over consolidate clays. The effects on the response of the system pile - ground of a prolonged load, instead, can be not negligible in cases of clays hold. The rate of movement of the pile differed in time, under constant loads, is a consequence of the progressive dissipation of interstitial overpressures that are induced in the ground during the test. The modeling of the phenomenon of consolidation, responsible for the reduction in the stiffness of the answer depends on many parameters, not all easily identifiable. Rarely, a static test reproduces the load mode to which the Foundation will be subjected in reality. However, for this test mode there is a clear correlation between the results obtained and the mechanical characteristics of the soil. In any case, the results of the static tests constitute the touchstone by which compare the results of tests with different modes of application of the load.

A cyclic load test envisages that reached a certain level of acting force, the same is made to vary in a predetermined number of times around the value reached. Also, the oscillation is performed in the surroundings of the displacement achieved. The aim of this test is to simulate the action of the wind, the waves, or the currents on the structures.

The effect of cycles results in a decreasing of the stiffness in the system pile - ground. In the initial portion of the curve p - y, in which the pattern is linear, the effect of cycles is negligible. When the magnitude of the displacements y is increased, the values of p decrease in function of the number of cycles in a significant manner. Even the ultimate value of resistance p_{ult} decreases. These effects, are evident in granular soils and in clays being placed above the level of aquifer and become particularly relevant for saturated clays placed below the phreatic level. Usually, when a certain number of cycles is reached, the response of the soil becomes independent from them.
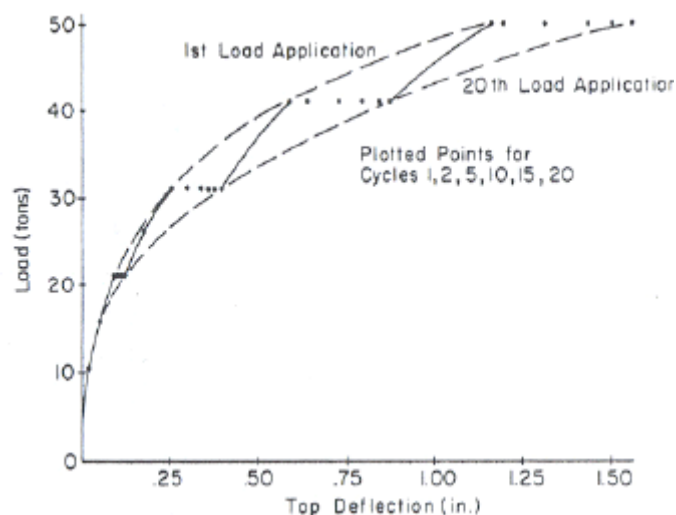
Figure 2-6 Variation of the curve loads - movements to the growing number of cycles (Reese & Welch, 1975).

The decreasing of the soil's resistance is due to a transfer of the stresses toward the bottom because of the interaction between the pile and the ground. Consequently, the distribution and the magnitude of the stresses in the pile, in terms of bending moment and shear, varies both in terms of quantity and in terms of the depth of the section of maximum stress.

The dynamic tests are carried out to simulate the forces generated on the structures due to traffic, industrial machinery, waves, earthquakes. However, the frequency of the loads due to the action of the traffic and the waves are usually low. For this reason, the development of the soil reactions p obtained in relation to the static or cyclic tests are enough to describe the effects (HADJIAN et al, 1992). The realization of a dynamic test provides the onset of inertial forces; to model these tests it is necessary therefore to consider the ground mass involved. Specific studies in this field have been undertaken in relation to the effects generated by rotating machinery (for example, WOODS & STOKOE, 1985) or by an earthquake (e.g., GAZETAS & MYLONAKIS, 1998).

The dynamic tests carried out are still few in number. It is therefore still difficult to establish general trends.

INFLUENCE OF THE CONSTRAINT CONDITION IN THE PILE HEAD

The test modes affect the response of the system pile - ground under horizontal actions since change the values of the ground reaction p. The response of a pile working under horizontal actions, in both extreme cases, head impeded from rotating and head free to rotate, is significantly different.

In particular, the values of displacement in the case of hindered rotation of the pile's head are considerably lower - about half (RANDOLPH, 1981) – of those in which the head is free to rotate, for a given acting load. This is a consequence of the fact that a pile impeded from rotating in the head, loaded by a horizontal force, interacts with the ground at a higher depth with respect to the pile whose head is free to rotate. The distribution of loads on an greater area of soil results in a reduction of the magnitude of the displacements of the pile.

The different constraint conditions in the pile's head predefine the distribution of the stresses on the pile. In the case of the pile with a free rotating head, the maximum moment comes along the shaft of the pile, at a depth in general quite superficial (few diameters of the pile). If the pile is rotational restrain, the maximum moment is registered in correspondence of the rotational restrain. The bending moment in the head for a rotationally restrained pile is significantly greater than the maximum moment acting on a pile whose head is free to rotate; the first one can be four times greater than the second one (Tooth & GULLÀ, 1983). To assure that the condition of constraint in the head is a perfect rotational restrain, it must be checked that the connection between the plate and the pile is indeed capable of resisting that high values of bending moment expected.

In the next figures are showed, for comparison purposes, the patterns of the deformed shape of the pile and the bending moment depending on the depth (made dimensionless with respect to the diameter). This was obtained by G.LANDI (2005) with a calculation program named NAPHOL for two piles with the same geometric and mechanical features, loaded under the same force, in soils with similar mechanical properties. The both piles are, respectively, free and impeded from rotating in the head. The purpose of the comparisons shown in the figures is purely qualitative.
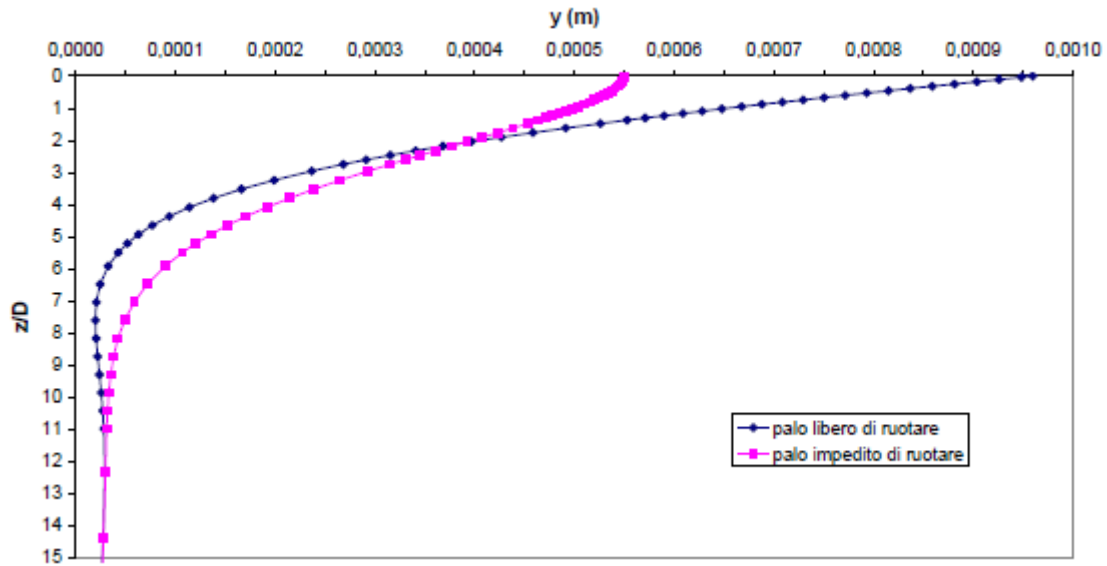
Figure 2-7 Deformed shapes of a pile with a free rotation head and a pile impeded from rotating on its head (G.LANDI, 2005).
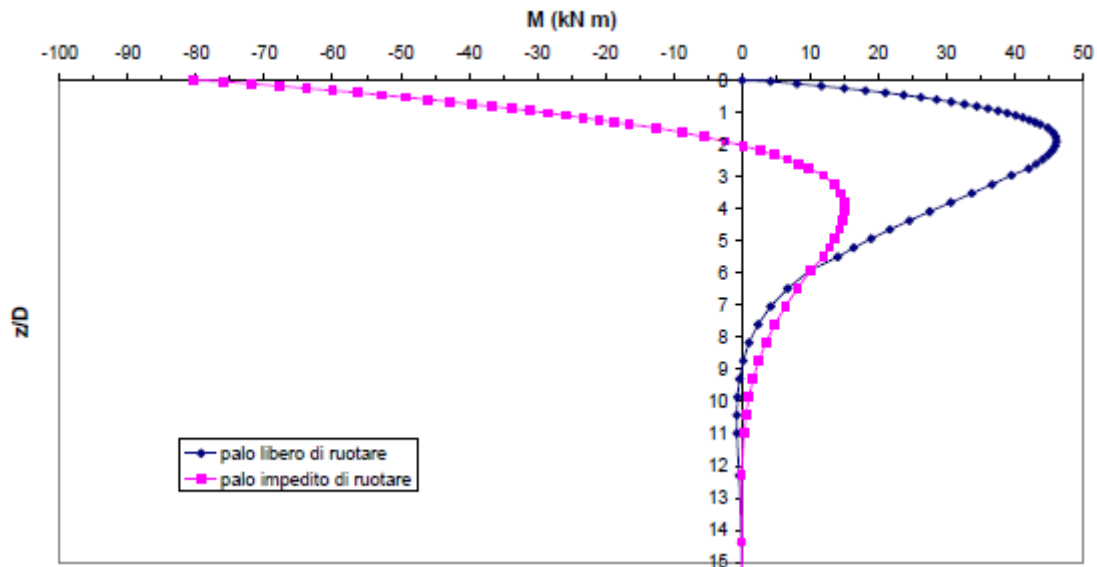
Figure 2-8 Bending moment diagram of a pile with a free rotation head and a pile impeded of rotating on its head (G.LANDI, 2005).

<u>INFLUENCE OF THE EXECUTION TECHNOLOGY OF THE PILE</u>

There are some technology to realize the piles. The technical innovations, with regards to the use of materials and machinery, have allowed, over the years, the development of different constructive procedures depending on the mechanical requests.

In general, the piles are divided, depending on the execution technology, into piles built by *removal of ground* (**rotary drilled piles**) and piles built by *displacement of the ground* (**driven piles)** There is also a third method to implement the piles consisting of a mix of both latter methods. According to this third procedure, the execution of the piles is performed by removing a portion of the ground and displacing another portion thereof.

The construction technique of a pile foundation affects significantly the response of the same to the axial stresses. It exists a high correlation between the way in which the piles are constructed and the stresses which are induced in the ground as a consequence of it. When deep foundations of piles are built by means of driving, due to the compression of the soil, the horizontal stresses along the pile increase. These forces grow up until the limit condition of failure is achieved. In the case of rotary drilled piles, horizontal tensions decrease as a consequence of the removal of a portion of ground until the limit condition of breaking by active pushing is reached. This modifications on the tensional state of the ground only affects a small area around the pile. In this portion of soil appear some shear stresses, which take part on the pile lateral resistance under axial loads. In addition to this, it is also needed to consider the axial tensions which are generated under the base of the pile. These also depends on the technology of construction of the piles. With regards to KISHIDA (1967), it must be considered a different friction angle depending on the construction technique of the piles.

Relating to the thesis of G.LANDI (2005), the effects on the tensional state due to the changes induced by the manufacturing technology of the piles, in its immediately surrounding area, when piles are loaded by horizontal actions are much smaller. This is motivated by the fact that the volume that affects the behavior of the pile under horizontal loads is much greater than that of the vertical loads, and therefore less influenced by the effects of the installation of the pile itself. In the next figure it is showed, a typical representation of the wedge of soil responsible of the answer under horizontal forces.
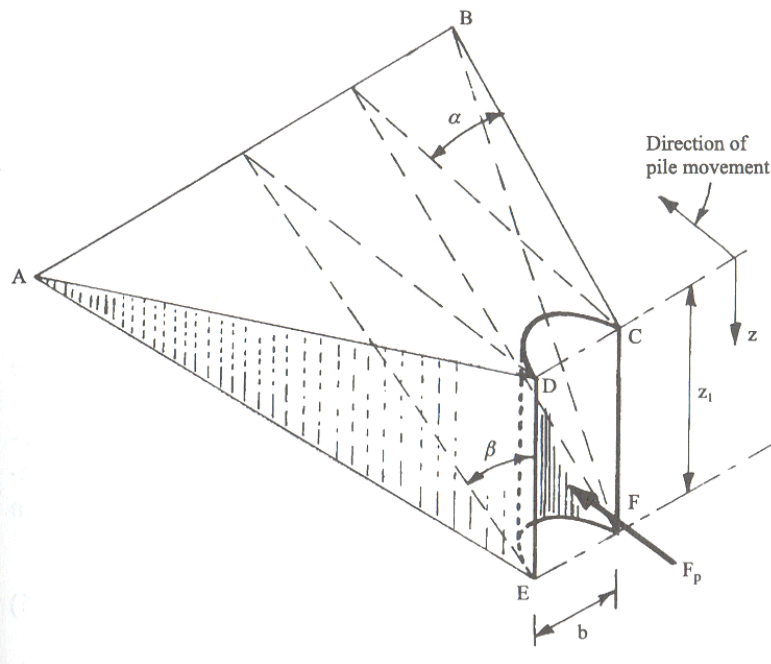
Figure 2-9 Wedge of soil responsible of the answer under horizontal forces (Reese & Van Impe, 2001).

Some authors (O'NEILL & DUNNAVANT, 1984; Huang et al, 2001) have tested piles built according to different modes, without obtaining definitive particulars on the influence of technology. The large experimental field described in ALIZADEH & DAVISSON (1970) foresaw

the creation of load tests on driven piles and on piles driven into the soil after the execution of a pre-hole. Also in this case, the obtained results offered not definitive indications.

It has been observed that the variability of the response due to the heterogeneity of the ground constitutes a more important factor of influence than that of technology.

In order to determine the pile answer under horizontal forces in operating conditions, the most widely used analysis method is based on the curves *p - y*. It is also necessary to emphasize in the choice of the kind of curve *p - y* taken to develop the analysis. Between the studies carried out by some authors (Terzaghi, 1955; McCLELLAND & FOCHT, 1958; Matlock, 1970; REESE et al, 1975) it can be checked that are taken into account many factors which can influence on the shape of the curves. Nevertheless, the manufacturing technology of the piles is not one of them.

It can be assumed that the kind of technology with which the construction of the piles is made up can influence the response of the piles working under horizontal loads when these are very low.

GEOMETRICAL AND MECHANICAL PROPPERTIES OF THE PILE

The response of the pile-ground system under horizontal loads is influenced by the geometrical features of the pile's section. Actually, the distribution of the horizontal forces along the edge of the pile, varies with the shape of its section (circular, square or rectangular, for H, etc.). Consequently, the value of the ground reaction *p* caused by the tensional state that acts on the edge of the pile, is modified. In the next image, it is showed, the state of stress on the lateral surfaces of some piles whose section's shape are different.
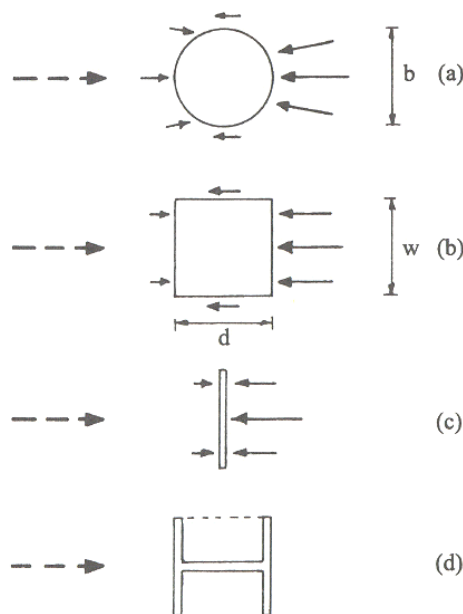
Figure 2-10 Tensional state acting on the pile's edge depending on the section's shape (G.LANDI, 2005).

In cases in which the section of the pile is not circular, it is possible to take into account the effects of the section's shape of the pile obtaining an circular equivalent diameter for each kind of section (REESE & VAN IMPE (2001)). It can be calculated by means of the next expression:

$$d_{eq} = w \cdot \left(\frac{p_{uc} + 2 \cdot \left(d - \frac{w}{2} \right) \cdot f_z}{p_{uc}} \right) \qquad (2.1.)$$

Where w is the dimension of the section which is perpendicular to the force direction, d is the length of the pile, p_{uc} is the limit load of a pile whose section is circular with a diameter w, f_z is the shear resistance along the edge of the rectangular surface of the pile at a depth z.

To calculate the shear resistance, it is necessary to distinguish between cohesive and granular soil. In the first case, the shear resistance is calculated by means of the next expression:

$$f_z = \alpha \cdot c_u \qquad (2.2.)$$

The parameter c_u is known as undrained cohesion at a specific depth. The determination of the α value must take into account the pile's behavior working under axial loads as well as the technology used to construct the piles. The value of α is comprised between $0,5 - 1$. On the other hand, in the case of granular soils, the shear resistance is calculated using the next formula:

$$f_z = K_z \cdot \gamma \cdot z \cdot \tan \phi \qquad (2.3.)$$

In which ϕ is the friction angle between the pile's surface and the ground at a specific depth, Υ is the specific weight of the soil, K_z is the lateral pushing ratio, which depends on the technology used to construct the piles.

Some studies have been carried out to determine if the geometry of the pile's section was supposed to be a relevant factor in the response of the system pile-ground. In fact, BROMS (1964a) noticed that the ultimate resistance in cohesive soils is influenced by the pile's shape when working under horizontal forces. On the other hand, in the calculation of the limit resistance in the case of granular soils (BROMS, 1964b), the influence of the pile's shape is considered negligible.

Moreover, some other authors (O'NEILL & DUNNAVANT, 1984) describe how the response of the ground, in terms of the curves $p - y$, keeps a non-linear connection with the diameter of the pile. It is necessary to pay special attention to this phenomenon when the diameter size is large.

According to the Ph.D.. Thesis developed by G.LANDI (2005), the reaction of the ground p is also conditioned by the material of which the pile is made up. Considering a pile with a squared section loaded perpendicularly to one of his edges, the shear stress values that are induced on the faces which are parallel to the action of the force, are quite different depending on the materials of which the pile is composed (concrete, steel, or wood). With regards to the formulas of REESE & VAN IMPE (2001), the type of material constituting the pile, influence the choice of the values of α and ϕ, for cohesive and granular soils.

In addition to this, BROMS (1964a), in order to determine the constant k to model the problem of a pile working under horizontal loads in cohesive soils, with the method of the curves $p - y$, identified a dependence of this parameter related to the material constituting the pile, with a coefficient called n_2. The value of this coefficient is equal to 1.00 for piles consisting of steel, 1,15 for concrete piles and 1,30 for wooden poles. Furthermore, to define the value of the limit resistance of the pile, depending on the section's shape, BROMS (1964a) also distinguishes the cases of interface pile – ground smooth or rough. The roughness features of the interface are a function of the pile's material.

The bending stiffness of the pile, defined as the product of the Young modulus of the material and the inertial moment of the pile's section $E_p I_p$ affects directly the system's response. For the same geometrical characteristics and kind of soil, a greater bending stiffness of the pile means that there will be induced stresses at a higher depth with respect to the flexible pile case. The external force is transmitted to an area of soil more extended; consequently, the stiffer the pile it is, the better will be the response of the system in terms of displacements.

Based on the comments made in the thesis carried out by G.LANDI (2005), the most significant factors that affect the response of the single pile, working under horizontal forces, are constituted by the heterogeneity of the mechanical properties of natural soils, which can be very different for a small area of land. In addition to this, it can be assumed that the influence of the load modality and the constraint condition in the pile's head are factors which take special importance on the pile-ground's system response. Meanwhile, the section shape and the construction technology of the pile represent secondary factors in the system's response.

2.4 Limit load of a single pile working under horizontal forces.

2.4.1 Granular soils.

When a pile is loaded with a horizontal force or a bending moment, the normal stresses placed in front of the pile are increased and the ground tend to split from the pile in radial direction. The normal stresses located on the back of the pile decrease, while the ground tends to move towards the pile in a radial direction. Next to the surface, the soil placed behind the pile tends to split from it. It is known that the ground located in front of the pile collapses when a break wedge is formed. With the increasing of the depth, the collapse mechanism of the ground takes place flowing along the pile's edge, without a relative spacing between the pile and the ground. These two breaking mechanisms result in the variation of the ground's limit pressure p_u which is induced on the pile depending on the depth.
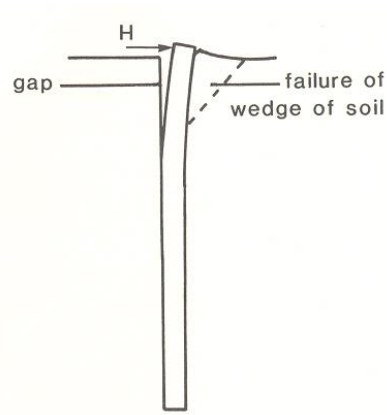
Figure 2-11 Break wedge of a ground working under horizontal loads (G.LANDI, 2005).

At a depth not higher than one diameter, the pile works like a load-bearing wall. When ultimate conditions of break are achieved, it appears a wedge of ground which is pushed by the pile. In this case, the limit pressure which will affect to the pile will be:

$$p_u = K_p \cdot \sigma'_z \qquad (2.4.)$$

Where σ'_z represents the ground's effective vertical tensional state and K_p is the passive earth pressure coefficient that depends on the friction angle ϕ and was suggested by Rankine as:

$$K_p = \frac{1 + \sin\phi}{1 - \sin\phi} \qquad (2.5.)$$

A widely used model in engineering to define the limit pressure profile of a granular soil is that one proposed by BROMS (1964b), which establish:

$$P_u = p_u \cdot D = 3 \cdot K_p \cdot \sigma'_v \cdot D \qquad (2.6.)$$

Where P_u is the value of the limit reaction per unit of length and D is the diameter of the pile. This calculated value of the ground's reaction tends to underestimate the limit load of a pile working under horizontal forces, in a 50 % (BROMS, 1946b) or in one third (POULOS & DAVIS, 1980). This model is highly used among the engineer designers because of the safety margin which provides.

According to the thesis of G.LANDI (2005), the formula of BROMS (1964b) was checked by the author, by comparing the values of the limit load obtained by its application to 32 different experimental cases. However, it must be pointed that, in these cases of analysis, at least 30 of

them correspond to piles with very small dimensions (length smaller than 1,5 meters). The two other cases are related to piles with ordinary dimensions (Length equal to 16,3 meters).

In addition to this, it has been proposed by REESE ET AL. (1974) another profile to describe the ultimate resistance of the ground. It is considered a difference between the values of the limit pressure induced by the soil in the area where takes place the break of the wedge, in which p_u is proportional to K_p, and the area where the ground outflows laterally to the pile, where p_u is proportional to $K_P{}^3$.

An intermedium profile between the both previous cases was proposed by BARTON, 1982. In this model p_u was adopted proportional to the square of the passive earth pressure coefficient $K_P{}^2$. The formula to calculate the ultimate resistance of the soil in this case is:

$$P_u = p_u \cdot D = K_p^2 \cdot \sigma'_v \cdot D \qquad (2.7.)$$

In the most of the cases, the friction angle in granular soils is equal or bigger than 30º. Consequently, $K_p^2 \geq 3 \cdot K_p$. This expression has been obtained based on the results of some centrifuge tests which have been run on piles properly instrumented. It has been measured the bending moments in these piles located within a ground consisting of dense uniform sands characterized by a friction angle of 43º. According to G.LANDI (2005) it has been concluded that the value for the ultimate resistance obtained with the model proposed by BARTON (1982) is underestimated approximately in a 6%.

In the next figure, taken from the Ph.D.. Thesis of G.LANDI (2005), are confronted the trends of the limit reaction per length unit obtained with regards to the models of REESE ET AL. (1974) and BARTON (1982). From the confrontation between the two models with the experimental data (black points), it can be noticed that until a depth equal to 1 – 1,5 D, the limit reaction per length unit can be obtained as:

$$p_u = K_p \cdot \sigma'_v \cdot D \qquad (2.8.)$$
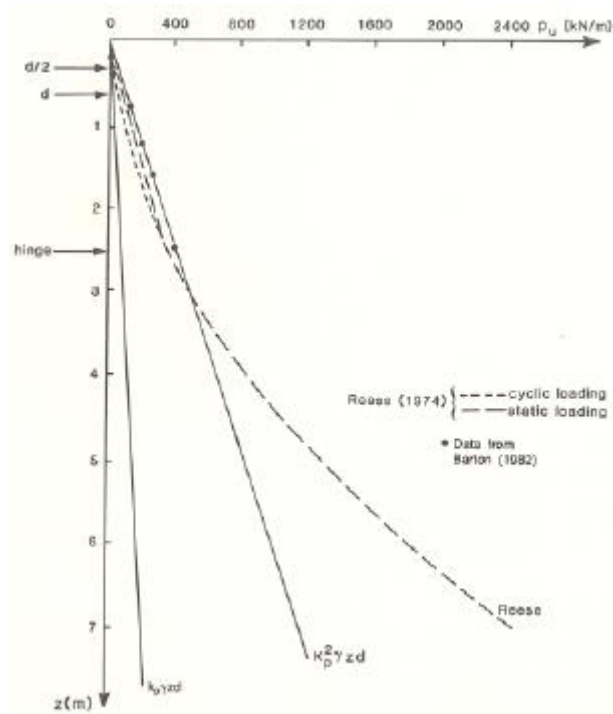
Figure 2-12 Confrontation between the trends of the limit reaction per length unit proposed by BARTON (1982) and REESE ET AL. (1974) showed on the Ph.D.. Thesis of G.LANDI (2005).

2.4.2 Cohesive soils.
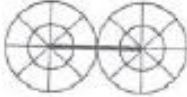
In cohesive soils, the break mechanism is based on the same principles as in granular soils. In the portion of ground next to the surface, the soil located behind the pile tends to split from it. In front of the pile is formed break wedge as was described in the case of granular soils. This break mechanism is called *block failure*. When the depth increases, the ground moves laterally to the pile, so that there is not a spacing between the soil placed on the pile's back and the pile. The value of the ultimate resistance of the ground is conditioned by these two break mechanisms. This value of the limit resistance is achieved at a depth next to the pile's base and depends on a parameter called undrained cohesion of the ground c_u.

Based on the plasticity's theory, some authors have obtained values of the resistance offered by a cohesive soil to the movement of a stiff element through it. These values correspond to tests developed in depths where the ground drains laterally with regards to the pile. In the case of cohesive soils, the ultimate resistance per length unit is calculated by means of the next expression:

$$P_u = p_u \cdot D = N \cdot c_u \cdot D \qquad (2.9.)$$

According to what was described in the Ph.D. Thesis of G.LANDI (2005), BROMS (1964a) proposed several values for the parameter *N*, which is function of the roughness and the shape of the solid elements considered. The values of this coefficient varies from 8,28 to 12,56. For a smooth circular pile, the parameter N comes 9,14. Nevertheless, BROMS (1964a) suggested to adopt regardless the shape and the roughness features of the pile a value equal to 9. This results in a very conservative estimation. However, this consideration is taken into account by

engineers in the most of the cases. In the next picture, are showed some values of the coefficient N depending on the shape and the features of roughness of pile proposed by BROMS (1964a).

SLIP FIELD PATTERN	SURFACE	ULTIMATE LATERAL RESISTANCE, q_{ub}/c_u
	ROUGH	12.56
	ROUGH	11.42
	SMOOTH	11.42
	SMOOTH	9.14
	SMOOTH	8.28

Figure 2-13 Parameter N depending on the shape and the roughness condition of the pile.

As shown in the Ph.D. Thesis of G.LANDI (2005), there are some other authors which have tried to determine the coefficient N for different values of the pile's roughness in cohesive soils. RANDOLPH & HOULSBY (1984) have considered a stiff-plastic ground model and observed that appeared two stiff small areas on the front and on the back side of the pile, and a range area of scrolling surrounding the pile. The obtained values of N between 9,14 (smooth pile) and 11,94 (perfectly rough pile). For this reason, RANDOLPH & HOULSBY (1984) suggested to take an average value of N equal to 10,5. It can be noticed that the values calculated in this case are similar to that obtained by BROMS (1964a).
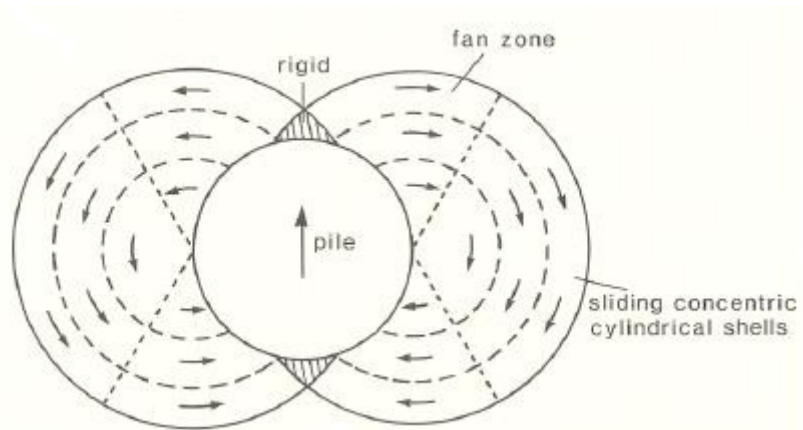
Figure 2-14 Break mechanism of the ground surrounding a pile working under horizontal loads described by RANDOLPH & HOULSBY (1984).

As it has been mentioned before, for cohesive soils, the failure mechanism near the ground surface, consists on the formation of a wedge of ground in the front side of the pile that tends to go upwards, and a splitting from the ground placed behind the pile. It can be concluded that the values of the limit resistance of the soil are lower near the ground surface. At bigger depths the mechanism of break consists on a lateral scrolling along the pile's shaft.
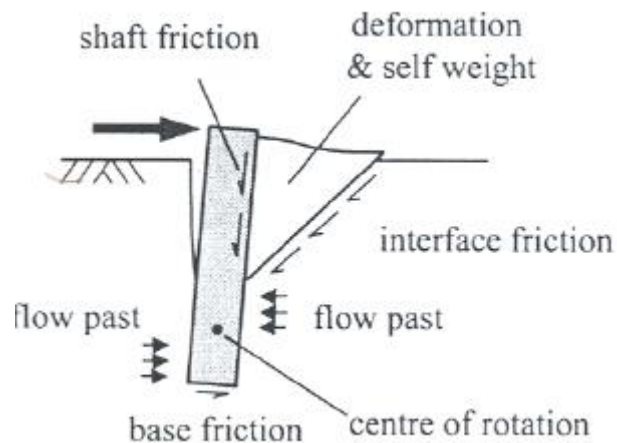
Figure 2-15 Break mechanism of the ground surrounding a pile loaded horizontally (RANDOLPH, 2003).

Otherwise, as it is described in the thesis of G.LANDI (2005), BROMS (1964a) concluded, from empirical tests, that for the firsts diameters of depth, the limit pressure of the ground, depending on the undrained cohesion c_u, experienced an almost linear variation from 2 c_u ,at the surface level, to 8 – 12 c_u at a depth of three diameters. For higher depths, the ultimate pressure can be considered as constant. However, to simplify the problem, the limit pressure is assumed equal to zero until a depth of 1,5 diameters. For higher depths, it is adopted a value

of the p_u obtained with regards to an undrained cohesion equal to 9 c_u. It must be pointed that this model proposed by BARTON (1964a) has not been compared to experimental data.
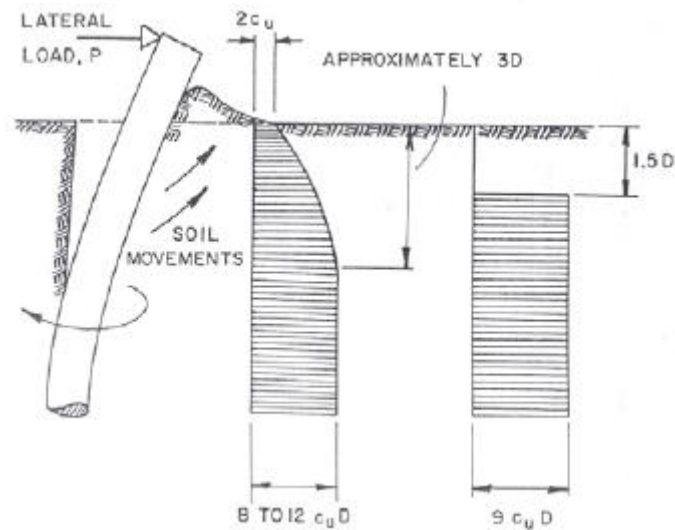
Figure 2-16 Resistance profile of the ground proposed by BARTON (1964a) for cohesive soils.

2.5   Block failure mechanism.

In the last point, some criteria to describe the response of an isolated pile working under horizontal forces have been described. Nevertheless, if a pile is within a group of piles with the same mechanical and material properties, the answer varies and it can be induced block breaking mechanisms which modify the resistance's profile described previously.
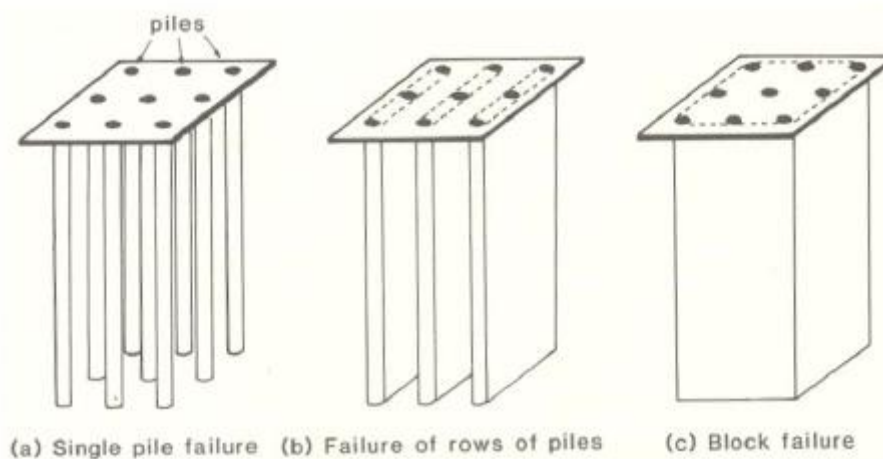
Figure 2-17 Block breaking model proposed by FLEMING ET AL., (1985).

When a horizontal load is applied on the same direction of the line which joins the pile's shafts of a group, the collapse mechanism is that showed in the case b) of the previous picture. This

26

failure mode is reached when the shear resistance of the ground placed between the piles, is lower than the limit resistance of the single isolated pile. If it is considered a pair of piles with a distance between its shafts equal to *s*, loaded with a horizontal force with the same direction as the line which joins the pile's shafts, the ultimate resistance per length unit of the piles is obtained with the next expression:

$$P_u = 2 \cdot s \cdot \tau_s \qquad (2.10.)$$

Where the τ_s is the shear resistance apperaring in the ground placed between both piles. It must be pointed that the calculation of parameter depends on the kind of soil; granular or cohesive.
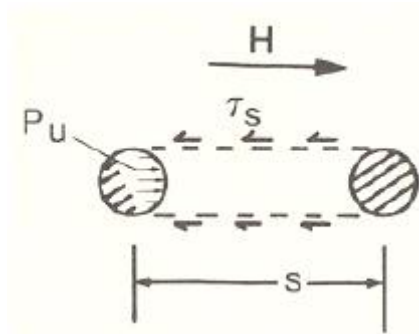
Figure 2-18 Block failure for a pair of piles (G.LANDI, 2005).

<u>GRANULAR SOILS</u>

In granular soils, the limit shear tensions acting on the ground is calculated with the following expression:

$$\tau_s = K \cdot \sigma'_v \cdot \tan \phi \qquad (2.11.)$$

Where σ'_v is the effective vertical tension at a determined depth, ϕ is the friction angle of the soil and *K* is the pushing coefficient that is comprised between K_0 and K_p. This coefficient *K* varies along the portion of soil placed between two piles. For this reason, it is very difficult to establish a single exact value for this parameter. According to the thesis developed by G.LANDI (2005), FLEMING ET AL. (1985) recommend as a first approximation to take this *K* equal to 1. Consequently, the ultimate resistance per length unit of a granular soil, when the block breaking of a pile is verified is obtained as:

$$P_u = 2 \cdot s \cdot K \cdot \sigma'_v \cdot \tan \phi \approx 2 \cdot s \cdot \sigma'_v \cdot \tan \phi \qquad (2.12.)$$

This value of P_u defines the ground's answer when is lower than the value obtained in the case of an isolated pile. Considering the model of the resistance proposed by BARTON (1982), where the P_u of the soil is provided by means of the expression:

$$P_u = K_p^2 \cdot \sigma'_v \cdot D \qquad (2.13.)$$

It can be concluded that the block breaking mechanism takes place when is verified the next condition:

$$\frac{s}{D} < \frac{K_p^2}{2 \cdot K \cdot \tan\phi} \approx \frac{K_p^2}{2 \cdot \tan\phi} \qquad (2.14.)$$

In the next graph is represented block breaking condition by means of the variation of the relative distance between the pile's shafts s/D when the friction angle of the soil is raised. It can be concluded that when the friction angle is increased, the block breaking mechanism can be verified at higher values of the relative distance between the pile's shafts s/D.
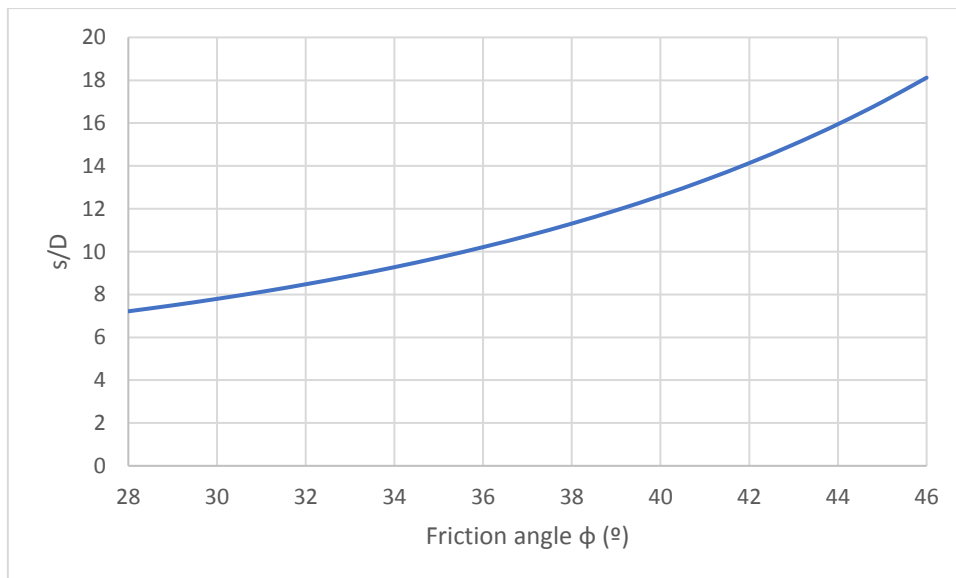
Figure 2-19 Limit values of the relative distance between the pile's shafts under which is verified the block failure mechanism in granular soils.

<u>COHESIVE SOILS</u>

In cohesive soils, the limit shear tension τ_s can be considered equal to the undrained cohesion c_u. In this case, the limit resistance per length unit that a cohesive soil induces on a pile when it is verified the breaking block mechanism, is calculated using the next formula:

$$P_u = 2 \cdot s \cdot c_u \qquad (2.15.)$$

In cohesive soils, the value for the ultimate resistance of the ground, with regards to the isolated single pile is equal to:

$$P_u = (9 \div 11) \cdot c_u \cdot D \qquad (2.16.)$$

So that, in this case, the block breaking mechanism is reached when it is verified the next condition:

$$\frac{s}{D} < \frac{(9 \div 11)}{2} = 4,5 \div 5,5 \qquad (2.17.)$$

It can be concluded that the values for the relative distance between the pile's shafts for which is verified the block failure condition in the case of cohesive soils, are lower than the values obtained for the same condition in granular soils. Moreover, according to the thesis of G.LANDI (2005), these values are close to those indicated in the literature as values to which the interaction between the piles working under horizontal forces are negligible.

In the next image, can be appreciated the differences between the variation of the relative distance of the pile's shafts in the cases of granular and cohesive soils, when the friction angle of the soil is increased.
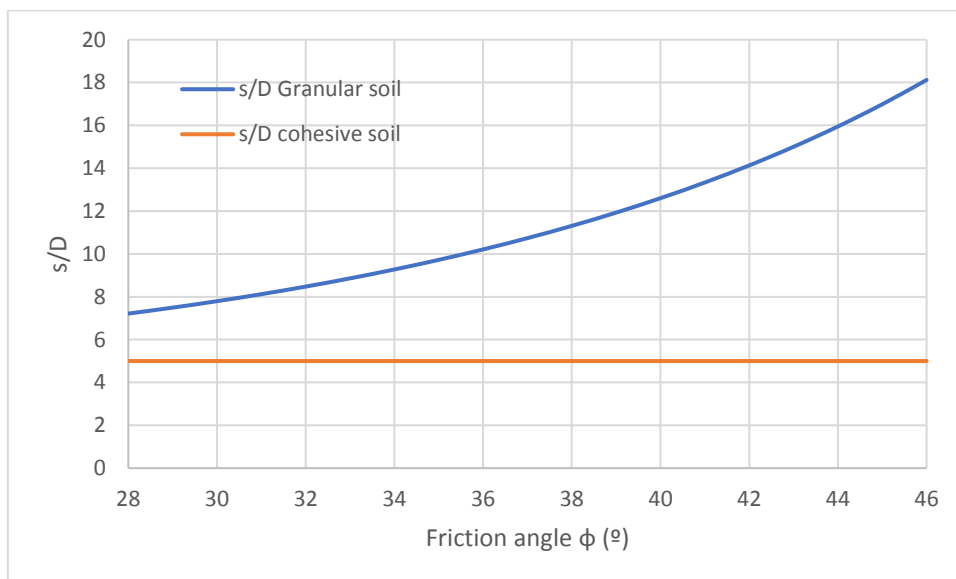
Figure 2-20 Confrontation between the variation of s/D when the friction angle is increased in the cases of cohesive and granular soils respectively.

2.6 Response of the pile group under horizontal loads.

In the last point it has been described the typical behavior that characterizes the response of a single pile working under horizontal loads. However, in reality the piles of a foundation placed under a structure are not isolated. These are put within a group of piles which are connected between them by a structure called plate. It has been checked that the response of an isolated pile under horizontal loads differs from the answer of a pile belonging to a group. In this paragraph are discussed some factors which influence the response of the pile's group working under horizontal loads.

The main aspects which influence the response of a group of piles and on the response of every pile within the group are listed below.

- mutual interaction pile – ground – pile.
- Interaction between the "plate" and the soil.
- Features of the plate stiffness.

With regards to the stiffness features of a foundation made up of piles connected by a connecting structure, it must be pointed out that the plate can be considered as an element infinitely stiff or infinitely flexible depending on its mechanical and geometrical properties. On one hand, when the plate is very stiff, the displacements of the pile's heads are the same for all of them as a consequence of the high stiffness which characterizes the joints between the piles with the plate. In this case, the loads acting on the pile's heads are different from one pile to another. On the other hand, when the plate can be considered flexible, the forces acting on the pile's heads will be same in all of them and equal to $H_i = H/m$. H is the total horizontal load acting on the foundation and m is the number of piles consisting on the foundation. In this second case, the displacements on the piles heads are different in all of them.

Otherwise, as it is detailed in the thesis of G.LANDI (2005), in the case of a group of piles loaded under axial forces, the bending stiffness of the plate and the axial stiffness of the piles can be bring into confrontation. In these circumstances, the effective value of the relative stiffness of the system plate – pile, is a factor with a high importance on the behavior of the group. However, in the case of a pile's group working under horizontal loads, the stiffness of the plate results substantially higher than the bending and shear stiffness of the piles, which opposed themselves to displacements that are perpendicular to their shafts. It can be adopted that under horizontal loads, the plate is an infinitely stiff structure, and for this reason, the displacements on the pile's head can be taken the same in all of them. The load tests run for some different group of piles have confirmed, without any exception, the validity of the ideas showed above.

To determine the interaction between the system pile – ground – pile, have been driven some static load tests on groups of piles with different configurations. It must be evidenced the difficulty to develop the tests with piles in real dimensions, due to its size and the costs which this kind of tests involve. For this reason, in the most of the cases the analysis are run on groups of piles whose dimensions are smaller than those of the real piles. The biggest pile group on which it has been run an analysis consists of 21 piles (3 x 7, MCVAY ET AL., 1998). In addition to this, RUESTA & TOWNSEND (1997) have carried out tests on group of piles consisting on 16 (4 x 4).

2.6.1   Experimental evidence.

When a group of piles is loaded under horizontal forces, the interaction between the piles and the soil, results in a decreasing of the system's stiffness. For the same horizontal load applied on the head of an isolated single pile and applied on the head of the piles pertaining to a group, it has been observed that the displacements of the pile's head in the case of the isolated single pile, are lower than those which are reached on the heads of the piles pertaining to a group. Otherwise, for the same displacement on the pile head in the case of the isolated single pile and in the case of the pile's group, the load which the isolated pile supports is higher than those loads that act on the pile's head of the group. Quantitatively, the interaction between the piles and the ground is defined by a concept known as efficiency η of the pile's group. This parameter links the medium acting load on a pile pertaining to the group H_g/m, where H_g is the horizontal force acting on the whole group, and the load which would experience the single isolated pile H_s when the displacements on the pile's head are the same.

$$\eta = \frac{H_g}{m \cdot H_s} \qquad (2.18.)$$

This interaction between the piles consisting of a group tends to be more important when the distance between the pile's shafts is reduced.

Because of the effect of reciprocal interactions that occur in a group, whose piles are connected by a structure infinitely stiff and not in contact with the ground, each pile behaves in a different way from the other. What can be realized is that on each pile of the group appears a different shear stress and different values of the bending moment. Furthermore, the maximum bending moment in each pile of the group is located at a different depth. This is the typical behavior observed in the case in which the pile's head are not restrained. The response of each pile of the group depends on the position that this occupies within the group. According to G.LANDI (2005), the answer of the single pile inside the group is conditioned by:

- The row of the group to which the pile in analysis pertains (*SHADOWING EFFECT*).
- The position of the pile within that row. (*EDGE EFFECT*).

The shadowing effect has a higher importance on the system's response. Overall, it can be observed that there is a considerable difference between the response of piles pertaining to the first row of the group, which seems to be stiffer, and the piles which are placed on the other rows of the group. The first row of the group is that one which receives the horizontal load in the first position, its piles push on an undisturbed soil.

The second phenomenon takes into account the differences which exist in the answer between the piles placed on the edges of a row and the piles which are inner to that row.

2.6.2   Efficiency.

As it has been developed in the previous paragraph, the answer of the piles into a group is influenced by the interaction which exists between them. It can be identified two modes of interaction between the piles. On the one hand, the *shadowing effects* refers to the different answer which experience the piles pertaining to different rows within the group. On the other

hand, the *edge effect* describe the different response which can be observed between the piles placed on a same row of the group; the behavior in the case of piles located on the edges is not the same as that which can be noticed in the piles which are located in the inner of the row. Due to these effects, the piles pertaining to a group are more yieldable than the isolated single pile. This results in a decreasing of the system's stiffness which is quantified by the efficiency η of the group. This parameter is highly related to the distance between the pile's shafts. In the most of the cases, the efficiency is lower than 1. However, when the distance between the pile's rows increases, η tends to increase its value until the unit is achieved.

Another aspect that should be mentioned is that the efficiency of the group also varies when the load level or the displacements of the pile's head are increased. For small values of the displacement the efficiency can be considered equal to the unit. Nevertheless, when the loads are enhanced, the phenomenon of interaction follows the same trend and the parameter η decreases until an asymptotic value is achieved. This behavior observed in the case of a group of piles working under horizontal loads is totally opposed to that appreciated when the same pile's group works under axial forces. In this second case, when the load is increased the interaction phenomena between the piles tend to be reduced.

In the next image, taken from the Ph.D. Thesis of G.LANDI (2005), is represented, for different configurations of the pile's group and several kind of soils, the variation of the group's efficiency when the displacements on the pile's heads (divided by the diameter of the pile) are increased. The trend observed is similar in all cases. It can be realised that the phenomenon of interaction between the piles grows up when the relative displacements on the piles head increase. There is an exception, which corresponds to the results obtained by RUESTA & TOWNSEND (1997, group 4 x 4). This is because of the high values of the load registered in the piles of the second row. Otherwise, the distance between the pile's shafts is equal to three times the diameter of the piles in all cases except in the tests run by ROLLINS ET AL. (2005a) and ROLLINS ET AL. (2005b), where the distance between the rows of piles were 3,3D and 3,92D respectively.
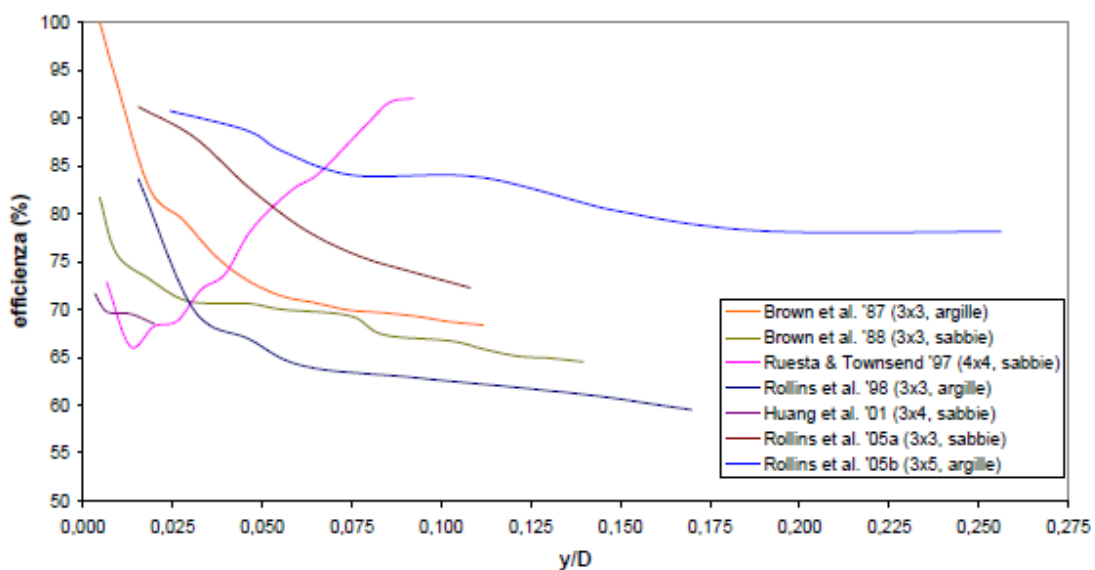

Figure 2-21 Variation of the efficiency of the group when the relative distance between the rows of the piles varies.

The factors of which the pile's group efficiency depends on are the next:

- The characteristics of the soil.
- The relative stiffness of pile – soil system.
- The relative distance between the piles shafts.
- The number of piles of the group and its geometrical properties.
- The size of the displacements on the piles head.

One of the effects which influences the efficiency of a piles group is the number of piles that compose the group. The study of this factor has been made possible thank to the tests run on groups of piles with reduced dimensions. It has been observed that when the number of pile's rows is increased over a determined number, the efficiency of the piles placed on the last rows tends to reach the unit. For this reason, in the thesis of G.LANDI (2005), it has been concluded that for a certain number of pile's rows, the influence of this factor on the efficiency becomes negligible. Another aspect which is mentioned is that, as the number of piles consisting of the group on which the tests have been run is low (equal to 21), it could not be a good decision to extend this conclusion to a group of piles whose number is higher because there is not experimental evidence.

As it has been mentioned above, the efficiency is not a constant parameter and depends on the size of the displacements on the pile's head. When these are enhanced to high levels, the efficiency tends to achieve an asymptotic value. It has been discussed by some authors the size of the displacements to which the efficiency achieves the asymptotic value. McVAY ET AL. (1998) proposed that the asymptotic value of the efficiency is achieved for displacements of *0,06D*, where *D* is the diameter of the piles. KOTTHAUS & JESSBERGER (1994) establish that the needed displacements on the pile's head to obtain the asymptotic value of the efficiency was *0,1D*. Otherwise, SCOTT (1995) proposed the introduction of a reference displacement on the bases of which evaluate the efficiency. This value given by SCOTT (1995) was *0,02D*.

On the other hand, some other authors such as REESE & VAN IMPE (2001) have tried to determine the response of the piles group working under horizontal loads on the basis of the response of the single isolated pile, by means of the identification of an efficiency value that does not depends on the size of the displacements. REESE & VAN IMPE (2001) have taken advantage of the tests run on groups of piles with real sizes and on groups of piles with reduced dimensions developed by the other authors. The efficiency value was referred to the displacement proposed by SCOTT (1995) equal to 0,02D, with the aim of confronting the different tests developed by the authors. Below, are showed the expressions obtained to calculate the efficiency between two piles which are aligned with the perpendicular and the same direction of the horizontal force acting on the group.

As it has been stablished on the Ph.D. Thesis of G.LANDI (2005), in the case of two piles aligned with the direction of the horizontal force, OCHOA & O'NEILL (1989) determined the formulas to calculate the different efficiencies between the pile facing the load in the first position and the pile located on its back.

The efficiency for the pile which faces the force in the first position is obtained as:

$$e = 0,70 \cdot \left(\frac{s}{D}\right)^{0,26} \quad for \quad \left(\frac{s}{D}\right) \leq 4,00 \qquad (2.19.)$$

For the pile located on its back, the efficiency comes:

$$e = 0,48 \cdot \left(\frac{S}{D}\right)^{0,38} \quad for \quad \left(\frac{S}{D}\right) \le 7,00 \qquad (2.20.)$$

If the piles are arranged orthogonally to the application of the force's direction, the interaction effects between the piles are symmetric, and the efficiency is calculated as:

$$e = 0,64 \cdot \left(\frac{S}{D}\right)^{0,34} \quad for \quad \left(\frac{S}{D}\right) \le 3,75 \qquad (2.21.)$$

For values of the relative distance between the piles higher than those showed in the expressions above, the efficiency can be taken equal to the unit ($e = 1$).

In this Master's Thesis, it will not be discussed cases in which the horizontal forces will attack the pile's group in a different direction from both mentioned above. However, it is presented the expression to calculate efficiency of the piles when the loads acting on the group have not the same or a perpendicular direction with regards to that from the force.

$$e = \sqrt{e_i^2 \cdot (\cos \beta)^2 + e_s^2 \cdot (\sin \beta)^2} \qquad (2.22.)$$

Where e_i is the efficiency of the piles placed on the same line, e_s is the efficiency of the piles arranged side by side and β is the angle between the force's direction and the direction of the line which joins two piles which are located in the same position but in different rows.

Finally, in a group of n piles, the efficiency of one of the piles of the group e_j, is calculated multiplying between them, the interactions that the other piles of the group make on the pile whose efficiency wants to be determined. The formula is given as:

$$e_j = \prod_{\substack{i=1 \\ i \ne j}}^{n} e_{ij} = e_{1j} \cdot e_{2j} \cdot \cdots \cdot e_{nj} \qquad (2.23.)$$

The obtained value of e_j attending to this procedure, is used as multiplier of the $p - y$ curve identified to describe the response of the single pile under horizontal actions:

$$p_{j\ group} = e_j \cdot p_{single} \qquad (2.24.)$$

With regards to the expression showed above, the answer of the single pile pertaining to a group can be determined.

2.6.3 The Shadowing effect.

According to the Ph.D. Thesis of G.LANDI (2005), the total load acting on a group of piles with distance between their shafts *s* sufficiently reduced ($s/D < 6$), subjected to horizontal static stresses, is distributed unevenly between the piles. The rate of the load absorbed by each pile is conditioned, mainly by the row to which the pile pertains within the group. One of the conclusions which can be obtained from the available tests, is that the row that absorbs the higher rate of load is the front one, which is also the row that faces a soil whose resistance is not disturbed by the presence of another rows of piles. The successive rows, instead, absorb lower rates of load. This phenomenon of uneven distribution of the loads depending on the row to which pertains a pile within the group is known as *Shadowing effect* (BROWN ET AL., 1988).

The behavior of the piles which pertains to the front row is similar to the response that experiences the single isolated pile. Apparently, there are not big differences between the curves load – displacement on the pile's head in the case of the piles pertaining to the front row o a group and the isolated single pile. These curves are practically the same.

Nevertheless, when piles head load –displacements curves are analyzed in the consecutive rows, it can be realized that these are more yieldable. The soil which face these subsequent rows of piles is disturbed by the action induced by the piles pertaining to the precedent rows, so that the resistance of the ground placed between the rows is lower than the resistance of the undisturbed soil which faces the front row. This effect, which is more significant in a depth next to the ground surface, results in a decreasing of the stiffness of the soil placed between the rows of piles.

What can be noticed from the analysis, is that the displacements of the piles head in the front row are higher than those obtained in the second row. This reduction of the displacements in the pile's heads is also observed between the second and the third row and in the case between the third and the fourth row. However, from the fourth row in advance, it can not be noticed a high difference between the displacements in the pile's head (images 2.22. and 2.23.). This means that, after the fourth row of piles, the loss in the soil's resistance is not significant. This behavior of the ground has been checked in the tests conducted on the piles with real sizes (ROLLINS ET AL., 2005b; image 2.26.) and on those with reduced dimensions (McVAY ET AL., 1998; image 2.25.).
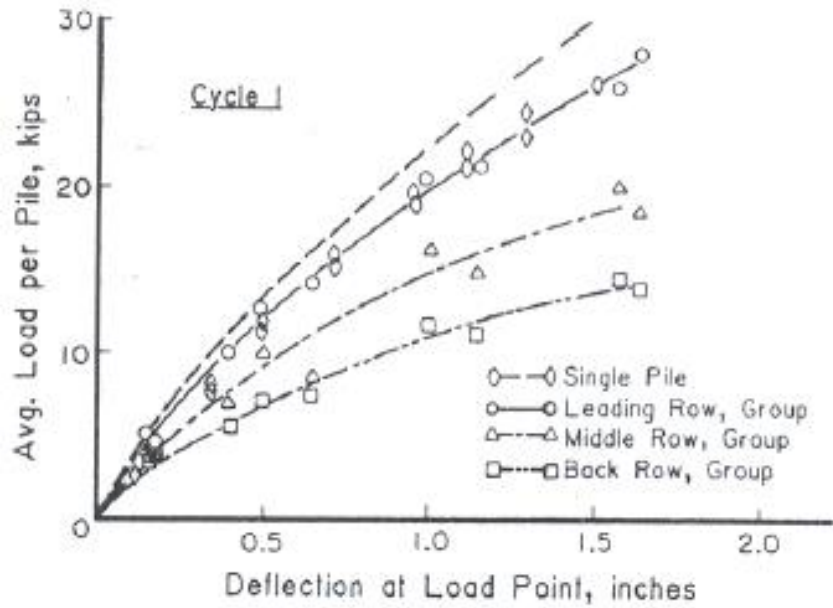
Figure 2-22 Curve medium load for pile – displacement for the single isolated pile and the rows in the case of a group of piles 3 x 3 (BROWN ET AL., 1988).
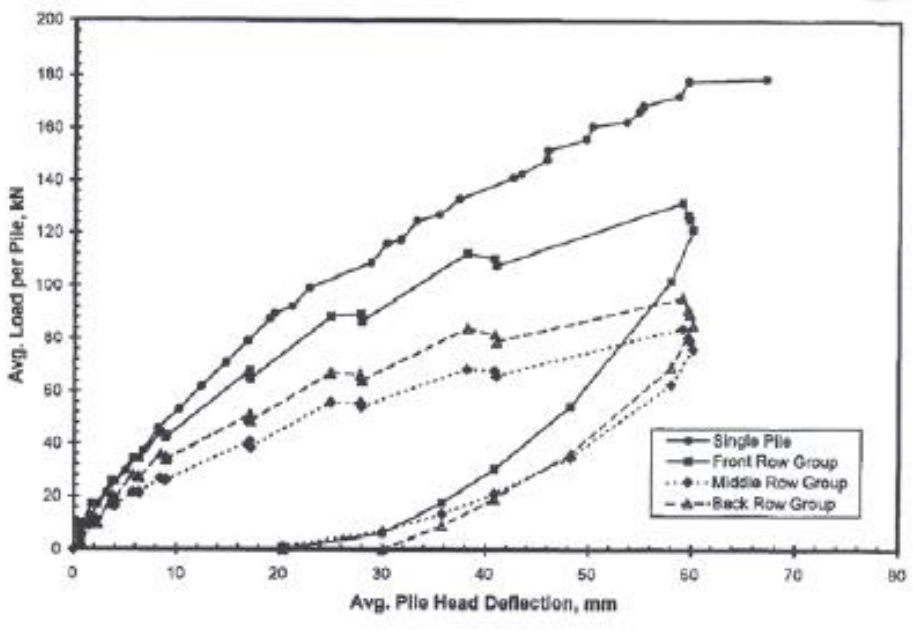
Figure 2-23 Curve medium load for pile – displacement for the single isolated pile and the rows in the case of a group of piles 3 x 3 (ROLLINS ET AL., 1998).
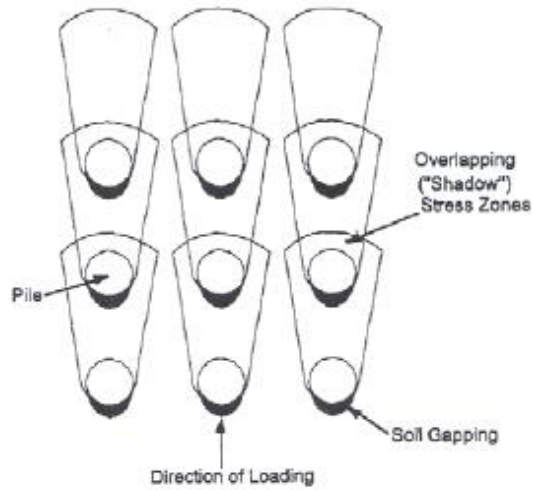
Figure 2-24 Schematic representation of the overlapping areas of the soil's resistance in a group working under horizontal actions (G.LANDI, 2005).
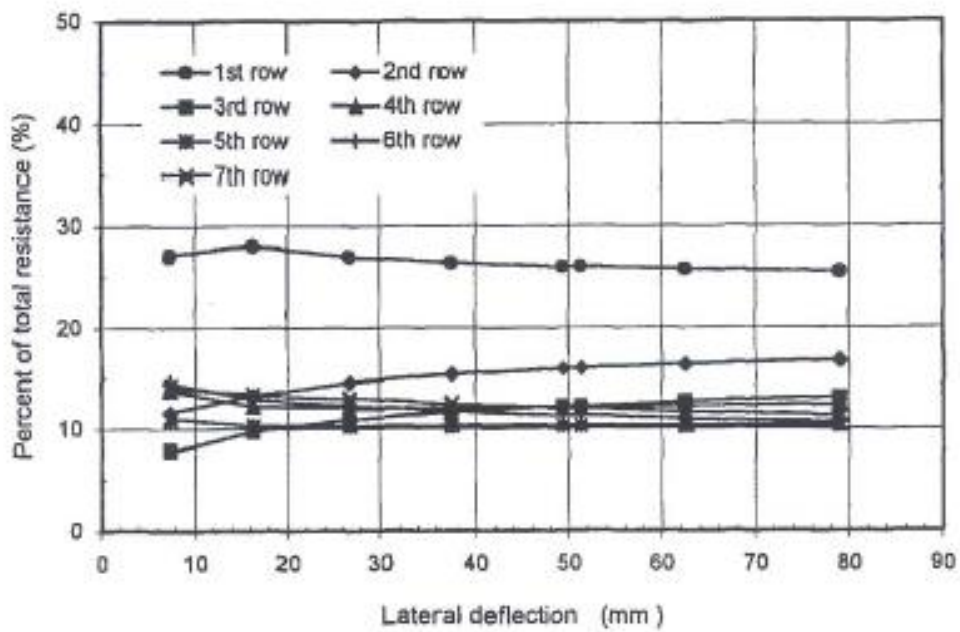
Figure 2-25 Variation of the load rate absorbed by the rows of a pile's group 3 x 7 in homogenously densified sands (McVAY ET AL., 1998).
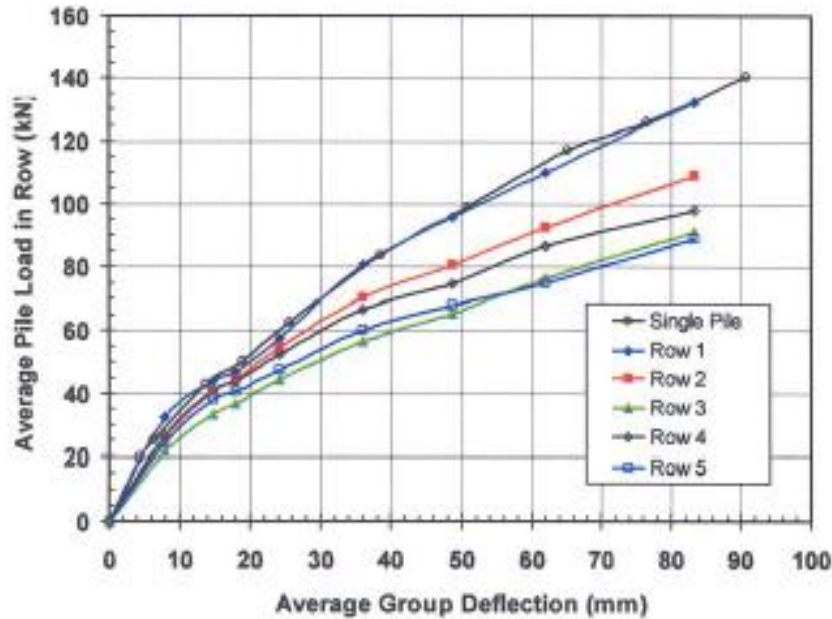
Figure 2-26 Curve medium load per pile – displacement for a single isolated pile and for the rows of a group 3 x 5 (ROLLINS ET AL., 2005b).

2.6.4   The edge effect.

The total load acting on a row of piles is distributed in an uneven way between the piles which pertain to the row. The reasons because of this particular load distribution are explained by the *edge effect*. This phenomenon is produced as a consequence of the overlapping of some shear resistance areas of the ground. The resistance which the soil offers to the thrust of the piles is explained by means of the onset of resistance wedges acting against the piles. When the external forces are increased, the volume of the wedges also grows up and, if the distance between the pile's shafts is low, then the wedges formed in front of adjacent piles of the row can overlap between them. This phenomenon is presented in the image 2.27. showed below.

This effect is more significant in the piles located in the inner of the row than those which are located on the edges. For this reason, it can be assumed that the inner piles absorb a lower load rate than those placed on the edges of the row, which are stiffer. The edge effect is considered less important than the shadowing effect in terms of the interaction phenomenon between the piles. In fact, some authors as BROMS ET AL., (1988); ROLLINS ET AL., (2005b), based on the experimentation have concluded that the loads acting on the pile's heads placed on the same row are approximately the same. This hypothesis justifies the method of the multiplying coefficients of the curves $p - y$ to model the behavior of the group. These coefficients are distinguished depending on the row to which the piles pertain and not to the position that the pile occupies within the same row.

As it is showed in the studies of some authors such as BAGUELIN ET AL., (1985), RUESTA & TOWNSEND (1997), ILYAS ET AL., (2004), ROLLINS ET AL., (2005a), the different distribution of the load between the piles pertaining to a same row it cannot be always negligible.

In the image 2.28., it has been represented the absorbed load by the center and the outer pile of a same row when the relative displacements are increased. The graph below shows the results obtained by the tests developed on real size group of piles by BAGUELING ET AL.,

38

(1895), group 3 x 2 and ROLLINS ET AL., (2005a), group 3 x 3. What can be appreciated in that graph, taken from the Ph.D. Thesis of G.LANDI (2005) are the ratios between the load absorbed by a pile placed on the first row and a pile occupying the same position but located on the second and on the third row of the group respectively.
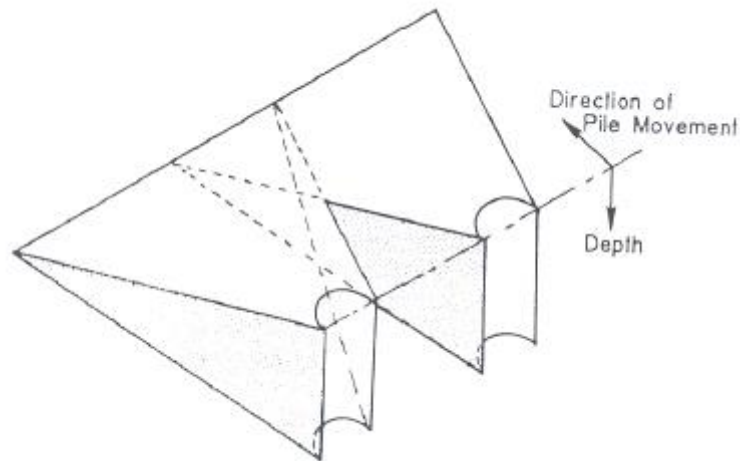
Figure 2-27 Overlapping of the shear resistance wedges of the ground for two piles pertaining to the same row. (BROWN ET AL., 1988).
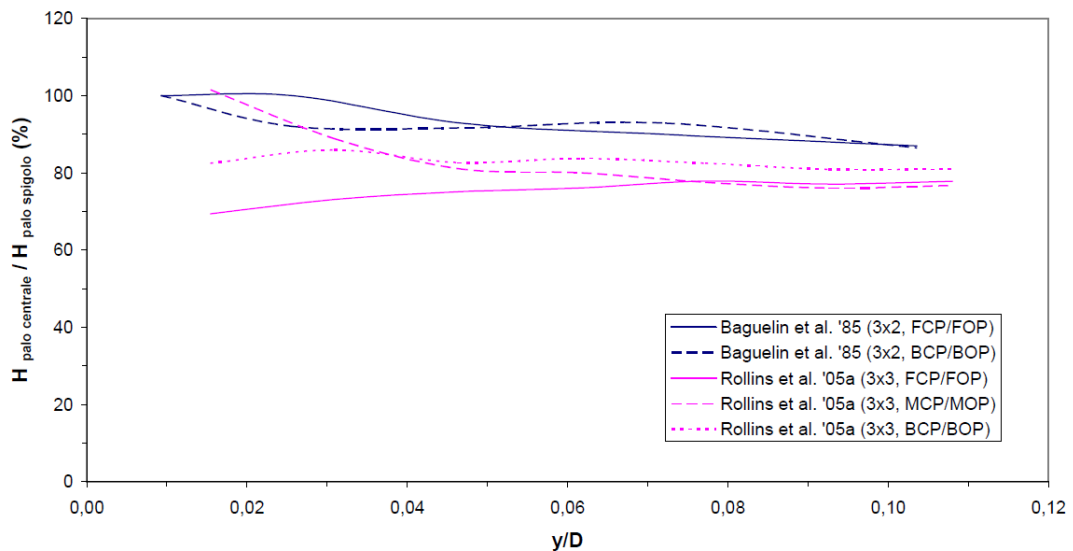
Figure 2-28 Percentage ratio between the load absorbed by the center and the outer piles of a same row in a group when the relative displacement is varied (G.LANDI, 2005).

From the graph showed above, it can be realized two important aspects. On the one hand, the edge effect also influences on the uneven distribution of the load between the piles pertaining

to a same row. On the other hand, this distribution of loads maintains itself constant when the displacements *y* are modified. Two conclusions can be learnt from this analysis. The first one is that the edge effect will not be able to be considered as negligible in all cases. Otherwise, the interaction between the piles caused by the shadowing effect is more significant than that caused by the edge effect.

2.6.5   The bending moment.

As a consequence of the different distribution of the forces in the pile's heads of the group, and the different capacity of the soil to offer resistance to the horizontal displacements of the piles, depending on the row to which these pertain, the bending moments acting on the piles of the group are also different.

As the piles pertaining to the rows placed after the front row work under lower forces, the bending moments under which the piles of the successive rows work, are also lower than those experienced by the piles pertaining to the first row (image 2.29.).
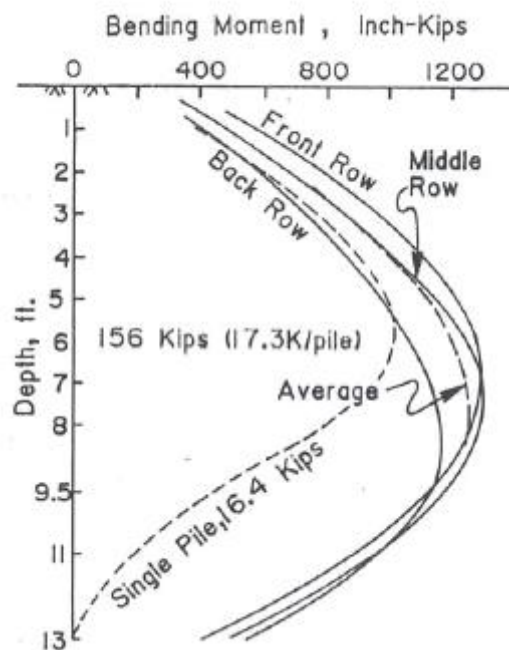
Figure 2-29 Medium bending moment profiles for the piles of a group 3 x 3 (BROMS ET AL., 1987).

With regards to the piles pertaining to the front row, it can be assumed that these work under a load similar to that under which the single pile works. The ground that the piles of the front row of a group faces is undisturbed by the action of piles located before this row. Consequently, the bending moment profile of a pile placed on the front row is very similar to that of the single pile. In fact, the maximum moment and the depth at which this is located are the same for both cases. This behavior can be observed in the next image (BROMS ET AL., 1988) taken from the Ph.D. Thesis of G.LANDI (2005).
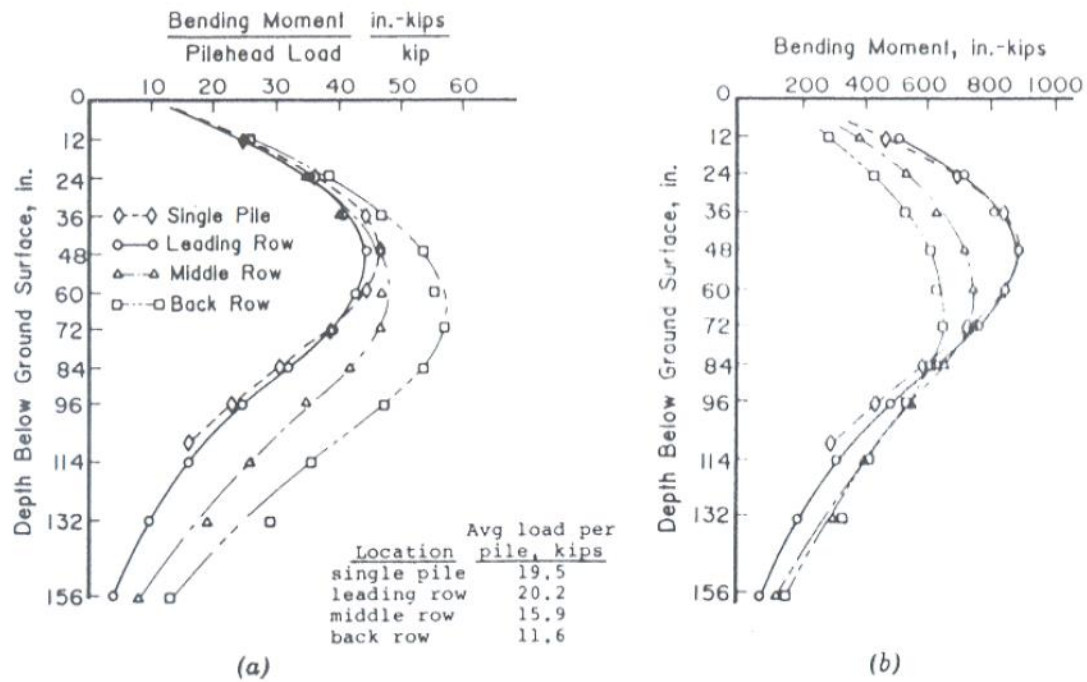
Figure 2-30 Bending moment profile for a single pile and for the piles of a group 3 x 3, standardized with regards to the shear acting on the pile's head (a) and in absolute value (b) (BROWN ET AL., 1988).

As it has been discussed on the thesis of G.LANDI (2005), if the value of the bending moment acting on a pile is standardized with regards to the stress acting on its head, it can be noticed that the greatest normalized moments arise in the piles of the rear rows (BROWN ET AL., 1988; ROLLINS et al, 2005a) (image 2.31.a). This is a consequence of the fact that these piles interact with a soil which is affected by the shadowing effect caused by the presence of the other piles of the group. Because of this effect, the soil has a lower resistance than the undisturbed ground to make front to the horizontal forces induced by the piles. Due to the fact that the most affected areas of soil by this interaction are those located next to the surface, the maximum bending moments, for the rows placed behind the front one, are reached gradually at higher depths (BROWN ET AL., 1987).
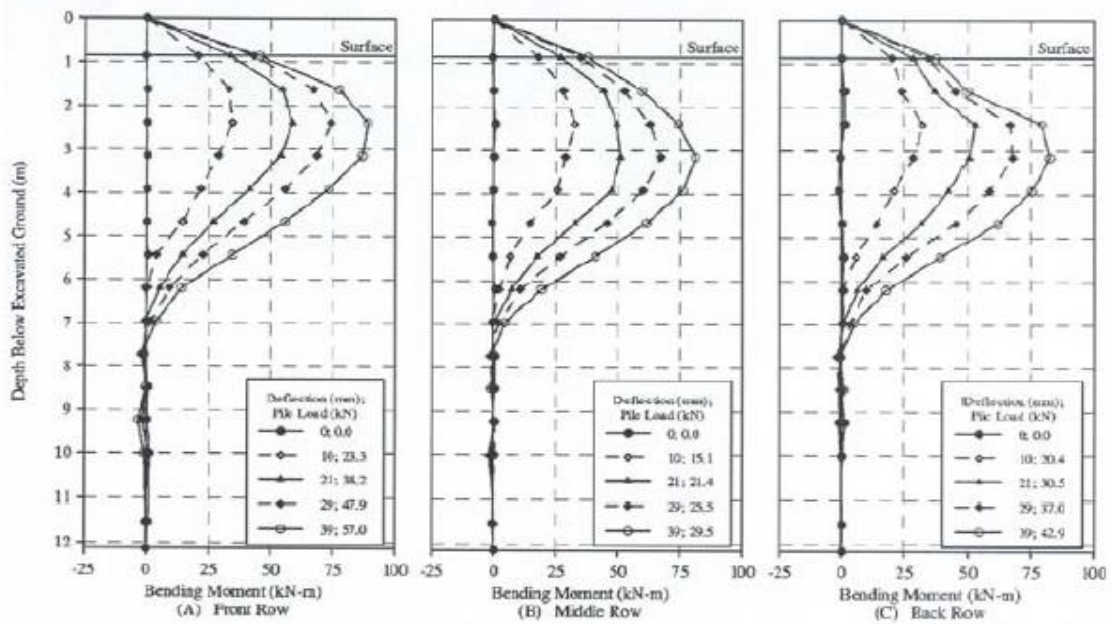
Figure 2-31 Bending moment profile for the piles locates on a group 3 x 3 for different load leves (ROLLINS ET AL., 2005).

In the next image, taken from the thesis of G.LANDI (2005), are represented the ratios between the maximum bending moments which act on the different rows of a group 3 x 3 and the maximum bending moment acting on the single pile when the displacements on the pile's heads in both cases are the same (BROWN ET AL., 1988; ROLLINS ET AL., 2005a). The reason because of the results have been obtained for the same displacements on the pile's head is that, the piles pertaining to a group, due to the interaction effects, achieve the same displacements that the single pile at a lower load. In the next graph can be appreciated that the piles of the group are less loaded than the single one.
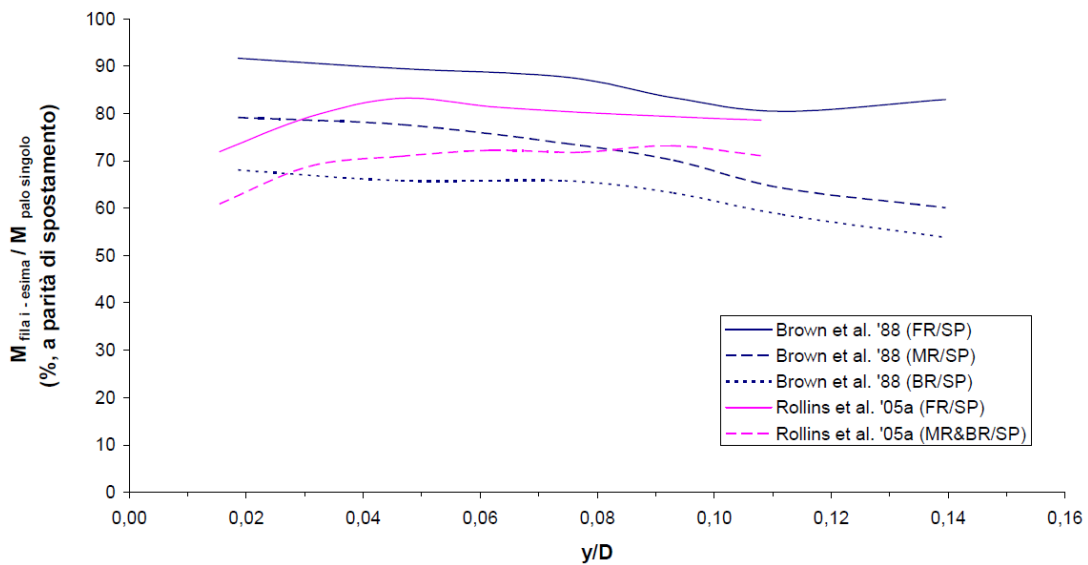
Figure 2-32 Percentage ratio between the maximum bending moment acting on the single pile and the piles of the group, when the displacements on the pile's head are the same (G.LANDI, 2005).

2.6.6 Effect of the construction technology of the piles in the system's response.

In the case of the single pile working under horizontal forces, it has been discussed the influence of the construction technology on the response of the *pile – soil* system. What has been concluded is that this factor does not affect as much as the other to the ground's properties.

Nevertheless, when the effect of the construction technology is studied in the case of groups of piles, this factor cannot be considered as negligible. When the relative distance between the shafts of the piles is small, the mechanic properties of the soil, placed on the surrounding areas of the piles, can be modified. Particularly, if the technology used induces displacements in the ground (*bored piles*), the mechanic features of the soil can be improved with regards to the condition of an undisturbed ground. The piles which would experience a higher improvement of the ground's properties would be those placed on the inner of the group. However, the piles located on the front row would follow facing a ground with undisturbed mechanical properties.

As it has been mentioned in the thesis of G.LANDI (2005), to quantify the changes in the mechanical properties of the ground induced by the construction technology, some authors run tests on side, to measure the variation of the characteristics of the soil before and after the construction of the piles (OCHOA & O'NEILL, 1989, with regards to the test run by BROWN ET AL., 1988; RUESTA & TOWNSEND, 1997; ROLLINS ET AL., 2005a). What was concluded by these authors was that the resistance of the ground could be improved between a 1,5 – 3,5 times from the resistance in the case of an undisturbed soil, when the piles were bored.

3 Single pile under horizontal load resistance calculation.

3.1 Broms Method.

In a granular soil, the failure mechanism of a pile can be produced in different ways. As it is established in the book *FONDAZIONI* di *CARLO VIGGIANI*, BROMS proposed two possible failure mechanisms of the piles depending on the constraint conditions on its head:

- *Piles not impeded of rotating on its head (Free-headed piles).*
- *Piles impeded of rotating on its head (restrained pile).*

FREE-HEADED PILES.

When the piles are not restrained on its head, BROMS proposed that the piles can behave in two different ways: *Short pile* or *Long pile*.

For the *short pile*, it has been found that the rotation comes around a point next to the bottom's edge of the pile. To simplify the analysis, BROMS suggested that it could be assumed the bottom surface of the pile as its rotation center without incurring in a big error. Moreover, It has also been proposed by BROMS to consider the resultant of the ground's stresses acting on this point by means of a concentrated force *F*.
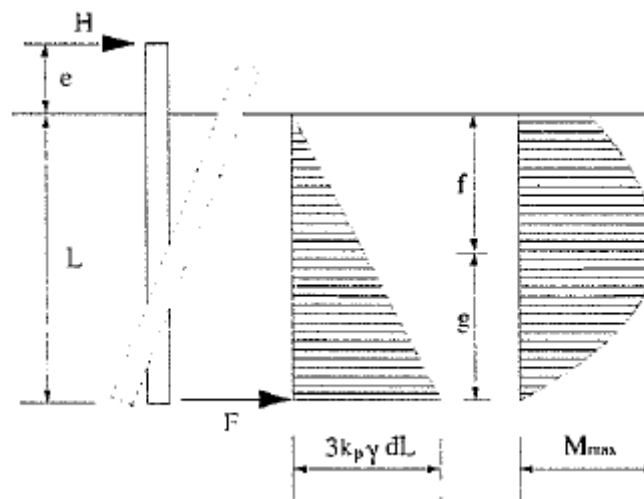
Figure 3-1 Short pile behavior in granular soils proposed by BROMS (FONDAZIONI, CARLO VIGGIANI).

If it is imposed a bending moment balance around the rotation center when it takes place the breaking condition, it can be calculated the maximum value of the horizontal force that the pile can resist before experiencing a change on its behavior from short to long pile.

$$H_{lim1} = k_p \cdot \gamma \cdot \frac{d \cdot L^3}{2 \cdot (e + L)} \qquad (3.1.)$$

As it can be noticed from the last expression, H_{lim} depends on the shear resistance of the soil (characterized by the specific weight *(Y)* and the passive coefficient of earth pressure *(K$_p$)* of the ground) and the geometrical features of the pile:

- **d** is the diameter of the pile.
- **L** is the length of the pile.
- **e** is the distance between the application point of the *H$_{lim}$* force and the ground's surface. Although in this thesis will be considered equal to 0.

The passive coefficient of earth pressure **K$_p$** is related to the friction angle of the soil by means of the next expression:

$$K_p = \frac{1 + \sin \phi}{1 - \sin \phi} \qquad (3.2.)$$

Where **ϕ** is the friction angle of the soil.

The pile will behave as *short pile* as long as the maximum bending moment acting on it, is lower than the yielding bending moment of the steel reinforcement of the piles $M_{max} \leq M_y$.

In the next picture, taken from the book *FONDAZIONI* (CARLO VIGGIANI), have been represented curves which show the variation of the horizontal force, depending on the ratios *e/d* and *L/d* respectively, under which the pile behaves as short pile. It has been represented both cases, the one in which the pile is restrained on its head and that corresponding to the free-headed pile.
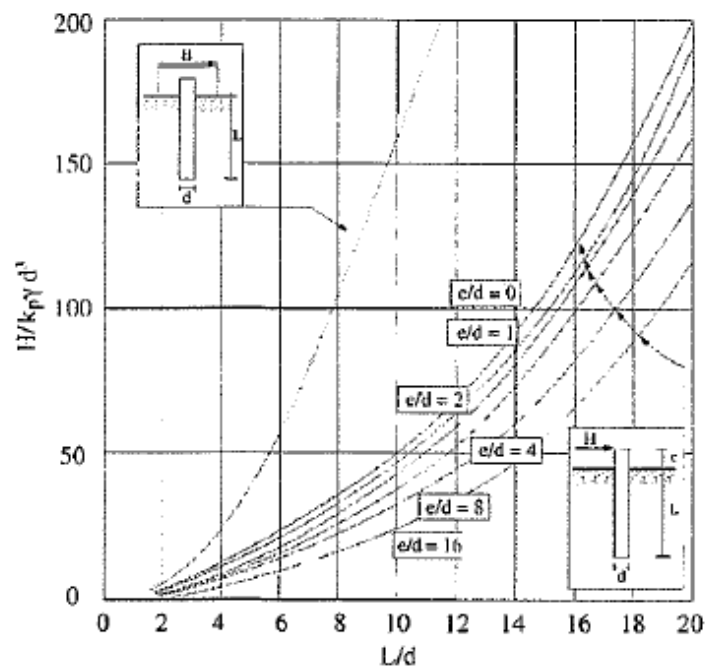
Figure 3-2 Limit value of the force H under which the pile behaves as short pile when the resistance of a granular soil is characterized by the model proposed by Broms. It has been represented both cases, Free-headed pile and Restrained pile.

Considering an axis referenced as **z** coinciding with the direction of the pile as it is showed in the image 3.3., it can be determined the expressions of the shear force (equation 3.3.) and the bending moment (equation 3.4.) along the pile in function of the depth z.
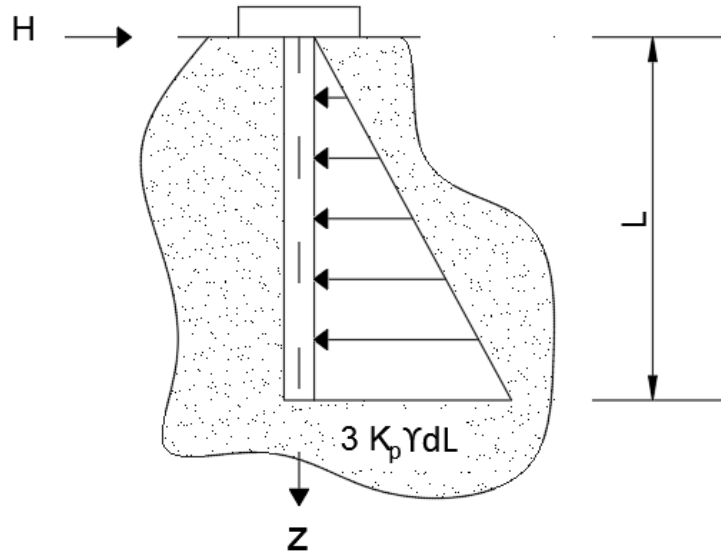
Figure 3-3 Scheme containing the forces acting on a pile when the resistance of the soil is obtained with regards to the model suggested by BROWN.

$$T = H - \frac{3}{2} \cdot K_p \cdot \gamma \cdot d \cdot z^2 \qquad (3.3.)$$

$$M = H \cdot (e + L) - \frac{3}{2} \cdot K_p \cdot \gamma \cdot d \cdot z^2 \cdot \frac{z}{3} \qquad (3.4.)$$

The depth at which the bending moment is maximum coincides with that at which the shear forces are equal to 0. Based on this statement, it has been obtained the depth **f** at which the bending moment is maximum as follows:

$$T = 0 \quad \rightarrow \quad f = 0{,}816 \cdot \sqrt{\frac{H}{k_p \cdot \gamma \cdot d}} \qquad (3.5.)$$

Consequently, the maximum bending moment acting on the pile is calculated by combining the equations 3.4. and 3.5.:

$$M_{max} = H \cdot (e + L) - \frac{3}{2} \cdot K_p \cdot \gamma \cdot d \cdot f^2 \cdot \frac{f}{3} \qquad (3.6.)$$

46

From the expressions 3.3. and 3.5., the second term at the second member is equal to $H \cdot f / 3$. For this reason:

$$M_{max} = H \cdot \left(e + \frac{2}{3} \cdot f\right) \qquad (3.7.)$$

Finally, substituting in the last expression the values of H (equation 3.1.) and f (equation 3.5.), the value of the maximum bending moment can be rewrite as:

$$\frac{M_{max}}{K_p \cdot \gamma \cdot d^4} = \frac{L}{2 \cdot (L + e)} \cdot \left(\frac{L}{d}\right)^3 \cdot \left(\frac{e}{L} + 0{,}544 \cdot \sqrt{\frac{L}{2 \cdot (L + e)}}\right) \qquad (3.8.)$$

With regards to this expression of the maximum bending moment, it is possible to verify the condition $M_{max} \leq M_y$. If the bending moment exceeds the yielding moment **M_y**, which is related to the mechanic properties of the reinforcement steel of the piles, it is progressively formed a plastic hinge on the pile at the same depth at which **M_y** has been exceeded by **M_{max}**. When the plastic hinge is completely formed, the pile does not behaves as a short pile anymore. This is the beginning of the pile's behavior as *long pile*.
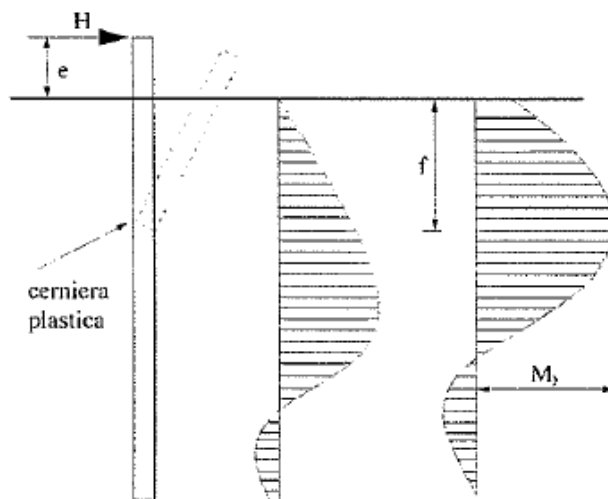
Figure 3-4 Long pile behavior in granular soils proposed by BROMS (FONDAZIONI, CARLO VIGGIANI).

As it has been mentioned above, when the yielding moment is exceeded and the plastic hinge appears, the pile starts behaving as the *long pile*. To determine the limit value of the horizontal force H_{lim} that results in the formation of the plastic hinge on the pile, it must be replaced the maximum bending moment **M_{max}** in the equation (3.9.) by the yielding moment **M_y**.

$$\frac{H}{K_p \cdot \gamma \cdot d^3} \cdot \left(\frac{e}{d} + 0,544 \cdot \sqrt{\frac{H}{K_p \cdot \gamma \cdot d^3}} \right) = \frac{M_y}{K_p \cdot \gamma \cdot d^4} \qquad (3.10.)$$

As it can be appreciated in the equation (3.10.), the value of the horizontal force does not depend on the pile's length, as long as it achieves at least a value to which the condition $M_{max} = M_y$ is verified. To determine this minimum length, it is enough with entering in the abacus showed below (image 3.5.) with the ratio $M_y/K_p\gamma d^4$. With regards to *e/d*, it can be obtained the value of *L/d*. As the diameter of the pile is known, it can be calculated the minimum length of the pile to which is verified the condition $M_{max} = M_y$.

In the case of study of the present Master's Thesis, it is considered a value of *e* equal to zero. For this reason, the expression 3.10. can be rewrite as:

$$e = 0 \quad \rightarrow \quad H_{lim2} = \left(\frac{M_y \cdot \sqrt{K_p \cdot \gamma \cdot d^3}}{0,544 \cdot d} \right)^{\frac{2}{3}} \qquad (3.11.)$$
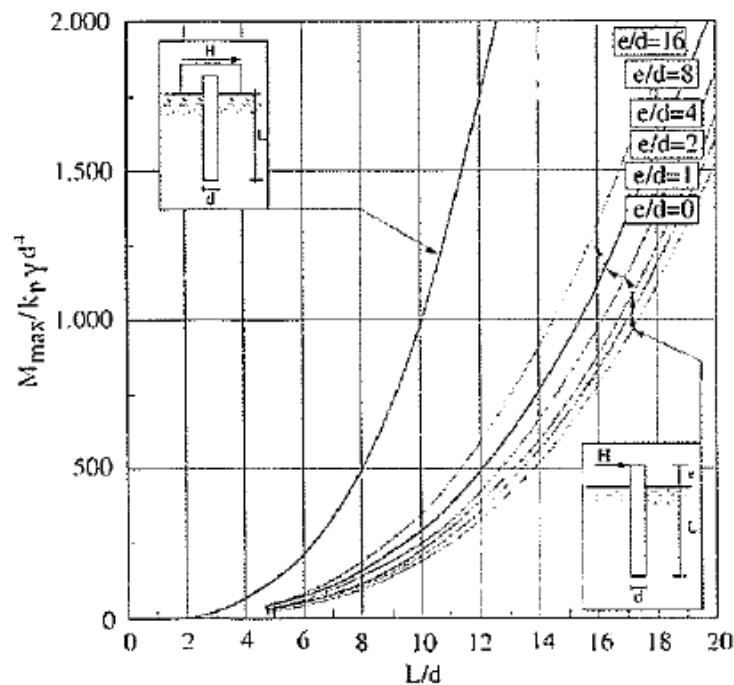
Figure 3-5 Maximum bending moment for the short pile, free or restrained to the rotation on its head, granular soils. (FONDAZIONI, CARLO VIGGIANI).

Otherwise, the value of H_{lim2} could also be obtained by means of the abacus showed in the image 3.6.. As it is known the yielding bending moment of the steel consisting on the reinforcement of the pile and its diameter, with regards to the ratio e/d, it can be determined the value of H_{lim2}.
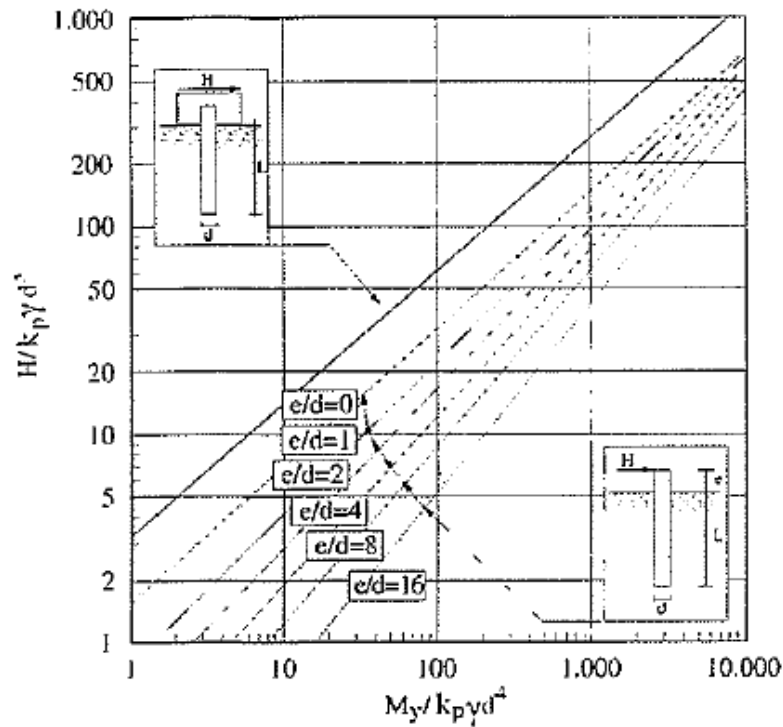
Figure 3-6 Limit value of the horizontal force H for the long pile when its head is not impeded of rotating and when the pile's head restrained.

Finally, the horizontal limit load of a pile in a granular soil is the minimum value between those calculated with regards to the equations given by (3.1.) and (3.11.).

$$H_{lim} = min(H_{lim1}, H_{lim2})$$

49

According to what it is disposed in the book _FONDAZIONI_ of CARLO VIGGIANI, BROMS suggests that a pile within a granular soil restrained to the rotation on its head, can behave in three different ways, as it is showed in the image 3.7..

- Short pile.
- Intermediate pile.
- Long pile.
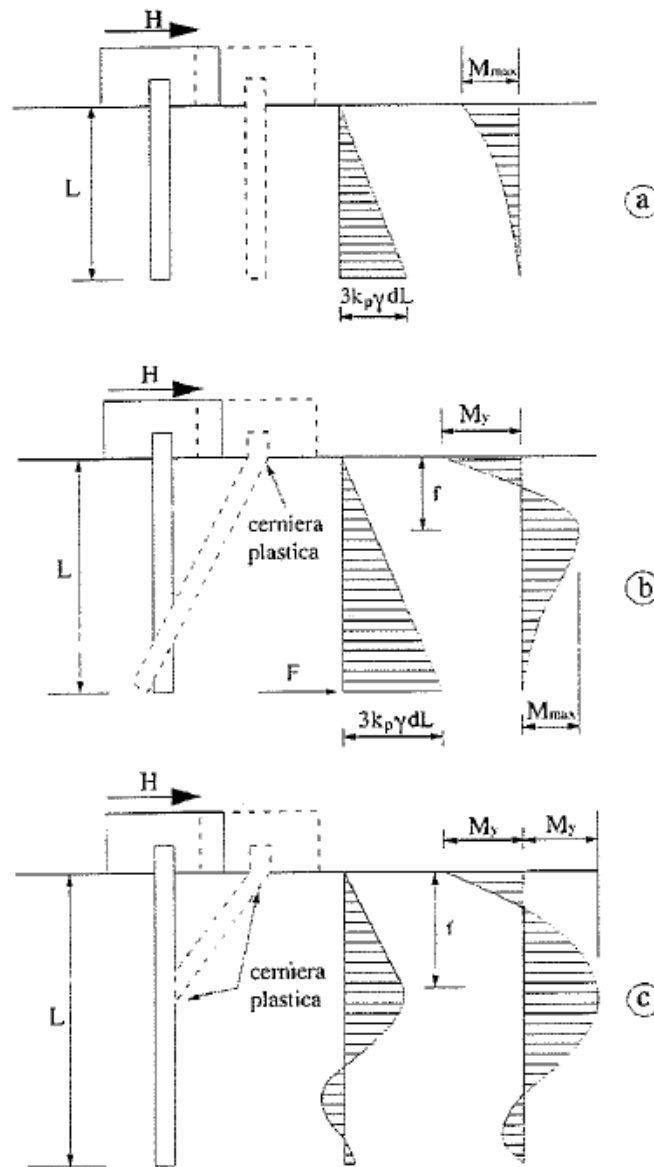
Figure 3-7 Pile restrained to the rotation on its head. A) Short pile; B) Intermediate pile; C) Long pile (FONDAZIONI, CARLO VIGGIANI).

For the short pile, a simple balance of the horizontal forces acting on the pile brings the next expression:

$$H_{lim1} = 1,5 \cdot L^2 \cdot K_p \cdot \gamma \cdot d \qquad (3.12.)$$

Which can be rewritten as:

$$\frac{H}{K_p \cdot \gamma \cdot d^3} = 1,5 \cdot \left(\frac{L}{d}\right)^2 \qquad (3.13.)$$

The equation 3.13. represents the value of the maximum horizontal force under which a pile, restrained to the rotation on its head, behaves as a *short pile*. As it can be observed, this force depends on the resistance features of the soil (γ, K_p) as well as the length (L) and the diameter of the pile (d). The equation 3.13. has been represented in the image 3.2. besides the curves of the horizontal force H related to the free-headed pile. Otherwise, to determine whether the pile's breaking mechanism corresponds to that of the *short pile* or the pile behaves as the *intermediate pile*, it must be verified the condition $M_y \leq M_{max}$. The maximum bending moment acting on the pile, before the appearance of the first plastic hinge, can be obtained as:

$$M_{max} = \frac{2}{3} \cdot H \cdot L \qquad (3.14.)$$

The equation 3.14. can be rewritten as:

$$\frac{M_{max}}{K_p \cdot \gamma \cdot d^4} = \left(\frac{L}{d}\right)^3 \qquad (3.15.)$$

The evolution of the ***M*_{max}** given by the equation 3.15. has been represented in the image 3.5. besides the curves of the maximum bending moment in the case of the free-headed pile.

When the maximum bending moment exceeds the yielding moment ***M*_y**, it is formed, progressively, a plastic hinge in the joint between the pile and the plate. When this first hinge is completely formed, the pile begins to behave as the *intermediate pile*. In addition to this, if it is imposed a balance to the horizontal displacements, it is obtained:

$$F = \frac{3}{2} \cdot L^2 \cdot K_p \cdot \gamma \cdot d - H \qquad (3.16.)$$

Taking into account the previous expression and imposing a balance to the rotation around the plastic hinge, it is obtained an equation which relates the yielding moment with the horizontal force under which the pile will behave as the *intermediate pile*.

$$M_y = \frac{1}{2} \cdot L^3 \cdot K_p \cdot \gamma \cdot d - H \cdot L \qquad (3.17.)$$

Which can be rewritten as:

$$\frac{H}{K_p \cdot \gamma \cdot d^3} = \frac{1}{2} \cdot \left(\frac{L}{d}\right)^2 + \frac{M_y}{K_p \cdot \gamma \cdot d^4} \cdot \frac{d}{L} \qquad (3.18.)$$

The equation 3.18. has been represented in the image 3.8. (C.VIGGIANI), which defines for each value of the yielding moment M_y, the interval of values of the ratio L/d ,which correspond to the three different failure mechanisms of the piles.
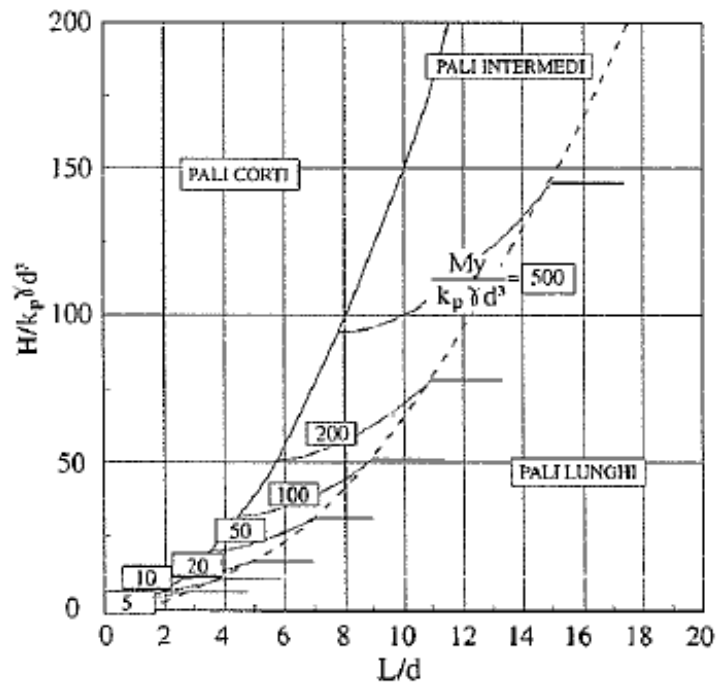
Figure 3-8 Limit value of the horizontal force which determines the intermediate pile's behavior when its head is impeded of rotating in a granular soil (FONDAZIONI, CARLO VIGGIANI).

The equation 3.18. can be rewritten to calculate the maximum value of the horizontal force over which the pile start behaving as the *long pile*. It is showed in the equation 3.19.

$$H_{lim2} = K_p \cdot \gamma \cdot d^3 \cdot \left(\frac{1}{2} \cdot \left(\frac{L}{d}\right)^2 + \frac{M_y}{K_p \cdot \gamma \cdot d^4} \cdot \frac{d}{L}\right) \qquad (3.19.)$$

When the maximum bending moment along the pile, which is achieved at a depth f (equation 3.5.), reaches the value of the yielding moment M_y, it is formed, progressively, a second

plastic hinge. When this hinge has been completely formed, the pile begins to behave as the *long pile*. The expression of the horizontal force which govern the long pile's behavior is obtained by means of establishing a bending moment's balance around the point in which the second hinge is formed. This results in:

$$\frac{2}{3} \cdot H \cdot f = 2 \cdot M_y \qquad (3.20.)$$

If in the previous expression is substituted the value of the depth **f** at which the maximum bending moment is achieved (equation 3.5.), it can be obtained the limit value over which the pile would start behaving as a mechanism, due to the appearance of a third plastic hinge. At this point, the pile would become useless.

$$H_{lim3} = K_p \cdot \gamma \cdot d^3 \cdot \sqrt[3]{\left(3{,}676 \cdot \frac{M_y}{K_p \cdot \gamma \cdot d^4}\right)^2} \qquad (3.21.)$$

As it occurred in the case of the free-headed pile, the horizontal limit force of a pile in a granular soil, is the minimum value between those calculated with regards to the equations given by (3.12.), (3.19.) and (3.21.).

$$H_{lim} = min(H_{lim1}, H_{lim2}, H_{lim3})$$

The real problem could present different conditions from those showed above, as it happens in the case of study which is being discussed on this Master's Thesis. Some of this different situations are listed in the next:

- The joint between the plate and the piles of the group could be placed at a certain height over the surface.
- The pile could intersect a soil composed by several different layers.
- The phreatic level could be located at a certain depth interacting with the piles.

In these previous cases, the theory proposed by Broms can be applied. However, the abacus and the formulas showed above are not applicable on them. The solution adopted in each problem will have to be specified in order to establish the correct failure mechanisms of the piles and satisfy the balance conditions.

In the next image, taken from FONDAZIONI (C.VIGGIANI), are represented the different situations described above.
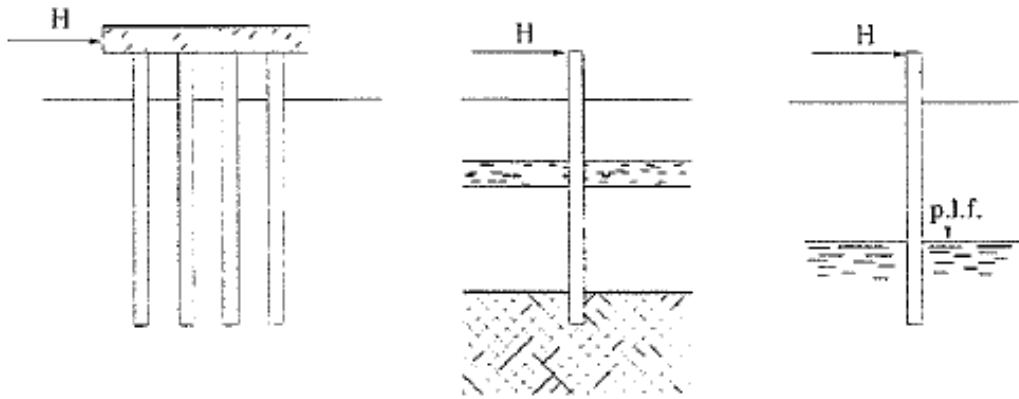
Figure 3-9 Cases which can be resolved by the BROMS's theory (FONDAZIONI, C.VIGGIANI).

3.2 Barton's method.

As it was explained in the point 2.1.3.1. of the present Master's Thesis, BROMS (1946b) suggested to model the forces which a granular soil induces on a pile considering the limit reaction of the soil equal to:

$$P_u = p_u \cdot D = 3 \cdot K_p \cdot \sigma'_v \cdot D \qquad (3.22.)$$

This model is highly used in geotechnical engineering. However, this value of the soil's resistance is underestimated in a 50%. For this reason, it has been discussed some other models to describe the reaction that the soil exercises on the piles pertaining to a deep foundation (REESE ET AL., (1974); PAULOS & DAVIS, (1980). Nevertheless, was BARTON (1982) the author who proposed a more accurate model for the resistance of the ground, due to the fact that his model only underestimates the soil's forces in a 6%. BARTON (1982) suggested that the resistance of the soil could be calculated by means of the next formula:

$$P_u = p_u \cdot D = K_p^2 \cdot \sigma'_v \cdot D \qquad (3.23.)$$

3.3 Comparison between Barton's and Brom's Methods

One of the aims of this Master's Thesis, is to bring into confrontation the models suggested by BROMS (1946b), whose equations are showed in the point 3.1. of this thesis, and the model proposed by BARTON (1982). This comparison has been made by substituting in the equations of BROMS (1946b), the resistance of the soil proposed by the same author for that suggested by BARTON (1982). In order to compare the both models, the first step was to obtain the equivalence between them. This has been done by matching the expressions of the soil's resistance proposed by the two authors:

$$3 \cdot K_p \cdot \sigma'_v \cdot D = K_p^2 \cdot \sigma'_v \cdot D$$

So that, to obtain the expressions according to the resistance model of the soil suggested by BARTON (1982), it must be done the next substitution in the equations developed by BROMS (1946b):

$$3 \cdot K_p \ (BROMS) \ \rightarrow \ K_p^2 \ (BARTON)$$

Finally, in the next table are showed the expressions obtained with regards to both models of the soil's resistance:

BROMS (1946b)	BARTON (1982)
Equation 3.1.	
$\dfrac{H}{K_p \gamma d^3} = \dfrac{d}{2(e+L)} \cdot \left(\dfrac{L}{d}\right)^3$	$\dfrac{3H}{K_p^2 \gamma d^3} = \dfrac{d}{2(e+L)}$
Equation 3.8.	
$\dfrac{M_{max}}{K_p \gamma d^4} = \dfrac{L}{2(L+e)} \cdot \left(\dfrac{L}{d}\right)^3 \cdot \left(\dfrac{e}{L} + 0{,}544 \sqrt{\dfrac{L}{2(L+e)}}\right)$	$\dfrac{3M_{max}}{K_p^2 \gamma d^4} = \dfrac{L}{2(L+e)} \cdot \left(\dfrac{L}{d}\right)^3 \cdot \left(\dfrac{e}{L} + 0{,}544 \sqrt{\dfrac{L}{2(L+e)}}\right)$
Equation 3.10.	
$\dfrac{M_y}{K_p \gamma d^4} = \dfrac{H}{K_p \gamma d^3} \cdot \left(\dfrac{e}{d} + 0{,}544 \sqrt{\dfrac{H}{K_p \gamma d^3}}\right)$	$\dfrac{3M_y}{K_p^2 \gamma d^4} = \dfrac{3H}{K_p^2 \gamma d^3} \cdot \left(\dfrac{e}{d} + 0{,}544 \sqrt{\dfrac{3H}{K_p^2 \gamma d^3}}\right)$
Equation 3.12.	
$\dfrac{H}{K_p \gamma d^3} = 1{,}5 \cdot \left(\dfrac{L}{d}\right)^2$	$\dfrac{3H}{K_p^2 \gamma d^3} = 1{,}5 \cdot \left(\dfrac{L}{d}\right)^2$
Equation 3.15.	
$\dfrac{M_{max}}{K_p \gamma d^4} = \left(\dfrac{L}{d}\right)^3$	$\dfrac{3M_{max}}{K_p^2 \gamma d^4} = \left(\dfrac{L}{d}\right)^3$
Equation 3.18.	
$\dfrac{H}{K_p \gamma d^3} = \dfrac{1}{2} \cdot \left(\dfrac{L}{d}\right)^2 + \dfrac{M_y}{K_p \gamma d^4}$	$\dfrac{3H}{K_p^2 \gamma d^3} = \dfrac{1}{2} \cdot \left(\dfrac{L}{d}\right)^2 + \dfrac{3M_y}{K_p^2 \gamma d^4}$
Equation 3.21.	
$\dfrac{H}{K_p \gamma d^3} = \sqrt[3]{\left(\dfrac{3{,}676 \cdot M_y}{K_p \gamma d^4}\right)^2}$	$\dfrac{3H}{K_p^2 \gamma d^3} = \sqrt[3]{\left(\dfrac{11{,}028 \cdot M_y}{K_p^2 \gamma d^4}\right)^2}$

According to the equations showed on the table located at the end of the previous point, have been calculated the values of the maximum horizontal forces for the single pile in four different cases. Those are listed below:

- *FREE-HEADED PILE (BROMS).*
- *FREE-HEADED PILE (BARTON).*
- *RESTRAINED PILE (BROMS).*
- *RESTRAINED PILE (BARTON).*

The main aim of the calculation of the H_{lim} has been to determine the pile's behavior in all the cases discussed in this Master' Thesis.

In this analysis, it has also been studied the effect of the variation of some parameters related to the mechanical features of the soil ($\phi \rightarrow K_p$), as well as the mechanical and geometrical properties of the piles (*L*, *D*) and the resistance of its reinforcement (M_y).

In the next table are showed the values of the *friction angle* **φ** and its corresponding *passive coefficient of earth pressure* **K_p** which have been taken into account in the analysis of the four cases of study listed above:

φ (º)	K_p
30	0,5236
32	0,5585
34	0,5934
36	0,6283
38	0,6632
40	0,6981

In addition to this, the specific weight of the soil which has been adopted in all cases is

$$\gamma = 20 \ kN/m^3$$

With regards to the mechanical and geometrical features of the piles which have been considered in the calculation of the limit horizontal forces, the diameters and the lengths of the piles are:

$$D = 600, 800, 1000, 1200 \ mm$$

$$L = 6, 10, 14, 20 \ m$$

In this analysis, it has been considered that the concrete of which the piles are made up of is the **B 450 C**.

Otherwise, it has also been varied the yielding bending moment of the reinforcement of the piles. The values of this **M_y** are listed in the next table besides the number and the diameter of the steel frames to which correspond these yielding moments:

Reinforcement	M_y (kNm)
12φ24	384,4
20φ24	994,9
22φ26	1672
26φ26	2330

Consecutively, are presented the values of the limit horizontal forces obtained with regards to the parameters previously identified. The calculation has been developed by means of an Excel worksheet. On these tables can be appreciated the different values of the H_{lim} calculated for all the possible combinations of the parameters. Subsequently, are showed the horizontal forces for the four different cases listed above:

FREE-HEADED PILE (BROMS)

In this case, the behavior of the single pile will be determined by the minimum value between the horizontal forces H_{lim1} and H_{lim2}. Otherwise, it has been obtained the maximum bending moment of the pile which will define whether the pile will behave as the short pile, in the case that this bending moment is lower than M_y, or as the long pile in the opossed case. These arguments are also applicable to the case of the free-headed single pile when the ground's resistance is characterized by the model of BARTON. The calculation of the H_{lim} and M_{max} has been carried out by means of the expressions showed below:

$$H_{lim1} = k_p \cdot \gamma \cdot \frac{d \cdot L^3}{2 \cdot (e + L)} \qquad (3.1.)$$

$$\frac{M_{max}}{K_p \cdot \gamma \cdot d^4} = \frac{L}{2 \cdot (L + e)} \cdot \left(\frac{L}{d}\right)^3 \cdot \left(\frac{e}{L} + 0,544 \cdot \sqrt{\frac{L}{2 \cdot (L + e)}}\right) \qquad (3.8.)$$

$$H_{lim2} = \left(\frac{M_y \cdot \sqrt{K_p \cdot \gamma \cdot d^3}}{0,544 \cdot d}\right)^{\frac{2}{3}} \qquad (3.11.)$$

And finally,

$$H_{lim} = min(H_{lim1}, H_{lim2})$$

D	L	My	φ	Kp	Hlim1 (3.1.)	Mmax (3.8.)	Hlim2 (3.11.)	Hlim	
(m)	(m)	kNm	º	-	(kN)	(kNm)	(kN)	(kN)	
0,6	6	384,4			648	1496	262	262	PALO LUNGO
0,8	6	994,9			864	1994	544	544	PALO LUNGO
1	6	1672			1080	2493	828	828	PALO LUNGO
1,2	6	2330			1296	2991	1097	1097	PALO LUNGO
0,6	10	384,4			1800	6924	262	262	PALO LUNGO
0,8	10	994,9			2400	9232	544	544	PALO LUNGO
1	10	1672			3000	11540	828	828	PALO LUNGO
1,2	10	2330			3600	13848	1097	1097	PALO LUNGO
0,6	14	384,4	30	3,0000	3528	18999	262	262	PALO LUNGO
0,8	14	994,9			4704	25333	544	544	PALO LUNGO
1	14	1672			5880	31666	828	828	PALO LUNGO
1,2	14	2330			7056	37999	1097	1097	PALO LUNGO
0,6	20	384,4			7200	55392	262	262	PALO LUNGO
0,8	20	994,9			9600	73856	544	544	PALO LUNGO
1	20	1672			12000	92320	828	828	PALO LUNGO
1,2	20	2330			14400	110784	1097	1097	PALO LUNGO

D	L	My	φ	Kp	Hlim1 (3.1.)	Mmax (3.8.)	Hlim2 (3.11.)	Hlim	
(m)	(m)	kNm	º	-	(kN)	(kNm)	(kN)	(kN)	
0,6	6	384,4			703	1623	269	269	PALO LUNGO
0,8	6	994,9			937	2163	558	558	PALO LUNGO
1	6	1672			1172	2704	850	850	PALO LUNGO
1,2	6	2330			1406	3245	1127	1127	PALO LUNGO
0,6	10	384,4			1953	7512	269	269	PALO LUNGO
0,8	10	994,9			2604	10015	558	558	PALO LUNGO
1	10	1672			3255	12519	850	850	PALO LUNGO
1,2	10	2330			3906	15023	1127	1127	PALO LUNGO
0,6	14	384,4	32	3,2546	3827	20612	269	269	PALO LUNGO
0,8	14	994,9			5103	27482	558	558	PALO LUNGO
1	14	1672			6379	34353	850	850	PALO LUNGO
1,2	14	2330			7655	41224	1127	1127	PALO LUNGO
0,6	20	384,4			7811	60093	269	269	PALO LUNGO
0,8	20	994,9			10415	80124	558	558	PALO LUNGO
1	20	1672			13018	100154	850	850	PALO LUNGO
1,2	20	2330			15622	120185	1127	1127	PALO LUNGO

D	L	My	φ	Kp	Hlim1 (3.1.)	Mmax (3.8.)	Hlim2 (3.11.)	Hlim	
(m)	(m)	kNm	º	-	(kN)	(kNm)	(kN)	(kN)	
0,6	6	384,4			764	1763	277	277	PALO LUNGO
0,8	6	994,9			1019	2351	574	574	PALO LUNGO
1	6	1672			1273	2939	874	874	PALO LUNGO
1,2	6	2330			1528	3527	1159	1159	PALO LUNGO
0,6	10	384,4			2122	8164	277	277	PALO LUNGO
0,8	10	994,9			2830	10885	574	574	PALO LUNGO
1	10	1672			3537	13606	874	874	PALO LUNGO
1,2	10	2330			4245	16327	1159	1159	PALO LUNGO
0,6	14	384,4	34	3,5371	4160	22401	277	277	PALO LUNGO
0,8	14	994,9			5546	29868	574	574	PALO LUNGO
1	14	1672			6933	37335	874	874	PALO LUNGO
1,2	14	2330			8319	44802	1159	1159	PALO LUNGO
0,6	20	384,4			8489	65310	277	277	PALO LUNGO
0,8	20	994,9			11319	87079	574	574	PALO LUNGO
1	20	1672			14149	108849	874	874	PALO LUNGO
1,2	20	2330			16978	130619	1159	1159	PALO LUNGO

D	L	My	φ	Kp	Hlim1 (3.1.)	Mmax (3.8.)	Hlim2 (3.11.)	Hlim	
(m)	(m)	kNm	º	-	(kN)	(kNm)	(kN)	(kN)	
0,6	6	384,4			832	1920	285	285	PALO LUNGO
0,8	6	994,9			1109	2560	591	591	PALO LUNGO
1	6	1672			1387	3200	899	899	PALO LUNGO
1,2	6	2330			1664	3840	1193	1193	PALO LUNGO
0,6	10	384,4			2311	8890	285	285	PALO LUNGO
0,8	10	994,9			3081	11853	591	591	PALO LUNGO
1	10	1672			3852	14817	899	899	PALO LUNGO
1,2	10	2330	36	3,8518	4622	17780	1193	1193	PALO LUNGO
0,6	14	384,4			4530	24394	285	285	PALO LUNGO
0,8	14	994,9			6040	32526	591	591	PALO LUNGO
1	14	1672			7550	40657	899	899	PALO LUNGO
1,2	14	2330			9060	48789	1193	1193	PALO LUNGO
0,6	20	384,4			9244	71120	285	285	PALO LUNGO
0,8	20	994,9			12326	94827	591	591	PALO LUNGO
1	20	1672			15407	118534	899	899	PALO LUNGO
1,2	20	2330			18489	142241	1193	1193	PALO LUNGO

D	L	My	φ	Kp	Hlim1 (3.1.)	Mmax (3.8.)	Hlim2 (3.11.)	Hlim	
(m)	(m)	kNm	º	-	(kN)	(kNm)	(kN)	(kN)	
0,6	6	384,4			908	2096	293	293	PALO LUNGO
0,8	6	994,9			1211	2794	608	608	PALO LUNGO
1	6	1672			1513	3493	926	926	PALO LUNGO
1,2	6	2330			1816	4191	1228	1228	PALO LUNGO
0,6	10	384,4			2522	9702	293	293	PALO LUNGO
0,8	10	994,9			3363	12936	608	608	PALO LUNGO
1	10	1672			4204	16170	926	926	PALO LUNGO
1,2	10	2330	38	4,2037	5044	19404	1228	1228	PALO LUNGO
0,6	14	384,4			4944	26623	293	293	PALO LUNGO
0,8	14	994,9			6591	35497	608	608	PALO LUNGO
1	14	1672			8239	44372	926	926	PALO LUNGO
1,2	14	2330			9887	53246	1228	1228	PALO LUNGO
0,6	20	384,4			10089	77618	293	293	PALO LUNGO
0,8	20	994,9			13452	103490	608	608	PALO LUNGO
1	20	1672			16815	129363	926	926	PALO LUNGO
1,2	20	2330			20178	155236	1228	1228	PALO LUNGO

D	L	My	φ	Kp	Hlim1 (3.1.)	Mmax (3.8.)	Hlim2 (3.11.)	Hlim	
(m)	(m)	kNm	º	-	(kN)	(kNm)	(kN)	(kN)	
0,6	6	384,4			993	2293	302	302	PALO LUNGO
0,8	6	994,9			1324	3057	627	627	PALO LUNGO
1	6	1672			1656	3821	954	954	PALO LUNGO
1,2	6	2330			1987	4585	1265	1265	PALO LUNGO
0,6	10	384,4			2759	10614	302	302	PALO LUNGO
0,8	10	994,9			3679	14152	627	627	PALO LUNGO
1	10	1672			4599	17690	954	954	PALO LUNGO
1,2	10	2330	40	4,5989	5519	21229	1265	1265	PALO LUNGO
0,6	14	384,4			5408	29126	302	302	PALO LUNGO
0,8	14	994,9			7211	38834	627	627	PALO LUNGO
1	14	1672			9014	48543	954	954	PALO LUNGO
1,2	14	2330			10817	58251	1265	1265	PALO LUNGO
0,6	20	384,4			11037	84914	302	302	PALO LUNGO
0,8	20	994,9			14717	113219	627	627	PALO LUNGO
1	20	1672			18396	141524	954	954	PALO LUNGO
1,2	20	2330			22075	169828	1265	1265	PALO LUNGO

The calculation of the **H**_lim_ and **M**_max_, in the case of the *free-headed single pile* when it is assumed the resistance model of the soil proposed by BARTON, has been carried out by means of the expressions showed below:

$$H_{lim1} = \frac{K_p^2 \cdot \gamma \cdot d \cdot L^3}{6 \cdot (e + L)} \qquad (3.1.')$$

$$\frac{3 \cdot M_{max}}{K_p^2 \cdot \gamma \cdot d^4} = \frac{L}{2 \cdot (L + e)} \cdot \left(\frac{L}{d}\right)^3 \cdot \left(\frac{e}{L} + 0{,}544 \cdot \sqrt{\frac{L}{2 \cdot (L + e)}}\right) \qquad (3.8.')$$

From the equation (3.10.'), corresponding to that used to calculate the **H**_lim2_, when the resistance of the soil is defined by the model of BARTON, considering $e = 0$, it can be obtained (3.11.') as:

$$H_{lim2} = \sqrt[3]{\left(\frac{1{,}0613 \cdot M_y \cdot \sqrt{K_p^2 \cdot \gamma \cdot d^3}}{d}\right)^2} \qquad (3.11.')$$

And finally,

$$H_{lim} = min(H_{lim1}, H_{lim2})$$

D	L	My	φ	Kp	Hlim1 (3.1.')	Mmax (3.8.')	Hlim2 (3.11.')	Hlim	
(m)	(m)	kNm	º	-	(kN)	(kNm)	(kN)	(kN)	
0,6	6	384,4			648	1496	262	262	PALO LUNGO
0,8	6	994,9			864	1994	544	544	PALO LUNGO
1	6	1672			1080	2493	828	828	PALO LUNGO
1,2	6	2330			1296	2991	1097	1097	PALO LUNGO
0,6	10	384,4			1800	6924	262	262	PALO LUNGO
0,8	10	994,9			2400	9232	544	544	PALO LUNGO
1	10	1672			3000	11540	828	828	PALO LUNGO
1,2	10	2330	30	3,0000	3600	13848	1097	1097	PALO LUNGO
0,6	14	384,4			3528	18999	262	262	PALO LUNGO
0,8	14	994,9			4704	25333	544	544	PALO LUNGO
1	14	1672			5880	31666	828	828	PALO LUNGO
1,2	14	2330			7056	37999	1097	1097	PALO LUNGO
0,6	20	384,4			7200	55392	262	262	PALO LUNGO
0,8	20	994,9			9600	73856	544	544	PALO LUNGO
1	20	1672			12000	92320	828	828	PALO LUNGO
1,2	20	2330			14400	110784	1097	1097	PALO LUNGO

D	L	My	φ	Kp	Hlim1 (3.1.')	Mmax (3.8.')	Hlim2 (3.11.')	Hlim	
(m)	(m)	kNm	º	-	(kN)	(kNm)	(kN)	(kN)	
0,6	6	384,4			763	1760	277	277	PALO LUNGO
0,8	6	994,9			1017	2347	574	574	PALO LUNGO
1	6	1672			1271	2934	874	874	PALO LUNGO
1,2	6	2330			1525	3520	1158	1158	PALO LUNGO
0,6	10	384,4			2118	8149	277	277	PALO LUNGO
0,8	10	994,9			2825	10865	574	574	PALO LUNGO
1	10	1672			3531	13582	874	874	PALO LUNGO
1,2	10	2330			4237	16298	1158	1158	PALO LUNGO
0,6	14	384,4	32	3,2546	4152	22361	277	277	PALO LUNGO
0,8	14	994,9			5536	29815	574	574	PALO LUNGO
1	14	1672			6920	37268	874	874	PALO LUNGO
1,2	14	2330			8304	44722	1158	1158	PALO LUNGO
0,6	20	384,4			8474	65192	277	277	PALO LUNGO
0,8	20	994,9			11299	86923	574	574	PALO LUNGO
1	20	1672			14123	108654	874	874	PALO LUNGO
1,2	20	2330			16948	130385	1158	1158	PALO LUNGO

D	L	My	φ	Kp	Hlim1 (3.1.')	Mmax (3.8.')	Hlim2 (3.11.')	Hlim	
(m)	(m)	kNm	º	-	(kN)	(kNm)	(kN)	(kN)	
0,6	6	384,4			901	2079	292	292	PALO LUNGO
0,8	6	994,9			1201	2772	607	607	PALO LUNGO
1	6	1672			1501	3465	924	924	PALO LUNGO
1,2	6	2330			1802	4158	1225	1225	PALO LUNGO
0,6	10	384,4			2502	9625	292	292	PALO LUNGO
0,8	10	994,9			3336	12834	607	607	PALO LUNGO
1	10	1672			4170	16042	924	924	PALO LUNGO
1,2	10	2330			5005	19251	1225	1225	PALO LUNGO
0,6	14	384,4	34	3,5371	4904	26412	292	292	PALO LUNGO
0,8	14	994,9			6539	35216	607	607	PALO LUNGO
1	14	1672			8174	44020	924	924	PALO LUNGO
1,2	14	2330			9809	52824	1225	1225	PALO LUNGO
0,6	20	384,4			10009	77003	292	292	PALO LUNGO
0,8	20	994,9			13345	102670	607	607	PALO LUNGO
1	20	1672			16682	128338	924	924	PALO LUNGO
1,2	20	2330			20018	154006	1225	1225	PALO LUNGO

D	L	My	φ	Kp	Hlim1 (3.1.')	Mmax (3.8.')	Hlim2 (3.11.')	Hlim	
(m)	(m)	kNm	º	-	(kN)	(kNm)	(kN)	(kN)	
0,6	6	384,4			1068	2465	309	309	PALO LUNGO
0,8	6	994,9			1424	3287	642	642	PALO LUNGO
1	6	1672			1780	4109	978	978	PALO LUNGO
1,2	6	2330			2136	4931	1296	1296	PALO LUNGO
0,6	10	384,4			2967	11414	309	309	PALO LUNGO
0,8	10	994,9			3956	15219	642	642	PALO LUNGO
1	10	1672			4946	19024	978	978	PALO LUNGO
1,2	10	2330			5935	22829	1296	1296	PALO LUNGO
0,6	14	384,4	36	3,8518	5816	31321	309	309	PALO LUNGO
0,8	14	994,9			7755	41761	642	642	PALO LUNGO
1	14	1672			9693	52202	978	978	PALO LUNGO
1,2	14	2330			11632	62642	1296	1296	PALO LUNGO
0,6	20	384,4			11869	91315	309	309	PALO LUNGO
0,8	20	994,9			15826	121753	642	642	PALO LUNGO
1	20	1672			19782	152191	978	978	PALO LUNGO
1,2	20	2330			23739	182629	1296	1296	PALO LUNGO

D	L	My	φ	Kp	Hlim1 (3.1.')	Mmax (3.8.')	Hlim2 (3.11.')	Hlim	
(m)	(m)	kNm	º	-	(kN)	(kNm)	(kN)	(kN)	
0,6	6	384,4			1272	2937	328	328	PALO LUNGO
0,8	6	994,9			1696	3915	681	681	PALO LUNGO
1	6	1672			2121	4894	1036	1036	PALO LUNGO
1,2	6	2330			2545	5873	1374	1374	PALO LUNGO
0,6	10	384,4			3534	13595	328	328	PALO LUNGO
0,8	10	994,9			4712	18127	681	681	PALO LUNGO
1	10	1672			5890	22659	1036	1036	PALO LUNGO
1,2	10	2330	38	4,2037	7069	27190	1374	1374	PALO LUNGO
0,6	14	384,4			6927	37305	328	328	PALO LUNGO
0,8	14	994,9			9236	49740	681	681	PALO LUNGO
1	14	1672			11545	62176	1036	1036	PALO LUNGO
1,2	14	2330			13854	74611	1374	1374	PALO LUNGO
0,6	20	384,4			14137	108762	328	328	PALO LUNGO
0,8	20	994,9			18850	145016	681	681	PALO LUNGO
1	20	1672			23562	181270	1036	1036	PALO LUNGO
1,2	20	2330			28274	217524	1374	1374	PALO LUNGO

D	L	My	φ	Kp	Hlim1 (3.1.')	Mmax (3.8.')	Hlim2 (3.11.')	Hlim	
(m)	(m)	kNm	º	-	(kN)	(kNm)	(kN)	(kN)	
0,6	6	384,4			1523	3515	348	348	PALO LUNGO
0,8	6	994,9			2030	4686	723	723	PALO LUNGO
1	6	1672			2538	5858	1100	1100	PALO LUNGO
1,2	6	2330			3046	7029	1459	1459	PALO LUNGO
0,6	10	384,4			4230	16271	348	348	PALO LUNGO
0,8	10	994,9			5640	21695	723	723	PALO LUNGO
1	10	1672			7050	27119	1100	1100	PALO LUNGO
1,2	10	2330	40	4,5989	8460	32543	1459	1459	PALO LUNGO
0,6	14	384,4			8291	44649	348	348	PALO LUNGO
0,8	14	994,9			11054	59531	723	723	PALO LUNGO
1	14	1672			13818	74414	1100	1100	PALO LUNGO
1,2	14	2330			16582	89297	1459	1459	PALO LUNGO
0,6	20	384,4			16920	130171	348	348	PALO LUNGO
0,8	20	994,9			22560	173561	723	723	PALO LUNGO
1	20	1672			28200	216951	1100	1100	PALO LUNGO
1,2	20	2330			33840	260342	1459	1459	PALO LUNGO

<u>*RESTRAINED PILE (BROMS)*</u>

In the case of the single pile whose head is restrained to the rotation as a consequence of the constraint condition which exists in the joint between the pile and the plate, the limit value of the horizontal force is obtained as the minimum between the three values of H_{lim} calculated for each different pile. In the tables below, it is also presented the maximum bending moment of the pile calculated to determine, by comparing it with M_y, whether the behavior of the pile corresponds to that of the short pile or to that of the intermedium pile. Nevertheless, in the cases in which the head of the piles is restrained to the rotation, the behavior of the pile will come from the minimum value of the H_{lim} obtained:

- If H_{lim1} coincides con H_{lim}, then the pile will behave as the *Short pile*.
- If H_{lim2} coincides con H_{lim}, then the pile will behave as the *Intermedium pile*.
- If H_{lim3} coincides con H_{lim}, then the pile will behave as the *Long pile*.

This argument has been also applied to the case of the restrained pile in which the soil's resistance has been obtained with the equations of BROMS particularized with the model proposed by BARTON for the resistance of the soil.

Otherwise, the **H_{lim1}**, **H_{lim2}** and **H_{lim3}**, as well as **M_{max}**, have been obtained with regards to the next formulas:

$$H_{lim1} = 1{,}5 \cdot L^2 \cdot K_p \cdot \gamma \cdot d \qquad (3.12.)$$

$$\frac{M_{max}}{K_p \cdot \gamma \cdot d^4} = \left(\frac{L}{d}\right)^3 \qquad (3.15.)$$

$$H_{lim2} = K_p \cdot \gamma \cdot d^3 \cdot \left(\frac{1}{2} \cdot \left(\frac{L}{d}\right)^2 + \frac{M_y}{K_p \cdot \gamma \cdot d^4} \cdot \frac{d}{L}\right) \qquad (3.19.)$$

$$H_{lim3} = K_p \cdot \gamma \cdot d^3 \cdot \sqrt[3]{\left(3{,}676 \cdot \frac{M_y}{K_p \cdot \gamma \cdot d^4}\right)^2} \qquad (3.21.)$$

And finally,

$$H_{lim} = min(H_{lim1}, H_{lim2}, H_{lim3})$$

D	L	My	φ	Kp	Hlim1 (3.12.)	Mmax (3.15.)	Hlim2 (3.19.)	Hlim3 (3.21.)	Hlim	
(m)	(m)	kNm	º	-	(kN)	(kNm)	(kN)	(kN)	(kN)	
0,6	6	384,4			1944	7776	712	416	416	PALO LUNGO
0,8	6	994,9			2592	10368	1030	863	863	PALO LUNGO
1	6	1672			3240	12960	1359	1314	1314	PALO LUNGO
1,2	6	2330			3888	15552	1684	1742	1684	PALO INTERMEDIO
0,6	10	384,4			5400	36000	1838	416	416	PALO LUNGO
0,8	10	994,9			7200	48000	2499	863	863	PALO LUNGO
1	10	1672			9000	60000	3167	1314	1314	PALO LUNGO
1,2	10	2330	30	3,0000	10800	72000	3833	1742	1742	PALO LUNGO
0,6	14	384,4			10584	98784	3555	416	416	PALO LUNGO
0,8	14	994,9			14112	131712	4775	863	863	PALO LUNGO
1	14	1672			17640	164640	5999	1314	1314	PALO LUNGO
1,2	14	2330			21168	197568	7222	1742	1742	PALO LUNGO
0,6	20	384,4			21600	288000	7219	416	416	PALO LUNGO
0,8	20	994,9			28800	384000	9650	863	863	PALO LUNGO
1	20	1672			36000	480000	12084	1314	1314	PALO LUNGO
1,2	20	2330			43200	576000	14517	1742	1742	PALO LUNGO

D	L	My	φ	Kp	Hlim1 (3.12.)	Mmax (3.15.)	Hlim2 (3.19.)	Hlim3 (3.21.)	Hlim	
(m)	(m)	kNm	º	-	(kN)	(kNm)	(kN)	(kN)	(kN)	
0,6	6	384,4			2109	8436	767	427	427	PALO LUNGO
0,8	6	994,9			2812	11248	1103	886	886	PALO LUNGO
1	6	1672			3515	14060	1450	1350	1350	PALO LUNGO
1,2	6	2330			4218	16872	1794	1789	1789	PALO LUNGO
0,6	10	384,4			5858	39055	1991	427	427	PALO LUNGO
0,8	10	994,9			7811	52073	2703	886	886	PALO LUNGO
1	10	1672			9764	65092	3422	1350	1350	PALO LUNGO
1,2	10	2330	32	3,2546	11717	78110	4139	1789	1789	PALO LUNGO
0,6	14	384,4			11482	107167	3855	427	427	PALO LUNGO
0,8	14	994,9			15310	142889	5174	886	886	PALO LUNGO
1	14	1672			19137	178612	6498	1350	1350	PALO LUNGO
1,2	14	2330			22964	214334	7821	1789	1789	PALO LUNGO
0,6	20	384,4			23433	312440	7830	427	427	PALO LUNGO
0,8	20	994,9			31244	416587	10464	886	886	PALO LUNGO
1	20	1672			39055	520734	13102	1350	1350	PALO LUNGO
1,2	20	2330			46866	624881	15739	1789	1789	PALO LUNGO

D	L	My	φ	Kp	Hlim1 (3.12.)	Mmax (3.15.)	Hlim2 (3.19.)	Hlim3 (3.21.)	Hlim	
(m)	(m)	kNm	º	-	(kN)	(kNm)	(kN)	(kN)	(kN)	
0,6	6	384,4			2292	9168	828	439	439	PALO LUNGO
0,8	6	994,9			3056	12224	1185	911	911	PALO LUNGO
1	6	1672			3820	15280	1552	1388	1388	PALO LUNGO
1,2	6	2330			4584	18336	1916	1840	1840	PALO LUNGO
0,6	10	384,4			6367	42446	2161	439	439	PALO LUNGO
0,8	10	994,9			8489	56594	2929	911	911	PALO LUNGO
1	10	1672			10611	70743	3704	1388	1388	PALO LUNGO
1,2	10	2330	34	3,5371	12734	84891	4478	1840	1840	PALO LUNGO
0,6	14	384,4			12479	116471	4187	439	439	PALO LUNGO
0,8	14	994,9			16639	155294	5617	911	911	PALO LUNGO
1	14	1672			20798	194118	7052	1388	1388	PALO LUNGO
1,2	14	2330			24958	232941	8486	1840	1840	PALO LUNGO
0,6	20	384,4			25467	339565	8508	439	439	PALO LUNGO
0,8	20	994,9			33956	452753	11369	911	911	PALO LUNGO
1	20	1672			42446	565941	14232	1388	1388	PALO LUNGO
1,2	20	2330			50935	679129	17095	1840	1840	PALO LUNGO

D	L	My	φ	Kp	Hlim1 (3.12.)	Mmax (3.15.)	Hlim2 (3.19.)	Hlim3 (3.21.)	Hlim	
(m)	(m)	kNm	º	-	(kN)	(kNm)	(kN)	(kN)	(kN)	
0,6	6	384,4			2496	9984	896	452	452	PALO LUNGO
0,8	6	994,9			3328	13312	1275	938	938	PALO LUNGO
1	6	1672			4160	16640	1665	1428	1428	PALO LUNGO
1,2	6	2330			4992	19968	2052	1893	1893	PALO LUNGO
0,6	10	384,4			6933	46222	2350	452	452	PALO LUNGO
0,8	10	994,9			9244	61629	3181	938	938	PALO LUNGO
1	10	1672			11556	77037	4019	1428	1428	PALO LUNGO
1,2	10	2330	36	3,8518	13867	92444	4855	1893	1893	PALO LUNGO
0,6	14	384,4			13589	126833	4557	452	452	PALO LUNGO
0,8	14	994,9			18119	169111	6111	938	938	PALO LUNGO
1	14	1672			22649	211389	7669	1428	1428	PALO LUNGO
1,2	14	2330			27179	253667	9226	1893	1893	PALO LUNGO
0,6	20	384,4			27733	369777	9264	452	452	PALO LUNGO
0,8	20	994,9			36978	493036	12376	938	938	PALO LUNGO
1	20	1672			46222	616294	15491	1428	1428	PALO LUNGO
1,2	20	2330			55466	739553	18605	1893	1893	PALO LUNGO

D	L	My	φ	Kp	Hlim1 (3.12.)	Mmax (3.15.)	Hlim2 (3.19.)	Hlim3 (3.21.)	Hlim	
(m)	(m)	kNm	º	-	(kN)	(kNm)	(kN)	(kN)	(kN)	
0,6	6	384,4			2724	10896	972	465	465	PALO LUNGO
0,8	6	994,9			3632	14528	1376	965	965	PALO LUNGO
1	6	1672			4540	18160	1792	1470	1470	PALO LUNGO
1,2	6	2330			5448	21792	2204	1949	1949	PALO LUNGO
0,6	10	384,4			7567	50445	2561	465	465	PALO LUNGO
0,8	10	994,9			10089	67260	3462	965	965	PALO LUNGO
1	10	1672			12611	84075	4371	1470	1470	PALO LUNGO
1,2	10	2330	38	4,2037	15133	100890	5277	1949	1949	PALO LUNGO
0,6	14	384,4			14831	138421	4971	465	465	PALO LUNGO
0,8	14	994,9			19774	184561	6663	965	965	PALO LUNGO
1	14	1672			24718	230702	8359	1470	1470	PALO LUNGO
1,2	14	2330			29662	276842	10054	1949	1949	PALO LUNGO
0,6	20	384,4			30267	403560	10108	465	465	PALO LUNGO
0,8	20	994,9			40356	538079	13502	965	965	PALO LUNGO
1	20	1672			50445	672599	16899	1470	1470	PALO LUNGO
1,2	20	2330			60534	807119	20294	1949	1949	PALO LUNGO

D	L	My	φ	Kp	Hlim1 (3.12.)	Mmax (3.15.)	Hlim2 (3.19.)	Hlim3 (3.21.)	Hlim	
(m)	(m)	kNm	º	-	(kN)	(kNm)	(kN)	(kN)	(kN)	
0,6	6	384,4			2980	11920	1057	479	479	PALO LUNGO
0,8	6	994,9			3973	15894	1490	995	995	PALO LUNGO
1	6	1672			4967	19867	1934	1515	1515	PALO LUNGO
1,2	6	2330			5960	23841	2375	2008	2008	PALO LUNGO
0,6	10	384,4			8278	55187	2798	479	479	PALO LUNGO
0,8	10	994,9			11037	73583	3779	995	995	PALO LUNGO
1	10	1672			13797	91978	4766	1515	1515	PALO LUNGO
1,2	10	2330	40	4,5989	16556	110374	5752	2008	2008	PALO LUNGO
0,6	14	384,4			16225	151433	5436	479	479	PALO LUNGO
0,8	14	994,9			21633	201911	7282	995	995	PALO LUNGO
1	14	1672			27042	252388	9133	1515	1515	PALO LUNGO
1,2	14	2330			32450	302866	10983	2008	2008	PALO LUNGO
0,6	20	384,4			33112	441495	11057	479	479	PALO LUNGO
0,8	20	994,9			44150	588660	14766	995	995	PALO LUNGO
1	20	1672			55187	735826	18479	1515	1515	PALO LUNGO
1,2	20	2330			66224	882991	22191	2008	2008	PALO LUNGO

RESTRAINED PILE (BARTON)

In the case of the restrained single pile, when the model adopted for the ground's resistance is that one proposed by BARTON, the calculation of the values of the limit horizontal force **H**_lim_, and the maximum bending moment **M**_max_, has been developed by means of the next equations:

$$H_{lim1} = \frac{1,5 \cdot K_p^2 \cdot \gamma \cdot d \cdot L^2}{3} \qquad (3.12.')$$

$$M_{max} = \frac{K_p^2 \cdot \gamma \cdot d \cdot L^3}{3} \qquad (3.15.')$$

$$H_{lim2} = \frac{K_p^2 \cdot \gamma \cdot d \cdot L^2}{6} + \frac{M_y}{L} \qquad (3.19.')$$

$$H_{lim3} = \frac{K_p^2 \cdot \gamma \cdot d^3}{3} \cdot \sqrt[3]{\left(\frac{11,028 \cdot M_y}{K_p^2 \cdot \gamma \cdot d^4}\right)^2} \qquad (3.21.')$$

And finally,

$$H_{lim} = \min(H_{lim1}, H_{lim2}, H_{lim3})$$

D	L	My	φ	Kp	Hlim1 (3.12.')	Mmax (3.15.')	Hlim2 (3.19.')	Hlim3 (3.21.')	Hlim	
(m)	(m)	kNm	º	-	(kN)	(kNm)	(kN)	(kN)	(kN)	
0,6	6	384,4			5832	7776	712	416	416	PALO LUNGO
0,8	6	994,9			7776	10368	1030	863	863	PALO LUNGO
1	6	1672			9720	12960	1359	1314	1314	PALO LUNGO
1,2	6	2330			11664	15552	1684	1742	1684	PALO INTERMEDIO
0,6	10	384,4			16200	36000	1838	416	416	PALO LUNGO
0,8	10	994,9			21600	48000	2499	863	863	PALO LUNGO
1	10	1672			27000	60000	3167	1314	1314	PALO LUNGO
1,2	10	2330	30	3,0000	32400	72000	3833	1742	1742	PALO LUNGO
0,6	14	384,4			31752	98784	3555	416	416	PALO LUNGO
0,8	14	994,9			42336	131712	4775	863	863	PALO LUNGO
1	14	1672			52920	164640	5999	1314	1314	PALO LUNGO
1,2	14	2330			63504	197568	7222	1742	1742	PALO LUNGO
0,6	20	384,4			64800	288000	7219	416	416	PALO LUNGO
0,8	20	994,9			86400	384000	9650	863	863	PALO LUNGO
1	20	1672			108000	480000	12084	1314	1314	PALO LUNGO
1,2	20	2330			129600	576000	14517	1742	1742	PALO LUNGO

D	L	My	φ	Kp	Hlim1 (3.12.')	Mmax (3.15.')	Hlim2 (3.19.')	Hlim3 (3.21.')	Hlim	
(m)	(m)	kNm	º	-	(kN)	(kNm)	(kN)	(kN)	(kN)	
0,6	6	384,4			6864	9152	827	439	439	**PALO LUNGO**
0,8	6	994,9			9152	12202	1183	911	911	**PALO LUNGO**
1	6	1672			11440	15253	1550	1387	1387	**PALO LUNGO**
1,2	6	2330			13728	18304	1914	1839	1839	**PALO LUNGO**
0,6	10	384,4			19066	42369	2157	439	439	**PALO LUNGO**
0,8	10	994,9			25422	56493	2924	911	911	**PALO LUNGO**
1	10	1672			31777	70616	3698	1387	1387	**PALO LUNGO**
1,2	10	2330	32	3,2546	38132	84739	4470	1839	1839	**PALO LUNGO**
0,6	14	384,4			37370	116262	4180	439	439	**PALO LUNGO**
0,8	14	994,9			49826	155015	5607	911	911	**PALO LUNGO**
1	14	1672			62283	193769	7040	1387	1387	**PALO LUNGO**
1,2	14	2330			74740	232523	8471	1839	1839	**PALO LUNGO**
0,6	20	384,4			76265	338955	8493	439	439	**PALO LUNGO**
0,8	20	994,9			101687	451940	11348	911	911	**PALO LUNGO**
1	20	1672			127108	564925	14207	1387	1387	**PALO LUNGO**
1,2	20	2330			152530	677910	17064	1839	1839	**PALO LUNGO**

D	L	My	φ	Kp	Hlim1 (3.12.')	Mmax (3.15.')	Hlim2 (3.19.')	Hlim3 (3.21.')	Hlim	
(m)	(m)	kNm	º	-	(kN)	(kNm)	(kN)	(kN)	(kN)	
0,6	6	384,4			8107	10810	965	464	464	**PALO LUNGO**
0,8	6	994,9			10810	14413	1367	963	963	**PALO LUNGO**
1	6	1672			13512	18016	1780	1466	1466	**PALO LUNGO**
1,2	6	2330			16215	21620	2190	1944	1944	**PALO LUNGO**
0,6	10	384,4			22520	50045	2541	464	464	**PALO LUNGO**
0,8	10	994,9			30027	66727	3436	963	963	**PALO LUNGO**
1	10	1672			37534	83409	4338	1466	1466	**PALO LUNGO**
1,2	10	2330	34	3,5371	45041	100090	5238	1944	1944	**PALO LUNGO**
0,6	14	384,4			44140	137324	4932	464	464	**PALO LUNGO**
0,8	14	994,9			58853	183099	6610	963	963	**PALO LUNGO**
1	14	1672			73566	228873	8293	1466	1466	**PALO LUNGO**
1,2	14	2330			88280	274648	9975	1944	1944	**PALO LUNGO**
0,6	20	384,4			90081	400362	10028	464	464	**PALO LUNGO**
0,8	20	994,9			120109	533816	13395	963	963	**PALO LUNGO**
1	20	1672			150136	667269	16765	1466	1466	**PALO LUNGO**
1,2	20	2330			180163	800723	20135	1944	1944	**PALO LUNGO**

D	L	My	φ	Kp	Hlim1 (3.12.')	Mmax (3.15.')	Hlim2 (3.19.')	Hlim3 (3.21.')	Hlim	
(m)	(m)	kNm	º	-	(kN)	(kNm)	(kN)	(kN)	(kN)	
0,6	6	384,4			9614	12819	1132	491	491	**PALO LUNGO**
0,8	6	994,9			12819	17092	1590	1019	1019	**PALO LUNGO**
1	6	1672			16024	21365	2059	1552	1552	**PALO LUNGO**
1,2	6	2330			19228	25638	2525	2057	2057	**PALO LUNGO**
0,6	10	384,4			26706	59347	3006	491	491	**PALO LUNGO**
0,8	10	994,9			35608	79129	4056	1019	1019	**PALO LUNGO**
1	10	1672			44510	98911	5113	1552	1552	**PALO LUNGO**
1,2	10	2330	36	3,8518	53412	118693	6168	2057	2057	**PALO LUNGO**
0,6	14	384,4			52344	162847	5843	491	491	**PALO LUNGO**
0,8	14	994,9			69792	217130	7826	1019	1019	**PALO LUNGO**
1	14	1672			87240	271412	9813	1552	1552	**PALO LUNGO**
1,2	14	2330			104688	325695	11798	2057	2057	**PALO LUNGO**
0,6	20	384,4			106824	474773	11889	491	491	**PALO LUNGO**
0,8	20	994,9			142432	633031	15876	1019	1019	**PALO LUNGO**
1	20	1672			178040	791289	19866	1552	1552	**PALO LUNGO**
1,2	20	2330			213648	949547	23855	2057	2057	**PALO LUNGO**

D	L	My	φ	Kp	Hlim1 (3.12.')	Mmax (3.15.')	Hlim2 (3.19.')	Hlim3 (3.21.')	Hlim	
(m)	(m)	kNm	º	-	(kN)	(kNm)	(kN)	(kN)	(kN)	
0,6	6	384,4			11451	15268	1336	521	521	PALO LUNGO
0,8	6	994,9			15268	20358	1862	1080	1080	PALO LUNGO
1	6	1672			19085	25447	2399	1645	1645	PALO LUNGO
1,2	6	2330			22902	30536	2933	2181	2181	PALO LUNGO
0,6	10	384,4			31809	70686	3573	521	521	PALO LUNGO
0,8	10	994,9			42412	94248	4812	1080	1080	PALO LUNGO
1	10	1672			53014	117810	6058	1645	1645	PALO LUNGO
1,2	10	2330	38	4,2037	63617	141372	7302	2181	2181	PALO LUNGO
0,6	14	384,4			62345	193962	6955	521	521	PALO LUNGO
0,8	14	994,9			83127	258616	9307	1080	1080	PALO LUNGO
1	14	1672			103908	323270	11665	1645	1645	PALO LUNGO
1,2	14	2330			124690	387924	14021	2181	2181	PALO LUNGO
0,6	20	384,4			127235	565487	14156	521	521	PALO LUNGO
0,8	20	994,9			169646	753983	18899	1080	1080	PALO LUNGO
1	20	1672			212058	942479	23646	1645	1645	PALO LUNGO
1,2	20	2330			254469	1130975	28391	2181	2181	PALO LUNGO

D	L	My	φ	Kp	Hlim1 (3.12.')	Mmax (3.15.')	Hlim2 (3.19.')	Hlim3 (3.21.')	Hlim	
(m)	(m)	kNm	º	-	(kN)	(kNm)	(kN)	(kN)	(kN)	
0,6	6	384,4			13705	18274	1587	553	553	PALO LUNGO
0,8	6	994,9			18274	24365	2196	1147	1147	PALO LUNGO
1	6	1672			22842	30456	2817	1746	1746	PALO LUNGO
1,2	6	2330			27410	36547	3434	2315	2315	PALO LUNGO
0,6	10	384,4			38070	84600	4268	553	553	PALO LUNGO
0,8	10	994,9			50760	112800	5739	1147	1147	PALO LUNGO
1	10	1672			63450	141000	7217	1746	1746	PALO LUNGO
1,2	10	2330	40	4,5989	76140	169200	8693	2315	2315	PALO LUNGO
0,6	14	384,4			74617	232142	8318	553	553	PALO LUNGO
0,8	14	994,9			99489	309523	11125	1147	1147	PALO LUNGO
1	14	1672			124362	386903	13937	1746	1746	PALO LUNGO
1,2	14	2330			149234	464284	16748	2315	2315	PALO LUNGO
0,6	20	384,4			152280	676799	16939	553	553	PALO LUNGO
0,8	20	994,9			203040	902399	22610	1147	1147	PALO LUNGO
1	20	1672			253800	1127999	28284	1746	1746	PALO LUNGO
1,2	20	2330			304560	1353598	33956	2315	2315	PALO LUNGO

What can be concluded from the analysis developed in the Excel worksheet is that in the most of the cases the behavior of the single pile corresponds to that one of the long pile. This is due to the fact that the minimum value of the H_{lim} coincides with the limit horizontal force H_{lim2} in the cases of the free-headed piles and with H_{lim3} in the cases of the restrained piles. As a consequence of these results, it can also be concluded that in this case of study, the values of the limit horizontal force do not depend on the length of the single pile.

Otherwise, as it can be realized in the cases of the restrained piles for both models of the soil resistance, it exists one unique case in which the single pile behaves as the intermediate pile. This anomalous data corresponds to a pile whose diameter is equal to 1,2 meters and whose length is equal to 6 meters. It must be pointed that these two data have been excluded from the discussion of the results developed in the next point of this Master's Thesis.

To compare the values of the limit horizontal forces obtained with regards to the resistance's models of the soil proposed by BROMS (1946b) and BARTON (1982), have been developed two different sorts of graphs. On the one hand, it was wanted to study the evolution of the limit horizontal force H_{lim} in function of the yielding bending moment M_y, depending on the constraint conditions on the pile's head. For this reason, have been graphed, for both models of the ground's resistance, the evolution of the horizontal force in the case of the free-headed pile and in the case of the restrained pile.

The results showed in the graphs below are represented in a logarithmic scale. The first of them corresponds to the results obtained with regards to the model of the soil's resistance proposed by BROMS (1946b). It can be outlined a linear increasing of the H_{lim}. This is due to the enhancement of three different factors, which are the diameter of the pile, the passive coefficient of earth pressure and the yielding bending moment of the pile's steel reinforcement. Another point to mention is that the values of the limit horizontal forces, when the piles are restrained to the rotation on its head, are higher than those obtained in the case of the free-headed piles. The reason of these differences between the H_{lim} values is due to the higher stiffness of the system pile – plate, when the pile's heads are restrained to the rotation.
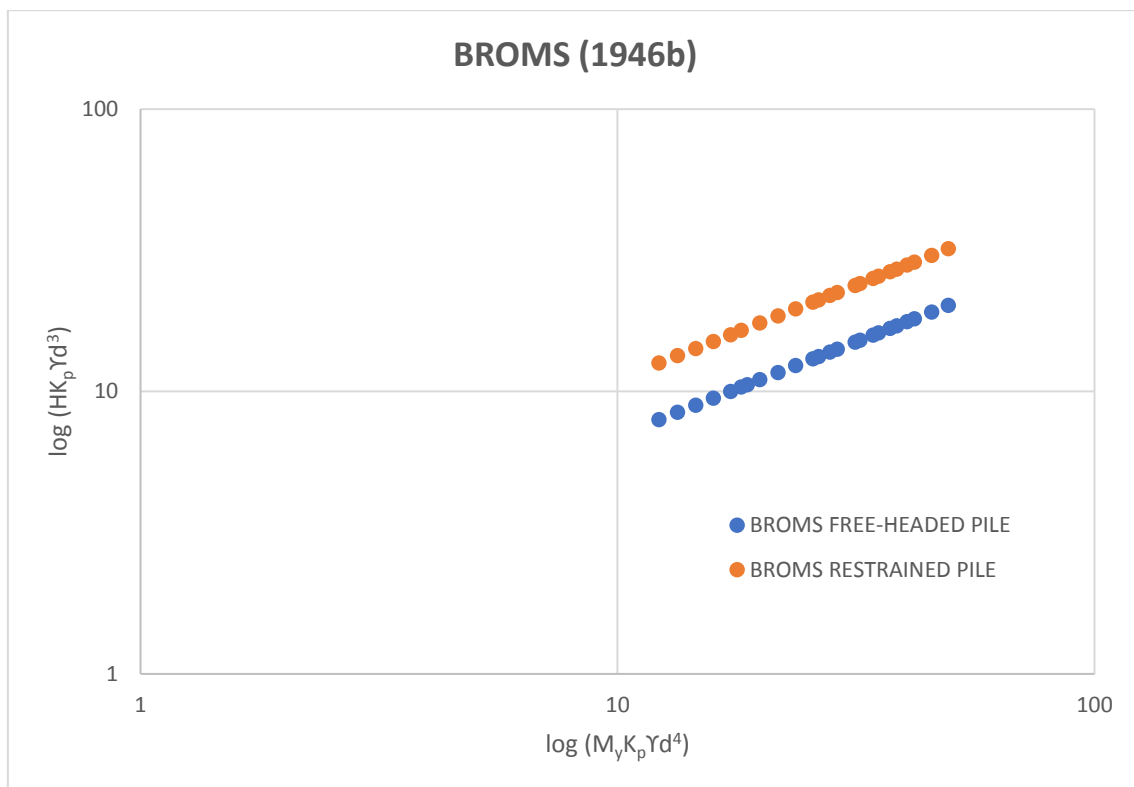
Figure 3-10 Variation of the H_{lim} when are modified the diameter of the piles, the passive coefficient of earth pressure and the yielding bending moment of the pile's reinforcement, when the resistance of the soil is characterized by the model proposed by BROMS (1946b). Are represented two cases: free-headed pile, restrained pile.

The second graph shows the variation of the limit horizontal load in function of the yielding bending moment M_y for the free-headed pile and for the restrained pile. In this case, it has been considered the model of BARTON for the soil's resistance. The trend of the results is

almost linear as it happened with the model of BROMS. As it has been explained for BROMS, this trend is also influenced by some other parameters such as the diameter of the pile and the passive earth pressure coefficient.
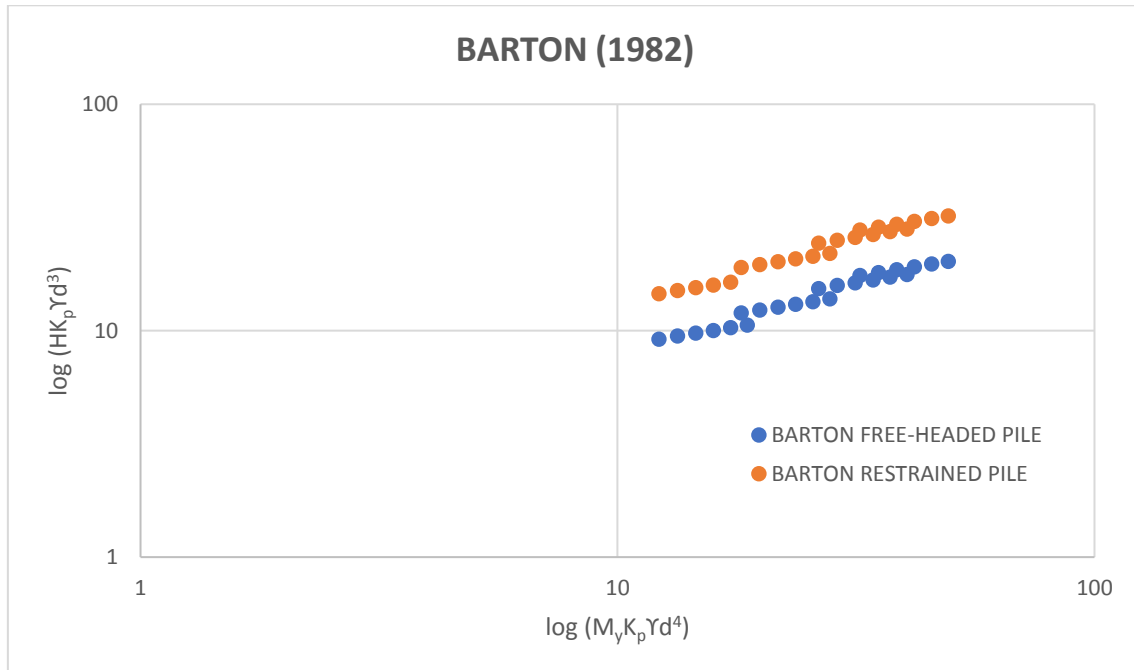
Figure 3-11 Variation of the H$_{lim}$ when are modified the diameter of the piles, the passive coefficient of earth pressure and the yielding bending moment of the pile's reinforcement, when the resistance of the soil is characterized by the model proposed by BARTON (1982). Are represented two cases: free-headed pile, restrained pile.

What can be concluded from this charts is that the increasing of the limit horizontal forces is linked to the raising of the yielding bending moment *M$_y$*, as well as the increasing of the passive coefficient of earth pressure *K$_p$*, which is related directly to the enhancement of the friction angle of the soil **ɸ**.

Otherwise, it has been analyzed the effect of the friction angle by plotting the limit horizontal forces *H$_{lim}$* with regards to the yielding bending moment *M$_y$* with which these *H$_{lim}$* have been calculated. In each of these graphs have been brought into confrontation the values obtained applying the equations of BROMS (1946b) for the ground's resistance with those obtained using these equations particularized with the model of BARTON (1982) for the resistance of the soil. The cases of study which has been compared for both models are:

- FREE-HEADED PILES BROMS (1946b) / BARTON (1982).
- RESTRAINED SINGLE PILE BROMS (1946b) / BARTON (1982).

Successively, are presented the graphs which contain the confrontations between the two models of resistance of the soil according to the constraint conditions on the head of the single pile. To determine the effects of the friction angle of the ground, it has been represented the variation of *H$_{lim}$* with regards to the *M$_y$* for the next values of the friction angle of the soil: 30, 32, 34, 36, 38, 40º.
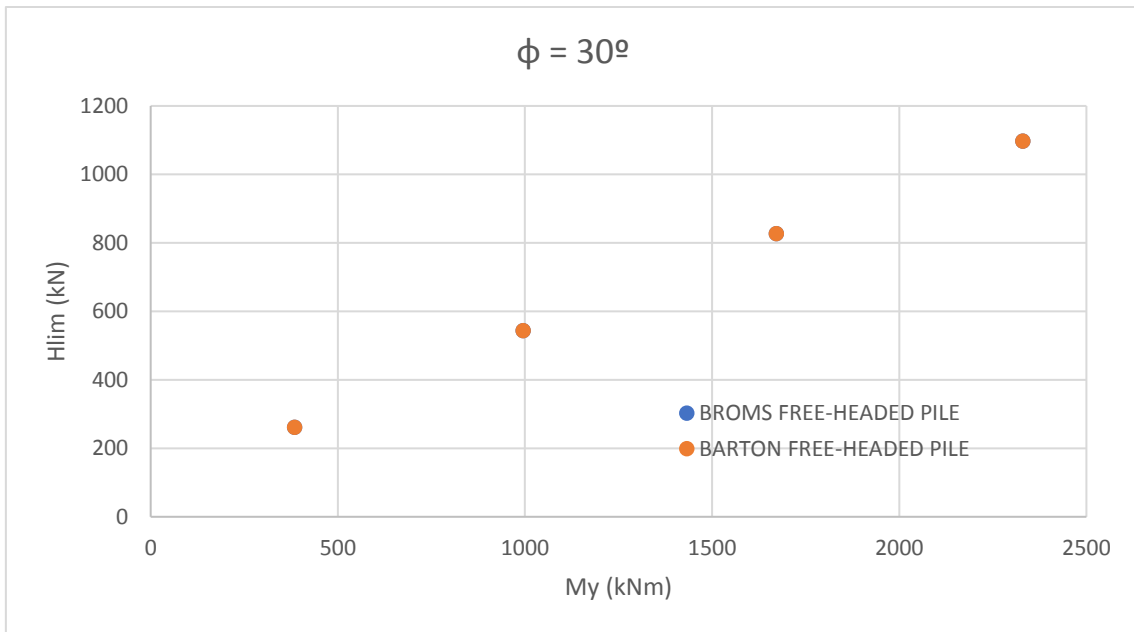
FREE-HEADED PILE

Figure 3-12 Confrontation between the Hlim values obtained according to the models of BROMS (1946b) and BARTON (1982) for the resistance of the soil in the case of the free-headed pile (Φ = 30º).
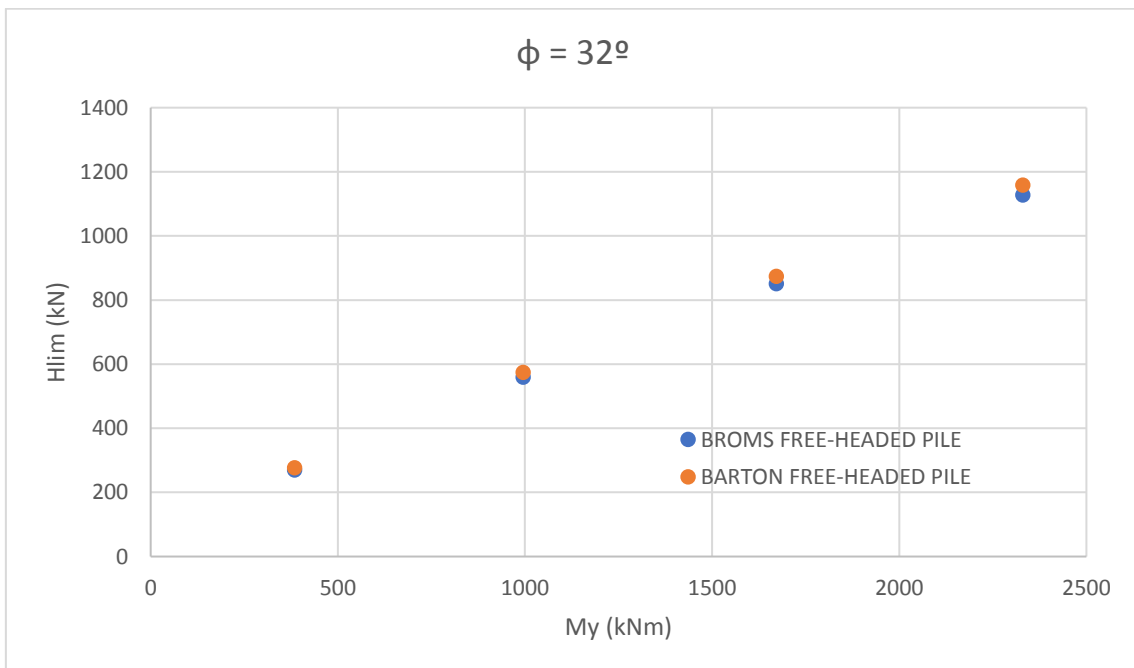
Figure 3-13 Confrontation between the Hlim values obtained according to the models of BROMS (1946b) and BARTON (1982) for the resistance of the soil in the case of the free-headed pile (Φ = 32º).
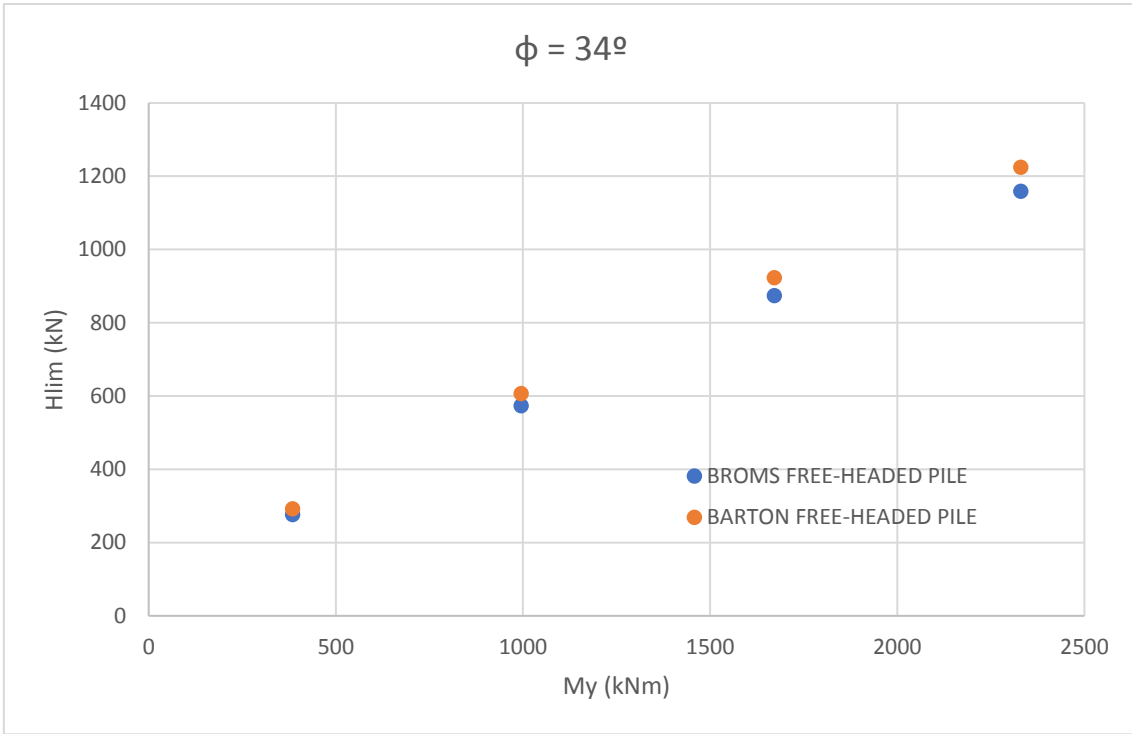
Figure 3-14 Confrontation between the Hlim values obtained according to the models of BROMS (1946b) and BARTON (1982) for the resistance of the soil in the case of the free-headed pile (Φ = 34º).
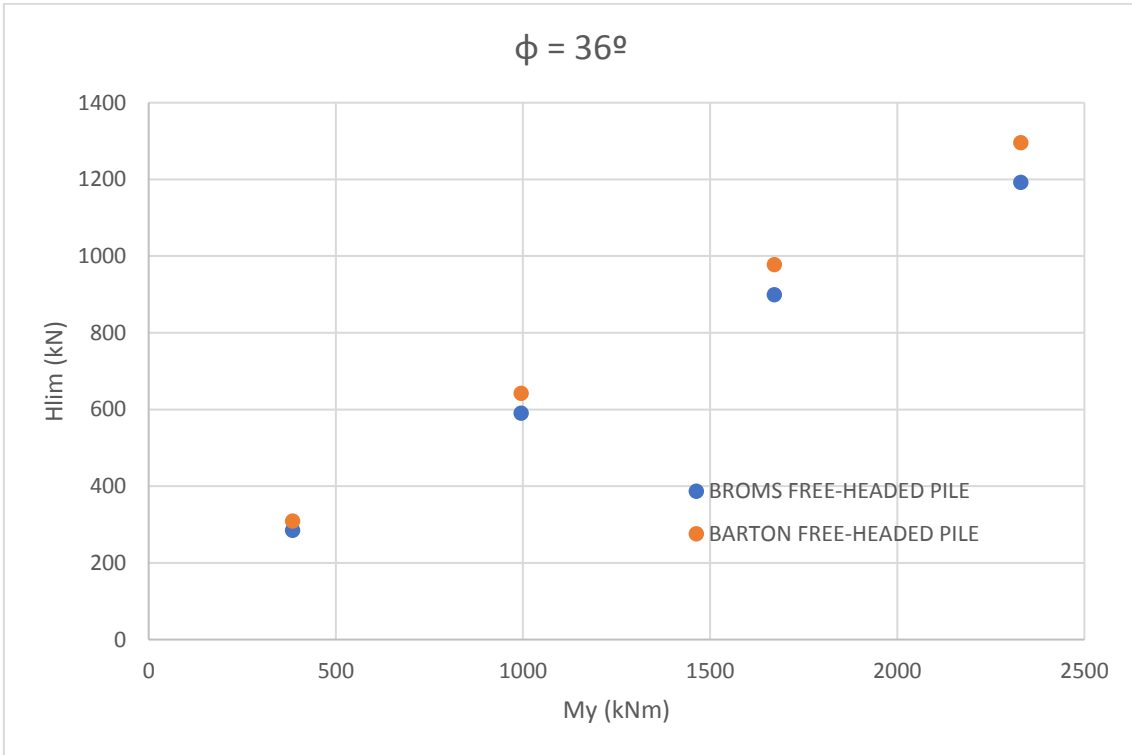
Figure 3-15 Confrontation between the Hlim values obtained according to the models of BROMS (1946b) and BARTON (1982) for the resistance of the soil in the case of the free-headed pile (Φ = 36º).
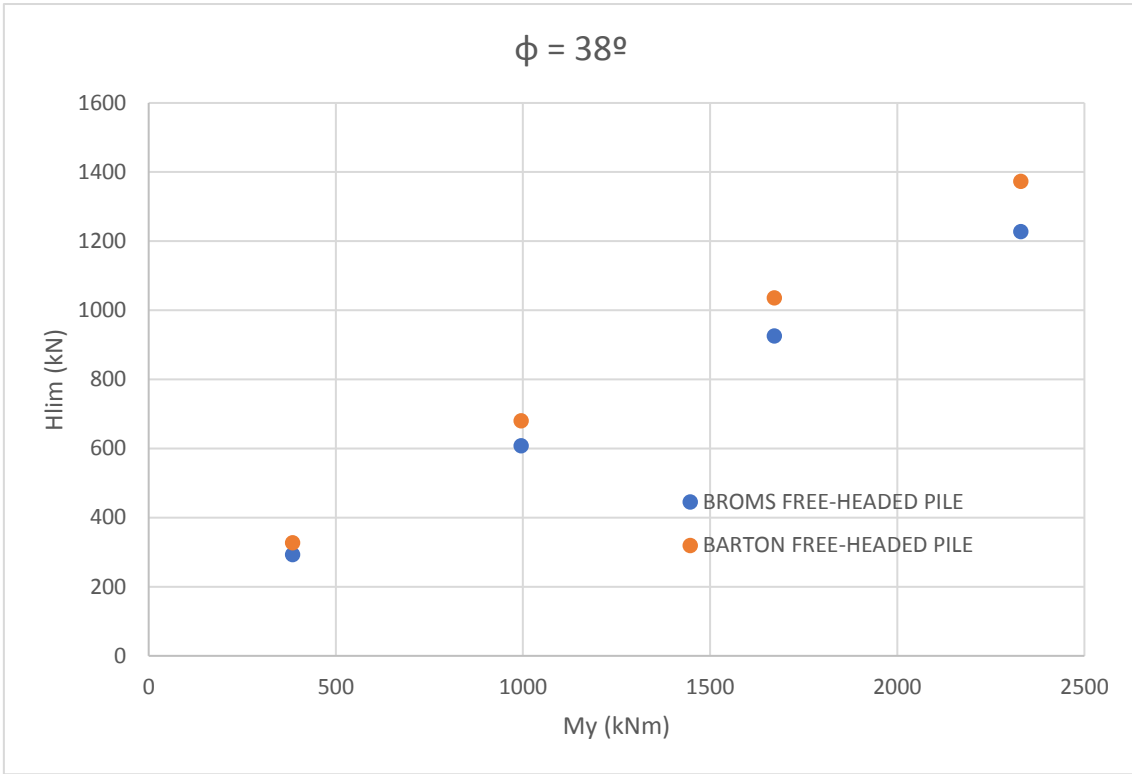
Figure 3-16 Confrontation between the Hlim values obtained according to the models of BROMS (1946b) and BARTON (1982) for the resistance of the soil in the case of the free-headed pile (Φ = 38º).
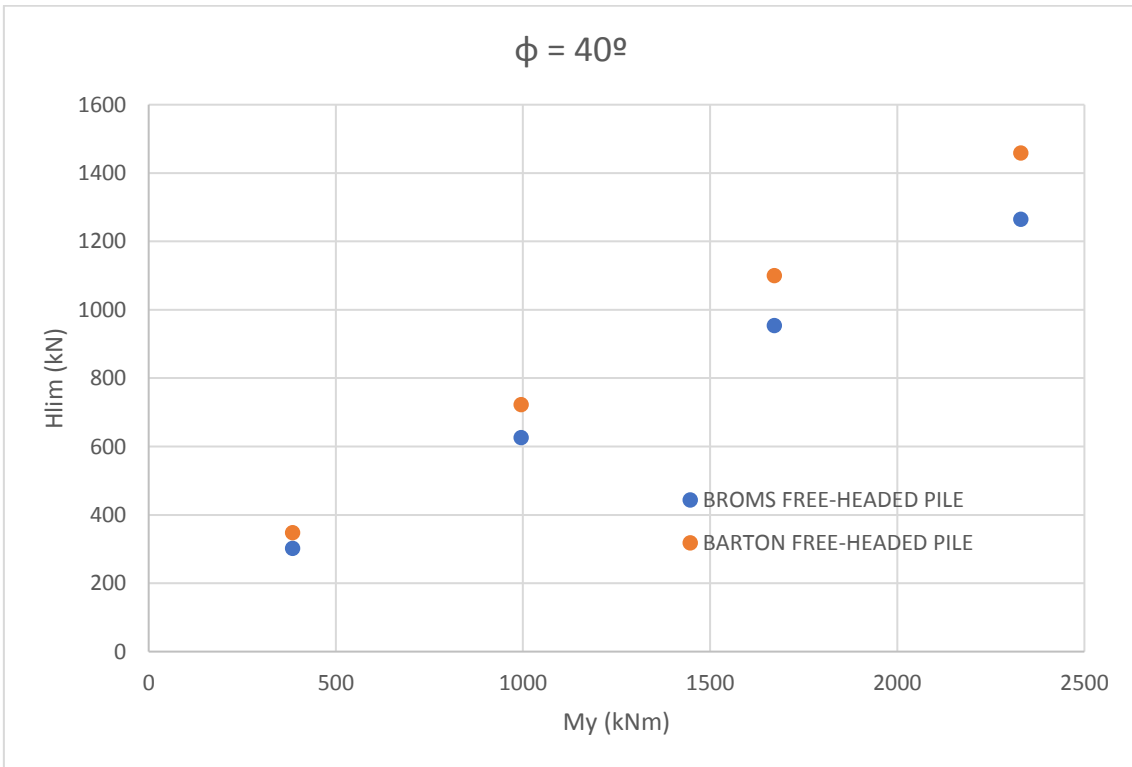
Figure 3-17 Confrontation between the Hlim values obtained according to the models of BROMS (1946b) and BARTON (1982) for the resistance of the soil in the case of the free-headed pile (Φ = 40º).
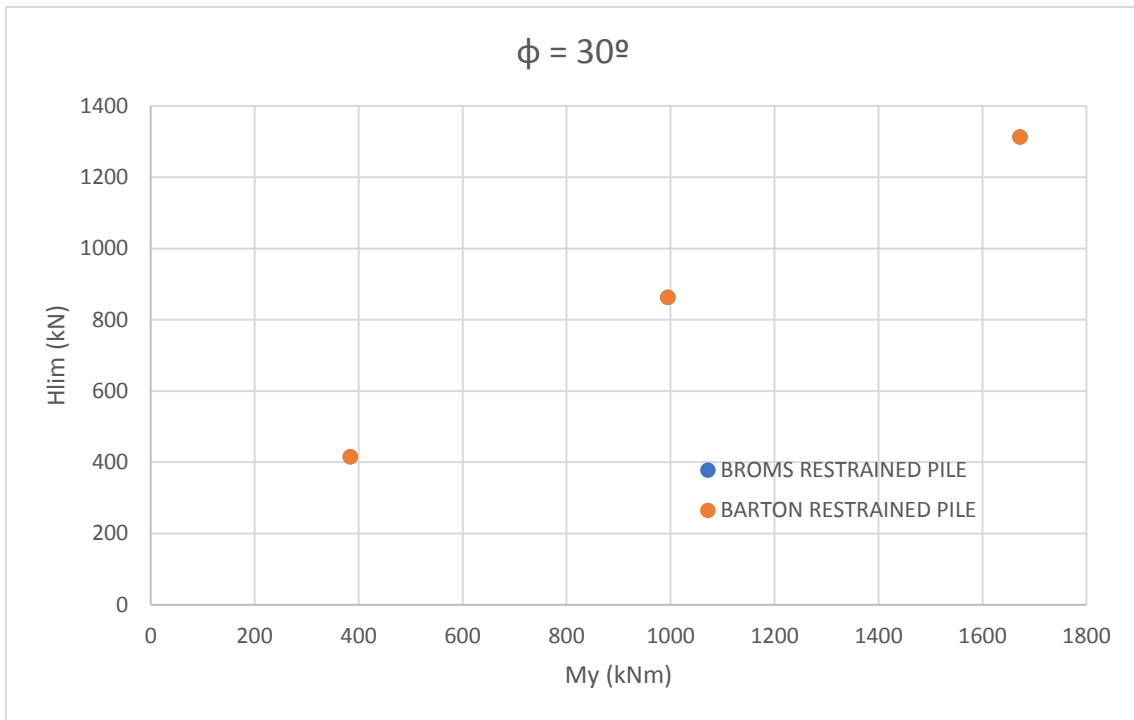
Figure 3-18 Confrontation between the Hlim values obtained according to the models of BROMS (1946b) and BARTON (1982) for the resistance of the soil in the case of the restrained pile (Φ = 30º).
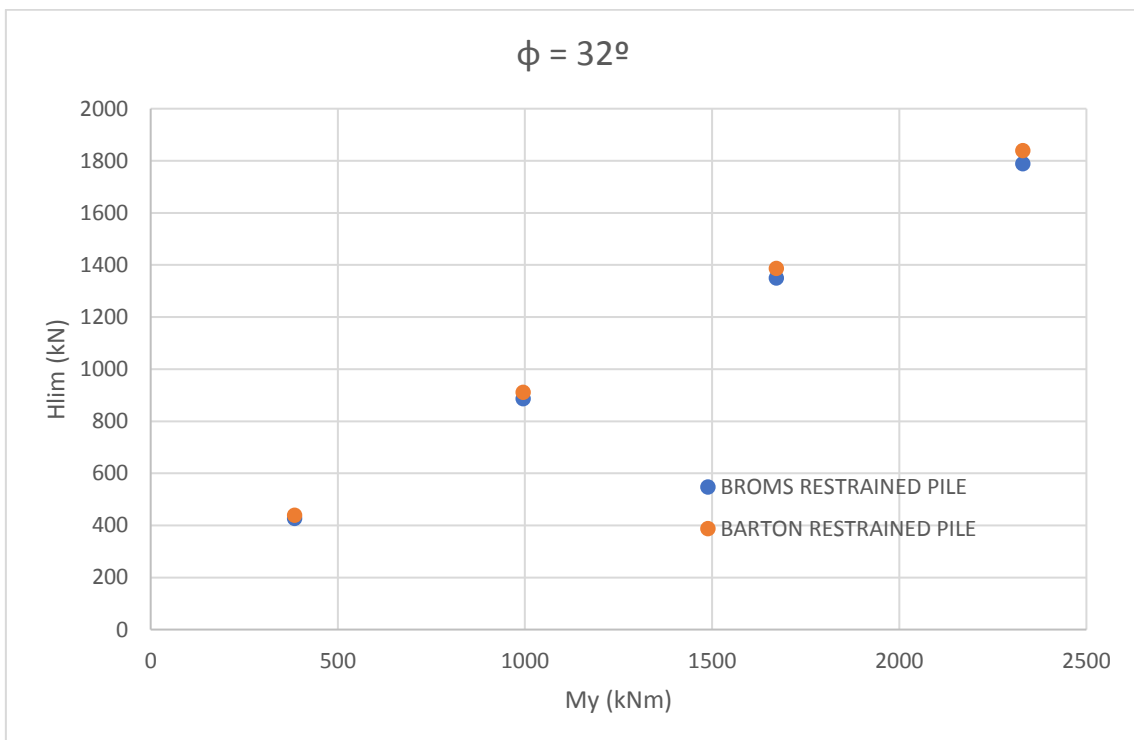
Figure 3-19 Confrontation between the Hlim values obtained according to the models of BROMS (1946b) and BARTON (1982) for the resistance of the soil in the case of the restrained pile (Φ = 32º).
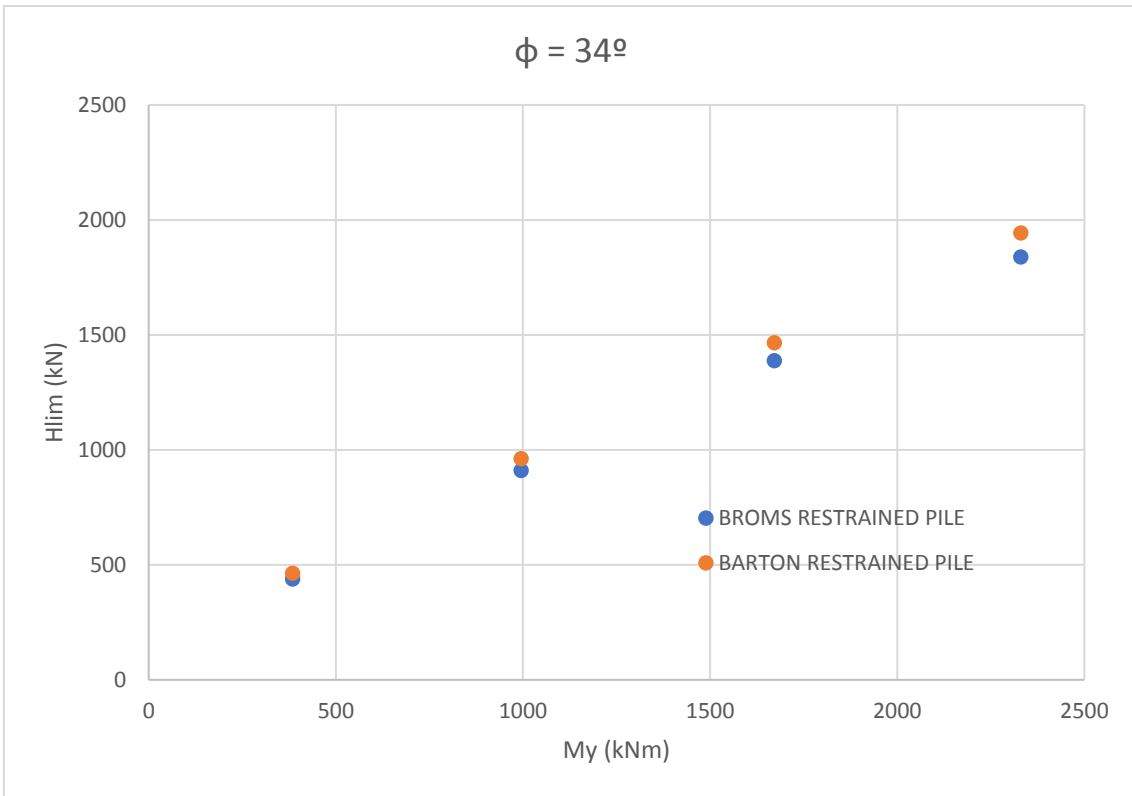
Figure 3-20 Confrontation between the Hlim values obtained according to the models of BROMS (1946b) and BARTON (1982) for the resistance of the soil in the case of the restrained pile (Φ = 34º).
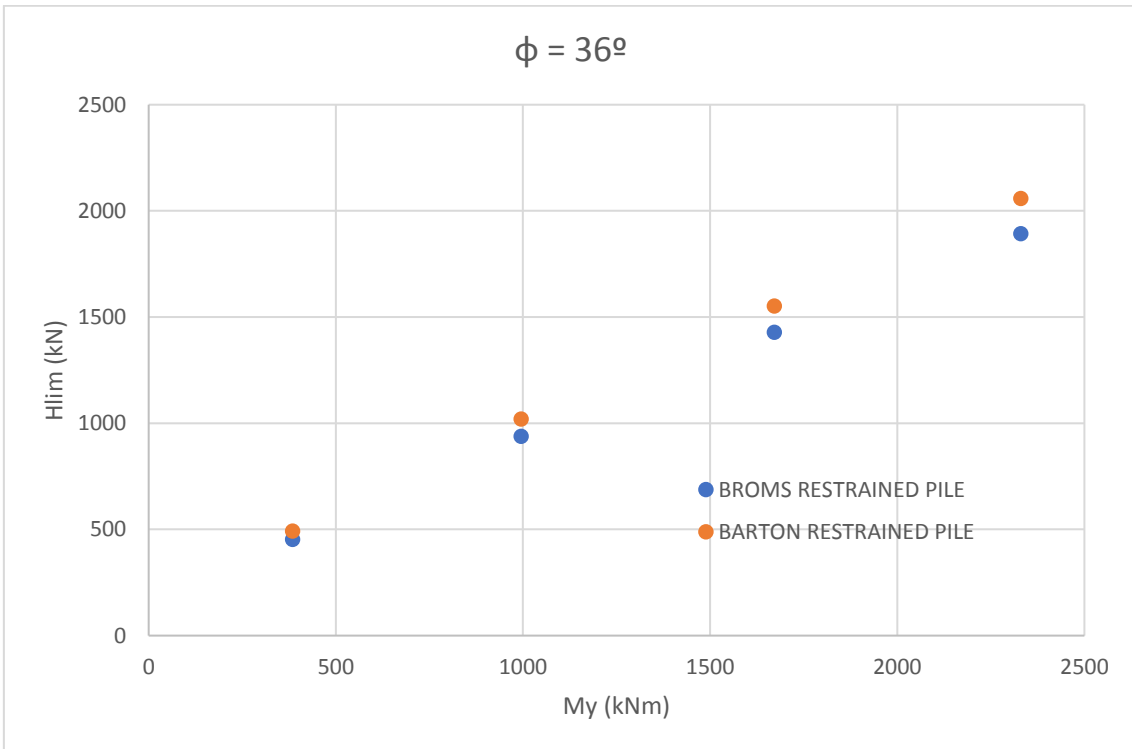
Figure 3-21 Confrontation between the Hlim values obtained according to the models of BROMS (1946b) and BARTON (1982) for the resistance of the soil in the case of the restrained pile (Φ = 36º).
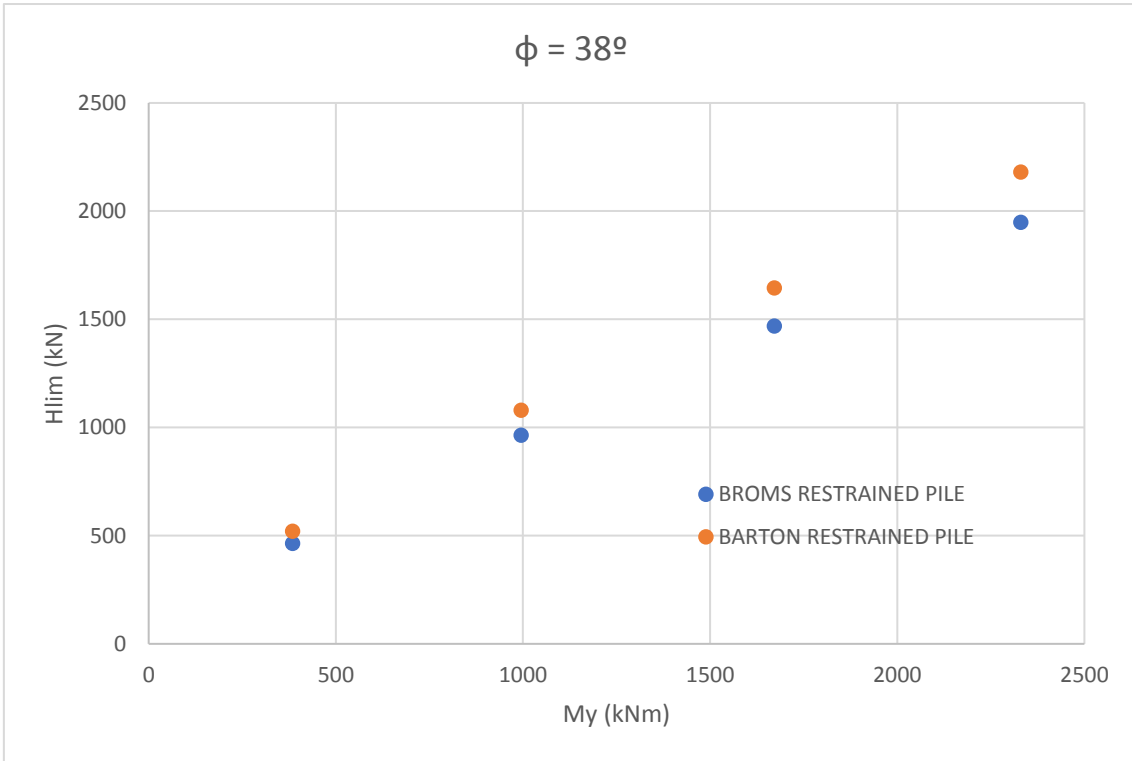
Figure 3-22 Confrontation between the Hlim values obtained according to the models of BROMS (1946b) and BARTON (1982) for the resistance of the soil in the case of the restrained pile (Φ = 38º).
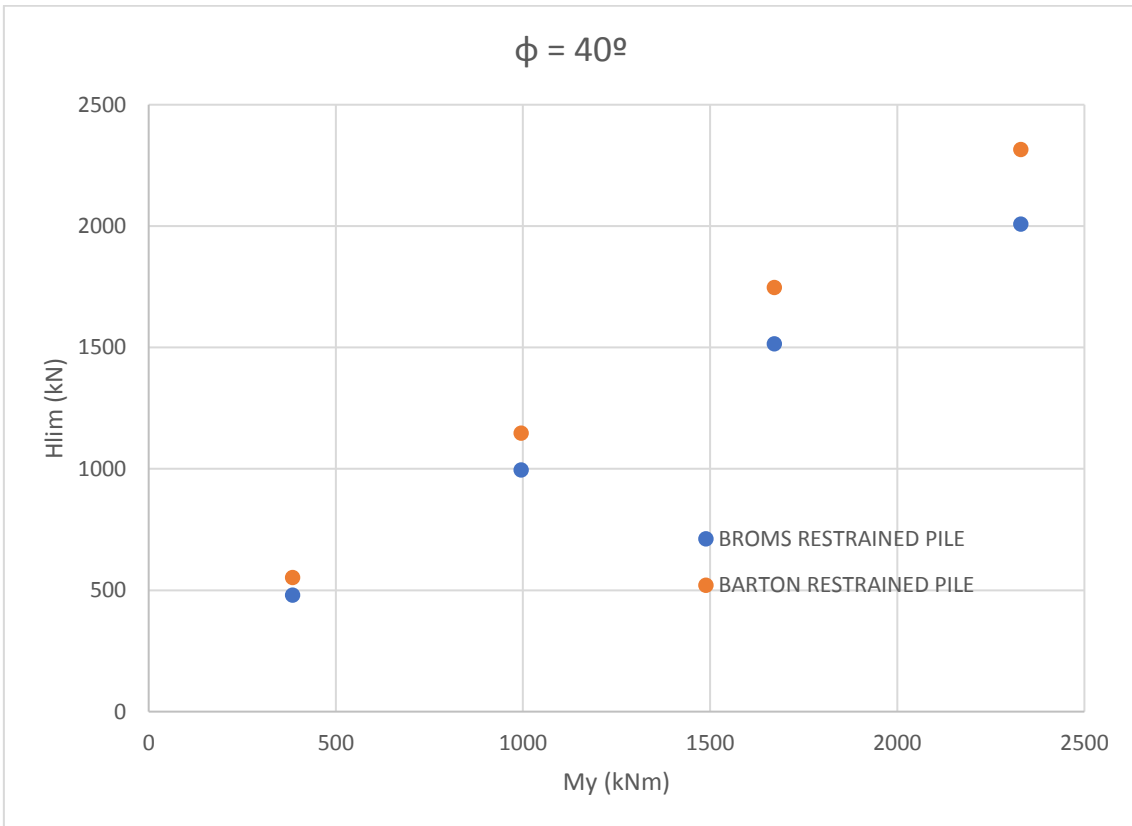
Figure 3-23 Confrontation between the Hlim values obtained according to the models of BROMS (1946b) and BARTON (1982) for the resistance of the soil in the case of the restrained pile (Φ = 40º).

From the confrontation carried out in the graphs, it can be realized that, with the increasing of the friction angle, the differences between the H_{lim} obtained by means of the two models of the resistance of the soil tend to grow up. As it has been established in previous points of this Master's Thesis, the passive coefficient of earth pressure is directly related to the friction angle of the ground. The different growth of the limit horizontal forces lies on the way in which H_{lim} is affected by the passive coefficient of earth pressure depending on the soil's resistance model which has been assumed. If it is considered the model proposed by BROMS (1946b) for the ground's resistance, the limit horizontal force grows up with regards to the factor $3 \cdot K_p$. Nevertheless, if the model adopted for the resistance of the soil is that one proposed by BARTON (1982), then the H_{lim} will increase according to the factor K_p^2. As it can be checked, the value of these factors is the same when the friction angle of the soil is equal to 30º. However, when it is increased (32, 34, 36, 38, 40º), what can be observed is that the values of the H_{lim} calculated with regards to the model of BARTON (1982) are higher than those obtained according to the model of BROMS (1946b). In the next table are presented the, for each friction angle, the values of the passive earth pressure coefficient, as well as the way in which these affect to the H_{lim} depending on the model of the ground's resistance chosen.

φ (º)	φ (rad)	K_p	$3K_p$ (*BROMS*)	K_p^2 (*BARTON*)
30	0,5236	3,0000	9,0000	9,0000
32	0,5585	3,2546	9,7638	10,5923
34	0,5934	3,5371	10,6114	12,5113
36	0,6283	3,8518	11,5555	14,8367
38	0,6632	4,2037	12,6112	17,6715
40	0,6981	4,5989	13,7967	21,1500

This behavior observed, is the same that was mentioned in the Doctoral Thesis of G.LANDI (2005), which established that the criterium proposed by BROMS (1946b) tended to underestimate the resistance of the soil in a 50%, while that, the criterium suggested by BARTON (1982) was only supposed to underestimate it in a 6%. This argument explains the reason because the values of the H_{lim} obtained according to BROMS (1946b) are lower than those calculated based on the model of BARTON (1982).

4 Group Efficiency

Until now, the studies developed in this Master's Thesis were referred to the single pile placed in a granular soil depending on the constraint conditions on its head: restrained, free-headed. However, the case of application that is being discussed on this Thesis, corresponds to a group of piles (4 x 4) working under horizontal loads. In addition to this, it must be pointed that the constraint condition of the group is that one of the restrained pile due to the size of the plate.

As it was mentioned in the introduction of the Thesis, it is being studied the behavior's improvement which would have had the system in the case in which the concrete block, placed between the mole on which the ship hit and the deep foundation of the control tower located on the dock of Genova, would have disposed of a deep foundation consisting on a group of piles 4 x 4. It was expected to find that, by adding the group of piles under the concrete block, the displacements experienced by it were reduced, so that this situation would have resulted in a decreasing of the displacements on the tower's head.
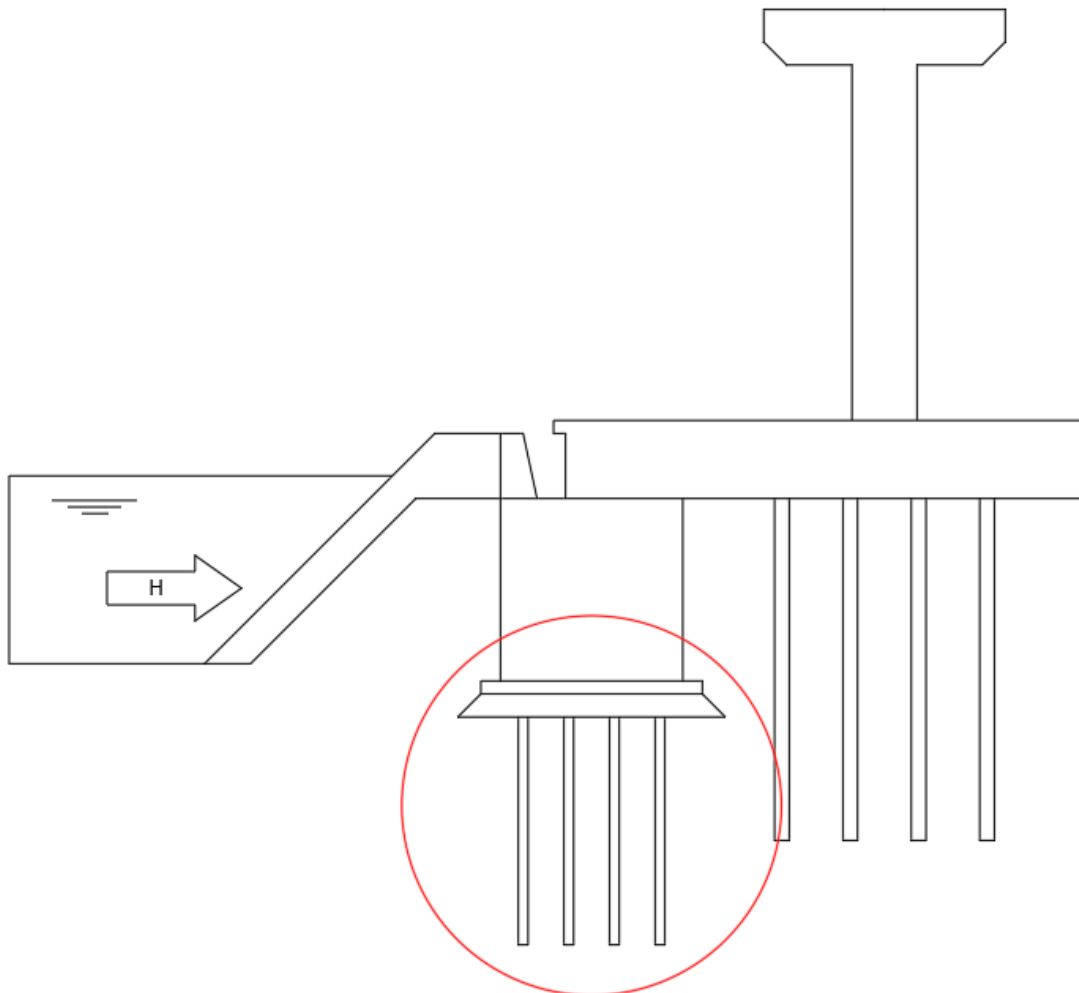
Image 3.24.- Scheme of the deep foundation placed under the concrete block which is being studied.

As it has been discussed on the theoretical base of the Thesis, the behavior which experiences a pile pertaining to a group working under horizontal forces, is not the same as the single pile supports. This is due to the interaction effects between the piles of the group which make that both kind of piles, the single and that one within the group, behave in different ways. One the one hand, the *shadowing effect* explains the different amount of load that is received by a pile located into a group depending on the row to which it pertains. As it was told, is the front row, the one which experiences similar load conditions to those of the single pile. This is because, the first row of the group faces a portion of soil which has not been previously disturbed by another rows of piles. As the soil placed between two rows of piles is disturbed as a consequence of the pushing on it due to the precedent rows, the amount of load absorbed by the piles pertaining to these inner rows is lower. One of the factors which highly influences this phenomenon is the distance between the rows of the group, so that, the higher is it, the less interaction between the piles there is. On the other hand, it must be mentioned the *edge effect*, which explains the different amount of load which receive the piles pertaining to a same row within the group. When the distance between them is low, the wedges of soil located on the back of the piles, formed due to the pushing of the piles in the soil, can overlap between them. This effect makes that the forces supported by the piles located on the edges of the group are higher than those experienced for the inner piles of the row. Nevertheless, this second effect of interaction is not as important as the *shadowing effect*.

The different behavior of the single pile and the pile pertaining to a group beacuse of the interaction effects, results in the appearance of the concept of *efficiency*, which correlates the average amount of load absorbed by the pile of the group and the force experienced by the single pile, when the displacements on their heads are the same. Some examples have been showed in the Theoretical base of the Thesis.

To discuss the effects of the pile's efficiencies in the group, have been carried out some studies on groups of piles with different dimensions. Specifically, have been calculated the efficiencies of the piles pertaining to two different groups (2 x 2; 4 x 4) working under horizontal forces. On these firsts cases of study the sizes of the piles are:

- Length equal to 20 meters.
- Diameter equal to 0,8 meters.

According to these efficiencies, have been also calculated the values of the forces acting on the piles of the group to determine the displacements that these would experience behaving as the single pile. The development of this process is going to be presented below.

4.1   Group 2 x 2.

First of all, it must be defined some of the features of the problem. The horizontal force acting on the group of piles 2 x 2, it has been considered $T_{Total} = 1900\ kN$. Moreover, it has been assumed an average value of the lateral reaction coefficient of the soil $k_h = 7{,}5\ N/cm^3$, according to what it is established in *FONDAZIONI* (CARLO VIGGIANI) for a soil composed by sands not immersed. As the number of piles of this group is equal to 4, the average force acting on each of them comes:

$$T_{pile} = \frac{T_{Total}}{4} = 475\ kN$$

In this analysis, it has been studied how the distance between the piles within the group influences on the efficiency. For this reason, have been calculated the efficiencies of the piles for different distances between the rows. These have been obtained considering a diameter of the piles equal to 0,8 meters and varying the relative distance between them s/D from 1 to 7.

Based on the model proposed by OCHOA & O'NEILL (1989), it is necessary to remind that, to calculate the efficiency of the piles pertaining to the row placed in the first position, it must be taken into account the next expression:

$$e_{r1} = 0,70 \cdot \left(\frac{S}{D}\right)^{0,26} \quad for \quad \left(\frac{S}{D}\right) \leq 4,00 \qquad (4.1.)$$

Subsequently, to determine the efficiency of the piles pertaining to the back row, it is necessary to consider:

$$e_{r2} = 0,48 \cdot \left(\frac{S}{D}\right)^{0,38} \quad for \quad \left(\frac{S}{D}\right) \leq 7,00 \qquad (4.2.)$$

To consider the edge effect in the calculation of the efficiencies of the piles, it must be used the expression proposed by these authors for the piles which are arranged orthogonally to the direction of the forces.

$$e_{orto} = 0,64 \cdot \left(\frac{S}{D}\right)^{0,34} \quad for \quad \left(\frac{S}{D}\right) \leq 3,75 \qquad (4.3.)$$

Consequently, the efficiencies of the piles pertaining to both rows have been obtained by means of the next expressions:

$$e_{pile-row1} = e_{r1} \cdot e_{orto} \qquad (4.4.)$$

$$e_{pile-row2} = e_{r2} \cdot e_{orto} \qquad (4.5.)$$

In the following table are presented the values of the efficiencies obtained for each pile of the group 2 x 2. It can be appreciated that the maximum value obtained for the efficiency is equal to 1. When the efficiency of a pile is equal to the unit, it means that there are not interaction

phenomenon between the piles. It can be observed that this situation is achieved when the relative distance between the rows of piles is approximately 7D, where D is the diameter of the piles.

s (m)	D (m)	s/D	e_{r1}	e_{r2}	e_{orto}	$e_{pile-row1}$	$e_{pile-row2}$
0,8		1	0,7000	0,4800	0,6400	0,4480	0,3072
1,2		1,5	0,7778	0,5600	0,7346	0,5714	0,4113
1,6		2	0,8382	0,6246	0,8101	0,6790	0,5060
2		2,5	0,8883	0,6799	0,8739	0,7763	0,5942
2,4		3	0,9314	0,7287	0,9298	0,8661	0,6776
2,8		3,5	0,9695	0,7727	0,9799	0,9500	0,7571
3,2	0,8	4	1,0000	0,8129	1,0000	1,0000	0,8129
3,6		4,5	1,0000	0,8501	1,0000	1,0000	0,8501
4		5	1,0000	0,8848	1,0000	1,0000	0,8848
4,4		5,5	1,0000	0,9174	1,0000	1,0000	0,9174
4,8		6	1,0000	0,9483	1,0000	1,0000	0,9483
5,2		6,5	1,0000	0,9776	1,0000	1,0000	0,9776
5,6		7	1,0000	1,0000	1,0000	1,0000	1,0000

Afterwards, have been calculated the horizontal forces acting on the single pile with regards to the average force, which would act on each pile of the group in the case in which the efficiency is equal to 1. According to the definition of the efficiency:

$$\eta = \frac{T_{pile}}{n \cdot T_{single\ pile}} \quad \rightarrow \quad T_{single\ pile} = \frac{T_{pile}}{\eta \cdot n} \qquad (4.6.)$$

Considering the values of the efficiency showed in the table above, the horizontal forces acting on the single piles are presented in the next table:

Tsp row 1 (kN)	Tsp row2 (kN)
1060,27	1546,22
831,31	1154,75
699,52	938,71
611,86	799,38
548,46	701,04
500,01	627,40
475,00	584,35
475,00	558,77
475,00	536,84
475,00	517,74
475,00	500,90
475,00	485,90
475,00	475,00

Finally, based on the horizontal forces presented in the previous table, have been calculated the displacements on the heads of the single piles in each case. To make this calculation, it has been used an Excel worksheet provided by *Engineering and Geotechnics SRL*. This has been particularized for the features of the piles and the mechanical properties of the ground.

RESTRAINED PILE WORKING UNDER HORIZONTAL FORCES

PROJECT:

INPUT DATA:

Diameter of the pile (D):	0,8	(m)
Length of the pile (L)	20	(m)
Lateral reaction coefficient (k_h):	7,5	(N/cm^3)
Acting horizontal force (T):	Previous table	(kN)
fck of the concrete:	30,0	(MPa)
fcm of the concrete:	38,0	(MPa)
Ecls ($E = 22000(fcm/10)^{0.3}$):	32837	(MPa)
J ($J = \pi*D^4/64$):	2010619	(cm^4)
λ (elastic length $\lambda = (4*EJ/k_h*D)^{1/4}$):	458,04	(cm)
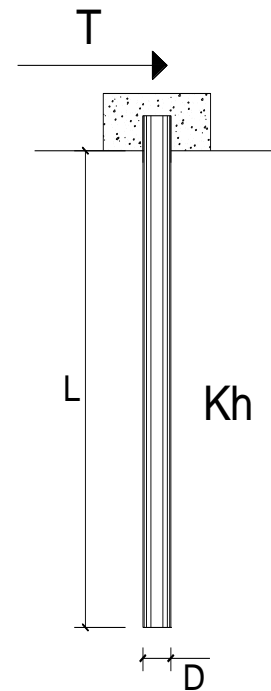
In the following table are presented the values of the displacements on the pile's head obtained with the Excel worksheet with regards to the parameters predefined and to the values of the forces calculated:

$T_{sp\ row1}$ (kN)	$T_{sp\ row2}$ (kN)	$u_{pile\ row1}$ (cm)	$u_{pile\ row2}$ (cm)
1060,27	1546,22	3,858	5,626
831,31	1154,75	3,025	4,202
699,52	938,71	2,545	3,416
611,86	799,38	2,226	2,909
548,46	701,04	1,996	2,551
500,01	627,40	1,819	2,283
475,00	584,35	1,728	2,126
475,00	558,77	1,728	2,033
475,00	536,84	1,728	1,953
475,00	517,74	1,728	1,884
475,00	500,90	1,728	1,823
475,00	485,90	1,728	1,768
475,00	475,00	1,728	1,728

Finally, to analyze the effect of the relative distance between the piles on the displacements experienced by their heads, it has been represented the ratio $u_{pile}/u_{single\ pile}$ with regards to the relative distance between the piles.

- u_{pile} corresponds to the displacements reached on the head of each pile of the group.
- $u_{single\ pile}$ is the displacement that would experience the single pile. It is equal to the displacement that is achieved in the head of a pile whose efficiency is equal to the unit.

u_{row1} (cm)	u_{row2} (cm)	$u_{row1}/u_{single\ pile}$	$u_{row2}/u_{single\ pile}$
3,858	5,626	2,232	3,255
3,025	4,202	1,750	2,431
2,545	3,416	1,473	1,976
2,226	2,909	1,288	1,683
1,996	2,551	1,155	1,476
1,819	2,283	1,053	1,321
1,728	2,126	1,000	1,230
1,728	2,033	1,000	1,176
1,728	1,953	1,000	1,130
1,728	1,884	1,000	1,090
1,728	1,823	1,000	1,055
1,728	1,768	1,000	1,023
1,728	1,728	1,000	1,000
$u_{singlepile}$		1,728	1,728
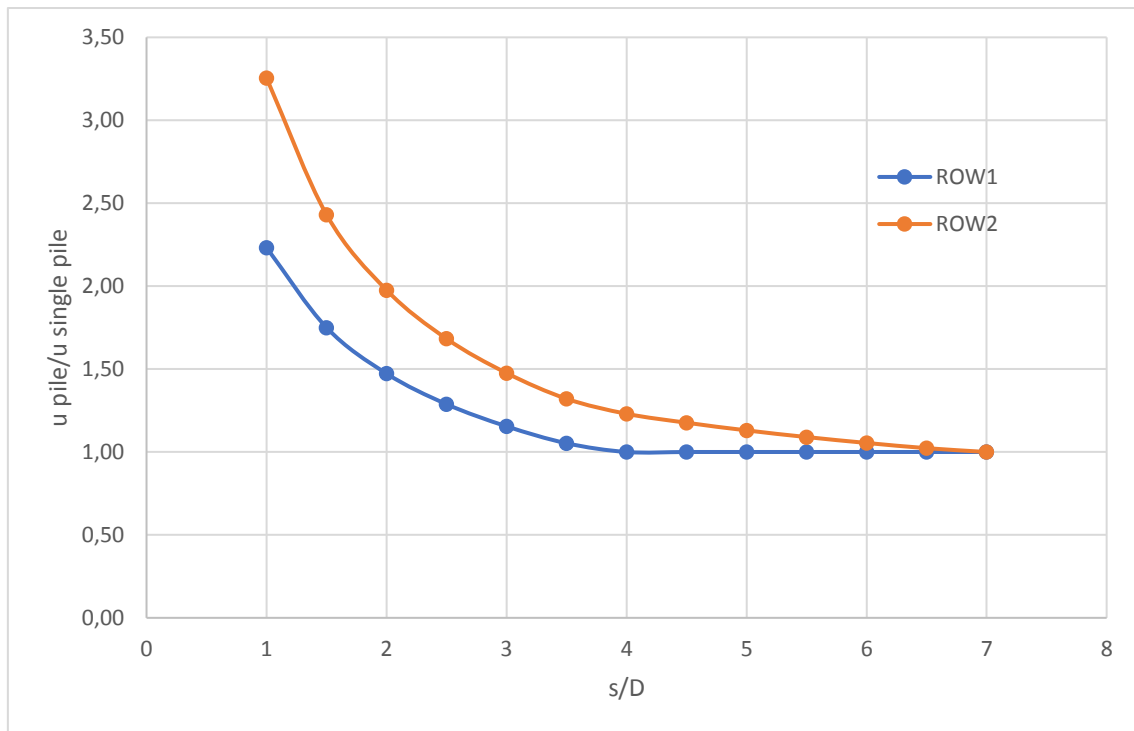
Figure 4-1 Variation of the relative displacements of the pile's head with regards to the relative distance between the piles and depending on the row to which the piles pertain within the group 2x2.

4.2 Group 4 x 4.

In the same way, it has been analyzed the case of a group composed by sixteen piles (4 x 4). The diameters of the piles are equal to 0,8 meters and their lengths are equal to 20 meters. In this case, it has been maintained the value of the lateral reaction coefficient as 7,5 N/cm^3. Otherwise, the horizontal force acting on the group has been increased until the 7700 kN. As the group consists of sixteen piles, the average load, which each pile of the group absorbs, is obtained as:

$$T_{pile} = \frac{T_{Total}}{16} = 481,25 \ kN$$

In the case of the group of piles 4 x 4, the calculation of the efficiencies has been also carried out by means of the equations proposed by OCHOA & O'NEILL (1989) for the piles placed on the front and on the back rows, as well as for the piles that are arranged orthogonally to the direction of the horizontal force. However, in this case, the process is more complex than in the group 2 x 2. To calculate the efficiencies of each pile, the group has to be subdivided in some subgroups.

Firstly, the plate composed by 16 piles has been split into two subgroups. The first subgroup consists on the 8 piles pertaining to the front and second rows of the group. The second subgroup is that one conformed by the 8 piles pertaining to the third and the back rows. To differentiate between the piles from the first and the second subgroup in the calculation of the

efficiencies, to the first subgroup it has been assigned the equation 3.22., while the equation 3.23. has been assigned to the piles pertaining to the second subgroup.

Secondly, each subgroup has been subdivided in two rows. The same process as that one followed to make the decomposition of the group into two subgroups has been assumed to divide the subgroups into two rows. Consequently, to calculate the efficiency of the piles pertaining to the front row of each subgroup it has been taken into account the equation 3.22.. Otherwise, the piles pertaining to the back row of each subgroup is affected by the equation 3.23.. These two equations refers to the expressions proposed by OCHOA & O'NEILL (1989) to calculate the efficiency of piles placed on the front and on the back row of a group respectively.

Successively, after considering the *shadowing effect* in the calculation of the efficiencies of the piles pertaining to a group 4 x 4, it must be introduce the *edge effect*. To do this, the first step is to subdivide each row in two sub rows. To consider this division on the calculation of the efficiencies, each efficiency from those obtained with regards to the process explained in the precedent paragraph, must be multiplied by the equation 3.24. from those proposed by OCHOA & O'NEILL (1989).

Finally, to determine the efficiency of each single pile of the group, it is necessary to subdivide the sub rows into two single piles. To take into account this new subdivision of the group, the efficiencies calculated according to the previous paragraph, must be multiplied another time by the expression 3.24. proposed by OCHOA & O'NEILL (1989), which refers to the efficiency of two piles arranged orthogonally to the direction of the force.

To clarify the decomposition process, described in the precedent paragraphs, it is presented the sequence followed by means of the image 3.26..
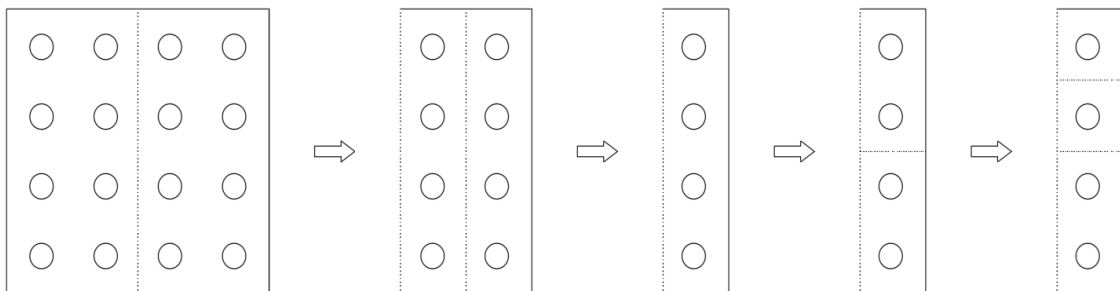
Figure 4-2 Process of decomposition of the group 4 x 4 to calculate the efficiencies of each single pile of the group. First of all, the group is divided into two subgroups. Secondly, each subgroup is subdivided into two rows. Successively each row is divided into two sub rows and finally, each sub row is divided into two piles.

Subsequently, are presented the expressions which have been considered to calculate the efficiency of the piles of the group. After the calculation, it has been noticed that the value of the efficiency for the piles located on the same row is the same. For these reason, the expressions considered to obtain the efficiencies of the four piles pertaining to the same row is the same.

$$e_{pile\ row\ 1} = e_{group1} \cdot e_{row1} \cdot e_{orto}^2 = \left[0{,}70 \cdot \left(\frac{S}{D}\right)^{0{,}26}\right]^2 \cdot \left[0{,}64 \cdot \left(\frac{S}{D}\right)^{0{,}34}\right]^2 \qquad (4.7.)$$

$$e_{pile\ row\ 2} = e_{group1} \cdot e_{row2} \cdot e_{orto}^2 = 0{,}70 \cdot \left(\frac{S}{D}\right)^{0{,}26} \cdot 0{,}48 \cdot \left(\frac{S}{D}\right)^{0{,}38} \cdot \left[0{,}64 \cdot \left(\frac{S}{D}\right)^{0{,}34}\right]^2 \quad (4.8.)$$

$$e_{pile\ row\ 3} = e_{group2} \cdot e_{row1} \cdot e_{orto}^2 = 0{,}48 \cdot \left(\frac{S}{D}\right)^{0{,}38} \cdot 0{,}70 \cdot \left(\frac{S}{D}\right)^{0{,}26} \cdot \left[0{,}64 \cdot \left(\frac{S}{D}\right)^{0{,}34}\right]^2 \quad (4.9.)$$

$$e_{pile\ row\ 4} = e_{group2} \cdot e_{row2} \cdot e_{orto}^2 = \left[0{,}48 \cdot \left(\frac{S}{D}\right)^{0{,}38}\right]^2 \cdot \left[0{,}64 \cdot \left(\frac{S}{D}\right)^{0{,}34}\right]^2 \qquad (4.10.)$$

According to the equations (3.28.), (3.29.), (3.30.) and (3.31.), have been obtained the efficiencies of the sixteen piles which conform the group 4 x 4. As it has been mentioned previously, the efficiency of the four piles that pertain to a same row within the group is the same. For this reason, in the table are only presented four columns which corresponds to the efficiencies of the piles placed on the front, second, third and fourth row respectively.

As in the case of the group 2 x 2, for the group 4 x 4, also has been studied the effect of the relative distance between the rows of piles s/D. Considering a diameter of the piles equal to 0,8 meters, the ratio s/D has been varied from 1 to 7. In the following table, have been colored in orange the cases which are difficult to find in the real projects. In addition to this, the most common cases in the real projects have been highlighted in the table in blue.

s (m)	D (m)	s/D	$e_{pile\ row1}$	$e_{pile\ row2}$	$e_{pile\ row3}$	$e_{pile\ row4}$
0,8		1	0,2007	0,1376	0,1376	0,0944
1,2		1,5	0,3265	0,2350	0,2350	0,1692
1,6		2	0,4611	0,3436	0,3436	0,2561
2		2,5	0,6027	0,4613	0,4613	0,3531
2,4		3	0,7501	0,5868	0,5868	0,4591
2,8		3,5	0,9025	0,7192	0,7192	0,5732
3,2	0,8	4	1,0000	0,8129	0,8129	0,6608
3,6		4,5	1,0000	0,8501	0,8501	0,7226
4		5	1,0000	0,8848	0,8848	0,7829
4,4		5,5	1,0000	0,9174	0,9174	0,8417
4,8		6	1,0000	0,9483	0,9483	0,8992
5,2		6,5	1,0000	0,9776	0,9776	0,9556
5,6		7	1,0000	1,0000	1,0000	1,0000

After having calculated the efficiencies, have been determined the horizontal forces acting on the single pile with regards to the average force, which would act on each pile of the group in

the case in which the efficiency is equal to 1. According to the definition of the efficiency (equation 3.27.) and the values of the efficiencies obtained for the piles of the four rows which conform the group, the horizontal forces acting on the single piles are presented in the next table:

s (m)	D (m)	s/D	$T_{sp\ row1}$ (kN)	$T_{sp\ row2}$ (kN)	$T_{sp\ row3}$ (kN)	$T_{sp\ row4}$ (kN)
0,8		1	2398	3497	3497	5100
1,2		1,5	1474	2048	2048	2844
1,6		2	1044	1401	1401	1880
2		2,5	799	1043	1043	1363
2,4		3	642	820	820	1048
2,8		3,5	533	669	669	840
3,2	0,8	4	481	592	592	728
3,6		4,5	481	566	566	666
4		5	481	544	544	615
4,4		5,5	481	525	525	572
4,8		6	481	507	507	535
5,2		6,5	481	492	492	504
5,6		7	481	481	481	481

Successively, based on the horizontal forces showed in the precedent table, have been calculated the displacements on the heads of the single piles in each case. To develop this calculation, it has been used the same Excel worksheet, provided by the *ENVIRONMENT AND GEOTECHNIC SRL*, which was used in the case of the group 2 x 2. This has been particularized for the characteristics of the piles and the mechanical properties of the soil predefined.

$u_{pile\ row1}$ (cm)	$u_{pile\ row2}$ (cm)	$u_{pile\ row3}$ (cm)	$u_{pile\ row4}$ (cm)
8,72498	12,72393	12,72393	18,55573
5,36358	7,45042	7,45042	10,34919
3,79777	5,09638	5,09638	6,83903
2,90560	3,79612	3,79612	4,95957
2,33463	2,98415	2,98415	3,81437
1,94036	2,43473	2,43473	3,05506
1,75114	2,15425	2,15425	2,65016
1,75114	2,05996	2,05996	2,42324
1,75114	1,97911	1,97911	2,23677
1,75114	1,90872	1,90872	2,08047
1,75114	1,84664	1,84664	1,94735
1,75114	1,79132	1,79132	1,83241
1,75114	1,75114	1,75114	1,75114

Finally, to analyze the effect of the relative distance between the piles *s/D* on the displacements experienced by their heads, it has been represented, for the piles of each one of the four rows, the ratio $u_{pile}/u_{single\ pile}$ with regards to *s/D*.

- u_{pile} corresponds to the displacements reached on the head of each pile of the group.
- $u_{single\ pile}$ is the displacement that would experience the single pile. It is equal to the displacement that is achieved in the head of a pile whose efficiency is equal to the unit.

On the one hand, the values of the **u_{pile}** have been taken from the previous table. On the other hand, the values of the $u_{single\ pile}$ are presented in the following table:

$u_{single\ pile\ row1}$ (cm)	$u_{single\ pile\ row2}$ (cm)	$u_{single\ pile\ row3}$ (cm)	$u_{single\ pile\ row4}$ (cm)
1,75114	1,75114	1,75114	1,75114

Consequently, the obtained values of the ratio **u_{pile} / $u_{single\ pile}$** with regards to the relative distance between the piles **s/D** are:

s/D	$u_{pile}/u_{single\ pile}$			
	PILE row 1	PILE row 2	PILE row 3	PILE row 4
1	4,982	7,266	7,266	10,596
1,5	3,063	4,255	4,255	5,910
2	2,169	2,910	2,910	3,905
2,5	1,659	2,168	2,168	2,832
3	1,333	1,704	1,704	2,178
3,5	1,108	1,390	1,390	1,745
4	1,000	1,230	1,230	1,513
4,5	1,000	1,176	1,176	1,384
5	1,000	1,130	1,130	1,277
5,5	1,000	1,090	1,090	1,188
6	1,000	1,055	1,055	1,112
6,5	1,000	1,023	1,023	1,046
7	1,000	1,000	1,000	1,000

These results have been plotted (image 3.27.) to discuss the different trends observed from the analysis. After that graph, have been exposed the conclusions to which it has been arrived after the analysis effected on the groups 2 x 2 and 4 x 4 respectively.
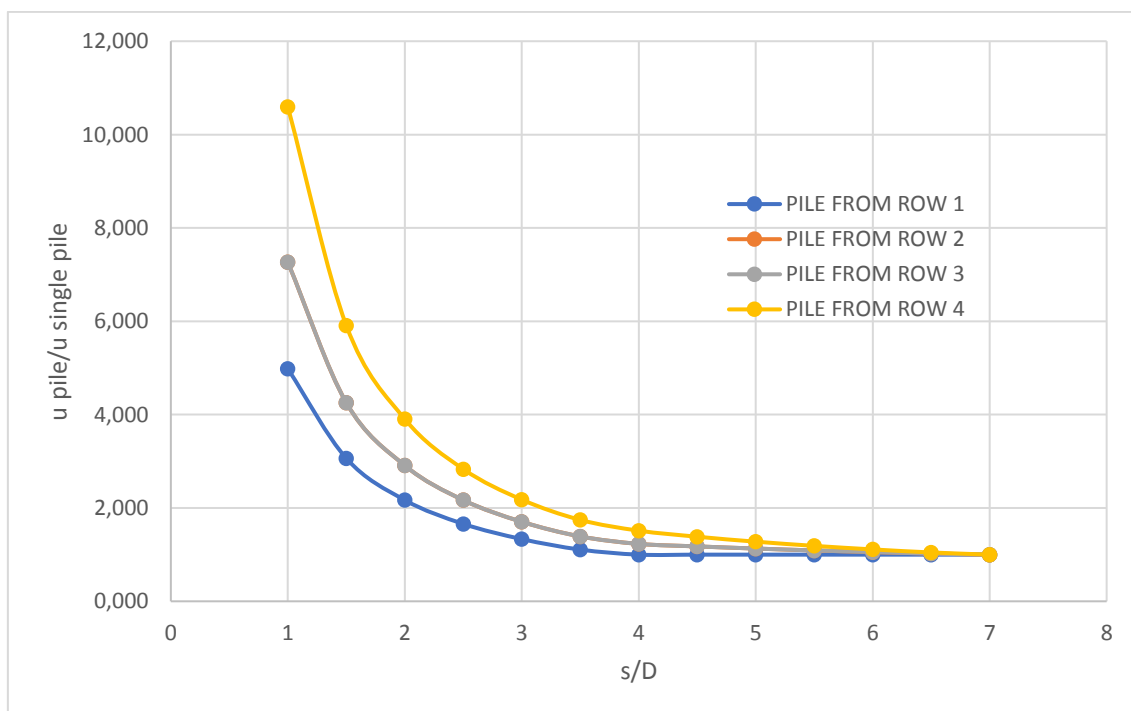
Figure 4-3 Variation of the relative displacements of the pile's head with regards to the relative distance between the piles and depending on the row to which the piles pertain within the group 4x4.

In both graphs, in which has been represented the variation of ratio $u_{pile,i}/u_{single\ pile}$ with regards to the relative distance between the piles (cases 2 x 2 and 4 x 4), have been observed the same trends. For low values of the ratio s/D, the difference between the displacement in the pile's head for each pile of the group and the displacement in the head of a pile whose efficiency is equal to 1, tends to be very high. It is also appreciated that the ratio $u_{pile,i}/u_{single\ pile}$ in the case of the front row is lower than in the back rows. This behavior means, as it was exposed in the theoretical base, that the front row tends to behave in a similar way that the single pile does when piles are working under horizontal loads.

Another aspect which has been realized in both cases (2 x 2, 4 x 4) is that, when the ratio s/D is increased, the differences between the displacement on the head of the piles pertaining to the group and the displacement on the head of a pile whose efficiency is equal to 1, tend to decrease achieving an asymptotic value of 1 for values of the distance between the piles higher than 4 times their diameters.

From the results obtained, what can be concluded is that, when the relative distance between the piles is very low, such as the cases comprised between $1 \leq s/D \leq 2$, it is very important to consider the efficiency of the piles. Otherwise, there is a high risk of underestimating the maximum displacements on the pile's head.

Obviously, the values of the efficiencies obtained for relative distances between $1 \leq s/D \leq 2$, are not usual in the real projects. The most commonly values of the relative distance in practice are those comprised between $3 \leq s/D \leq 4$.

5   Application to a real scale case: The Pilot tower of Genova Docks

The study which is being carried out on this Master's Thesis is related to an incident which took place a few years ago in the dock of Genova. A cargo ship impacted against the mole of the dock. The problem surged because the control tower was located very near to the point where the ship hit the mole. This resulted in the collapse of the tower as a consequence of the high displacements which were achieved on its head. The ship pushed the mole, so that the soil placed between the foundation of the tower and the inclined wall of the mole in which the ship beat was highly compressed. This phenomenon induced important loads on the foundation of the tower. However, the true responsible of pushing the foundation was a concrete block which was located next to the piles between the mole and the tower's foundation. The compression of the soil gave place to the displacement of the block, pushing the piles consisting on the foundation of the tower.

In the real case, the concrete block was not restrained into the soil by a deep foundation. It is thought that, this lack of the piles under the block was the responsible of the big displacements which it experienced and that resulted in the collapse of the tower's foundation. As it was described in the foreword, the main aim of this Master's thesis is to determine which would have happened in the case in which the concrete block would have disposed of a deep foundation under its bottom surface.

The described problem has been modeled by a finite elements software called *PLAXIS* to determine the size of the real displacements and the stresses in both cases, the real case (no piles under the concrete block) and the case of study in which the concrete block contained a pile's foundation. The aim of this analysis was to compare the reduction of the displacements achieved in the pilot tower's head in both cases. It must be underlined that, it has been also discussed the differences between a static and dynamic analysis. On purpose, have been conducted four different calculation with the software *PLAXIS* which are listed below:

- Static analysis when the concrete block does not contain the pile's foundation.
- Static analysis when the concrete block is restrained by the pile's foundation.
- Dynamic analysis when the concrete block does not contain the pile's foundation.
- Dynamic analysis when the concrete block is restrained by the pile's foundation.

The aim of these four analysis with *PLAXIS* is to obtain the displacements reached by the concrete block in the case when it is restrained by the foundation and in the real case. Afterwards, considering the output results provided by the software, specifically the equivalent force obtained from the shear stresses' diagram, it has been developed an analysis to determine the displacements on the pile's heads of the group in the real case, with regards to the same process which has been carried out in the cases of the groups 2 x 2 and 4 x 4 respectively, based on the methods proposed by BROMS (1496b) and BARTON (1982). This second analysis has been developed in order to compare the differences between the displacements obtained from *PLAXIS* and those calculated with regards to the analytical process.

Consecutively, are defined the geometrical parameters of the problem. The foundation proposed to restrain the displacements of the concrete block is composed by a group of 16 piles (4 x 4). The principal features of this foundation are listed below:

- Diameter of the piles: 1,2 meters.

- Length of the piles: 20 meters.
- Plate dimensions: 13,5 x 13,5 m^2.
- Relative distance between the piles *s/D = 2,75*.
- Distance between the piles: 3,3 meters.
- Distance between the pile and the edge of the plate: 1,8 meters.

The next image, corresponding to the hypothetical foundation placed under the concrete block, shows the geometrical properties of the plate and the disposition of the piles within the group 4 x 4.
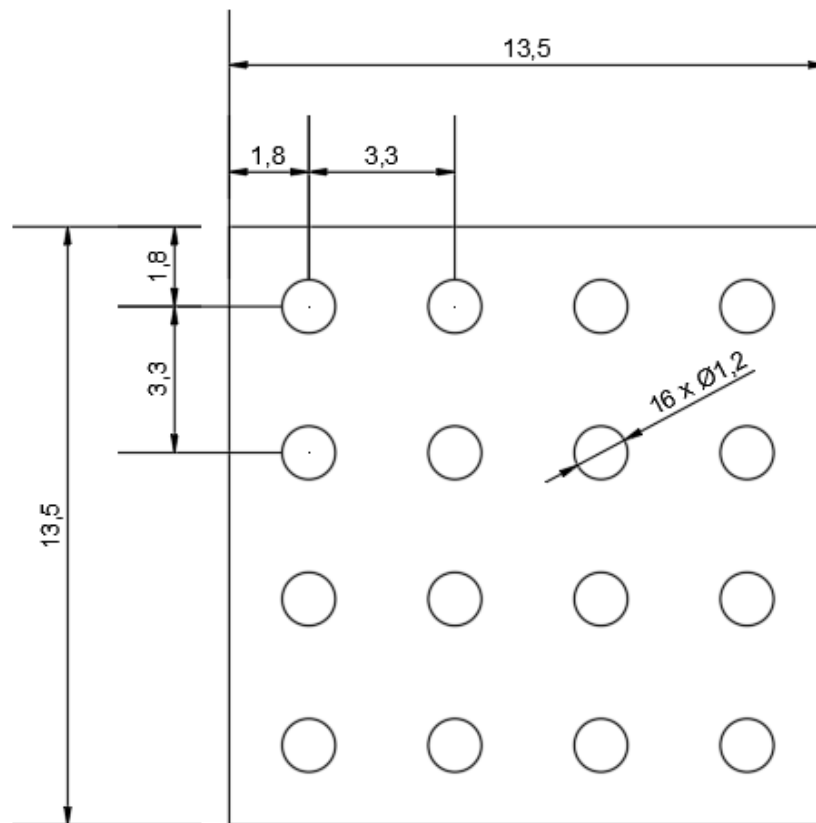
Figure 5-1 Geometrical features of the hypothetical pile foundation placed under the concrete block, whose displacements are being studied. The dimensions are presented in meters.

5.1 Dock layout

The new pilot tower of the Genova's dock is intended to be built next to the east mouth of the port as it has been presented in the figures 1 and 2 respectively. It has been presented two different possible configurations of the mole in the zone of the dock affected by the construction of the new pilot tower:

- To the north, towards the mouth of the Bisagno's stream it has been suggested a geometry F – F featured by the presence of a layer in artificial boulders with a slope of 2/3 and a maximum depth at the foot of the mole equal to 8 meters.

- To the south, a geometry referenced as G – G (Figure 5-5) characterized by the presence of a course composed by artificial boulders with a slope of 1/2, a small retaining structure placed at the foot and a maximum depth of the mole equal to 12 meters.
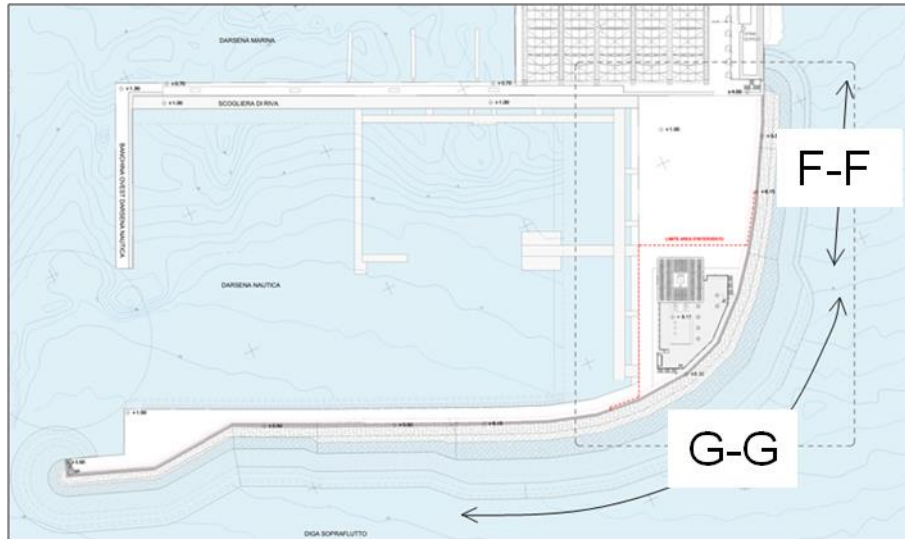
Figure 5-2 Layout of the Genova's dock and location of the new pilot tower (courtesy of CETENA and ACQUATECNO).
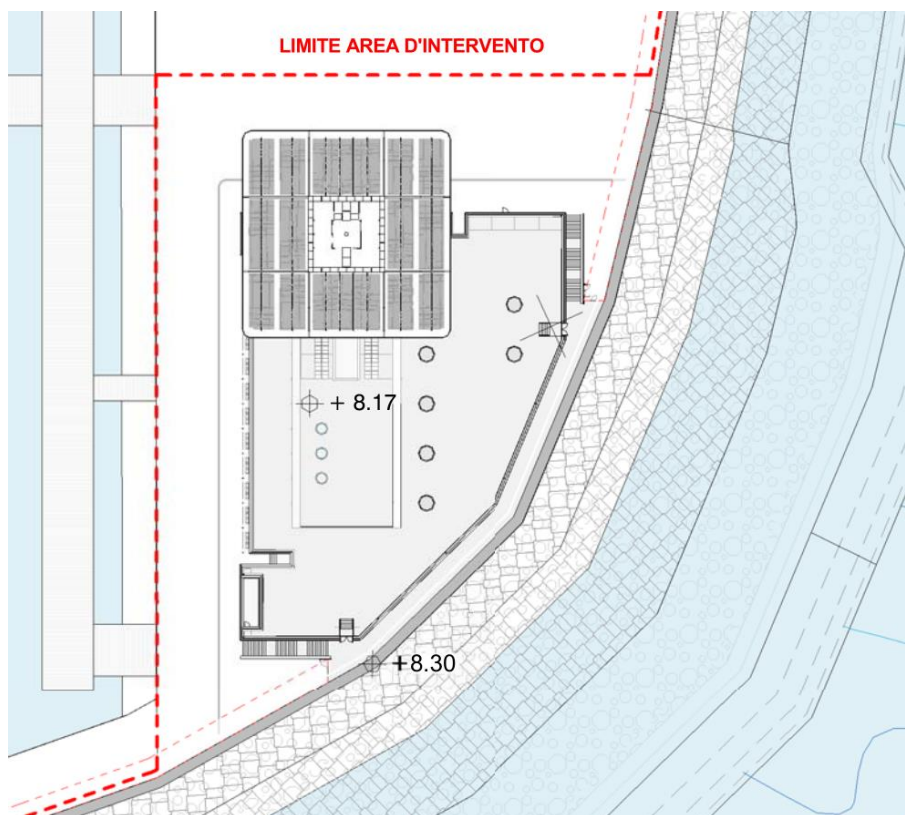
Figure 5-3 General planimetry of the new pilot tower (courtesy of CETENA and ACQUATECNO).
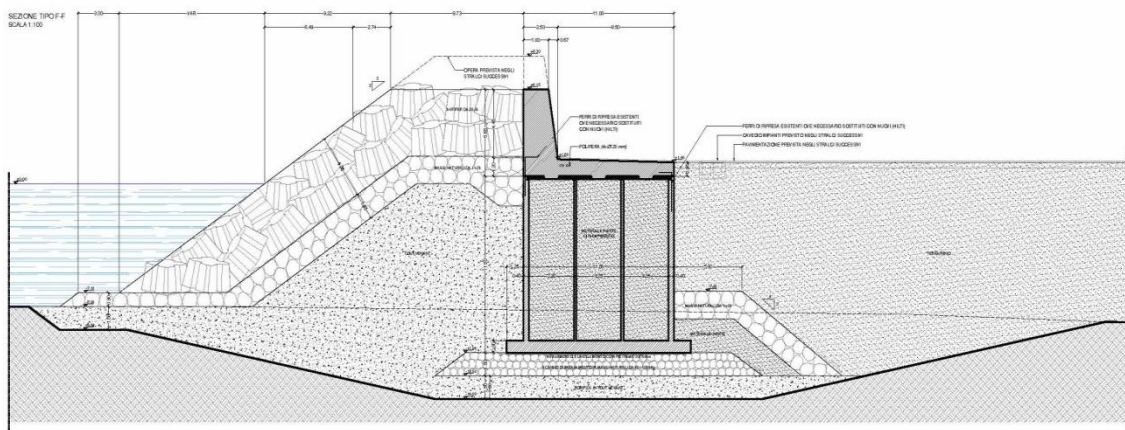
Figure 5-4 Typical section of the mole F – F (courtesy of CETENA and ACQUATECNO).
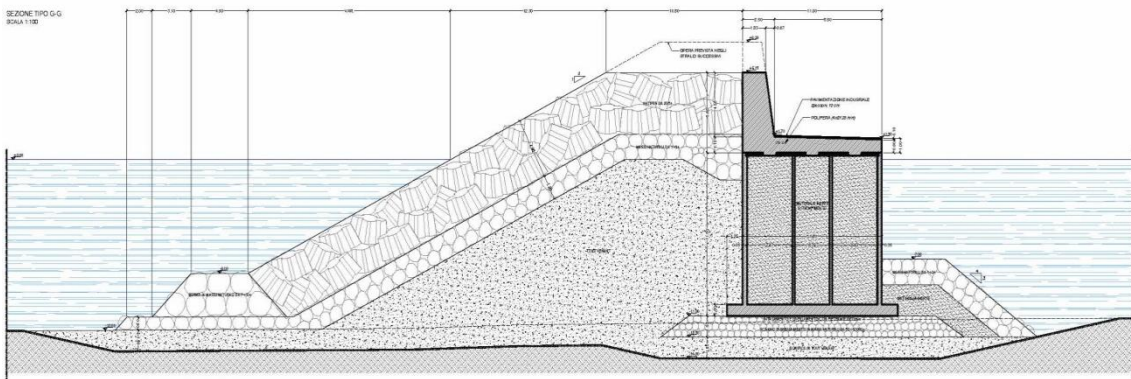
Figure 5-5 Typical section of the mole G – G (final stretch without embankment) (courtesy of CETENA and ACQUATECNO).

The main characteristics of the materials consisting on the breakwater dam of the Genova's dock are listed below (Figure 11):

- Superficial course of the mole's slope composed by artificial boulders with concrete kind Antifer 20,5 tons.
- Support structure of the layer of artificial boulders placed at the foot of the mole in the section G – G consisting of natural boulders of category IV (7-10 t).
- Filter layer: Natural boulders of category II (1-3 t).
- Core: Tout Venant of quarry at a trapezoidal section.
- Block composed by reinforced concrete filled with Tout Venant.
- Embankment, which represents the premises of the foundation of the new pilot tower.

At the back of the breakwater and the concrete block, there is platform on which it is supposed to be built the control tower. It consists of a low structure (one single floor) and a very slender tower of 62 meters in height (Figure 5-6).

The foundation under the pilot tower and the structures placed on the base next to the tower, has been conform by rotary drilled piles of medium-high diameters and 30 meters in length (Figure 5-7, Figure 5-8).
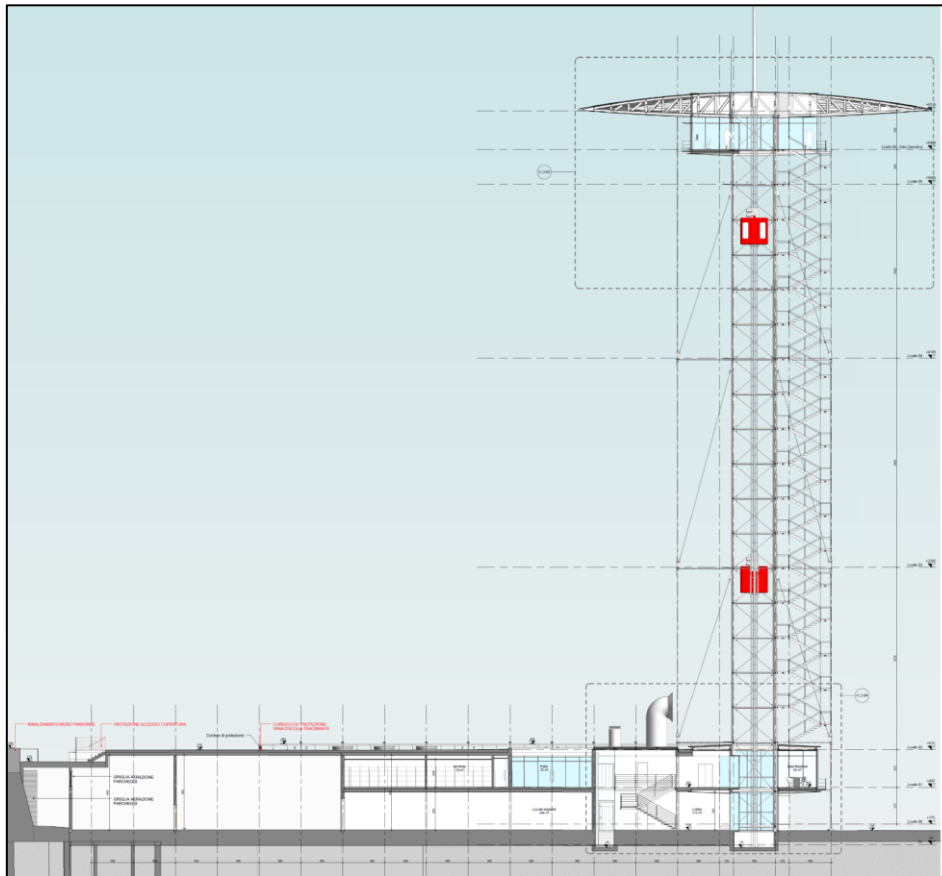
Figure 5-6 Scheme of the section of the New Pilot Tower on the Genova's dock. (courtesy of CETENA and ACQUATECNO).
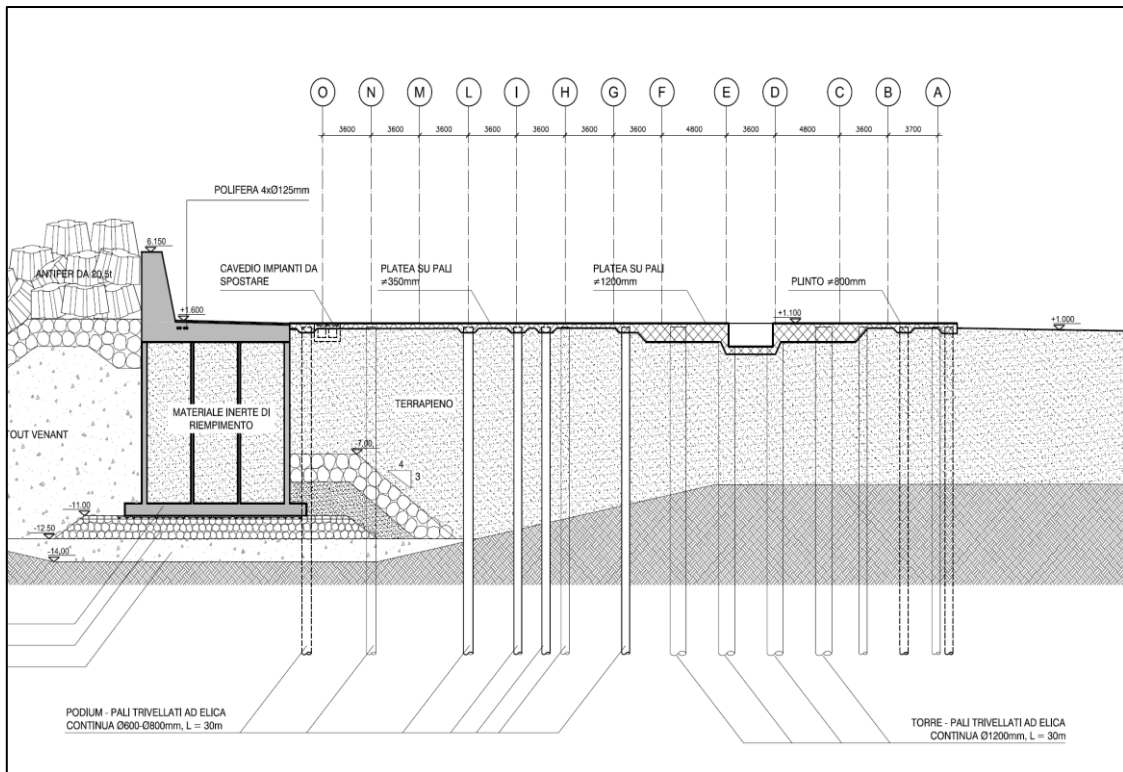
Figure 5-7 Foundations of the structure located in the pilot area (section) (courtesy of CETENA and ACQUATECNO).
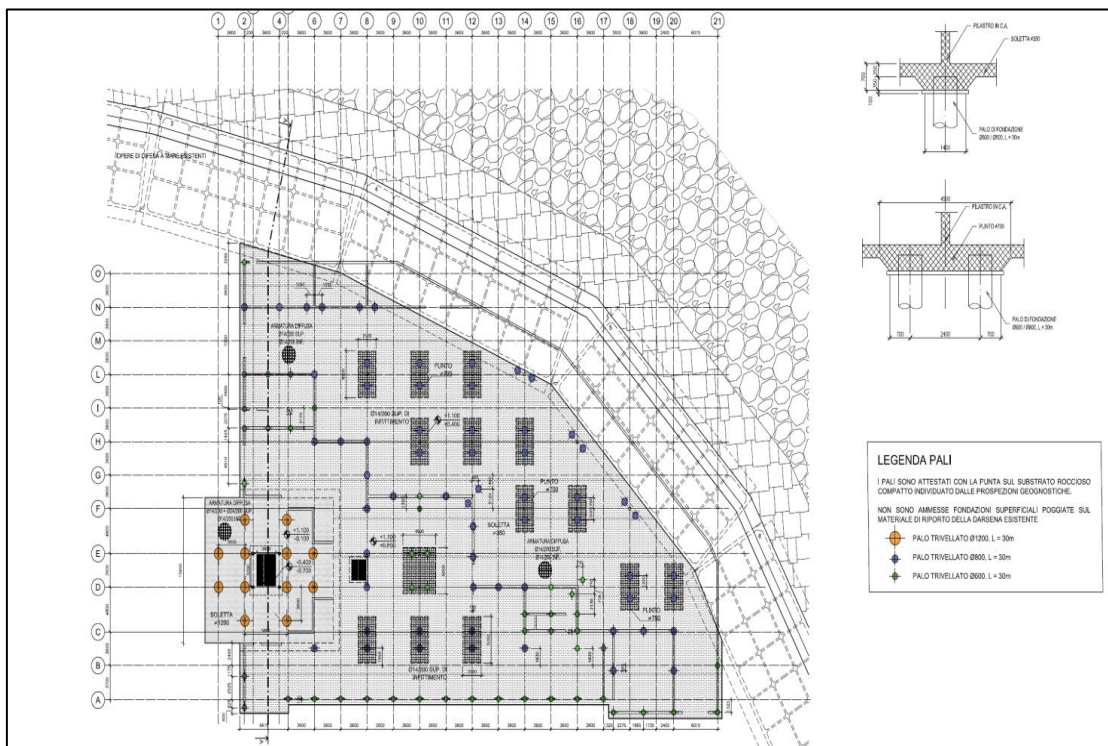
Figure 5-8 Foundations of the structure located in the pilot area (plan view) (courtesy of CETENA and ACQUATECNO).

With regards to the graphic schemes showed in the following figures (5-9, 5-10), it is possible to observe the angle, almost orthogonal, formed between the line of the navigation route in the worst situation, which is equal to 303º N, according to what was disposed by a group of pilots, and the perimeter of the breakwater. Particularly, in the figure 5-10, it is underlined the location of the cross section of the project (figure 5-11.) to which correspond the minimum distance between the structure of the new pilot tower and the impact point of cargo ship on the breakwater.

The analysis developed in the following paragraphs are referred to these geometrical conditions as representative of the worst scenario with respect to the structural vulnerability of the project.
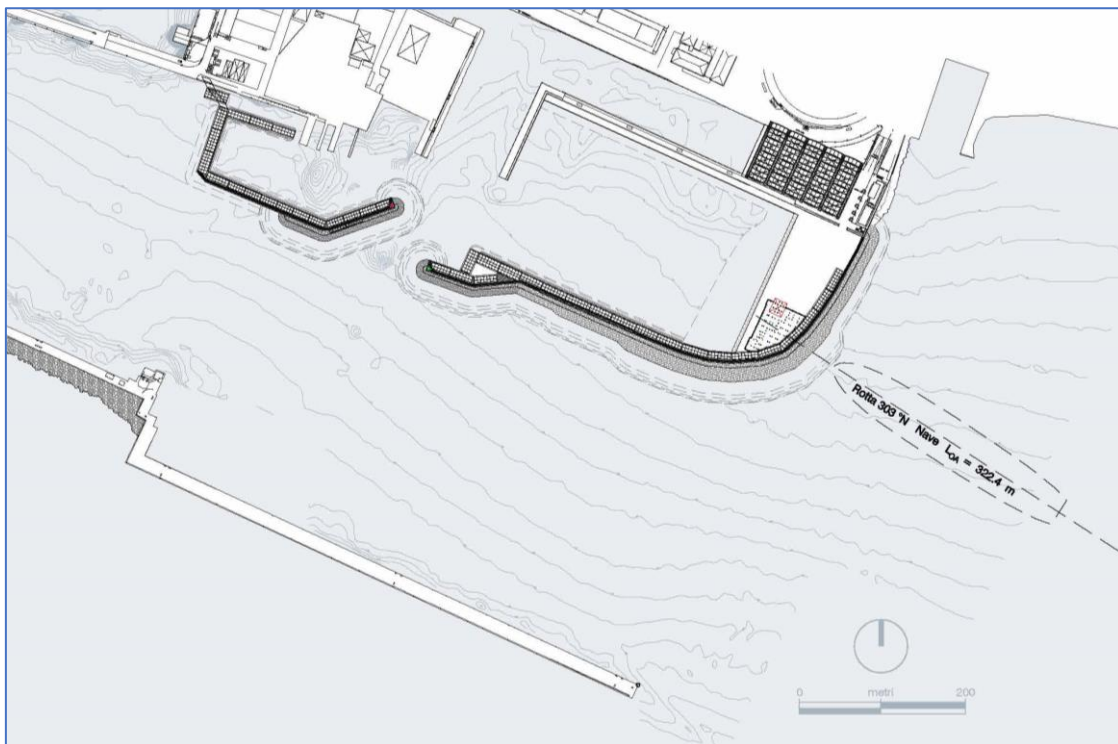
Figure 5-9 Worst impact route suggested by the group of pilots (303 °N) (courtesy of CETENA and ACQUATECNO).
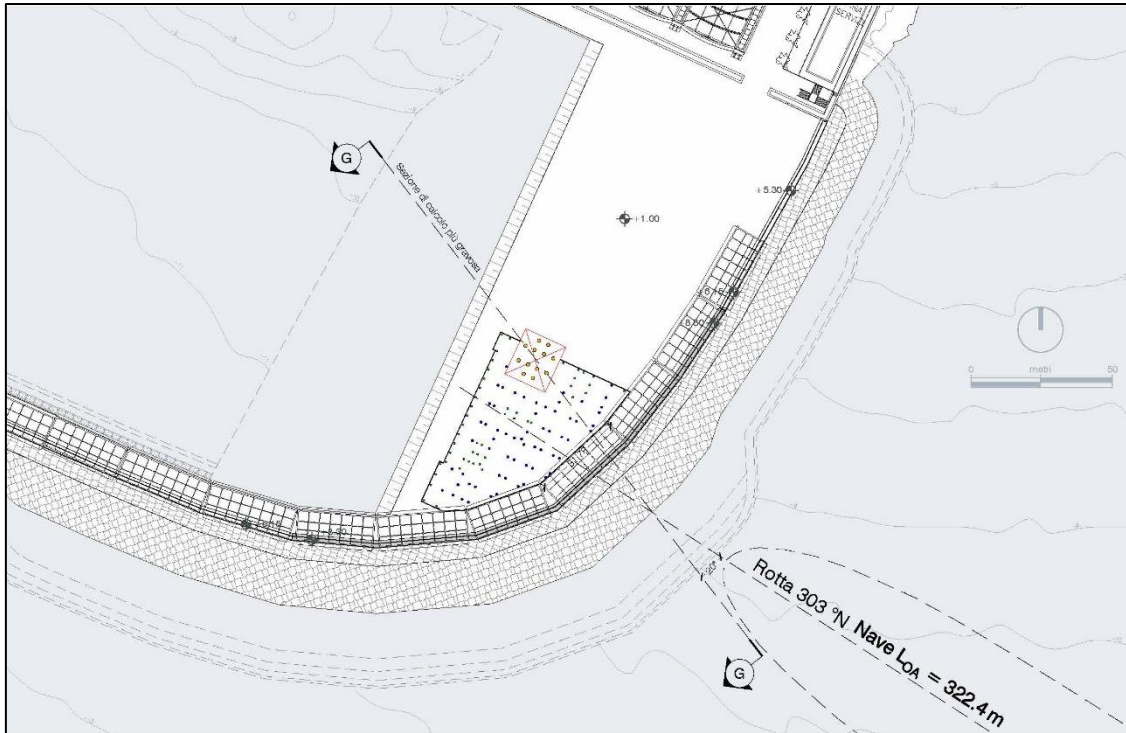
Figure 5-10 Location of the minimum distance between the Pilot Tower and the impact point (courtesy of CETENA and ACQUATECNO).
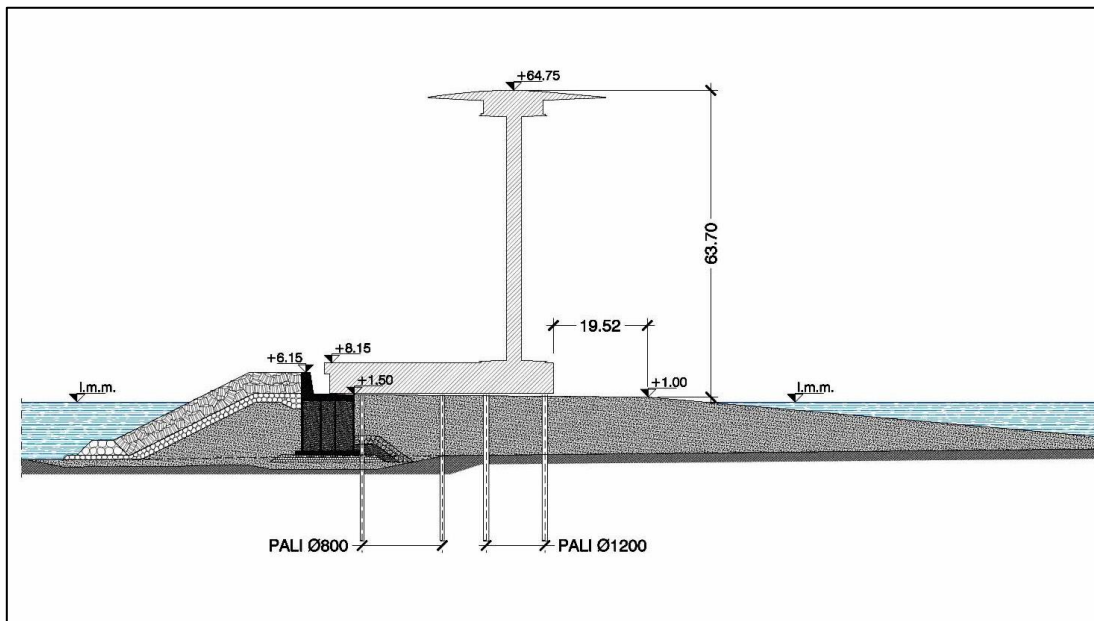
Figure 5-11 Section of minimum distance between the Pilot Tower and the impact point (Sea side) (courtesy of CETENA and ACQUATECNO).

5.2 Impact force estimation

To estimate the force with which the cargo ship stroke on the mole of the dock of Genova, have been required the services of *CETENA* (*Centro per gli Studi di Tecnica Navale*) in collaboration with *AQCUATECNO*, which is an expert partner in civil engineering projects. To develop the model, it was necessary some information which the port authorities gave to both companies with regards to the kind of ship and the direction of the force which must be considered during the analysis. The problem was modeled by means of calculation software, based on the finite elements models.

After some discussions between the two partners, it was agreed to consider a ship characterized by a configuration with bulb in its bow, because it was concluded that the most of the ships of large size contain the bulb in its bow. At least, some of the features of the cargo ship that were considered in the analysis are:

- Length of the ship = 300 meters.
- Displacement = 78000 t.
- Width = 50 meters.
- Project immersion = 8,8 meters.
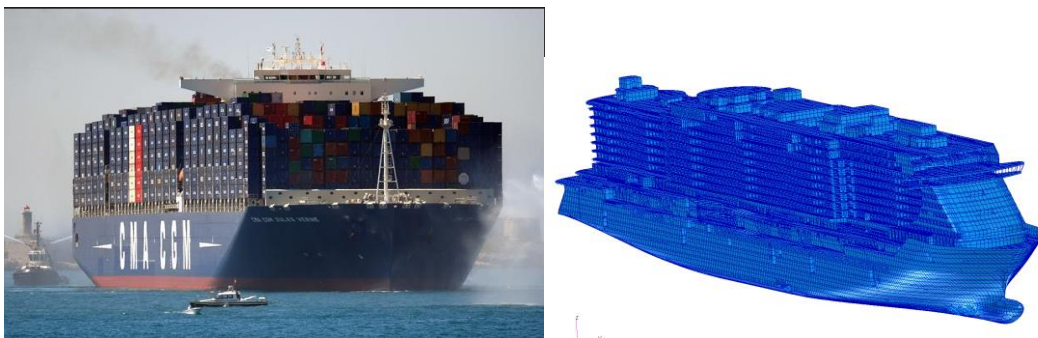
Figure 5-12 Cargo ship and FEM which was taken as reference in the modeling of the problem in the Genova's dock.

The models of finite elements (FEM) used to estimate the impact forces which were induced on the mole by the cargo ship have been developed with the commercial calculation code of finite elements MSC Marc. It is an implicit sort of code capable of simulating with accuracy non-linear phenomena such as the collision of the deformable bodies through the contact analysis.

With the aim of reducing the onerous process of calculation in terms of the tuning of the model and the calculation time, the models have been limited in extension to the bow's ship. In spite of considering the whole ship in the analysis, it has been only taken into account the bow of the shift (approximately 33 out of 300 meters of the cruise). This assumption is justified due to the fact that the deformations produced as a consequence of an impact are concentrated in a zone quite limited.

The part of the craft which has not been modeled is taken into account in terms of a mass with the aim of representing correctly the amount of kinetic energy involved in the phenomenon (figure 5-13). The mass pertaining to the part of the ship which has been modeled is positioned

in a point coinciding with the barycenter of the craft and it has been joined to the bow by means of a rigid element (*element RBE2 from the bookstore of the software MSC Marc*). It has been disposed that the ship can rotate around the perpendicular axis (inclined) thanks to a kinematic system modeled with resilient springs.

Finally, it must be underlined that the model of the bow's ship has been carried out with 2D shell elements and 1D beam elements.
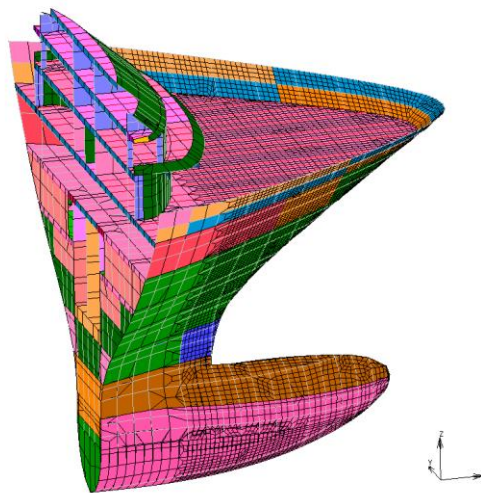
Figure 5-13 FEM model (bow's zone) used to simulate the collision of the ship against the mole of the dock of Genova (courtesy of CETENA and ACQUATECNO).

elemento rigido di connessione tra massa nave (nel baricentro) e parte di prua modellata

massa rappresentativa della parte di nave non modellata (baricentro nave)

molle di richiamo elastico per rappresentare la lbertà di rotazione della nave attorno all'asse trasversale (beccheggio)
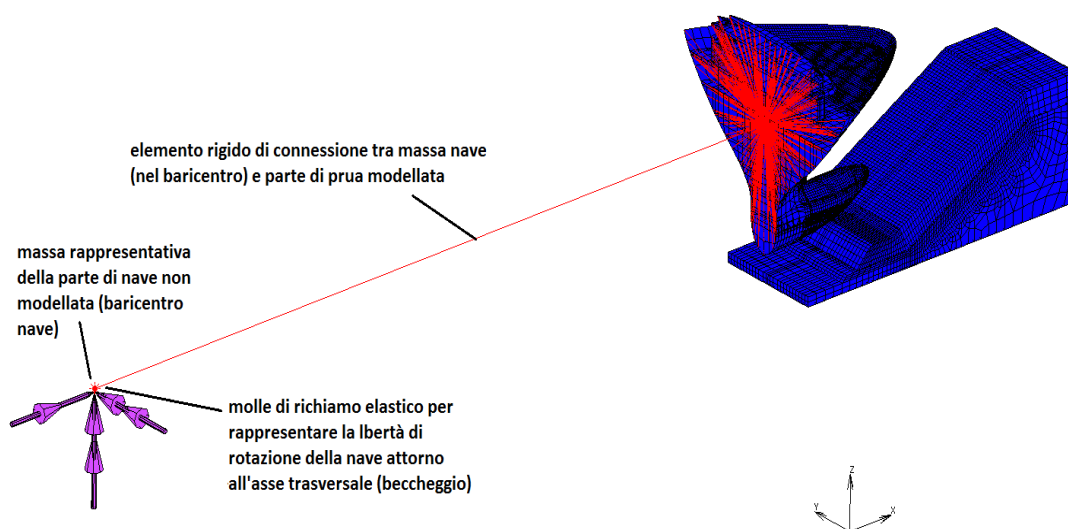
Figure 5-14 Representation of the ship's mass connected to the bow's craft by means of a rigid element (courtesy of CETENA and ACQUATECNO).

Otherwise, the external part of the mole (breakwater) has been represented considering 3D elements for both configurations F – F and G – G respectively (figure 5-15). The model of the mole developed with the finite elements consists of a superficial layer made up of representative elements of artificial bounders (*antifer*). This first layer is disposed over a second coat of material, which represents a filter layer. This is composed by natural bounders and lies on a core characterized by *tout venant*. The interaction phenomena between both substrates has been regulated by a relationship of contact with friction. In the following figure is showed the breakwater of the dock of Genova modeled with finite elements using the software *MSC Marc*.
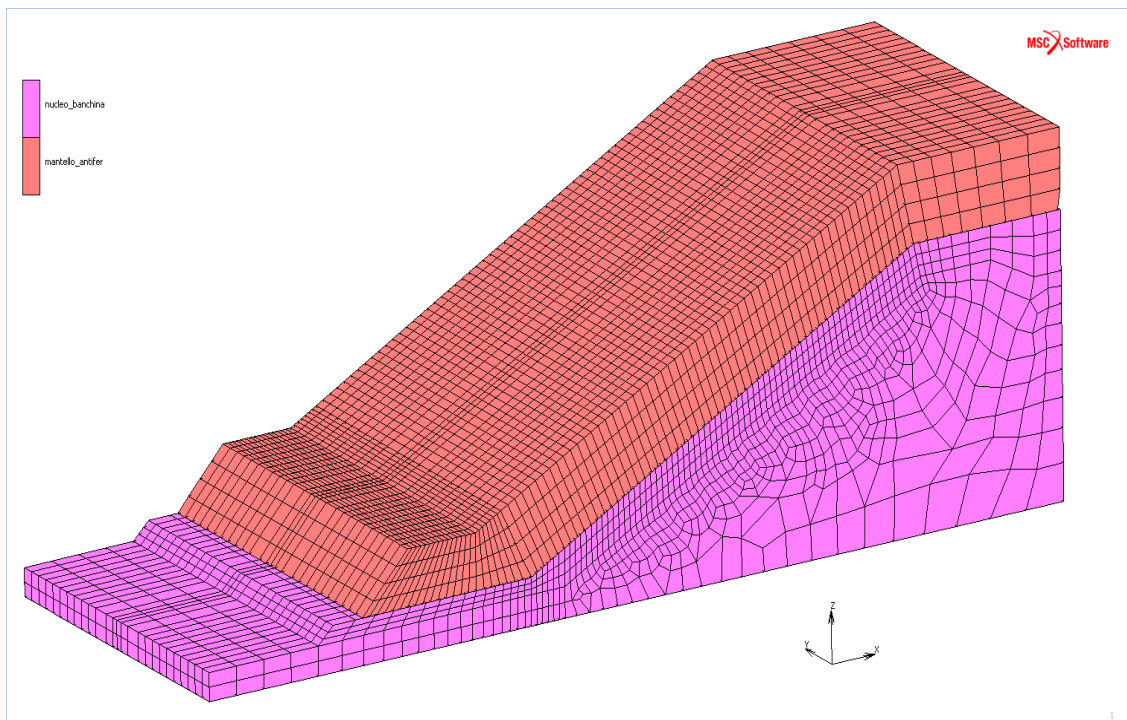
Figure 5-15 Finite elements model of the mole of the Genova's dock (type G – G) (courtesy of CETENA and ACQUATECNO).

In addition to this, are listed below some of the mechanical properties of the mole's materials and conditions which have been considered in the analysis of the problem of the Genova's dock:

- Isotropic materials.
- Mole's superficial layers of bounders with a Young's modulus equal to 200 MPa.
- Core of the mole with a Young's modulus equal to 500 MPa.
- Friction angle between the ship's bulb and the mole's superficial layer equal to 26,57º.
- Friction angle between the superficial layers and the core of the mole equal to 19,30º.

5.2.1   Impact force estimation FEM Model

In the following figure, it is showed the main result obtained from the calculation process according to the model of collision of the cargo ship against the dock of Genova which was developed by the finite elements software *MSC Marc* (Figure 5-16). It represents the values of the impact forces in function of the time. Nevertheless, to make these results suitable for the geotechnical FEM calculation, the forces must be discomposed in a perpendicular and in a tangential component to the surface of contact between the bulb's ship and the mole.

The scheme of calculation considered to transform the contact forces into pressures is specified in the figure 5-16. As it has been indicated in the figure 5-18, the contact area has been considered as the rectangle which circumscribes the contact zone between the bulb and the mole.
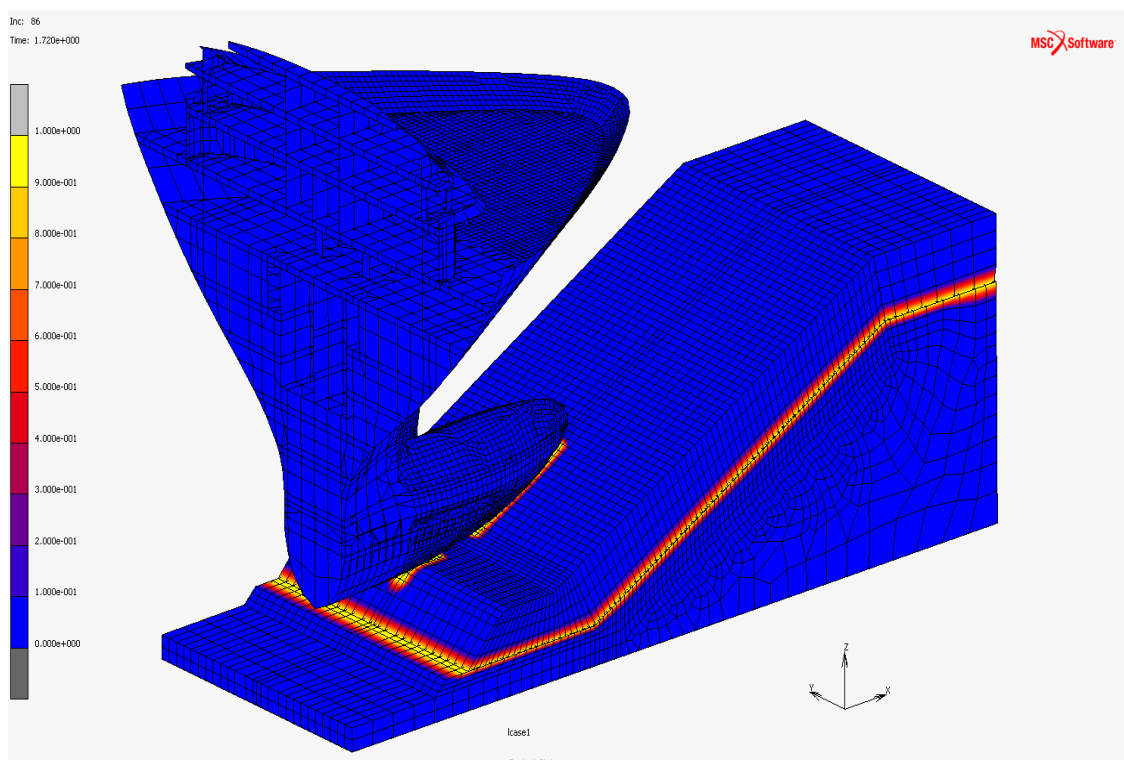
Figure 5-16 Main results obtained from the calculation process of the model of Impact of the cargo ship against the mole of the Genova's dock (courtesy of CETENA and ACQUATECNO).
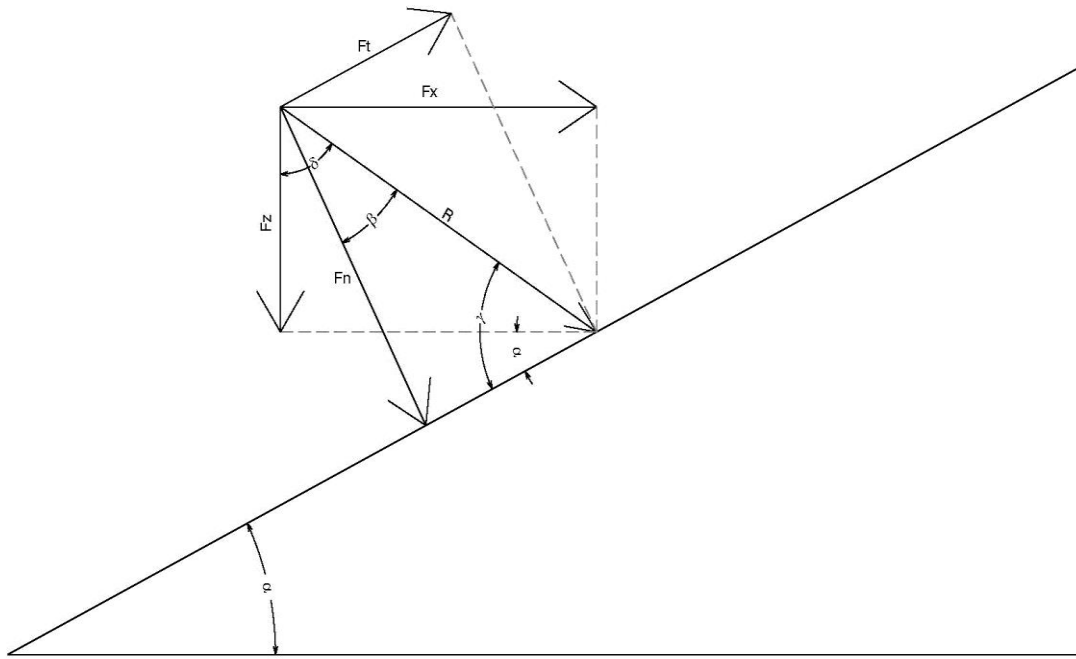
Figure 5-17 Decomposition of the forces obtained with MSC Marc on their normal and tangential components (courtesy of CETENA and ACQUATECNO).
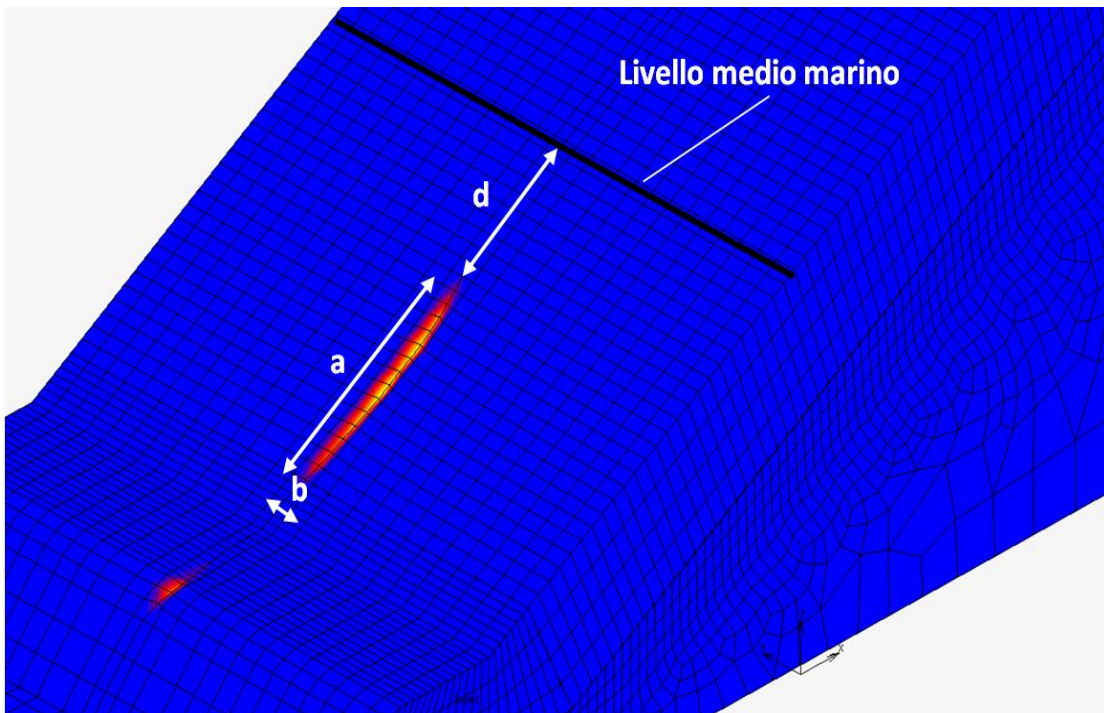
Figure 5-18 Calculation of the contact area and distance to the average marine level (courtesy of CETENA and ACQUATECNO).

In the next table have been presented the values of the contact forces (resultant and components) and their respective stresses (normal and tangential) for the case of a cargo ship of 300 meters in length.

The numeric values of the impact forces and their corresponding pressures, useful in the calculation and subsequent valuation of the consequences due to the collision of the ship against the mole of the Genova's dock, are presented in the following table. These results have been also plotted to analyze the variation of the forces and their components, as well as the contact area between the ship's bulb and the mole in function of the time in the figures 5-19, 5-20 and 5-21 respectively.

The scheme of application of the contact forces to the geotechnical model is presented in the figure 5-22.

t	a	B	A	d	FX	FZ	R	δ	β	FN	FT	s	t
(s)	(m)	(m)	(m²)	(m)	(N)	(N)	(N)	(°)	(°)	(N)	(N)	(MPa)	(MPa)
0.20	4.70	1.62	7.61	4.60	-1.15E+07	9.40E+06	1.48E+07	50.6	23.6	1.36E+07	5.93E+06	1.78	0.78
0.40	7.36	1.57	11.56	3.90	-5.54E+07	4.06E+07	6.87E+07	53.8	26.8	6.13E+07	3.09E+07	5.31	2.68
0.60	8.74	1.57	13.72	3.51	-9.85E+07	6.65E+07	1.19E+08	56.0	29.0	1.04E+08	5.76E+07	7.58	4.19
0.80	9.76	1.56	15.23	3.04	-1.20E+08	7.70E+07	1.43E+08	57.4	30.4	1.23E+08	7.21E+07	8.08	4.73
1.00	10.00	1.58	15.80	2.76	-1.33E+08	8.60E+07	1.58E+08	57.1	30.1	1.37E+08	7.95E+07	8.67	5.03
1.20	10.84	1.57	17.02	2.53	-1.25E+08	8.11E+07	1.49E+08	57.0	30.0	1.29E+08	7.45E+07	7.58	4.38
1.40	10.44	1.58	16.50	2.35	-1.19E+08	7.92E+07	1.43E+08	56.4	29.4	1.25E+08	7.04E+07	7.56	4.27
1.60	9.88	1.59	15.71	2.11	-1.06E+08	6.92E+07	1.26E+08	56.8	29.8	1.10E+08	6.26E+07	6.97	3.99
1.80	9.47	1.59	15.06	1.87	-8.69E+07	5.65E+07	1.04E+08	57.0	30.0	8.98E+07	5.17E+07	5.96	3.44
2.00	9.37	1.59	14.90	1.62	-6.72E+07	4.50E+07	8.09E+07	56.2	29.2	7.06E+07	3.95E+07	4.74	2.65
2.20	8.91	1.61	14.35	1.37	-5.33E+07	3.60E+07	6.44E+07	56.0	29.0	5.63E+07	3.12E+07	3.92	2.17
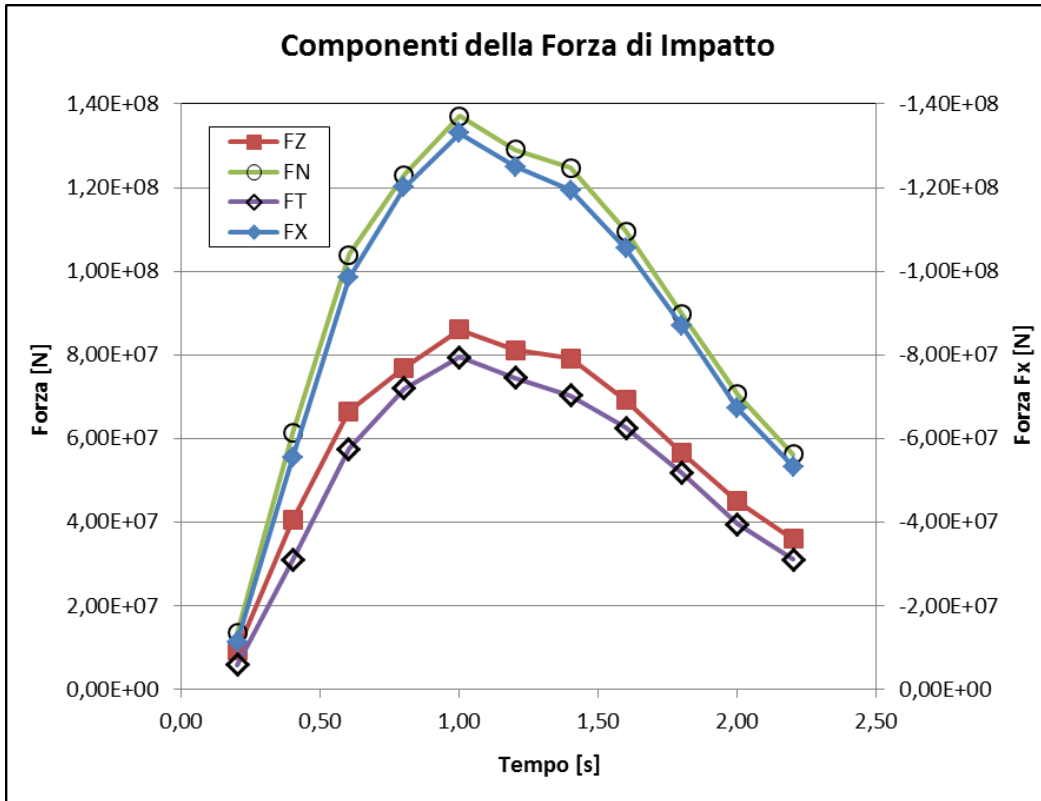
Figure 5-19 Components of the impact forces in function of the time for a cargo ship of 300 meters in length (courtesy of CETENA and ACQUATECNO).
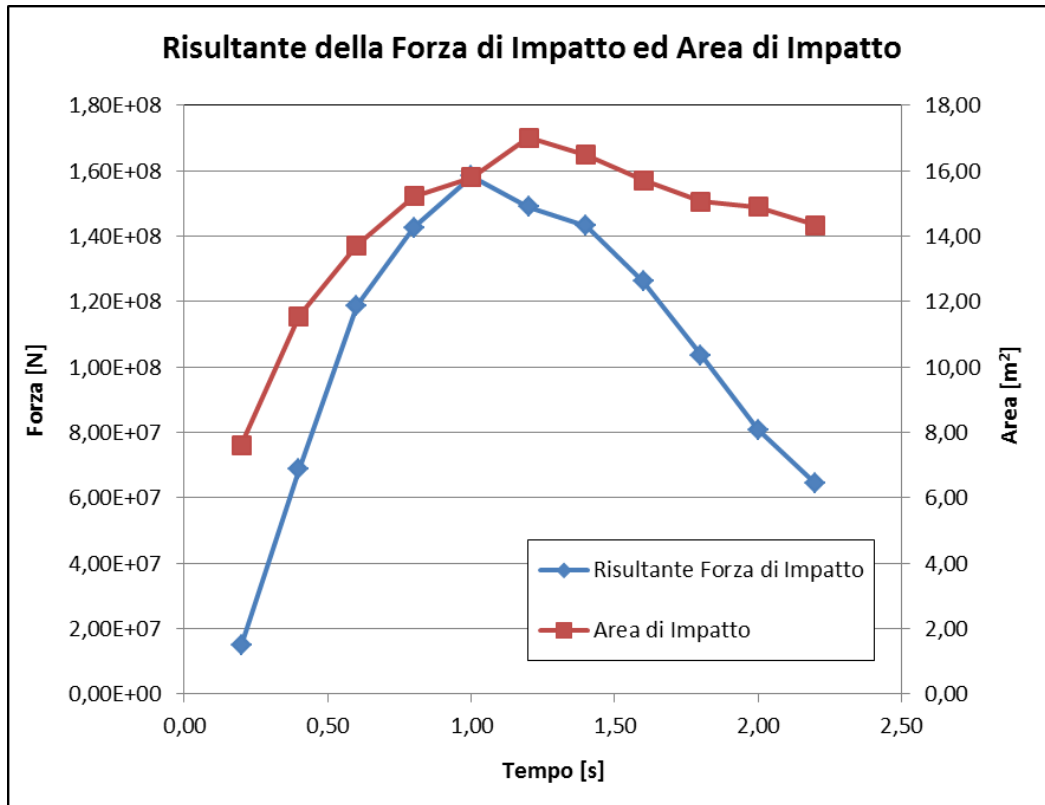
Figure 5-20 Resultant impact forces and contact area in function of the time for a cargo ship of 300 meters in length (courtesy of CETENA and ACQUATECNO).
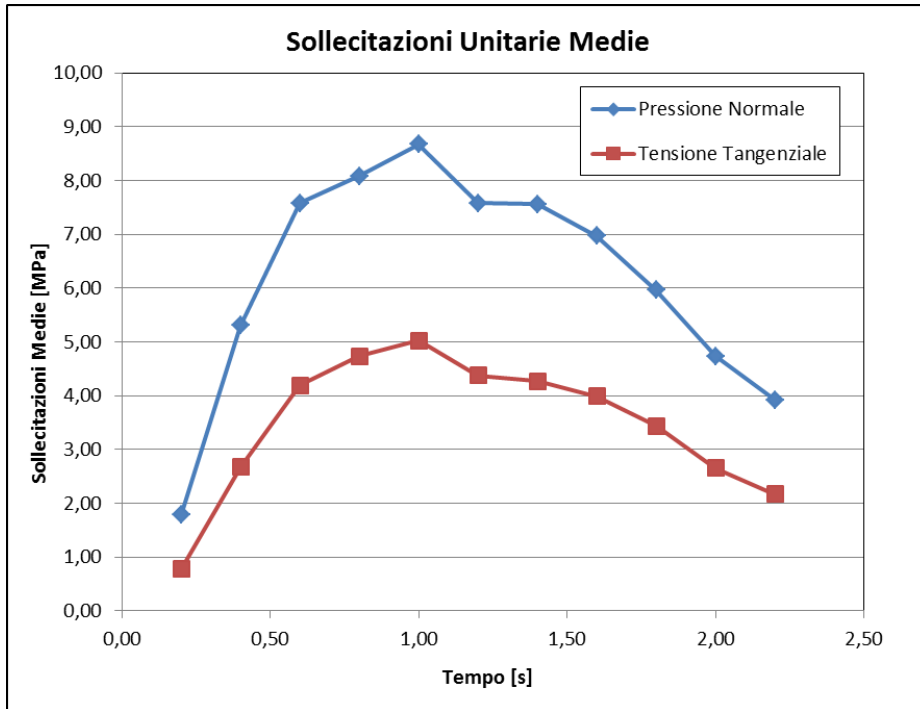
Figure 5-21 Normal and tangential components of the impact forces in function of the time for a cargo ship of 300 meters in length (courtesy of CETENA and ACQUATECNO).
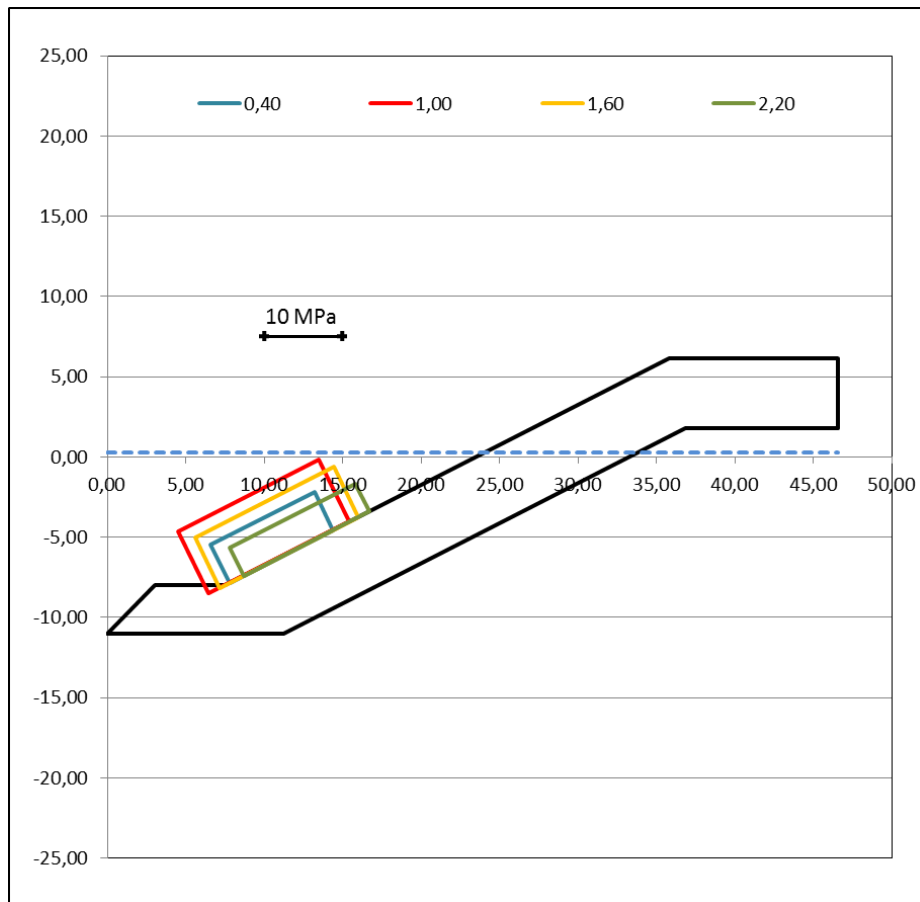
Figure 5-22 Variation of the pressures and contact area in function of the time for a cargo ship of 300 meters in length (courtesy of CETENA and ACQUATECNO).

5.3 Geotechnical model

The geotechnical characterization of the area and in general, the geological-geotechnical model have been agreed from the geological and geotechnical report and from the Implementation Project developed for the construction of the new mole and increasing of the Technical Breakwater located on the Genova's dock written by the society *Appolonia*.

5.3.1 Stratigraphy

The geotechnical report of the Implementation Project of the breakwater of the Genova's dock has individuated the following layers of material in the seabed:

- Marine and/or Fluvial deposit (from 5 to 8 meters in width).
- Calcareous layer of soil under de fluvial deposit (50 meters in width).

5.3.2 Soil Mechanical properties

In the following table, has been reported the mechanical characterization of the seabed disposed in the report of the Implementation Project of Breakwater of the Genova's dock.

Soil	Width (m)	Υ_t (kN/m³)	Φ (º)	c (kPa)	UCS (MPa)	E (MPa)	Y (-)
Silty sands	5 - 8	19	28	0	-	5	0,15
Smashed Calcareous from Antola	2 - 3	20	n.d.	n.d.	0,4 – 0,8	n.d.	n.d.
Undamaged calcareous from Antola	>50	26	n.d.	n.d.	35	n.d.	n.d.

6   Finite Element Analysis of the case

6.1   Brief description of the method

A Finite Elements analysis requires the previous creation (input phase) of a geometrical model in two dimensions in the plane x – y composed by points, lines and some other components. In this real case of study have been used triangular elements of 15 nodes to model the different layers of soil and the other materials of the model (volume elements – clusters). The triangle of 15 nodes provides a fourth order interpolation for the displacements and the numeric integration uses 12 points of Gauss (stress points) on which are calculated the tensional state, as well as the state deformations. Consequently, the 15 nodes triangle constitutes a very accurate element and provides optimate solutions even in very complex problems. Otherwise, the use of triangular elements of 15 nodes comports a very high calculation time and high requirements of memory.

A 15 nodes element can be considered as the composition of four 6 nodes elements, due to the fact that the total number of nodes and the integration points are the same. However, it must be underlined that one element consisting on 15 nodes is more reliable than those composed by four elements of 6 nodes.
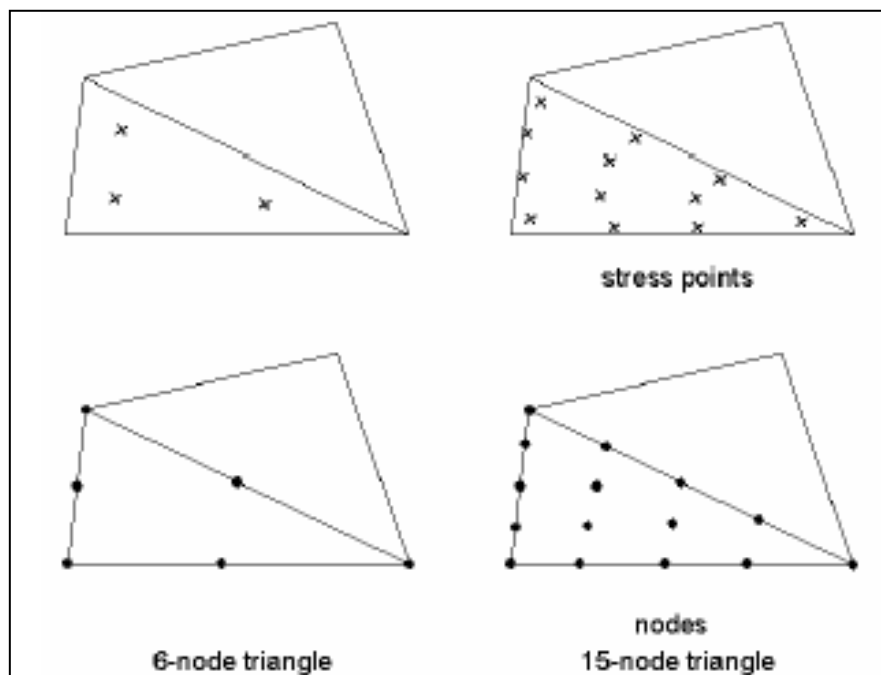
Figure 6-1 Elements consisting on 6 and 15 nodes respectively.

As it has been mentioned, the creation of a geometrical model composed by points, lines and clusters is the starting point for the numeric analysis. Furthermore, these base components can be assigned to the models of different structural objects working under specific conditions in order to simulate each kind of project: lining of galleries, plates, geosynthetics, drainage systems, objects defined to simulate the interaction phenomena soil-structure or external

loads such as distributed and concentrates forces. The geometrical model must comprise, with analogue approach, the initial situation, as well as the different phases which take place during the process of calculation (for example, the several construction phases).

When the geometrical model has been completely defined and all of the geometrical components have their own initial properties, can be generated the finite elements mesh. This mesh is determined by the FEM model used in the analysis.

After having defined the geometry of the problem, assign the different materials to the clusters of soil, assign the values to the present beam elements and having positioned the phreatic level corresponding to that of the project, the model is ready to proceed with the calculation of the in situ tensions, as well as the interstitial pressures at the beginning.

Afterwards, must be defined the different phases of digging and must be activated the several elements which compose the problem in analysis. This is carried out in the calculation module which precedes the phase of the real calculation.

6.2 Brief description of the constitutive models

For a few years, the software *PLAXIS* disposes of a constitutive model called *Hardening Soil*, (*HS*) which permits to the user to take advantage and to reproduce the main aspects of the stress-strain behavior of the natural materials, with the subsequent advantages of the simulation of problems with geotechnical nature, overall those of digging.

As in the most of the constitutive models, the HS is assumed as a continuous porous medium in order to be able to conduct coupled analysis. The main feature of the constitutive connection is the presence of a closed yielding surface to which, is associated an isotropic mechanism of hardening regulated by the plastic volumetric deformations (with a flow law associated) and by the plastic distortions (with a flow law not associated).

The main characteristics of the model *Hardening Soil HS* are listed below:

- Different constitutive bonds for the tensional state of the first load (towards the external part of the yielding surface) and that of load – unload (in the inner part of the yielding surface).
- Development of plastic deformations due to the increasing of the diverter tensions, with a flow law not associated, as well as the enhancement of the spherical tensions, with flow law associated.
- Failure criterium of Möhr-Coulomb.

The secant stiffness modulus E_{50} for tensional states of the first load cycle (towards the outer part of the yielding surface) is function of the confinement tension applied and the material resistance.

$$E_{50} = E_{50,ref} \cdot \left[\frac{(c' \cdot \cos \varphi' - \sigma'_{min} \cdot \sin \varphi')}{(c' \cdot \cos \varphi' + p_{ref} \cdot \sin \varphi')} \right]^{m} \qquad (6.1.)$$

Where:

- p_{ref} is the pressure of reference which is equal to 100 kPa.
- σ'_{min} is the minor main stress.
- E_{50ref} is the secant stiffness modulus at the reference pressure ($\sigma'_{min} = p_{ref}$).
- *m* is an exponential coefficient which regulates the dependence between the stiffness and the tensional state.
- E_{50} is the secant stiffness modulus (at the 50% of the failure) referred to the tension σ'_{min}.

The stiffness modulus E_{ur}, which characterizes the tensional states inner to the yielding surface is function of the confinement tension applied and the material's resistance:

$$E_{ur} = E_{ur,ref} \cdot \left[\frac{(c' \cdot \cos \varphi' - \sigma'_{min} \cdot \sin \varphi')}{(c' \cdot \cos \varphi' + p_{ref} \cdot \sin \varphi')} \right]^m \qquad (6.2.)$$

Where:

- p_{ref} is the pressure of reference which is equal to 100 kPa.
- σ'_{min} is the minor main stress.
- E_{50ref} is the secant stiffness modulus at the reference pressure ($\sigma'_{min} = p_{ref}$).
- *m* is an exponential coefficient which regulates the dependence between the stiffness and the tensional state.
- E_{ur} is the secant stiffness modulus at a tension σ'_{min}.
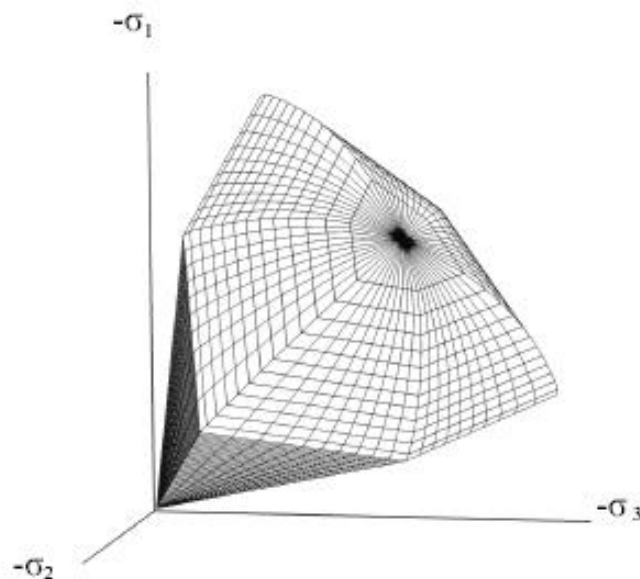
Figure 6-2 Closed yielding surface (Hardening Soil model).

q = σ₁-σ₃

axial strain ε₁
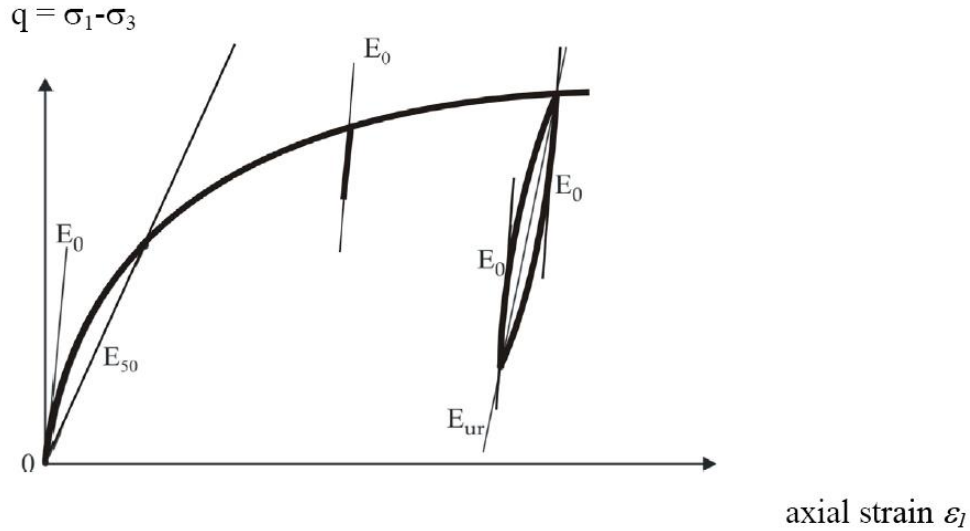
Figure 6-3 Definition of the parameters E_0, E_{50} and E_{ur} in the constitutive model "HS".

6.3   The critical time step

In all the dynamic analysis carried out with *PLAXIS*, it is defined a calculation time by the user. To be able to obtain optimal solutions from the calculation process, it must be also defined the minimum number of the calculation steps which has to be considered in each of these analysis. To determine this minimum number of steps it is necessary to calculate previously the critical time step.

Despite the advantages of the implicit integration, the time step used in the calculation is subject to some limitations. If the time step is to large, the solution will display substantial deviations and the calculated response will be unreliable. The critical time step depends on the maximum frequency and the coarseness (fineness) of the finite element mesh. In general, the following expression can be used for a single element (Pal, 1998):

$$\Delta t_{critical} = \frac{l_e}{\alpha \cdot \sqrt{\dfrac{E \cdot (1-v)}{\rho \cdot (1+v) \cdot (1-2v)}} \cdot \sqrt{1 + \dfrac{B^4}{4S^2} - \dfrac{B^2}{2S} \cdot \left[1 + \dfrac{1-2v}{4} \cdot \dfrac{2S}{B^2}\right]}} \qquad (6.3.)$$

In the equation 6.3., the term B and S respectively denote the largest dimension of the finite element and the surface area of the finite element. The first root term represents the velocity of a (compression) wave in the material model. The factor **α** depends on the element type. For a 6-node element $\alpha = 1/(6\sqrt{c_6})$, with $c_6 \approx 5{,}1282 \cdot 10^{-2}$, and for a 15-node element $\alpha = 1/19\sqrt{c_{15}}$, with $c_{15} \approx 4{,}9479 \cdot 10^{-3}$ (Zienkiewicz & Taylor, 1991). The other determining factors are the Poisson's ratio, **υ**, and the average length of an element, **l_e**. In a finite element model, the critical time step is equal to the minimum value of **Δt** according to equation 6.3.

over all the elements. This time step is chosen to ensure that a wave during a single step does not move distance larger than the minimum dimension of an element.

In this case of application, the parameters which have been considered to calculate critical time step, are presented in the next table:

α (15-node element)	E	υ	B	S = B²/2
0,003702	30000000	0,23	0,1	0,005

Consequently, according to the equation 6.3., the critical time step is equal to:

$$\Delta t_{critical} = 0{,}036239523 \, s$$

As the simulation time has been considered equal to 6 seconds, the minimum number of steps which must be considered in the calculation process comes:

$$n_{steps,min} = \frac{6}{0{,}036239523} = 165{,}565 \, steps$$

To obtain optimal results in the dynamic analysis, it has been considered a higher number of calculation steps than that obtained above. It has been thought that a good estimation of the number of steps of the calculation process would be:

$$n_{steps,chosen} = 400 \, steps > 165{,}565 \, steps$$

6.4   Finite Element Model Description

It has been modeled the problem which happened in the dock of Genova a few years ago, in which a cargo ship impacted against the mole in a zone next to the pilot tower of the dock. As a consequence of the impact, the tower collapsed. To model this situation, it has been used the finite elements software *PLAXIS*, whose base has been described in the previous points of this Master's Thesis.

The main aim of this Thesis is to determine the reduction of the displacements in the head of the pilot tower by adding to the concrete block, placed between the foundation of the tower and the structures located next to it, and the wall consisting of the mole, a foundation composed by a group of 16 piles (4 x 4) with a diameter of 1,2 meters and 20 meters in length. To analyze the differences between the real situation a that hypothetical proposed in this Thesis, have been developed two different files. The first one, corresponds to the real case in which the concrete block does not contain the pile's foundation. In the second case, have been introduced the piles under concrete block to determine the improvement in the system's response.

The first step consists on modeling the mole of the Genova's dock in *PLAXIS*. This has been carried out according to the information which was obtained from the geotechnical and geophysical analysis of the soil in the Genova's dock. As it has been explained, the first thing that must be done, when a problem is being modeled by means of a finite elements software like *MSC Marc*, is to define the points, the lines and the clusters to create a draw in 2D that represents the geometry of the problem based on the real sizes. The next step consists on defining the different kind of materials which conform the model according to what has been disposed in the previous paragraphs. At this point, for each defined material, must be introduced their mechanical properties such as the Young's Modulus, the Poisson coefficient and the kind of behavior which is more suitable for it: elastic, plastic. Afterwards, it must be assigned to each closed contour of the model its corresponding material from those created in the previous step.

After having drawn the contours that represent the structures, foundations, and layers of soil pertaining to the model and having assigned to them their respective materials, it must be created the mesh. As it has been discussed in precedent paragraphs, the mesh consists on geometrical elements which are defined by a particular number nodes. As it has been described, in this model have been adopted triangular elements of 15 nodes because the results obtained from the analysis in this case, are more accurate than those obtained by subdividing the triangle of 15 nodes in four elements of 6 nodes.

It must be pointed that, the created mesh is not uniform. As it can be appreciated in the figure 6-4, there are zones in the model proposed in which the density of elements is higher, and consequently, their sizes are lower. These zones with a higher density of elements and nodes correspond to those which are more significant in the analysis and which are more sensitive to the changes in the loads. As it can be observed, the highest amounts of nodes are located in the concrete block and in the foundation and the head of the pilot tower. It has been selected 8 different points of the model from which have been obtained and analyzed the displacements. As it can be observed in figure 6-5, these have been referenced as *A*, *B*, *C*, *D*, *E*, *F*, *G* and *H* respectively.

- The point A is placed on the zone of the breakwater where the ship impacted.
- The point B is located on a corner on the top side of the concrete block.
- The point C corresponds to a node which is placed on the head of the piles pertaining to the front row of the concrete block's foundation.
- The point D corresponds to a node which is placed on the head of the piles pertaining to the second row of the concrete block's foundation.
- The point E corresponds to a node which is placed on the head of the piles pertaining to the third row of the concrete block's foundation.
- The point F corresponds to a node which is placed on the head of the piles pertaining to the back row of the concrete block's foundation.
- The point G is a node located at the bottom of the pilot control tower.
- The point H is a node placed on the head of the pilot control tower.

Subsequently, it must be introduced in the models the acting loads. In this case, the application mode of the loads and their sizes considered, correspond to the results obtained from the analysis carried out by *CETENA* and *ACQUATECNO* based on the information, given by a group of pilots of the Genova's dock, which referred to the worst impact tracks against the mole. The obtaining process of the forces has been described in precedent points of this Master's Thesis.

After having introduced all the parameters of the model, the analysis must be extended a 3D situation. This has been done by introducing in the model a certain depth in the perpendicular direction to those which define the plane x – y.

As it has been mentioned above, have been proposed two different models to determine the diverse responses of the system in the cases in which the concrete block contains a foundation or not. In addition to this, from each of these models, have been created two files. This has been carried out to discuss the differences in the response when it is run an static or a dynamic analysis. In order to obtain the different behaviors, one of the files has been particularized with a static calculation process, while the other one has been individualized for a dynamic analysis.

In the following points of the Thesis are presented the results of the four cases obtained by means of the calculation process with *PLAXIS*, as well as the discussion and comparison of them.
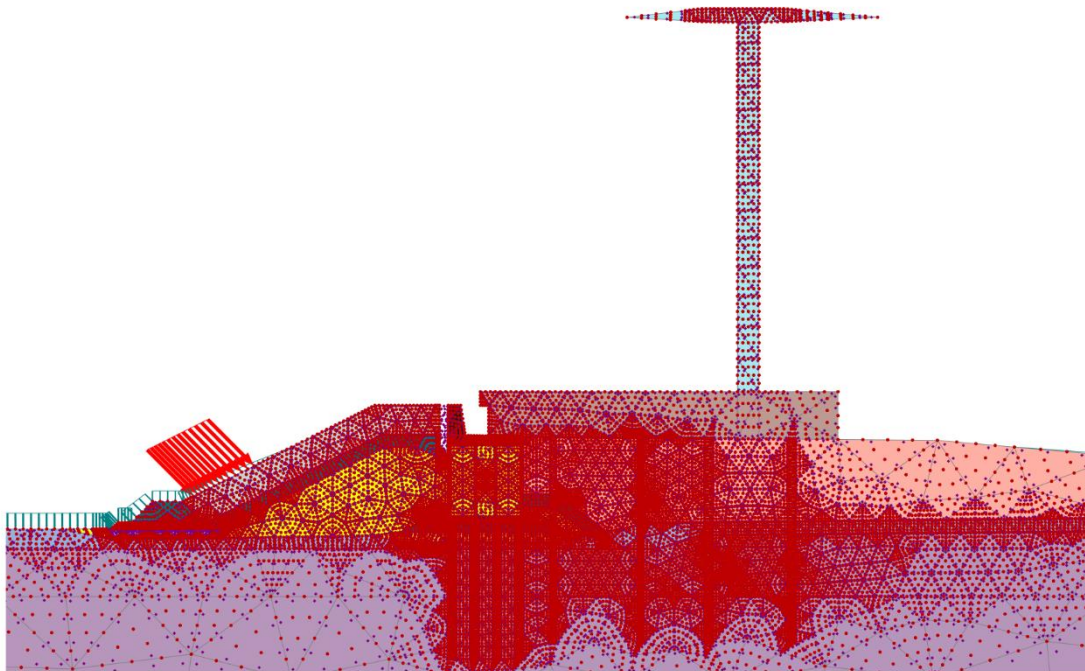
Figure 6-4 PLAXIS model of the mole of the Genova's dock containing the nodes which have been taken into account in the analysis.
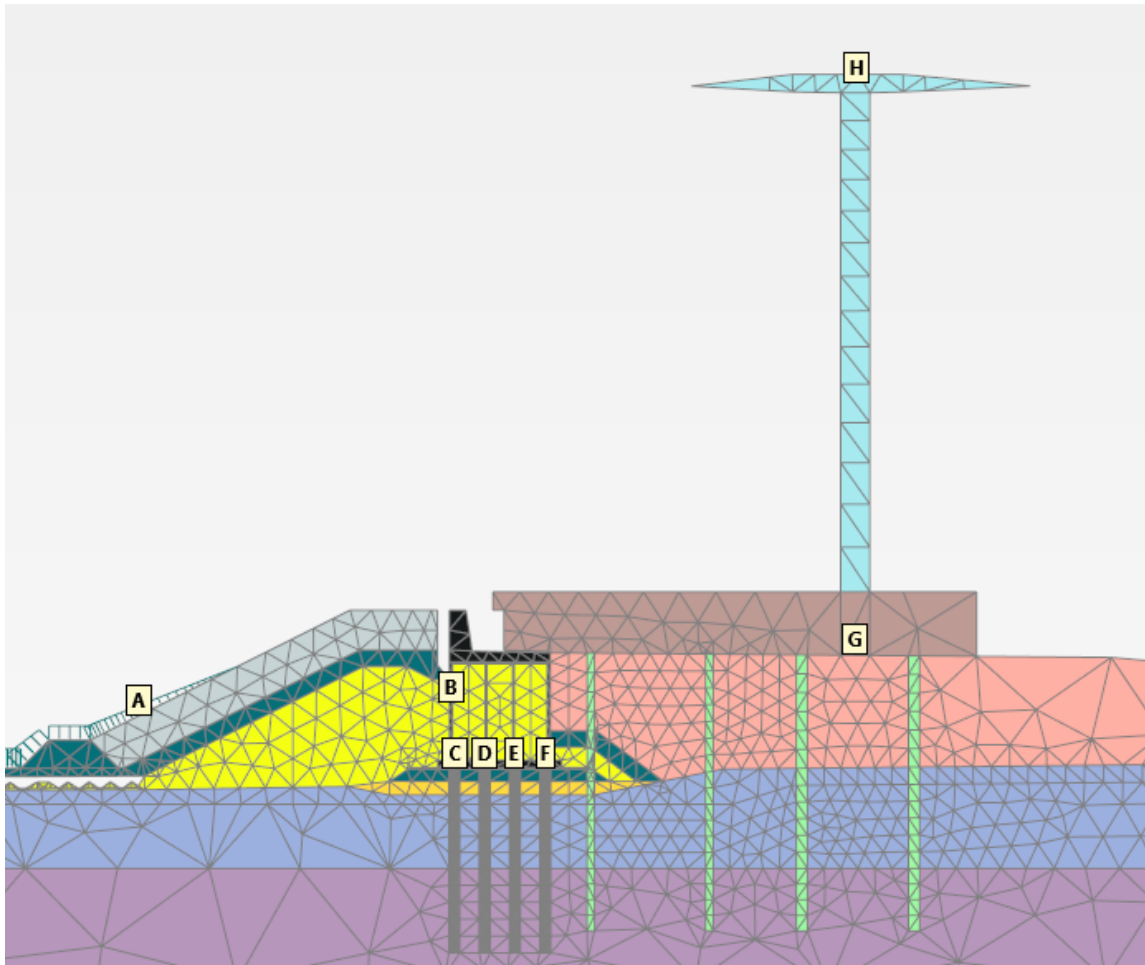
Figure 6-5 Nodes of the model whose displacements obtained from the static and the dynamic analysis have been compared.

6.5 Finite Element Model Results

As it has been mentioned in the previous point, have been run four different analysis corresponding to the cases listed below:

- STACTIC ANALYSIS in the case in which the concrete block contains a PILE's FOUNDATION.
- STACTIC ANALYSIS in the case in which the concrete block does not contain a PILE's FOUNDATION.
- DYNAMIC ANALYSIS in the case in which the concrete block contains a PILE FOUNDATION.
- DYNAMIC ANALYSIS in the case in which the concrete block does not contain a PILE's FOUNDATION.

From the static analysis have been extracted the next results:

- The deformed mesh.
- The plastic points.
- The principal effective stresses σ'_1.
- The displacements u_x.
- The displacements u_y.
- The total displacements $|U|$.

Otherwise, from the dynamic analysis have been extracted the next results:

- The deformed mesh.
- The plastic points.
- The principal effective stresses σ'_1.
- The displacements u_x.
- The displacements u_y.
- The total displacements $|U|$.
- The extreme displacements $u_{x,max}$.
- The extreme displacements $u_{Y,max}$.
- The extreme total displacements $|U_{max}|$.

In the following points are presented the obtained results for the different cases of analysis which have been carried out with *PLAXIS*. Afterwards, it has been done a discussion of the results by comparing the displacements obtained from the static and dynamic analysis in the points *A*, *B*, *C*, *D*, *E*, *F*, *G* and *H* respectively.

6.5.1   STATIC CASE-without Piles

The first analysis which has been carried out, corresponds to the static case in which the concrete block does not contain the pile's foundation under its bottom surface. In the first place, it has been presented the deformed mesh which has been obtained by means of the static analysis run with PLAXIS.
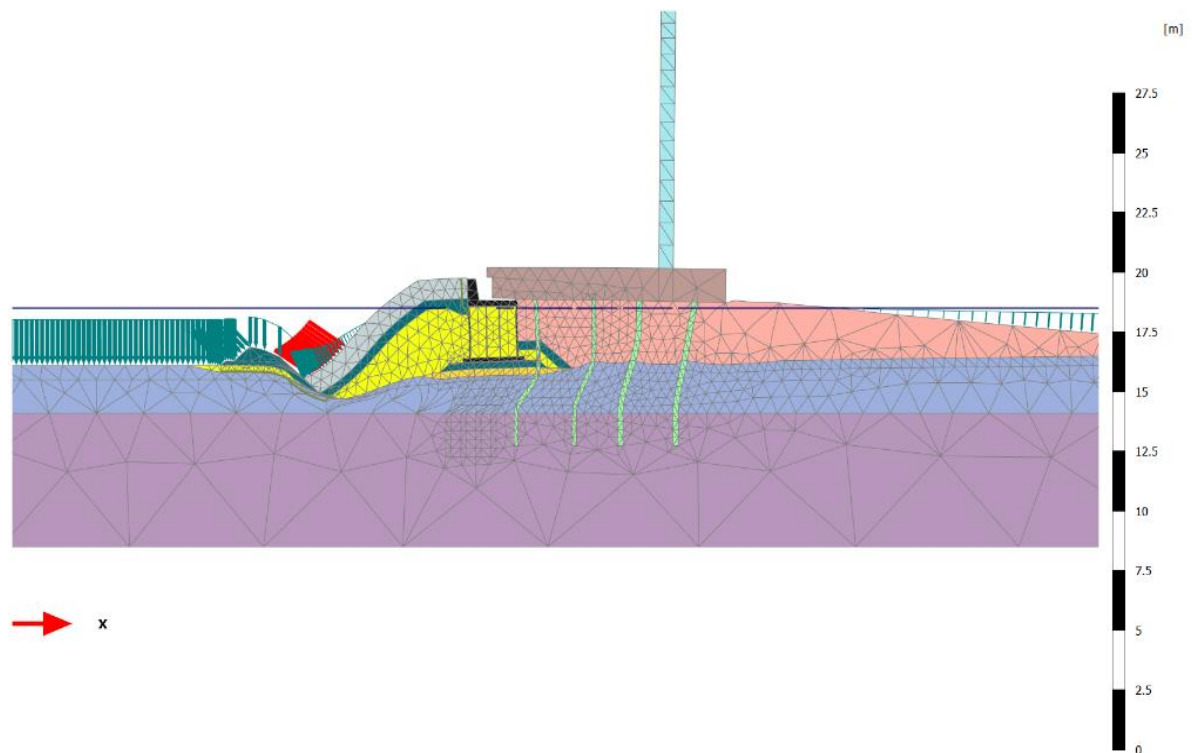
Figure 6-6 Deformed mesh of the model without piles under the concrete block obtained from the static analysis.

Subsequently, are presented in the next figure the plastic points surged in the model as a consequence of the application of the loads by means of the static analysis run by *PLAXIS*. In the figure can be noticed different kind of points in different colors. Each one of them has a different meaning:

- The red small squares represent the failure points of the model.
- The blue triangles correspond to the cap points of the model.
- The green triangles characterize the hardening points of the model.
- The white squares represents the tension cut-off points of the model.
- The brown spots correspond to the cap-hardening points of the model.

What can be noticed from the figure is that the most of the failure points are located in the layers of soil next to the surface. The highest amounts of points are concentrated in the concrete block, as well as in the layer of soil placed immediately below the platform which is at the bottom of the tower (between the piles of the foundation of the pilot tower). Otherwise, the cap points are concentrated below the concrete block, but these blue triangles also can be appreciated in the back of the piles pertaining to the foundation of the pilot tower of the Genova's dock. Concretely, in this case, the highest amount of the cap points is located in the back of the piles pertaining to the back row of the group of piles pertaining to the foundation of the tower. Finally, the other kind of points which must be mentioned in this case are the cap-hardening points, which are mostly concentrated under the concrete block and in the second layer of soil placed under the foundation of the pilot tower.
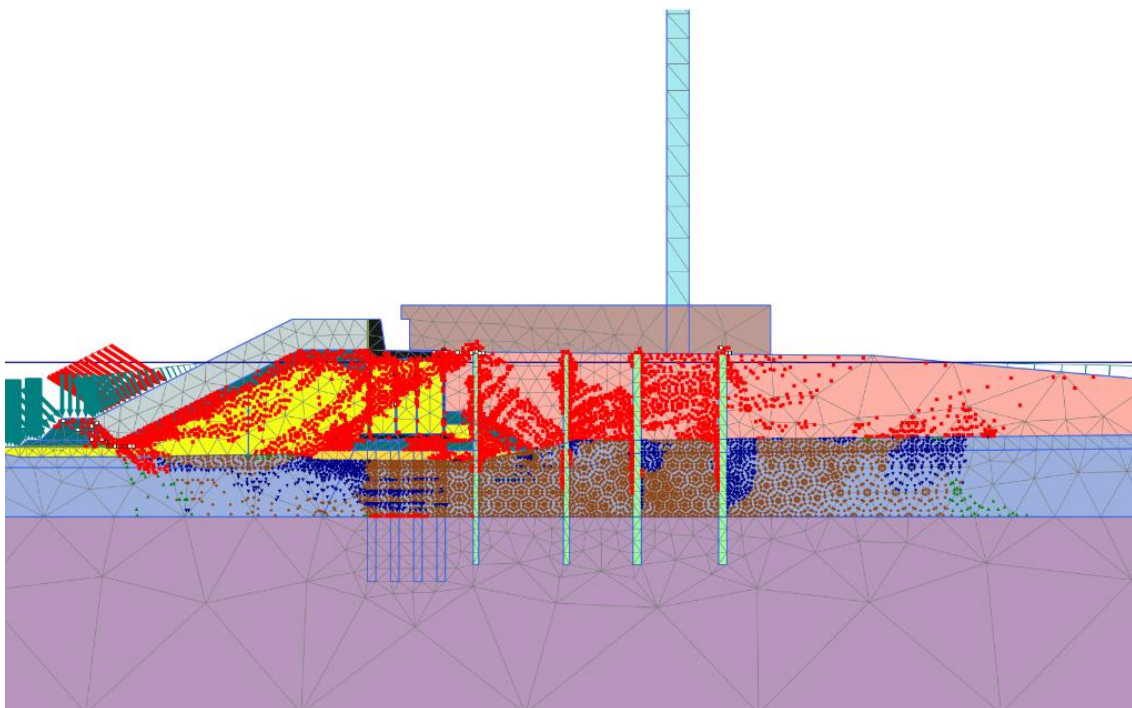
Figure 6-7 Plastic points of the model without piles under the concrete block obtained from the static analysis.

Afterwards, in the following figure have been presented the principal effective stresses σ'$_1$ which have been obtained in each point of the finite elements model developed by PLAXIS as a consequence of the static analysis run. From the results, it has been obtained a maximum

value of the principal stress σ'$_1$, equal to 741,4 kN/m2. This maximum stress has been reached in the element 169 at Node 4207, which is located on the back of the piles pertaining to the first row of the group that consists of the foundation of the pilot tower. Particularly, this element is located next to bottom surface of the piles of this front row.
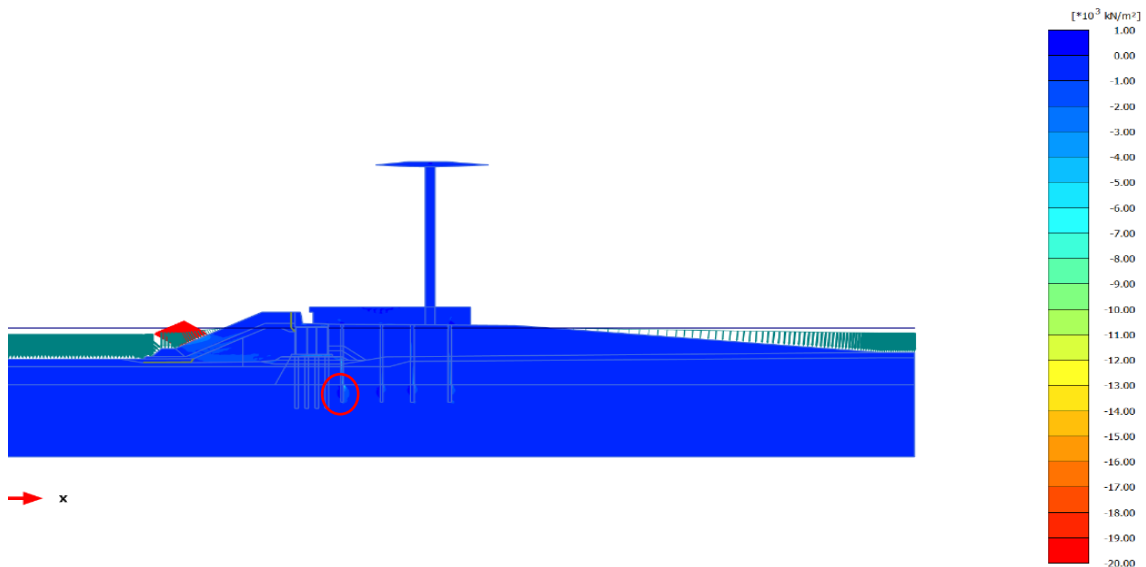
Figure 6-8 Principal effective stress σ'$_1$ of the model without piles under the concrete block obtained from the static analysis.

In the next figures are showed the total displacements of the different elements which conform the model in both directions. In the first figure are represented the magnitude of the total displacements with regards to the direction x (**u$_x$**). As it can be appreciated, according to the legend, the highest displacements take place in the portion of soil located immediately after of the breakwater of the Genova's dock. As it can be checked, in this zone the displacements reach values higher than 1,40 meters. Concretely, the maximum displacement achieved in the direction of the axis x is equal to 1,626 meters. This is produced in the element 913 at node 16441. Otherwise, the displacements in the head of the pilot tower are higher than 1 meter, which is too much and explains the collapse of the tower. Finally, as it is being studied the behavior of the concrete block, it must be underlined that the displacements of it are comprised between 0,80 – 1 meters.
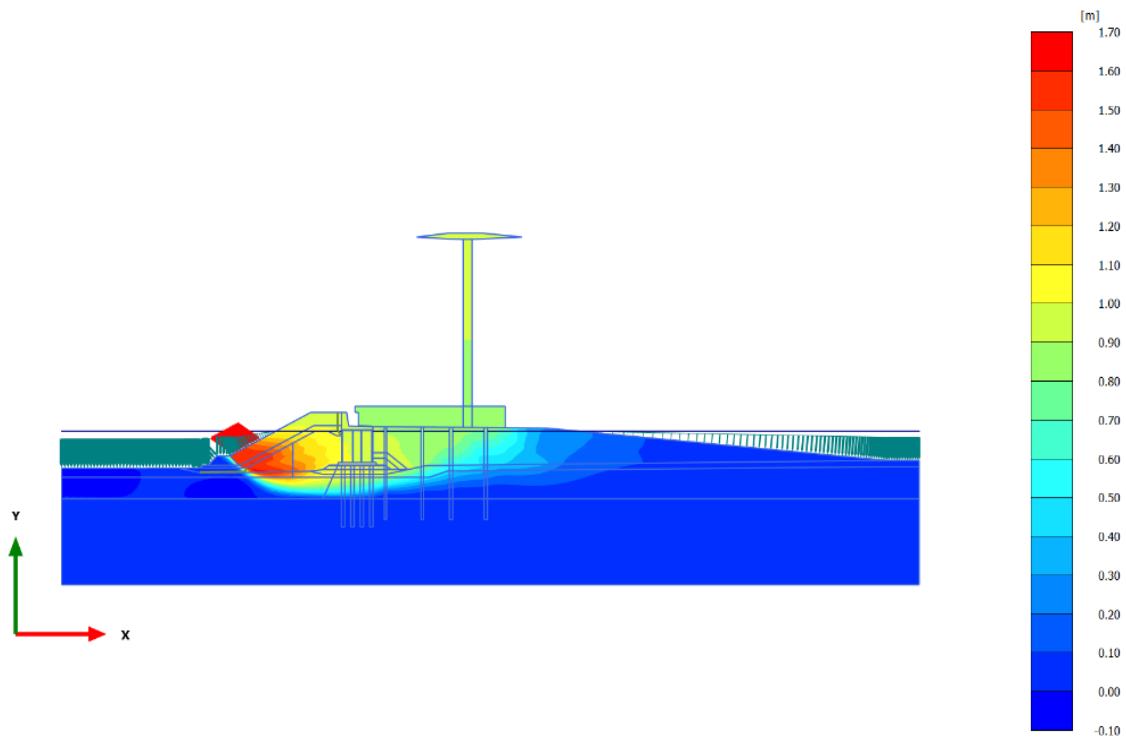
Figure 6-9 Total displacements u_x achieved in the different nodes of the model without piles under the concrete block obtained from the static analysis.

Subsequently, in the next figure are represented the total displacements in the direction of the axis y. As it can be checked, the magnitude of these displacements is much lower than those displacements achieved according to the direction x. In this case, the highest displacements are reached in the breakwater, particularly, in the zone of the mole where the cargo ship is supposed to impact. The maximum displacement in this case has been produced in the negative direction of the axis y and is equal to 1,36 meters. This has been reached in the element 225 at node 17947. The other points of interest in the model are those consisting on the concrete block. As it can be checked, the displacements of it are not higher than 0,20 meters. In the head of the pilot tower the displacements in the direction of the axis y are high, its magnitude is as much as 0,10 meters, which in comparison with those displacements achieved in the direction of the axis x are negligible.
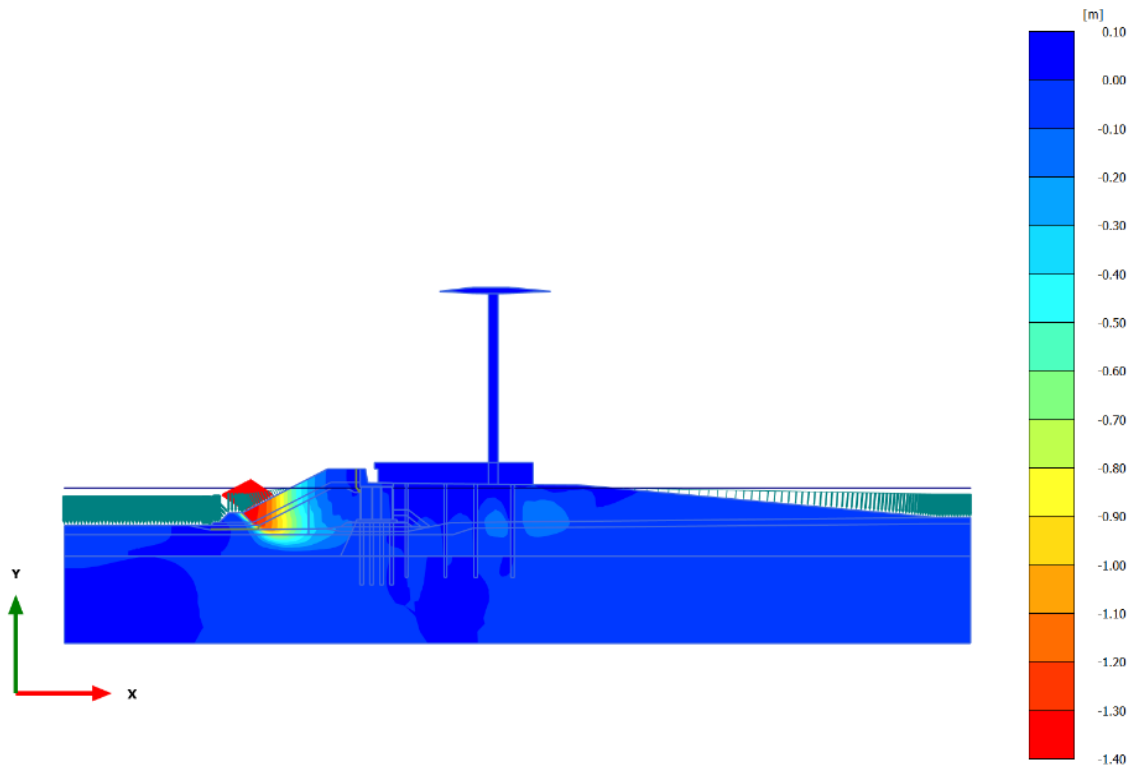
Figure 6-10 Total displacements u_y achieved in the different nodes of the model without piles under the concrete block obtained from the static analysis.

Finally, in the next figure have been showed the total displacements |U| achieved in the different elements of the model after having run a static analysis. The results obtained in this case are more similar to those obtained in the case of the displacements in the direction of the axis x. The maximum displacement which has been reached in this case is equal to 2,084 meters. It corresponds to the element 236 at node 17904, which is located in the impact zone of the cargo ship in the mole. In addition to this, the total displacements reached in the concrete block are comprised between 0,80 – 1,20 meters, and those achieved in the head of the pilot tower are comprised between 0,80 – 1 meter. As it has been told above, the magnitude of the displacements reached in the head of the pilot tower of the Genova's dock, which have been obtained in this analysis, justify the collapse of the tower.
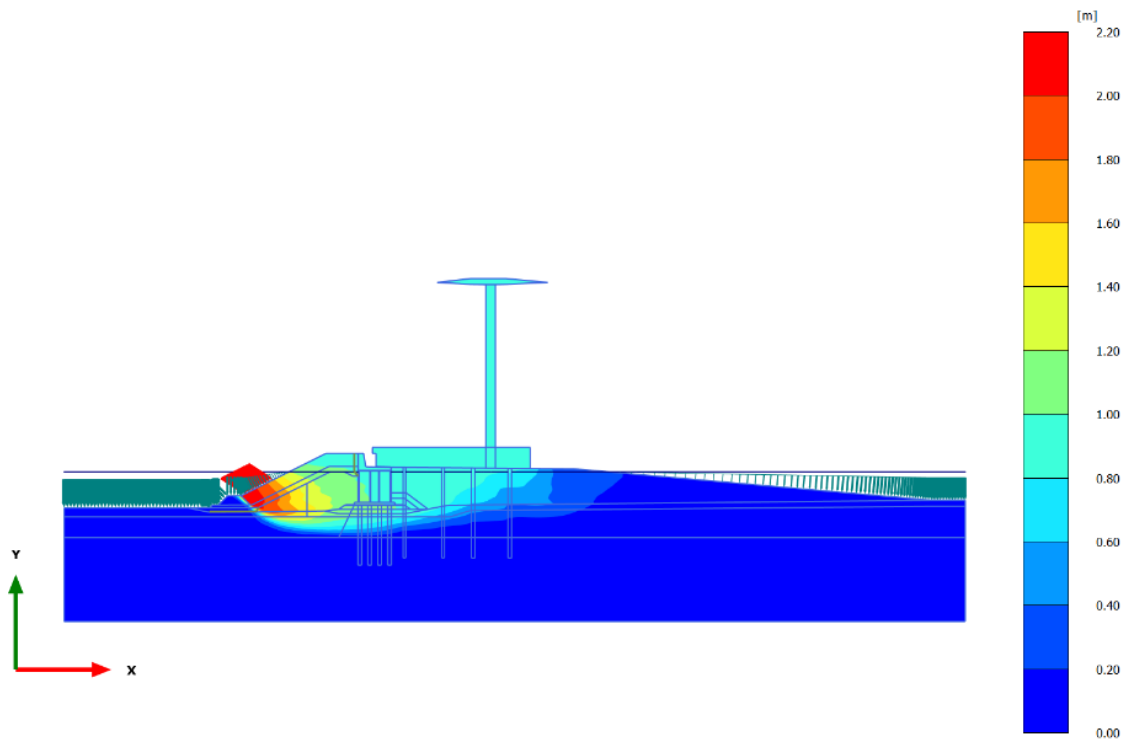
Figure 6-11 Total displacements |U| achieved in the different nodes of the model without piles under the concrete block obtained from the static analysis.

6.5.2   DYNAMIC CASE-without Piles

In this point are going to be discussed the results obtained in the model of the Genova's dock developed with *PLAXIS*, in the case in which the concrete block does not contain the pile's foundation under its bottom surface. The simulation has been carried out by means of a dynamic calculation process extended to a period of time equal to 6 seconds.

Firstly, it has been presented the deformed mesh of the model after having run a dynamic analysis. With regards to the deformed mesh obtained for the static analysis, it must be told that both are very similar. However, the maximum displacement achieved with the dynamic analysis is a little bit higher than that reached with the static analysis. As it can be appreciated, the highest deformations are produced at the bottom of the breakwater, in the piles pertaining to the foundation of the Genova's dock and in the head of the pilot tower, as well as in the platform on which the tower lies.
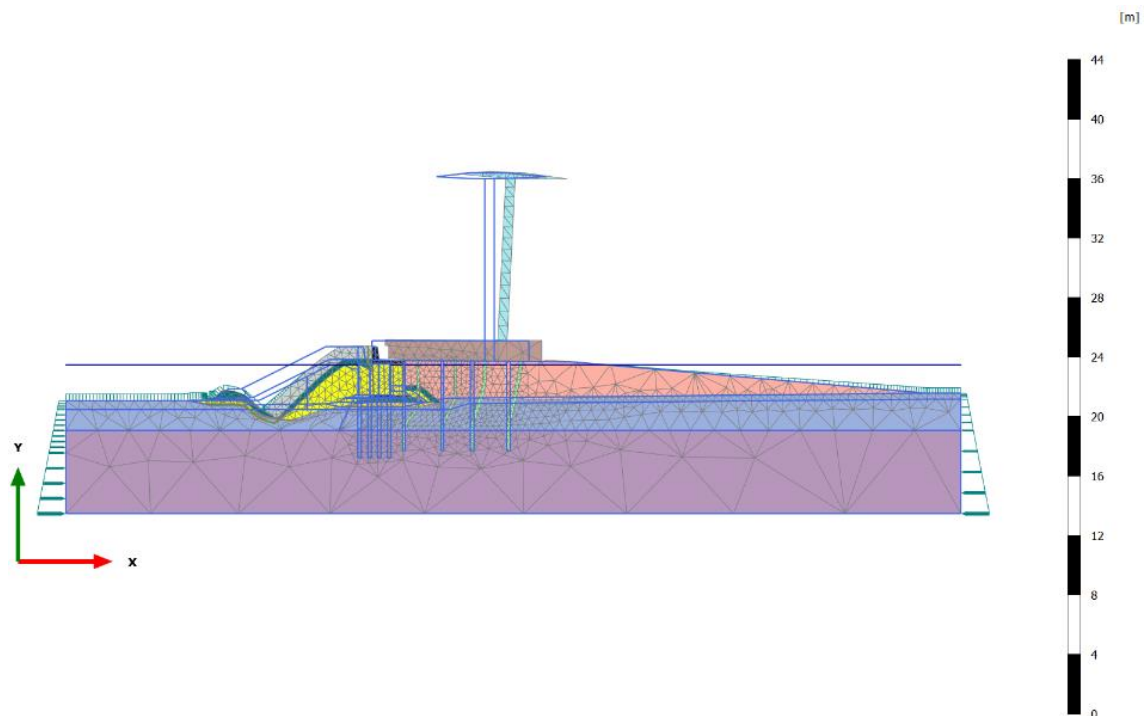
Figure 6-12 Deformed mesh of the model without piles under the concrete block obtained from the dynamic analysis.

Successively, in the next figure are presented the plastic points which have appeared in the model during the analysis as a consequence of the loads induced on the mole due to the impact of the cargo ship. One of the main details which must be underlined is that, unlike the results obtained in the static analysis, the amount of the plastic points has been highly reduced. In fact, in this case can only be appreciated two kind of plastic points from the six sorts which could be noticed in the static analysis.

-    The red small squares represent the failure points of the model.
-    The white squares represents the tension cut-off points of the model.

From these results, it can be checked that the failure points are placed mostly in the structure on which the foot of the breakwater rests, which is next to the impact zone of the cargo ship. As it is logical, this zone of the model corresponds to that where the highest stresses are produced. In this portion of soil can also be appreciated a few tension cut-off points, represented by the white small squares. In addition to this, the other failure points, which have resulted from the analysis, are located in the concrete block. Concretely, in the four corners which delimit the block in the model. Moreover this failure points, it can also be found a tension cut-off point in the concrete block.
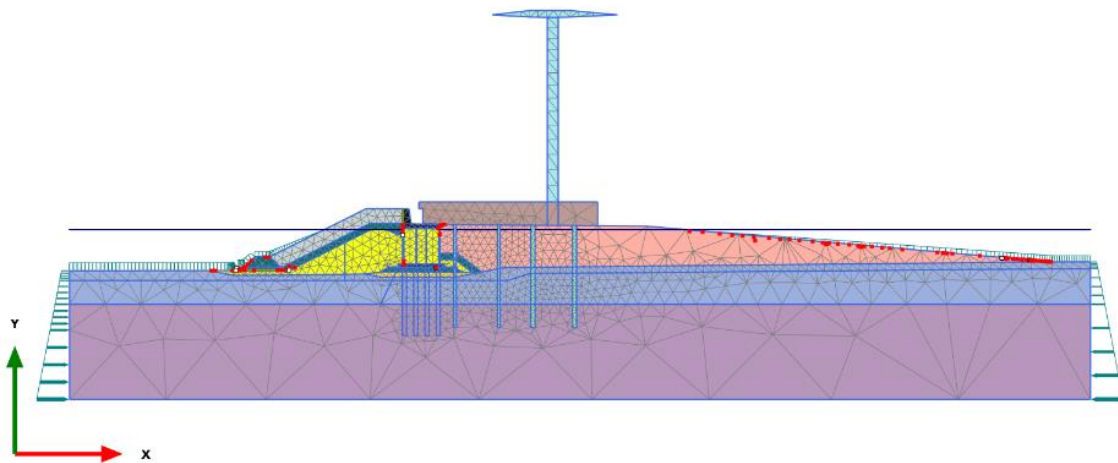
Figure 6-13 Plastic points of the model without piles under the concrete block obtained from the dynamic analysis.

Afterwards, in the following figure are presented the principal effective stress σ'$_1$ reached in each point of the model for the simulation of the real case, without the piles under the concrete block. These stresses have been obtained by means of a dynamic analysis. The maximum effective stress, which has been achieved in the element 1810 at Node 10350, is equal to 18030 kN/m^2. The node in which has been reached this maximum value of principal effective stress is located in the back of the piles pertaining to the front row of the foundation of the control pilot tower of the Genova's dock. Particularly, this maximum stress has been achieved at a depth next to the bottom surface of the piles. In addition to this, it can be appreciated in the figure that the maximum values of the effective stresses σ'$_1$, are placed on the back of the piles pertaining to the foundation of the pilot tower at the same depth as the maximum effective stresses of the front row.
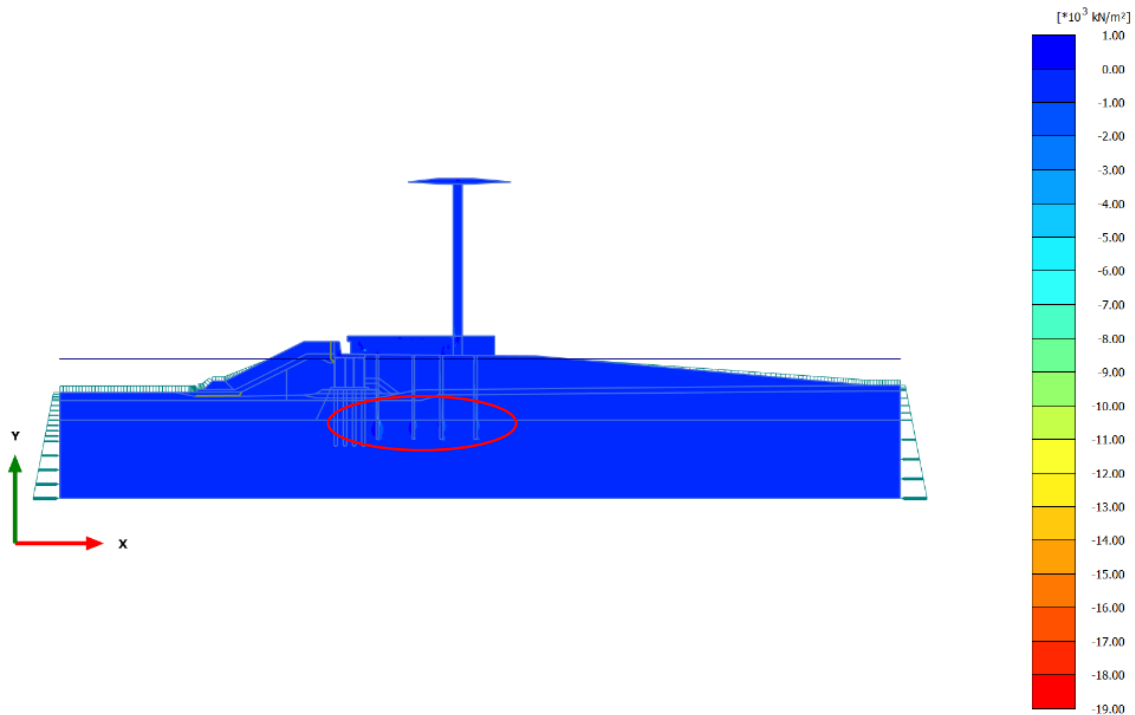
Figure 6-14 Principal effective stress σ'₁ of the model without piles under the concrete block obtained from the dynamic analysis.

Subsequently, are showed the total displacements achieved in the nodes of the model of the real case, which have been obtained with *PLAXIS* from a dynamic analysis. It must be underlined that these displacements are those reached at the end of the simulation time which is equal to 6 seconds. These must be differenced from the extreme total displacements, which corresponds to the maximum values of the displacements achieved in the simulation period. As it has been done for results obtained from the static analysis, firstly are presented the components of the displacements with regards to the two principal directions, which are those defined by the axis x and y respectively u_x and u_y.

In the following figure are showed the total displacements at the end of the simulation time with regards to the direction coinciding with the axis x. As it can be notice, the magnitude of these displacements is higher than those obtained for those values in the direction of the axis y. The maximum value of the total displacements in the direction x, which is equal to 1,709 meters, has been achieved in the element 210 at node 17899. This node is located at the bottom of the breakwater, which corresponds to that zone in the model where the cargo ship is supposed to impact. This is due to the fact that the highest forces are induced in this zone of the mole. Otherwise, according to this dynamic analysis run on the model developed for the real case with the software PLAXIS, it can be concluded that the displacements achieved in the head of the pilot tower are higher than 1,40 meters. These values of the displacements u_x at the end of the simulation time, justify the collapse of the pilot tower in the real case because of the huge displacements in the head of the tower. Finally, it must be mentioned that the displacements in the concrete block at the end of the simulation, are approximately equal to 1 meter, which is almost the same result as it has been reached by means of the static analysis for the same case.
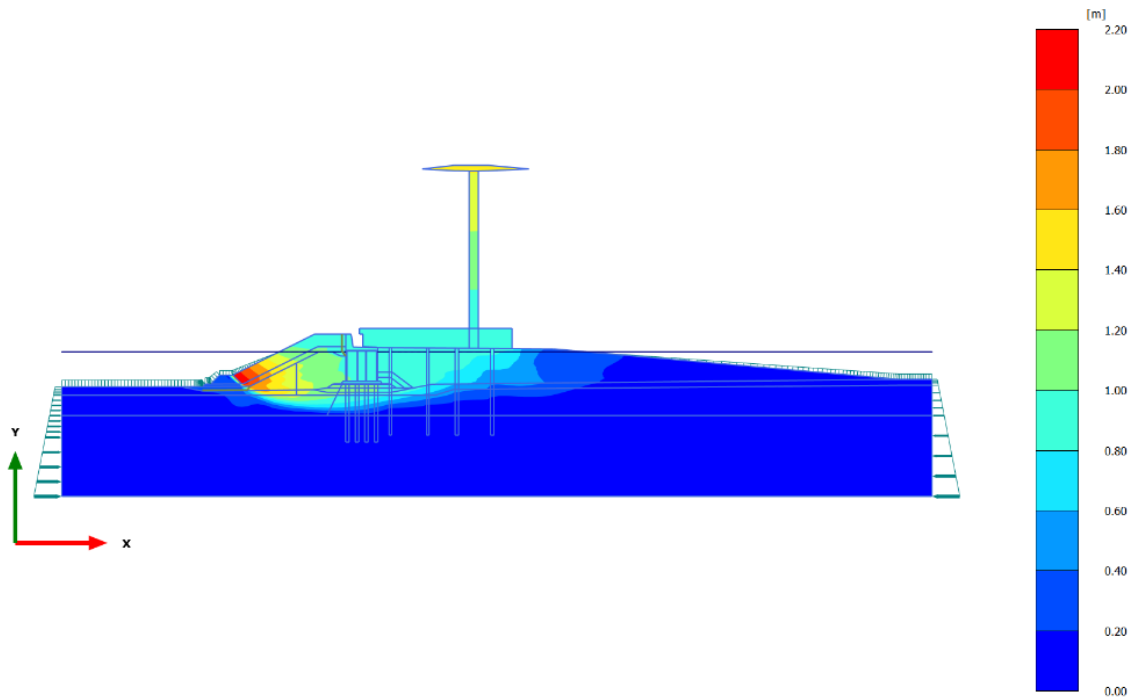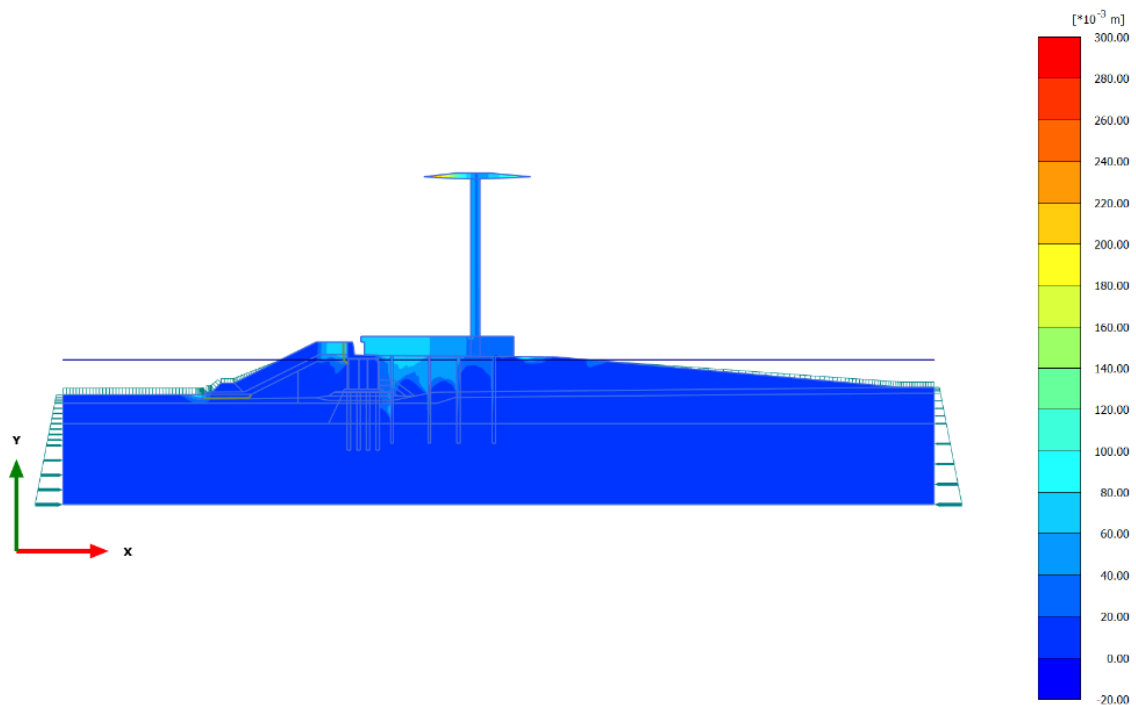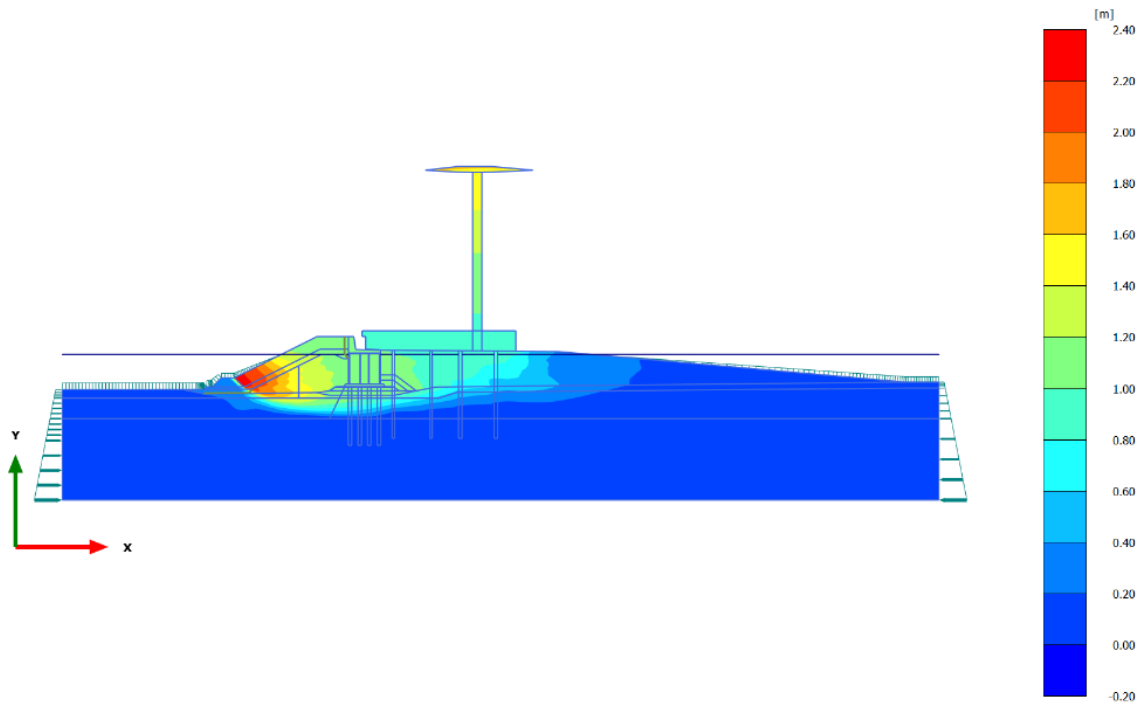
124
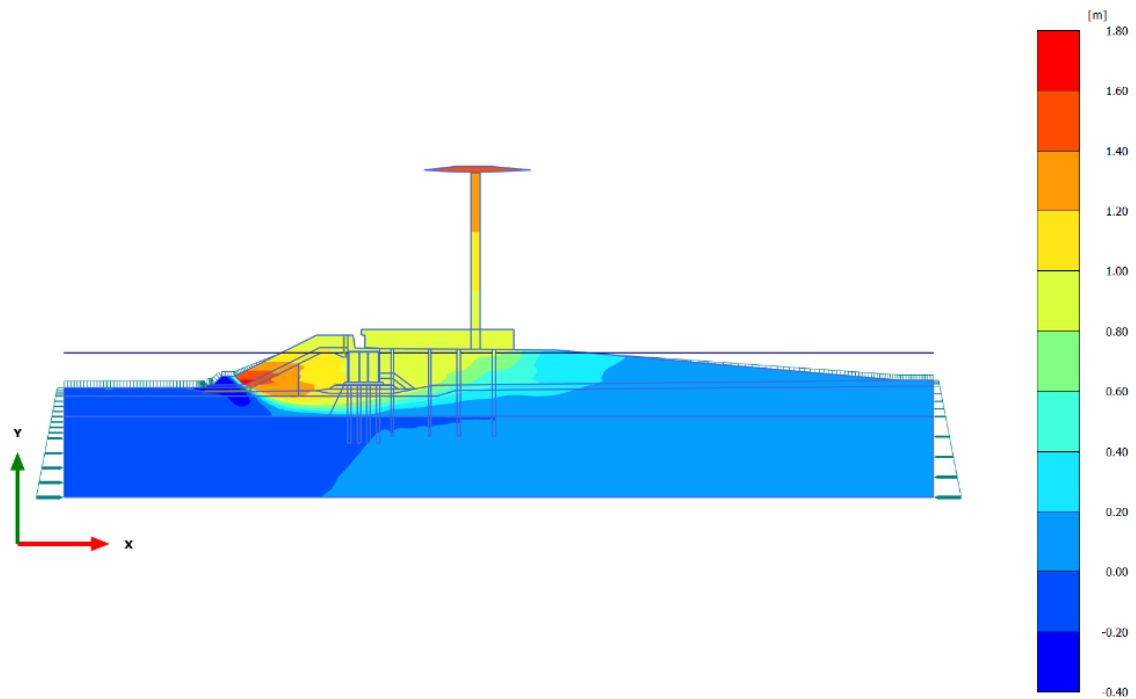
Figure 6-15 Total displacements u_x achieved in the different nodes of the model without piles under the concrete block obtained from the dynamic analysis.

The next figure presents the total displacements in the direction of the axis y, achieved in the model at the end of the simulation time, after having run a dynamic analysis. As it has been mentioned above, the magnitude of the displacements is lower than those reached on the direction of the axis x. In this case, the maximum displacement has been achieved in the element 225 at node 17947. It is equal to 1,547 meters and it has been produced in the negative direction of the axis y. This node is located at the bottom of the breakwater next to the impact point of the ship on the mole of the Genova's dock. Otherwise, the highest displacements uy reached in the head of the tower at the end of the simulation time are comprised between 0,10 – 0,30 meters. The displacements achieved in the concrete block in this case are approximately equal to 0,10 meters, which are similar to those obtained with the static analysis for the same case.
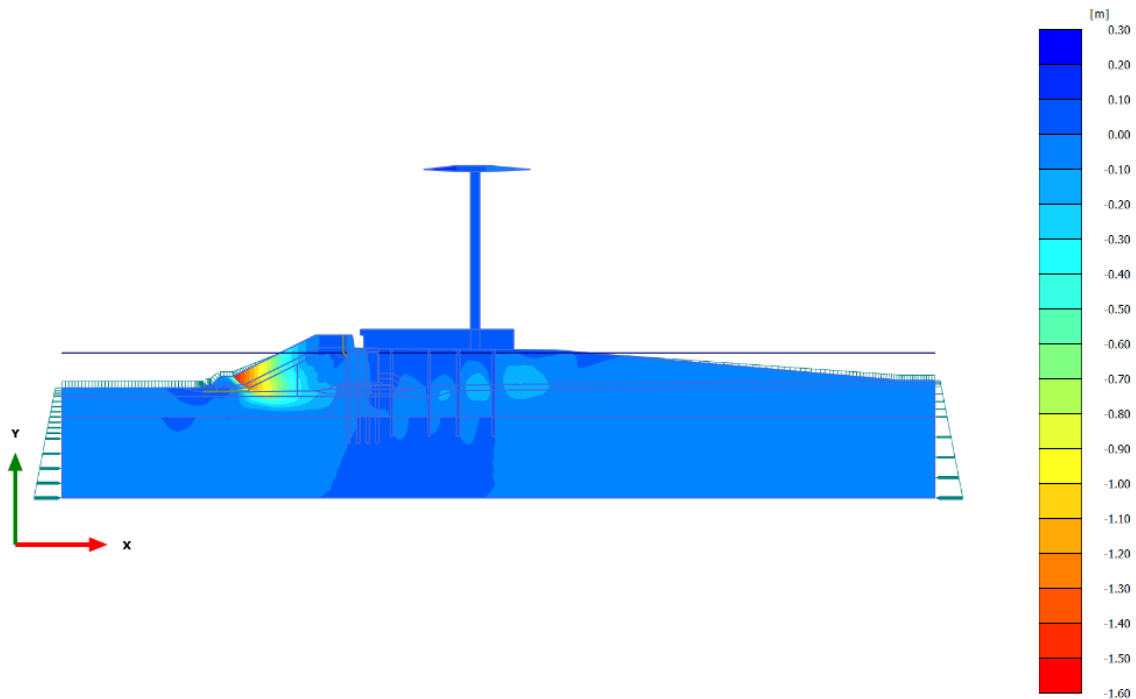
Figure 6-16 Total displacements u_y achieved in the different nodes of the model without piles under the concrete block obtained from the dynamic analysis.

The total displacements |U| achieved at the end of the simulation time of 6 seconds, in the model of the real case developed by PLAXIS, are represented in the following figure. The maximum value of the total displacements, which has been reached in the element 210 at node 17899, is equal to 2,181 meters. This value is a little bit higher than the maximum value of the total displacements obtained in the static analysis. The node in which the maximum displacement is reached, is located in the zone of the model where the ship impacted against the breakwater.

The total displacements |U| reached at the end of the simulation time in the head of the tower are higher than 1,40 meters. These values of the displacements are huge. Finally, it must be mentioned that the displacements in the concrete block which have been obtained in this case are comprised between 0,80 – 1 meter.

Figure 6-17 Total displacements |U| achieved in the different nodes of the model without piles under the concrete block obtained from the dynamic analysis.

Consecutively, are presented the values of the extreme total displacements in the directions of the axis x and y. These values of the displacements correspond to the maximum values which have been reached along the simulation time of 6 seconds for each node of the model. In the first place are showed the values of the extreme total displacements in the direction of the axis x. The maximum displacement, which has been achieved in the element 210 at node 17755, is equal to 1,832 meters. This node is located in the zone of the breakwater where the cargo ship is supposed to hit. It must be underlined that the maximum displacements reached in the head of the pilot tower are higher than 1,60 meters. As it can be noticed, the maximum displacements exceed those obtained at the end of the simulation time, which are around 1,40 meters. In addition to this, the maximum displacements achieved in the concrete block are comprised between 1 – 1,20 meters.
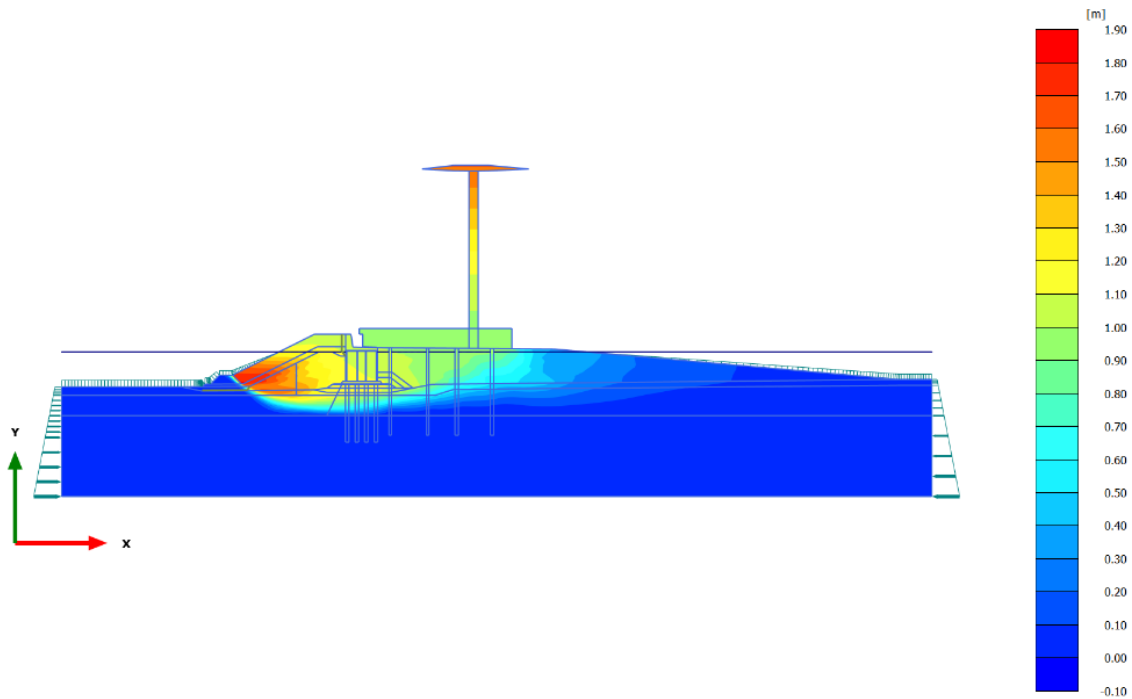
Figure 6-18 Maximum displacements u_x achieved in the different nodes of the model without piles under the concrete block obtained from the dynamic analysis.

Subsequently, are presented the maximum displacements in the direction of the axis y which have been reached in the nodes of the model along the simulation time. The maximum displacement in the direction of the axis y has been achieved in the head of the pilot tower of the Genova's dock. It is equal to 0,2845 meters and has been produced in the element 1 at node 1. Apart from this, the highest displacements in the direction y have been reached in the platform placed at the bottom of the pilot tower, particularly over the two firsts rows of piles pertaining to the foundation of the tower. The magnitude of these displacements is approximately equal to 0,10 meters. It has been also achieved similar displacements at the top and at the bottom of the breakwater.

Figure 6-19 Maximum displacements u_y achieved in the different nodes of the model without piles under the concrete block obtained from the dynamic analysis.

Finally, in the next figure are showed the extreme total displacements $|U|_{max}$ which have been achieved in the nodes composing the model developed by PLAXIS, along the simulation time. The maximum displacement has been reached at the bottom of the breakwater, which is the impact zone. Concretely, this maximum value of $|U|$, which has been achieved in the element 210 at node 17899, is equal to 2,317 meters. Otherwise, the displacements achieved in the head of the tower are higher than 1,50 meters. The magnitude of these displacements is huge, sufficient to produce the collapse of the pilot tower as a consequence of the ship's impact. Finally, the displacements which have been achieved in the concrete block are comprised between 1 – 1,20 meters.

Figure 6-20 Maximum displacements |U|max achieved in the different nodes of the model without piles under the concrete block obtained from the dynamic analysis.

The previous model developed by the FEM software *PLAXIS*, corresponds to the real problem that happened in the Genova's dock a few years ago, in which a cargo ship impacted against the breakwater and as a consequence of it, the pilot control tower of the dock collapsed. It has been run a static and a dynamic analysis to determine the stresses and the displacements in different nodes of the model. It has been concluded that the values of the displacements achieved are huge, so that, in the following points is going to be studied the improvement in the system's response in the case in which the concrete block, placed between the breakwater and the pile's foundation of the pilot tower, would have contained a pile's foundation which would have restrained its displacements through the soil. The foundation of the concrete block which has been proposed, is composed by a group of 16 piles (4 x 4) of 20 meters in length with a diameter of 1,20 meters.

6.5.3   STATIC CASE-with Piles

After having discussed the results obtained from the static and dynamic analysis in the case in which the concrete block does not contain the pile's foundation under its bottom surface, are going to be commented those results obtained from the analysis run in the case in which the concrete block is restrained to the soil by a foundation consisting on a group of 16 piles (4 x 4) that are 20 meters in length and whose diameters are equal to 1,2 meters.

Firstly, are going to be discussed the results corresponding to the static analysis. In the first figure, it can be observed the deformed mesh of the model after the calculation process. As it can be noticed, the deformations in the piles pertaining to the foundation of the pilot tower of the Genova's dock are much lower than those reached in the case in which the concrete block does contain the pile's foundation under its bottom surface. This is an evidence about the improvement in the behavior system which has been achieved as a consequence of the inclusion of the pile's foundation under the concrete block.
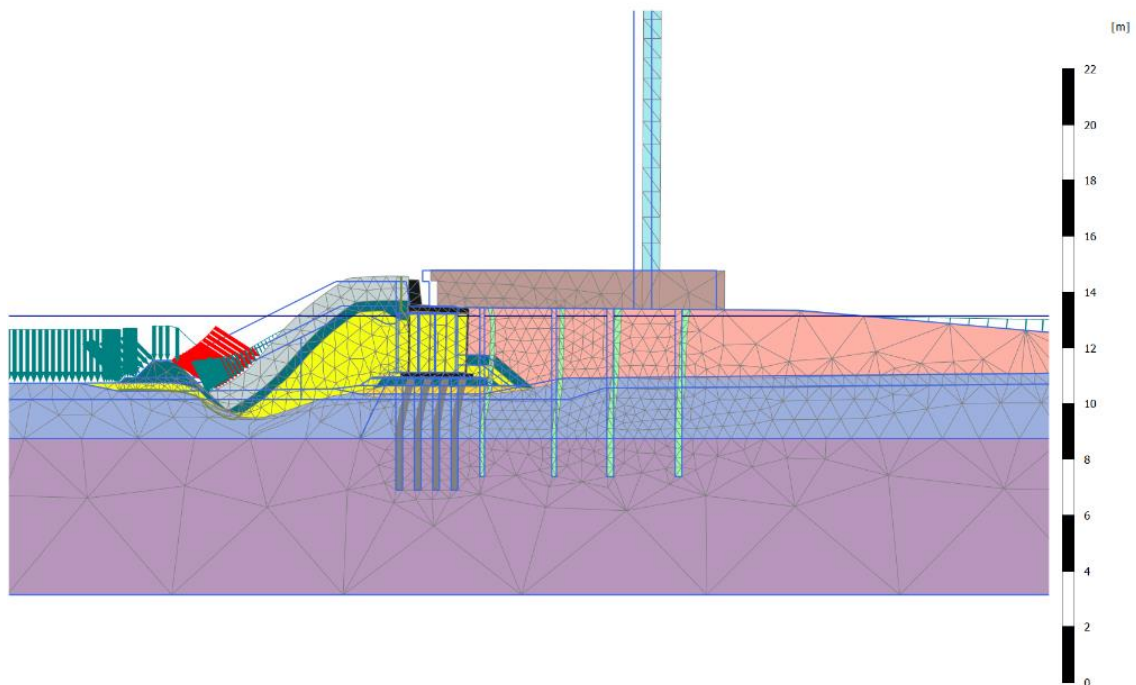
Figure 6-21 Deformed mesh of the model with piles under the concrete block obtained from the static analysis.

Subsequently, are presented in the next figure the plastic points surged in the model as a consequence of the application of the loads by means of the static analysis run by *PLAXIS*. In the figure can be noticed different kind of points in different colors. Each one of them has a different meaning:

- The red small squares represent the failure points of the model.
- The blue triangles correspond to the cap points of the model.
- The green triangles characterize the hardening points of the model.
- The white squares represents the tension cut-off points of the model.
- The brown spots correspond to the cap-hardening points of the model.

In this case, the failure points of the model are concentrated in several zones. Firstly, it can be appreciated a high amount of these small red squares in the portion of soil placed immediately below the breakwater in the impact zone where the cargo ship hit the mole. This is due to the fact that the stresses in this zone are the highest. Otherwise, there is huge quantity of failure points in the concrete block, overall, in the head of the piles pertaining to the foundation of the block. This is because of the high forces which this foundation absorbs. As it can be noticed, these failure points are located, concretely, in the front of the piles of this foundation. This zone corresponds to that where the soil tends to split from the piles. This behavior is also observed in the piles pertaining to the foundation of the pilot tower. In addition to this, it can be appreciated a huge amount of failure points between the piles of the foundation of the pilot tower. It must be underlined that the failure points are mostly concentrated on the layer of soil located immediately below to the platform placed at the bottom of the pilot tower. On the other hand, the cap points (blue triangles) are highly concentrated in the back of the piles pertaining to both foundations. As it was mentioned, these portions of soil are those where the piles push the soil and as a consequence of it, are formed the wedges. This behavior has been observed in the layer of soil placed at a depth of 3 – 4 meters under the phreatic level. In this layer are also concentrated the brown spots which represent the cap-hardening point of the model. Another phenomenon that must be mentioned are the tension cut-off points, which are represented by white squares. It is curious, because these points are placed on the head of the piles pertaining to both foundations. Finally, in the portion of soil located between the back row of the concrete block's foundation and the front row of the tower's foundation, at a depth of 4 meters approximately, are placed the hardening points which have appeared due to the stresses induced in the soil by the impact of the cargo ship.
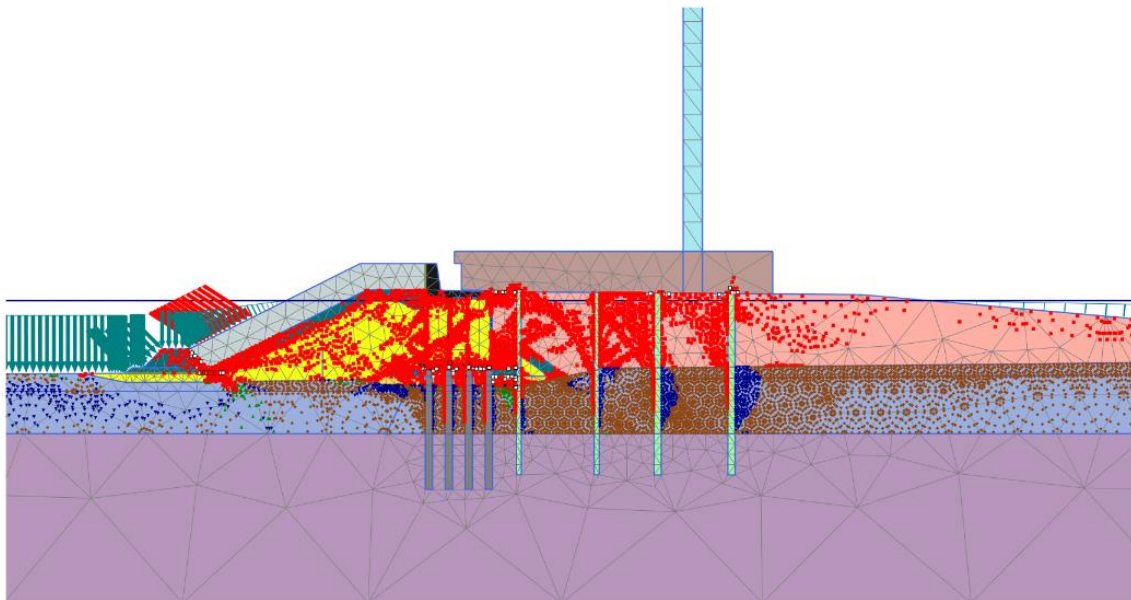
Figure 6-22 Plastic points of the model with piles under the concrete block obtained from the static analysis.

Afterwards, in the following figure have been presented the principal effective stresses σ'_1 which have been obtained in each point of the finite elements model developed by PLAXIS as a

consequence of the static analysis run. From the results, it has been obtained a maximum value of the principal stress σ'_1, equal to 62580 kN/m^2. This maximum stress has been reached in the element 1740 at Node 14555, which is located on the back of the piles pertaining to the first row of the group that consists of the foundation of the concrete block. The difference with the static analysis run in the other case is that, the highest principal stresses in this case are located on the back side of the piles pertaining to the foundation of the concrete block. Consequently, the principal effective stresses σ'_1, in the piles of the pilot tower's foundation have been reduced.
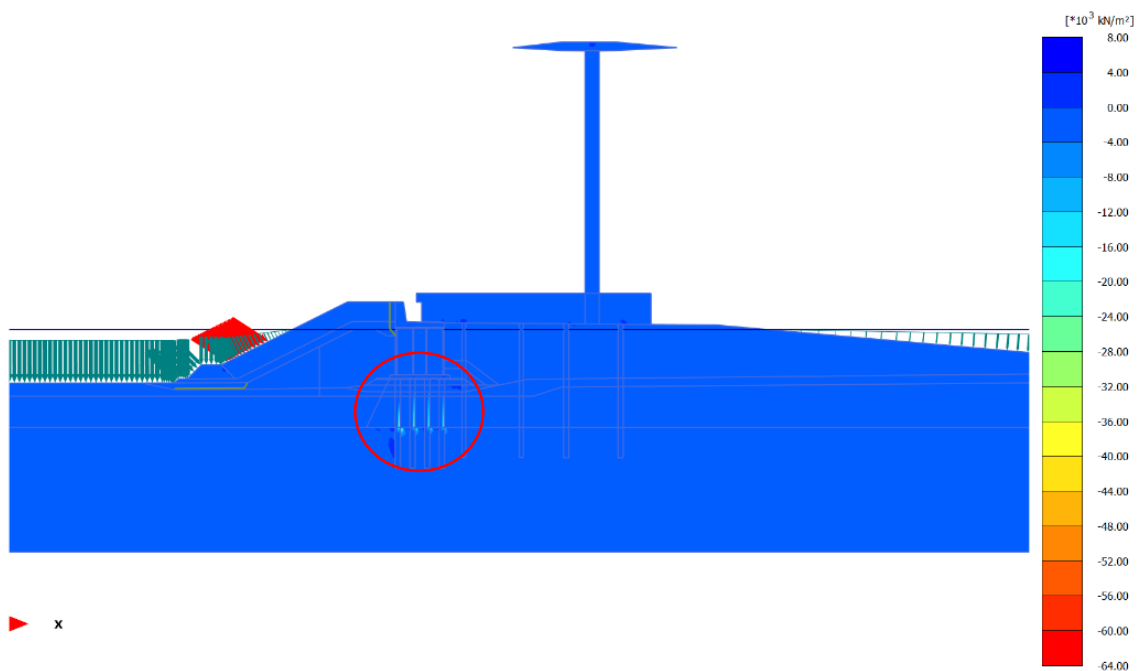
Figure 6-23 Principal effective stress σ'_1 of the model with piles under the concrete block obtained from the static analysis.

In the next figures are showed the total displacements of the different elements which conform the model in both directions. In the first figure are represented the magnitude of the total displacements with regards to the direction x (u_x). As it can be appreciated, according to the legend, the highest displacements take place in the portion of soil located immediately after of the breakwater of the Genova's dock. As it can be checked, in this zone the displacements reach values higher than 1,10 meters. Concretely, the maximum displacement achieved in the direction of the axis x is equal to 1,154 meters. This is produced in the element 913 at node 16441. Otherwise, it can appreciated that the displacements in the head of the pilot tower have been reduced significantly with regards to the case in which concrete block does not contain the pile's foundation under its bottom surface. However, the displacements achieved are still higher than 0,40 meters, which continuous being too much. With the piles under the concrete block, the displacements are quite reduced. However, these are high and the collapse of the tower cannot be impeded. Finally, as it is being studied the behavior of the

concrete block, it must be underlined that the displacements reached on it are comprised between 0,30 – 0,50 meters.
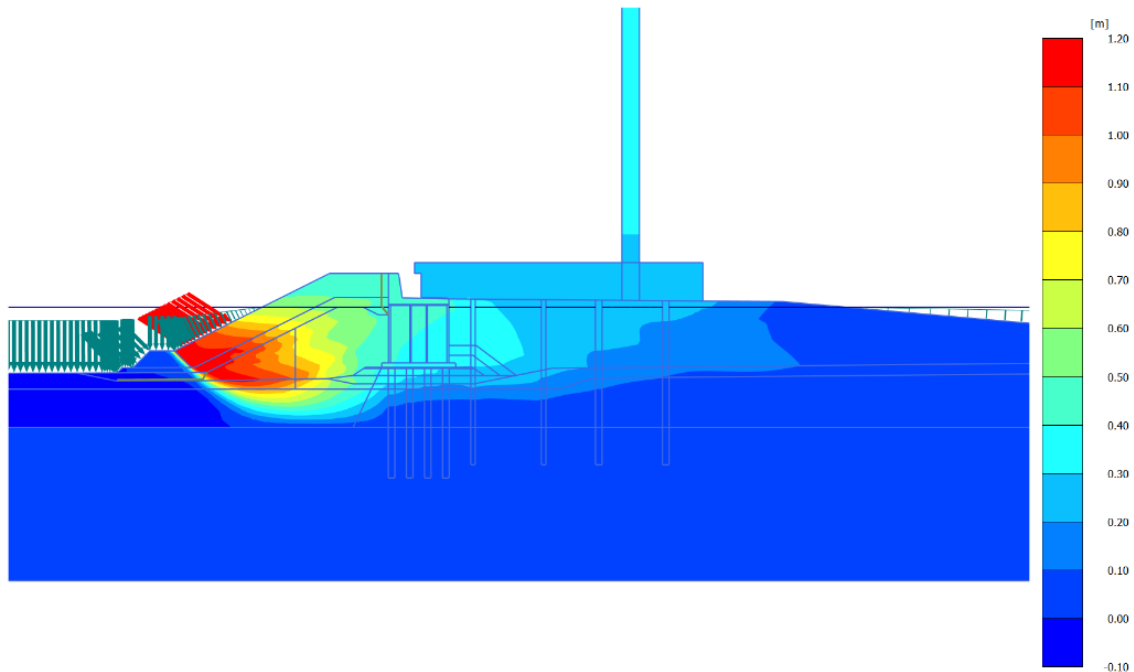
Figure 6-24 Total displacements u_x achieved in the different nodes of the model with piles under the concrete block obtained from the static analysis.

Subsequently, in the next figure are represented the total displacements in the direction of the axis y. As it can be checked, the magnitude of these displacements is much lower than those displacements achieved according to the direction x. In this case, the highest displacements are reached in the breakwater, particularly, in the zone of the mole where the cargo ship is supposed to impact. The maximum displacement in this case has been produced in the negative direction of the axis y and is equal to 1,166 meters. This has been reached in the element 195 at node 17869. The other points of interest in the model are those consisting on the concrete block. As it can be checked, the displacements of it have been also reduced and are comprised between 0,05 – 0,10 meters. In the head of the pilot tower the displacements in the direction of the axis y are higher than those obtained in the direction of the axis x, its magnitude has been increased with regards to the static analysis without piles under the concrete block, and these are higher than 0,10 meters.
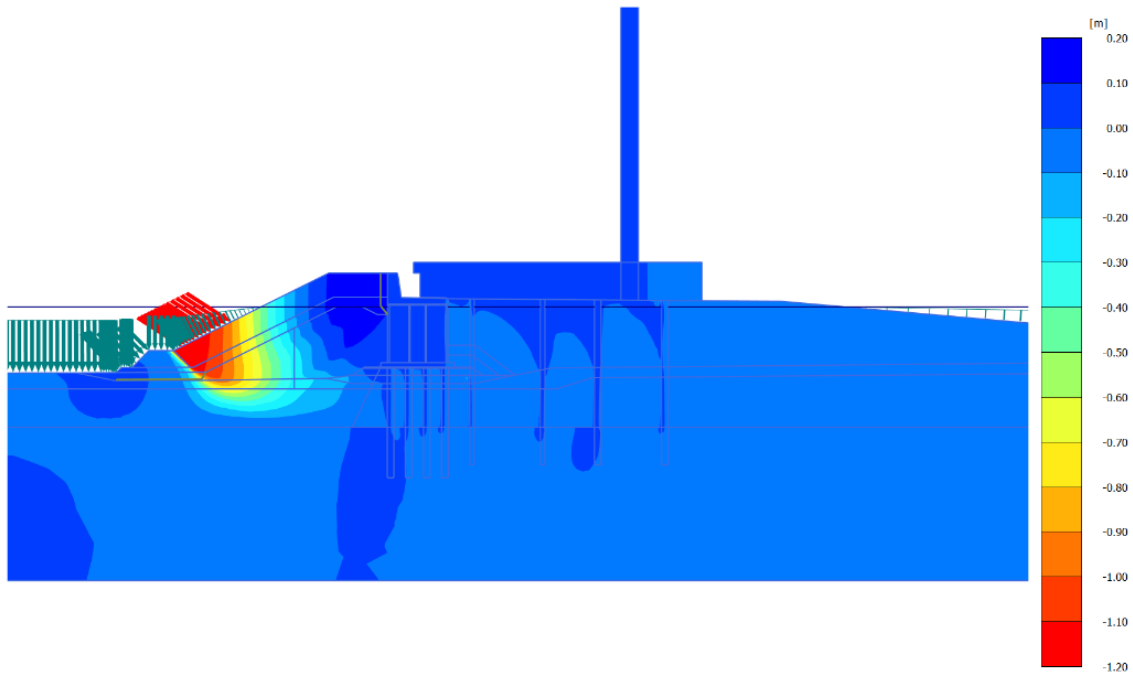
Figure 6-25 Total displacements u_y achieved in the different nodes of the model with piles under the concrete block obtained from the static analysis.

Finally, in the next figure have been showed the total displacements |U| achieved in the different elements of the model after having run a static analysis. The results obtained in this case are more similar to those obtained in the case of the displacements in the direction of the axis x. The maximum displacement which has been reached in this case is equal to 1,614 meters. It corresponds to the element 195 at node 17869, which is located in the impact zone of the cargo ship in the mole. In addition to this, the total displacements reached in the concrete block have been lowered by adding the piles under the concrete block. These are comprised between 0,30 – 0,60 meters, and those achieved in the head of the pilot tower are comprised between 0,30 – 0,40 meters. In conclusion, the effect of the piles under the concrete block has been positive, so that the displacements in the head of the pilot tower and on the concrete block have been reduced. Nevertheless, these are still high and the collapse of the pilot of the Genova's dock cannot be impeded.
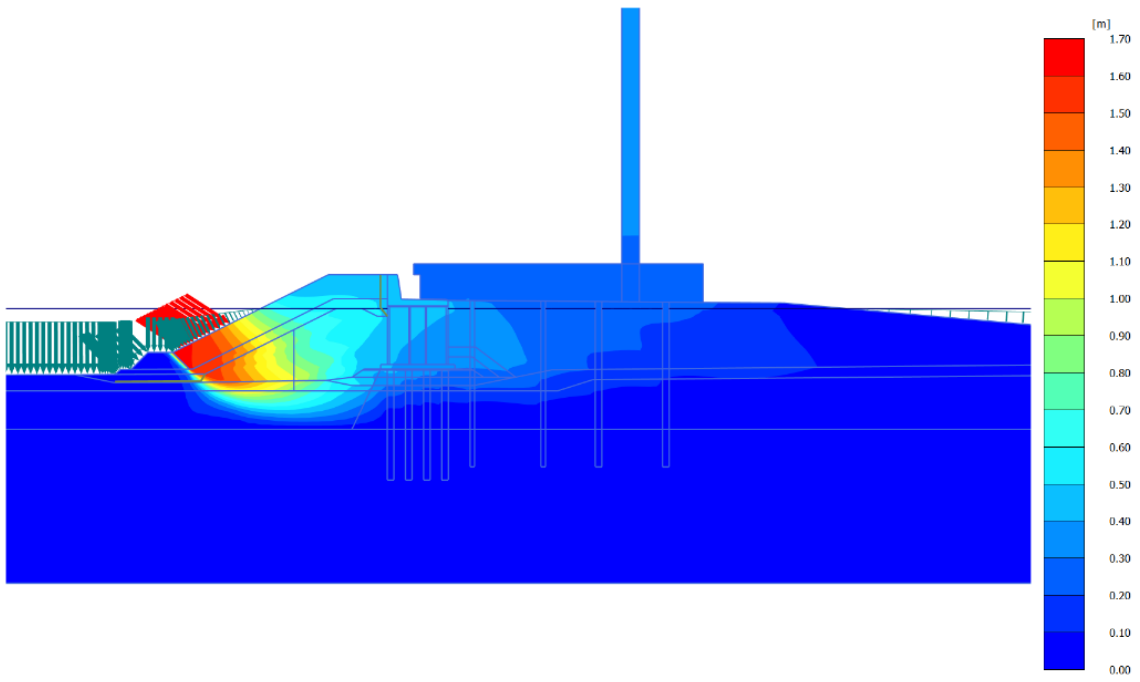
Figure 6-26 Total displacements |U| achieved in the different nodes of the model with piles under the concrete block obtained from the static analysis.

6.5.4   DYNAMIC CASE-with Piles

Finally, are presented the results obtained from the dynamic analysis run on the model developed by *PLAXIS*, in which the concrete block contains a foundation composed by 16 piles (4 x 4) of 20 meters in length and whose diameters are equal to 1,20 meters. In the first place, it is showed deformed mesh of the model. As it can be realized, the displacements in the heads of the piles pertaining to the foundation of the pilot tower have been reduced. This is due to the fact that the higher stiffness of the system after adding the piles under the concrete block. The deformations at the bottom of the breakwater, which coincides with the impact zone, are still high.
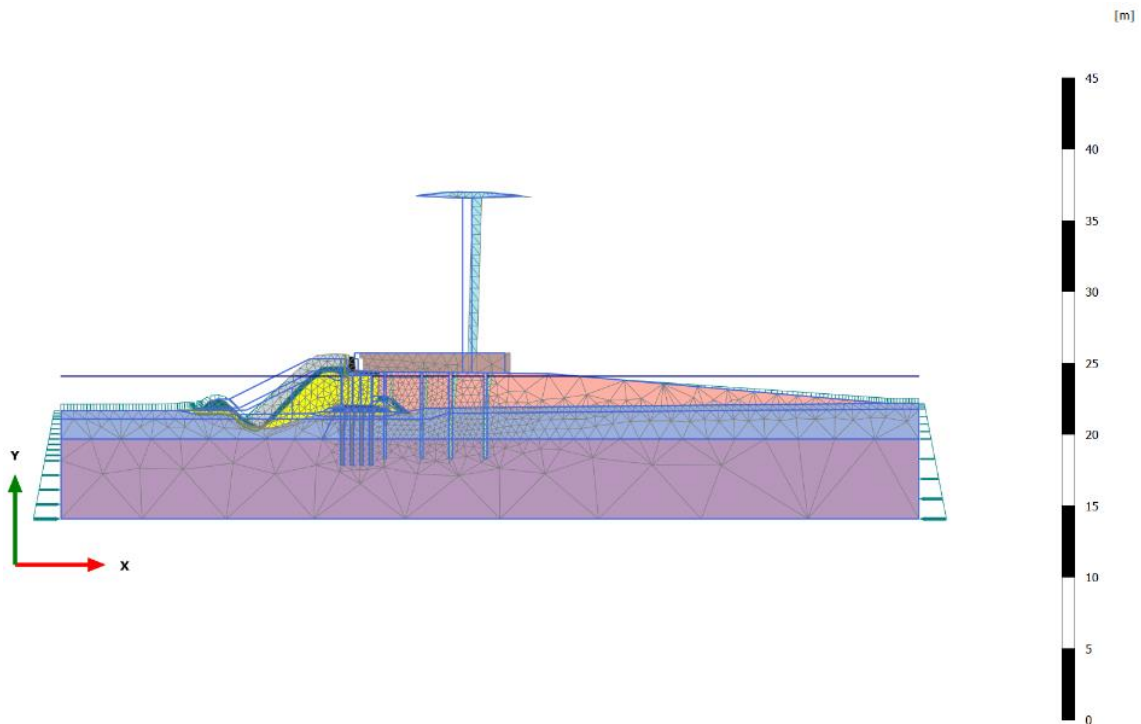
Figure 6-27 Deformed mesh of the model with piles under the concrete block obtained from the dynamic analysis.

Afterwards, is presented a figure which includes the plastic points surged in the model after running the dynamic analysis. One of the main details which must be underlined is that, unlike the results obtained in the static analysis, the amount of the plastic points has been highly reduced. In fact, in this case can only be appreciated two kind of plastic points from the six sorts which could be noticed in the static analysis.

- The red small squares represent the failure points of the model.
- The white squares represents the tension cut-off points of the model.

The most of the failure points have appeared in the head of the piles pertaining to the foundation of the concrete block. This is due to the fact that the highest stresses are reached in the top half of these piles as it can be observed in the figure 6-29. It can also be appreciated a group of failure points on the top of the concrete block, as well as in the heads of the piles pertaining to the foundation of the pilot control tower of the Genova's dock. It can be concluded that, the weakest points of the models are those placed in the heads of the piles.

In addition to this, it can be also appreciated a few tension cut-off points, which are located in the head of the piles of both foundations, as well as at the bottom of the breakwater.
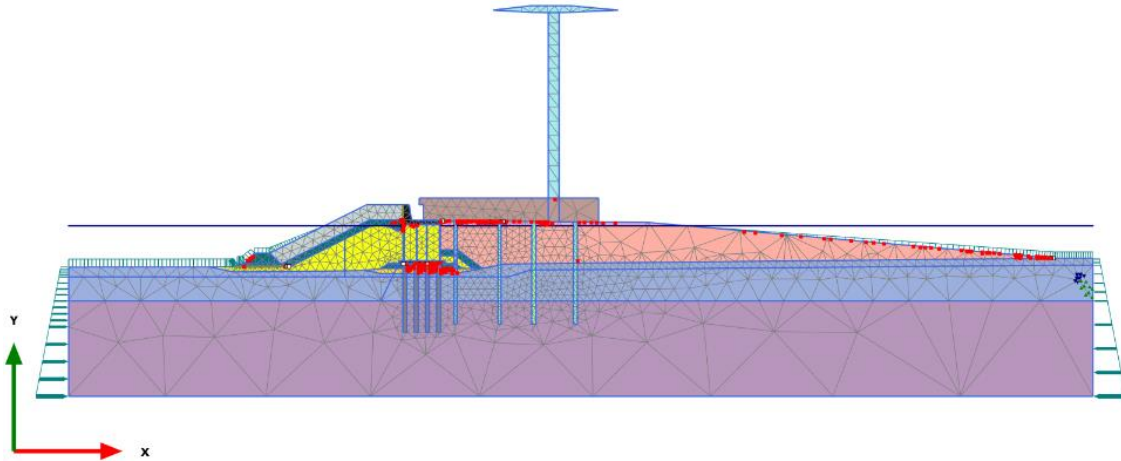
*Figure 6-28 Plastic points of the model with piles under the concrete block obtained from the dynamic analysis.*

Successively, are showed the principal effective stresses σ'_1 which have been achieved in the nodes consisting on the model, after having run the dynamic analysis. As it has been mention above, the highest effective stresses have been reached in the top half of the piles pertaining to the foundation of the concrete block. The maximum principal stress, which has been produced in the element 1740 at node 14555, is equal to 47210 kN/m^2. This node is placed on the back of the piles pertaining to the first row of the pile's foundation of the concrete block.
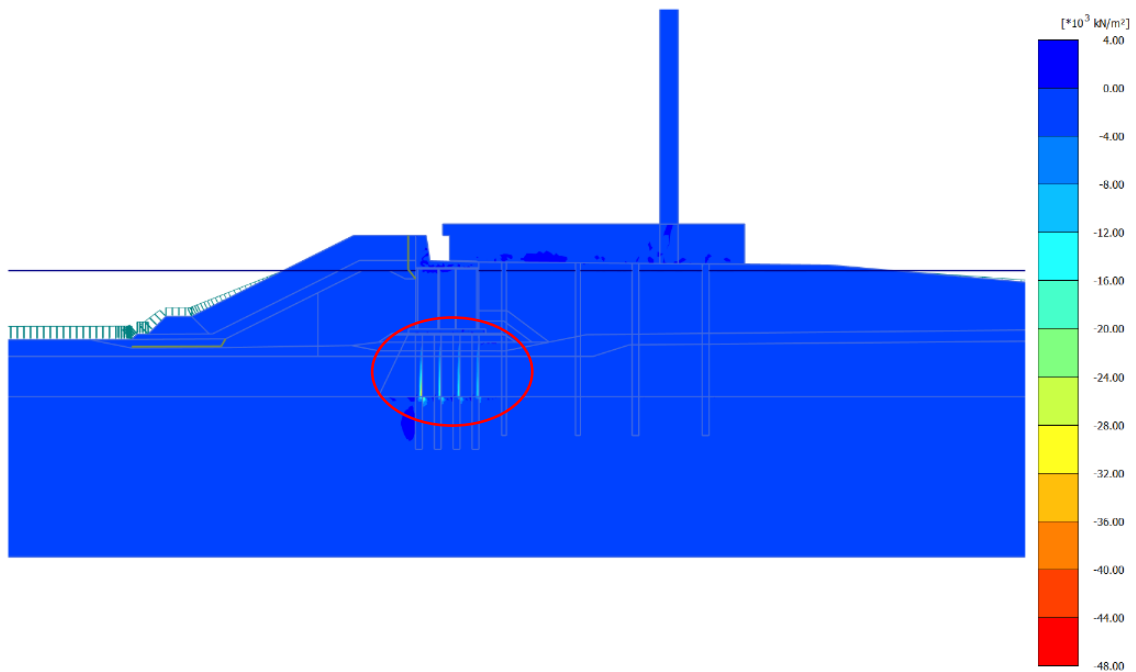
Figure 6-29 Principal effective stress σ'₁ of the model with piles under the concrete block obtained from the dynamic analysis.

Subsequently, are showed the total displacements achieved in the nodes of the model when the concrete block contains a pile's foundation under its bottom surface, which have been obtained with *PLAXIS* from a dynamic analysis. It must be underlined that these displacements are those reached at the end of the simulation time which is equal to 6 seconds. These must be differenced from the extreme total displacements, which corresponds to the maximum values of the displacements achieved in the simulation period. As it has been done for results obtained from the static analysis, firstly are presented the components of the displacements with regards to the two principal directions, which are those defined by the axis x and y respectively u_x and u_y.

In the following figure are showed the total displacements at the end of the simulation time with regards to the direction coinciding with the axis x. As it can be notice, the magnitude of these displacements is higher than those obtained for those values in the direction of the axis y. The maximum value of the total displacements in the direction x, which is equal to 1,469 meters, has been achieved in the element 210 at node 17899. This node is located at the bottom of the breakwater, which corresponds to that zone in the model where the cargo ship is supposed to impact. This is due to the fact that the highest forces are induced in this zone of the mole. Otherwise, according to this dynamic analysis run with *PLAXIS*, it can be concluded that the displacements achieved in the head of the pilot tower are comprised between 0,70 – 0,90 meters. As it can be noticed, the displacements in the head of the pilot tower have been reduced with regards to those obtained in the dynamic analysis of the real case, thanks to the action of the piles placed under the concrete block. Despite of the decreasing in the displacements u_x at the end of the simulation time, it cannot be impeded the collapse of the pilot tower because of the huge displacements in its head. Finally, it must be mentioned that the displacements in the concrete block at the end of the simulation, are comprised between 0,40 – 0,60 meters, which is almost the same result as it has been reached by means of the static analysis for the same case.
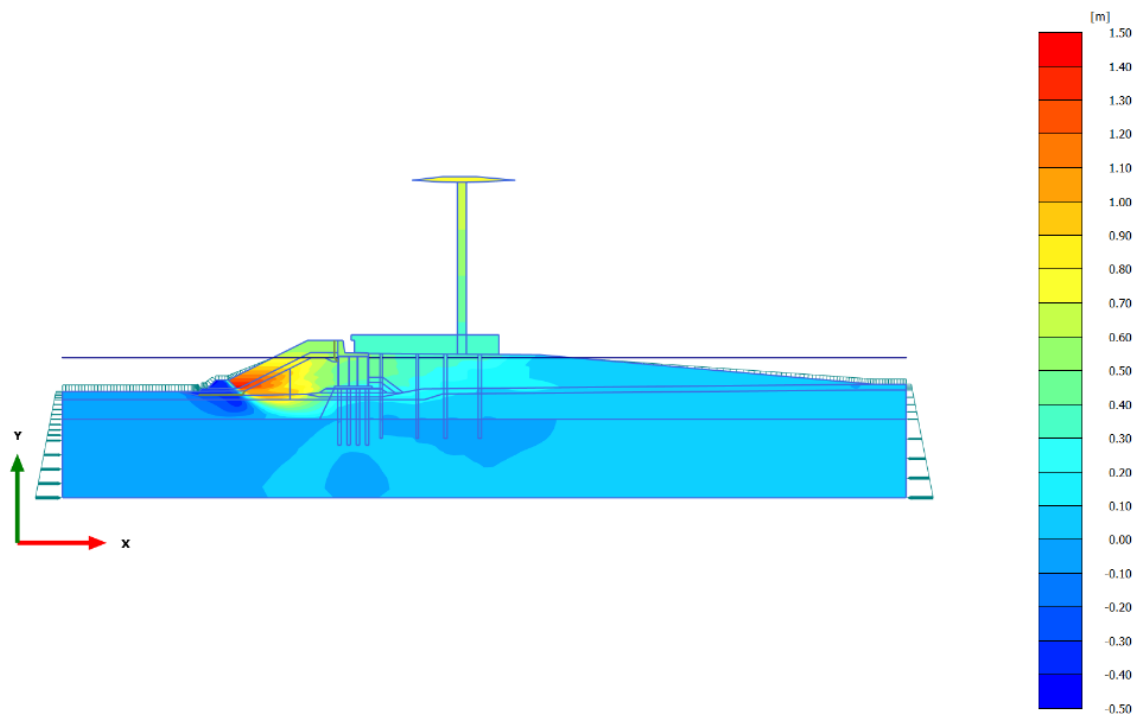
Figure 6-30 Total displacements u_x achieved in the different nodes of the model with piles under the concrete block obtained from the dynamic analysis.
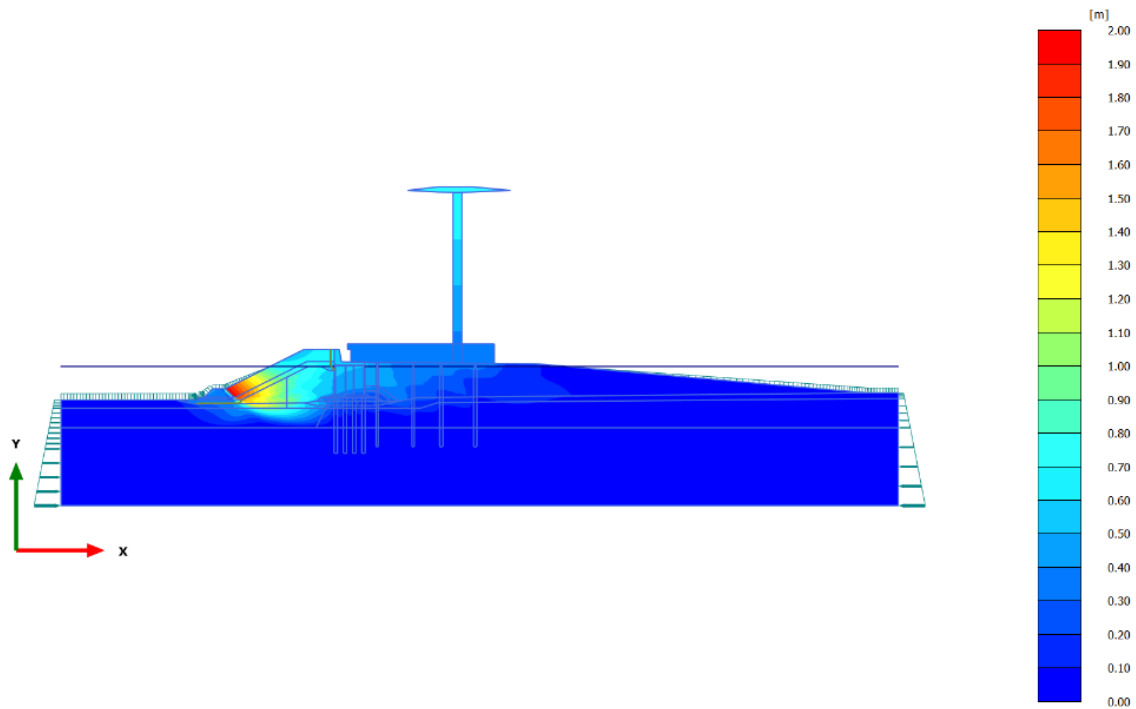
The next figure presents the total displacements in the direction of the axis y, achieved in the model at the end of the simulation time, after having run a dynamic analysis. As it has been mentioned above, the magnitude of the displacements is lower than those reached on the direction of the axis x. In this case, the maximum displacement has been achieved in the element 225 at node 17947. It is equal to 1,557 meters and it has been produced in the negative direction of the axis y. This node is located at the bottom of the breakwater next to the impact point of the ship on the mole of the Genova's dock. It must be underlined that, by adding the piles under the concrete block, the displacements in the direction of the axis y have been increased with regards to those obtained by means of the dynamic analysis in the real case. Otherwise, the highest displacements u_y reached in the head of the tower at the end of the simulation time are comprised between 0,10 – 0,20 meters. The displacements achieved in the concrete block in this case are approximately equal to 0,10 meters, which are similar to those obtained with the static analysis for the same case.
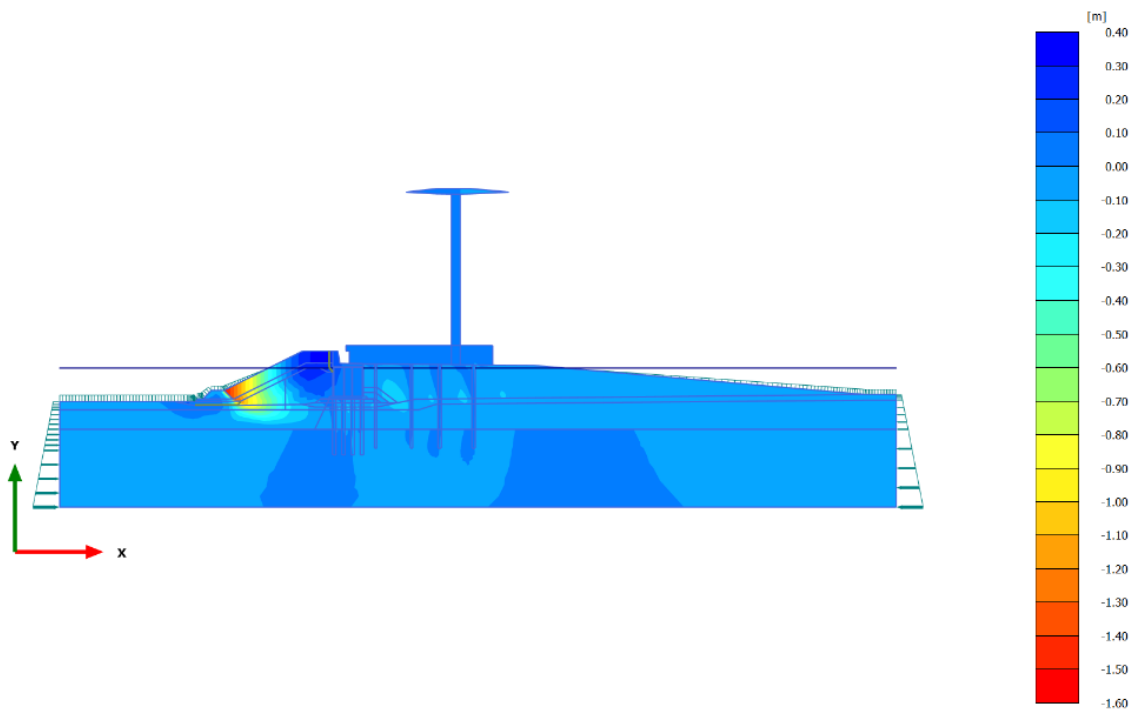
Figure 6-31 Total displacements uᵧ achieved in the different nodes of the model with piles under the concrete block obtained from the dynamic analysis.

The total displacements |U| achieved at the end of the simulation time of 6 seconds, in the model developed with *PLAXIS*, in which the concrete block contains a pile's foundation under its bottom surface, are represented in the following figure. The maximum value of the total displacements, which has been reached in the element 225 at node 17947, is equal to 1,996 meters. This value is higher than the maximum value of the total displacements obtained with the static analysis in the same case. The node in which the maximum displacement is reached, is located in the zone of the model where the ship impacted against the breakwater.

The total displacements |U| reached at the end of the simulation time in the head of the tower are comprised between 0,60 – 0,80 meters. These values of the displacements are still high, so that the collapse of the pilot tower of the Genova's dock cannot be impeded. Finally, it must be mentioned that the displacements in the concrete block which have been obtained in this case are comprised between 0,30 – 0,70 meters.

Figure 6-32 Total displacements |U| achieved in the different nodes of the model with piles under the concrete block obtained from the dynamic analysis.

Consecutively, are presented the values of the extreme total displacements in the directions of the axis x and y. These values of the displacements correspond to the maximum values which have been reached along the simulation time of 6 seconds for each node of the model. In the first place are showed the values of the extreme total displacements in the direction of the axis x. The maximum displacement, which has been achieved in the element 210 at node 17755, is equal to 1,666 meters. This node is located in the zone of the breakwater where the cargo ship is supposed to hit. As it can be appreciated, by adding the piles under the concrete block, the maximum displacements u_x have been lowered with regards to those obtained by means of the dynamic analysis run for the real case. This is the result of the increasing in the stiffness of the model which has been introduced by the action of the piles consisting on the foundation of the concrete block. It must be underlined that the maximum displacements reached in the head of the pilot tower have been also lowered until values of 0,90 – 1 meters. As it can be noticed, the maximum displacements exceed those obtained at the end of the simulation time, which are around 0,80 meters. In addition to this, the maximum displacements achieved in the concrete block are comprised between 0,40 – 0,60 meters.
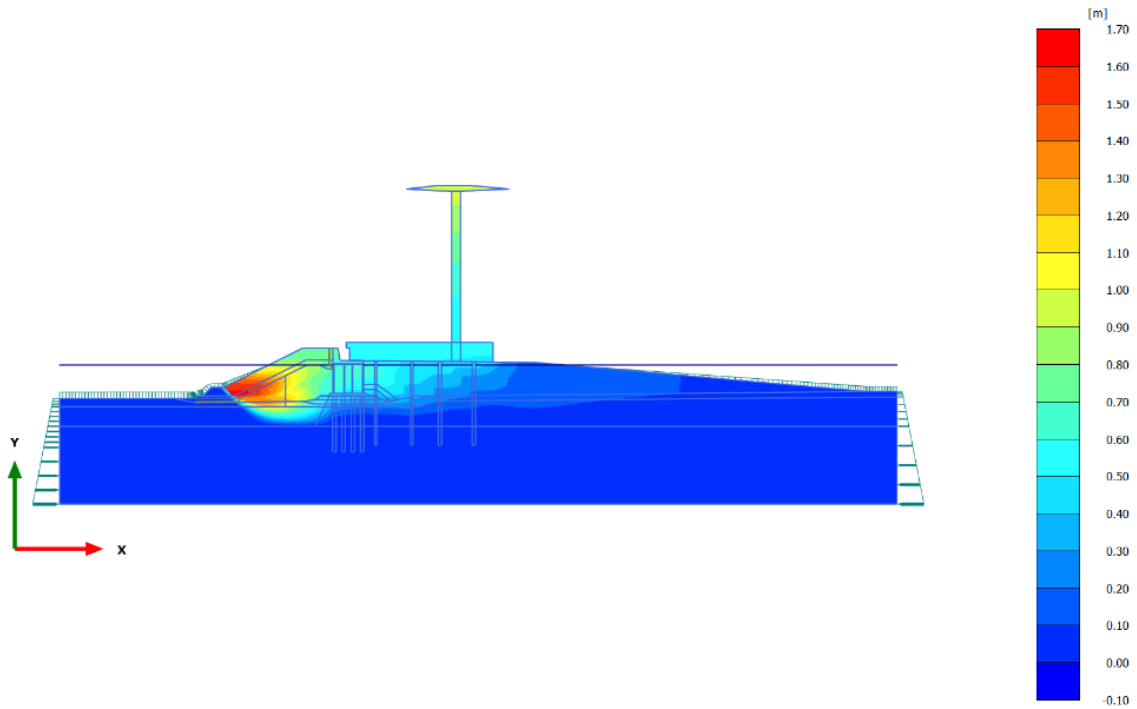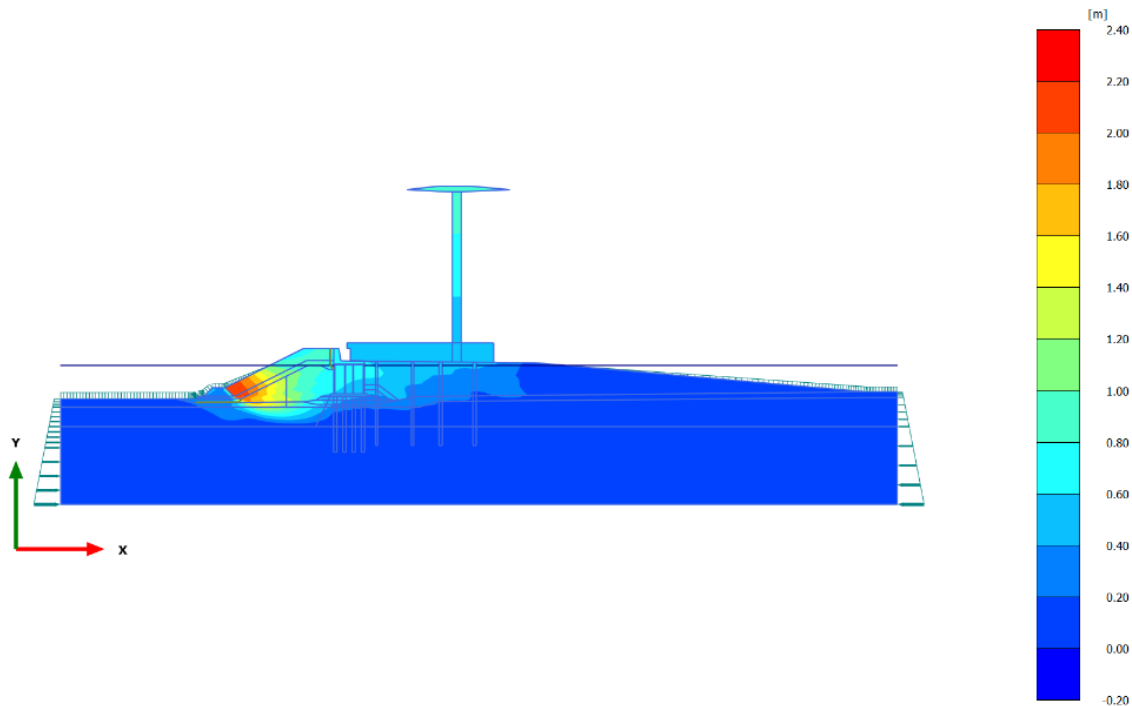
Figure 6-33 Maximum displacements u_x achieved in the different nodes of the model with piles under the concrete block obtained from the dynamic analysis.

Subsequently, are presented the maximum displacements in the direction of the axis y which have been reached in the nodes of the model along the simulation time. The maximum displacement in the direction of the axis y has been achieved on the top of the breakwater of the Genova's dock. It is equal to 0,3559 meters and has been produced in the element 221 at node 13891. Apart from this, the following highest displacements in the direction y have been reached at the bottom surface of the structure placed at the foot of the breakwater of the Genova's dock. The magnitude of these displacements is approximately equal to 0,10 − 0,12 meters.
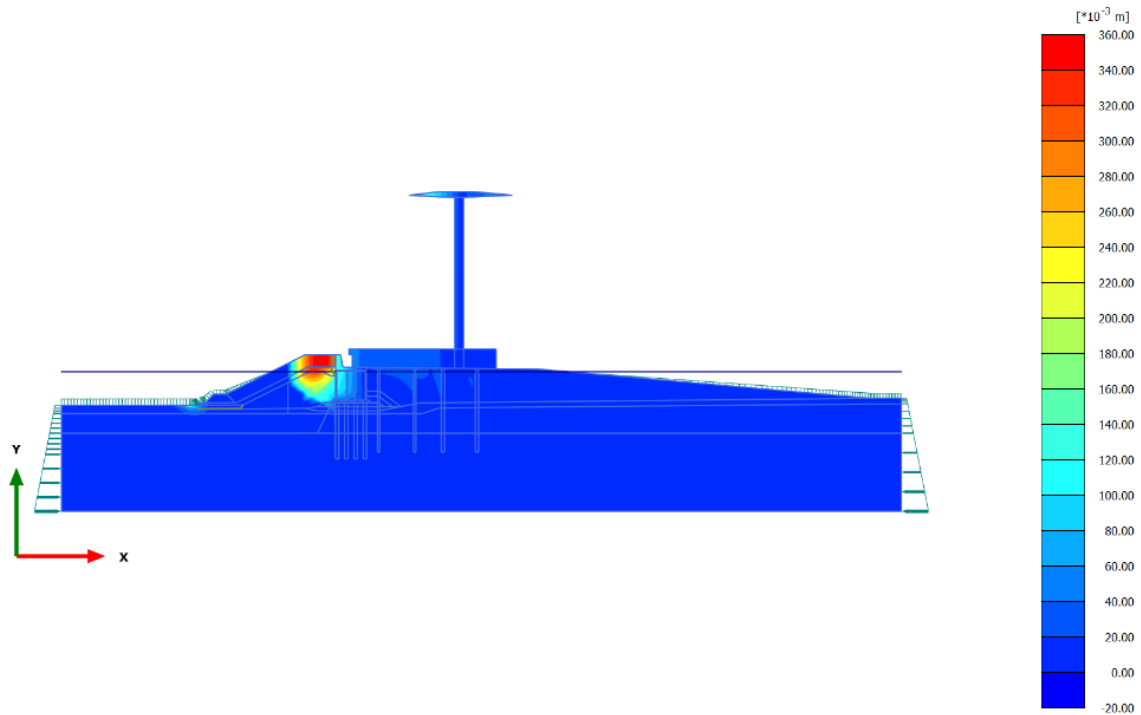
Figure 6-34 Maximum displacements u_y achieved in the different nodes of the model with piles under the concrete block obtained from the dynamic analysis.

Finally, in the next figure are showed the extreme total displacements $|U|_{max}$ which have been achieved in the nodes composing the model developed by PLAXIS, along the simulation time. The maximum displacement has been reached at the bottom of the breakwater, which corresponds to the impact zone. Concretely, this maximum value of $|U|$, which has been achieved in the element 210 at node 17899, is equal to 2,202 meters. As it can be appreciated, the displacements achieved in this case, have been lowered as a consequence of the increasing of the model's stiffness due to the action of the pile's foundation added to the bottom surface of the concrete block. Otherwise, the displacements achieved in the head of the tower have been also reduced until values comprised between 0,60 − 0,80 meters. Despite the reduction of the displacements, the magnitude of these is still high, sufficient to produce the collapse of the pilot tower as a consequence of the ship's impact. Finally, the displacements which have been achieved in the concrete block are comprised between 0,40 − 0,80 meters.

Figure 6-35 Maximum displacements |U|$_{max}$ achieved in the different nodes of the model with piles under the concrete block obtained from the dynamic analysis.

6.5.5   Results comparison

In this point, are going to be compared the results obtained from the static and the dynamic analysis. It is going to be made a comparison between the maximum displacements u_x in the nodes referenced in the figure 6-5 as A, B, C, D, E, F, G and H respectively, which have been obtained from the static analysis, with those which have been reached, in the same nodes, at the end of the simulation time of the dynamic analysis. On the one hand, the displacements obtained from the static analysis are represented as constant values along the simulation time. On the other hand, it can be observed the evolution of the displacements in the referenced nodes along the simulation time, which correspond to the results obtained from the dynamic analysis run with *PLAXIS*.

It can be differenced two sorts of graphs, those which correspond to the analysis run on the model of the real case, that one in which there are not piles under the concrete block placed between the breakwater and the foundation of the pilot tower, and those which are related to the case of study that has been proposed on this Master's Thesis to determine the reduction of the displacements which would have been achieved in the case in which the concrete block would have been restrained by a pile's foundation.

*CASE A. CONCRETE BLOCK WITHOUT A PILE'S FOUNDATION.*

The first graph shows the evolution of the displacements in the node A, which is placed on the impact area where the cargo ship hit the mole of the Genova's dock. The magnitude of the displacements reached at this node is only comparable with the magnitude of the displacements achieved in the head of the pilot control tower (node H). In these two cases, the displacements u_x are the highest.

In addition to this, it must be mentioned that the highest displacements are achieved with the dynamic analysis. However, the final displacement reached in the dynamic analysis is approximately 0,20 meters lower than the displacement obtained in the static analysis.
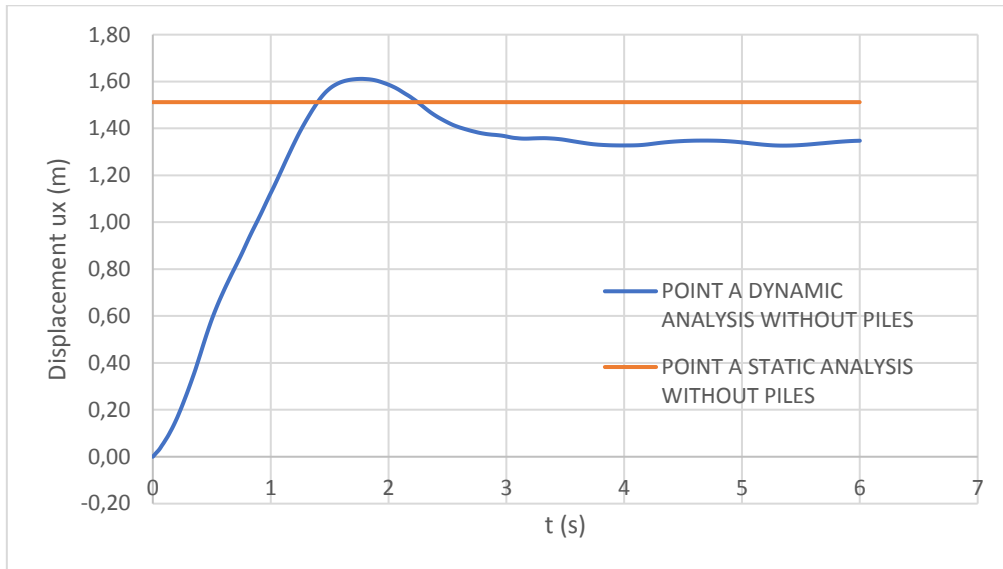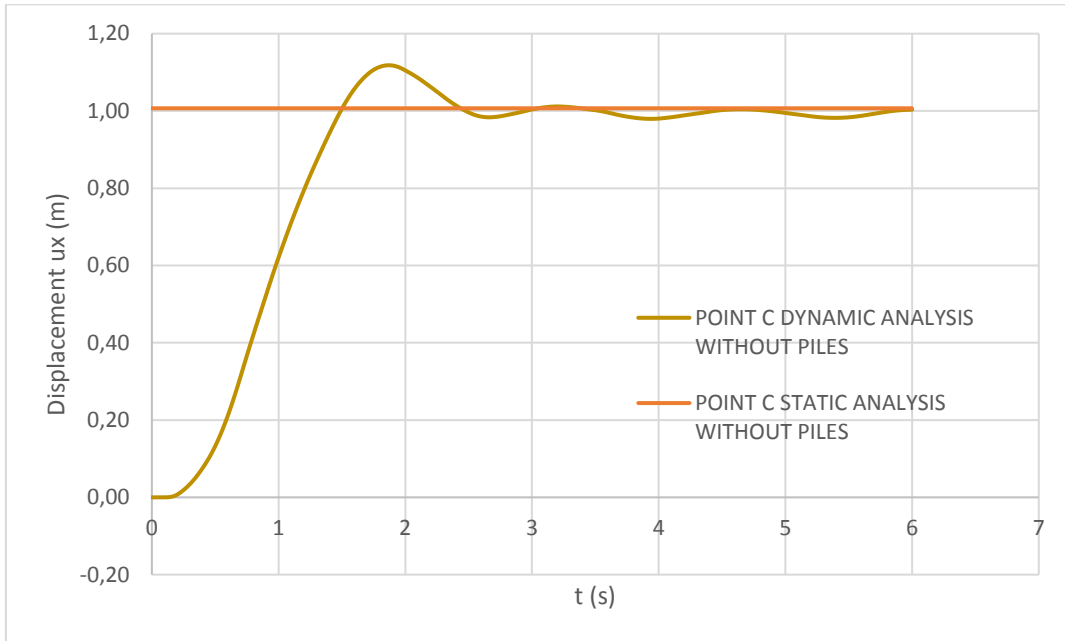

Figure 6-36 Comparison of the displacements in the node A when there are not piles under the block.

The node B is located in the top half of the concrete block. As it can be realized, the maximum displacement obtained from the dynamic analysis is equal to 1,10 meters. The final values of the displacements achieved are approximately equal to 1 meter in both analysis: static and dynamic.
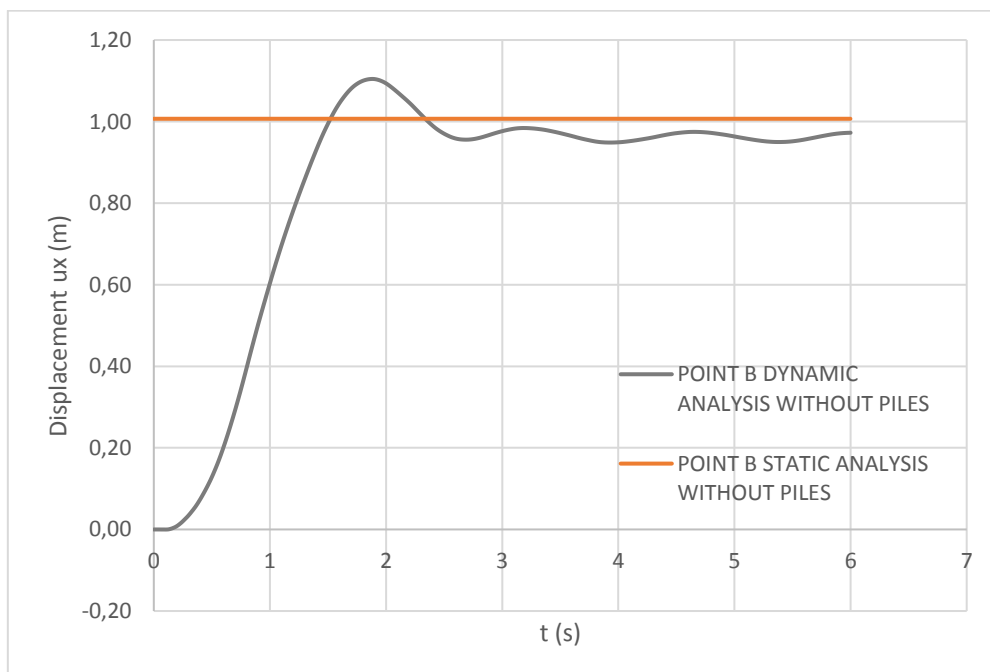
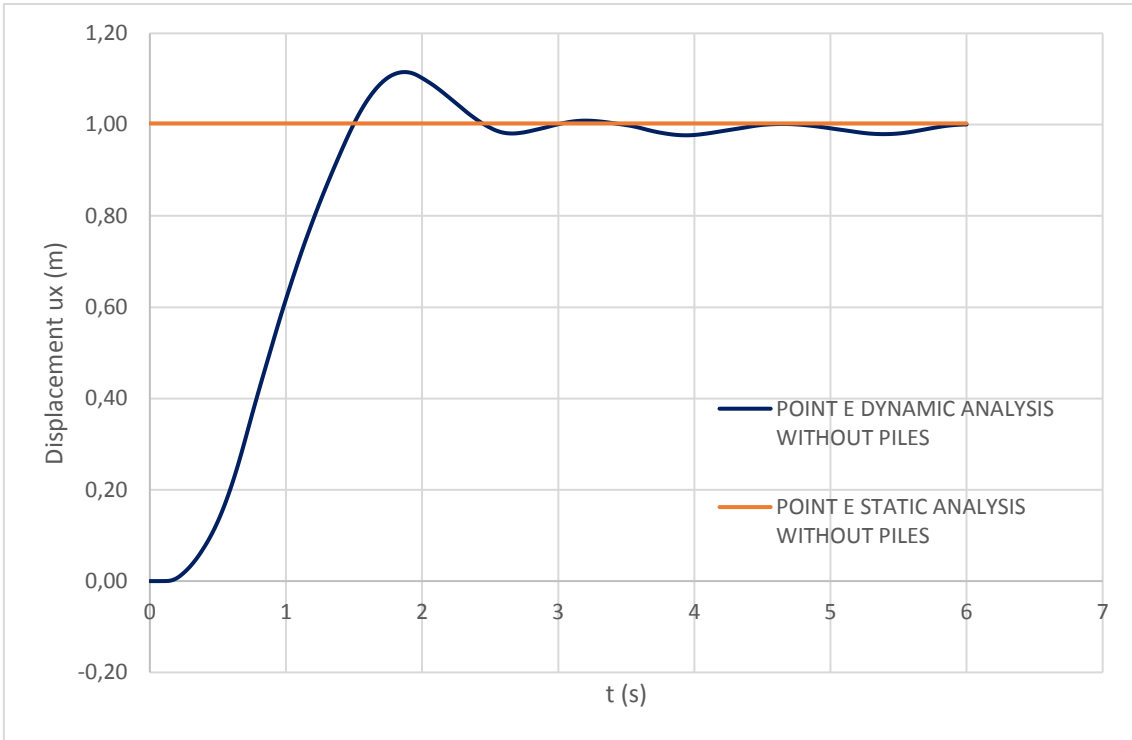*Figure 6-37 Comparison of the displacements in the node B when there are not piles under the block.*

Subsequently, the nodes C, D, E and F are placed under the bottom surface of the concrete block. In this case, the displacements observed in these four nodes u_x are practically the same. In the dynamic analysis, it is achieved a maximum value of the displacements u_x equal to 1,12 meters at the instant of time 1,8 seconds. In addition to this, it is observed that, at the end of the simulation time, both analysis converge in a same value of the displacements u_x equal to 1 meter. This behavior is observed in the four nodes.
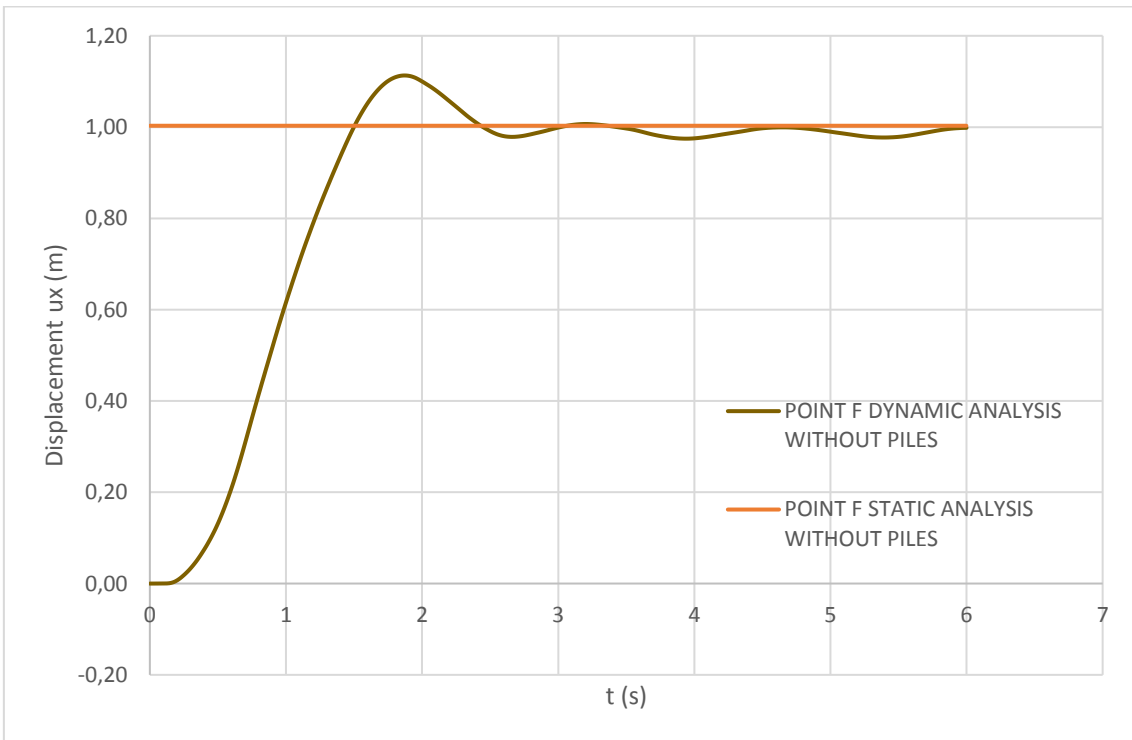

Figure 6-38 Comparison of the displacements in the node C when there are not piles under the block.
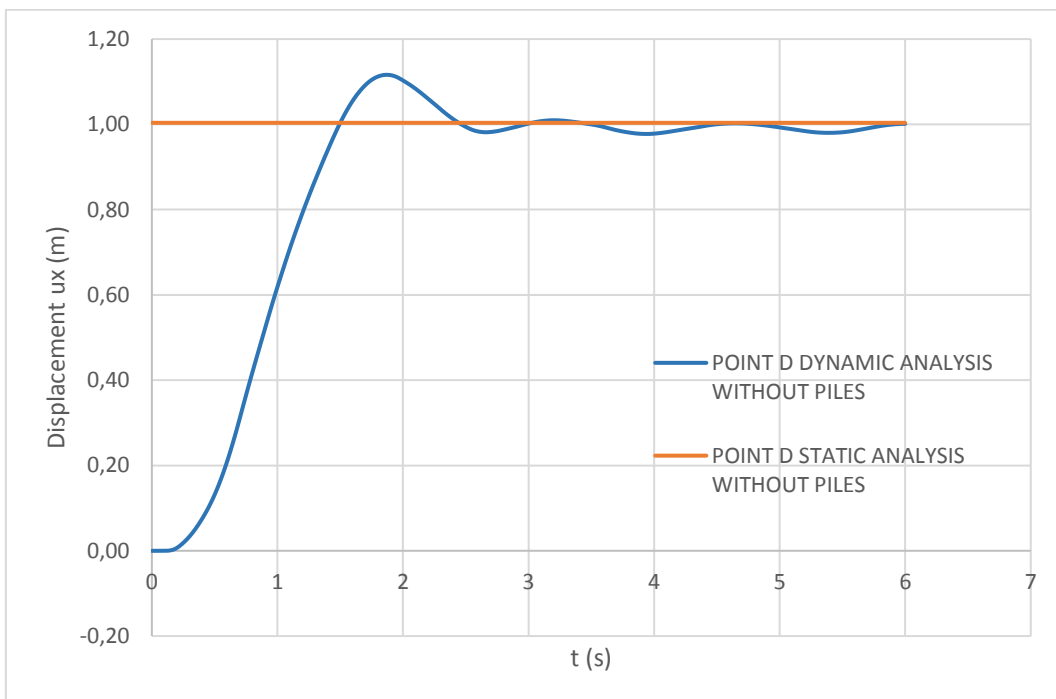
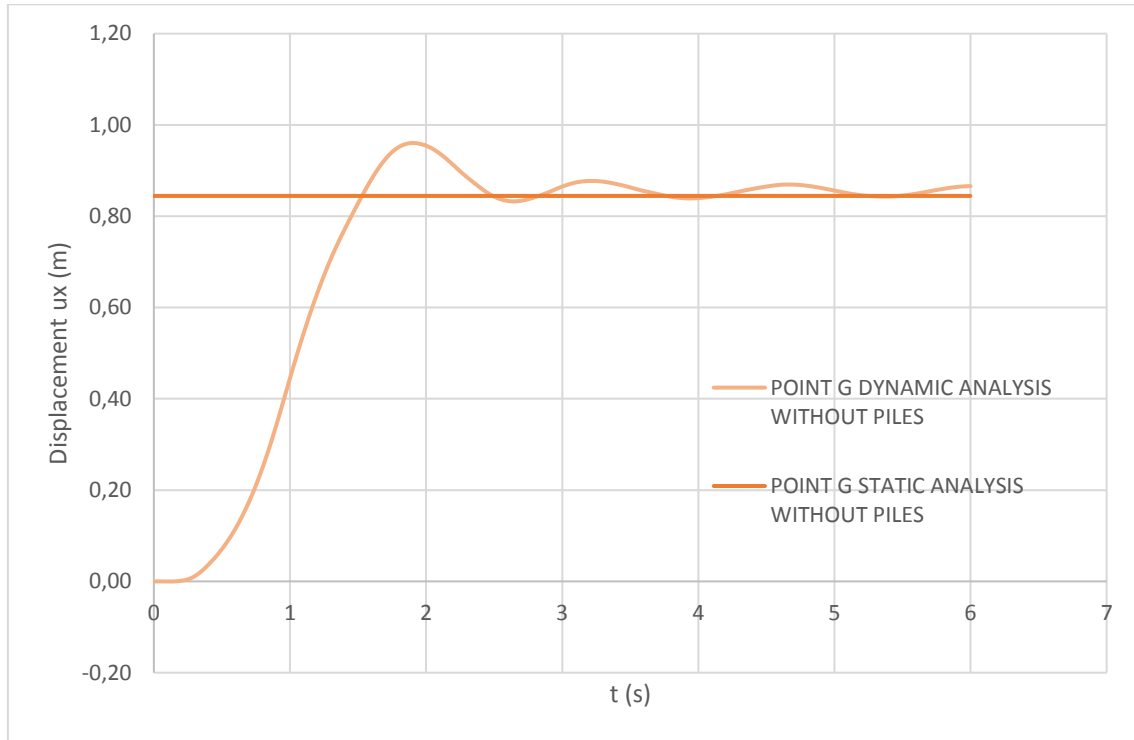*Figure 6-39 Comparison of the displacements in the node D when there are not piles under the block.*

147

Figure 6-40 Comparison of the displacements in the node E when there are not piles under the block.

Figure 6-41 Comparison of the displacements in the node F when there are not piles under the block.

Finally, have been compared the displacements obtained by means of both analysis in the node G, located at the bottom of the pilot tower, and the node H, placed on the head of the

tower. The displacements reached in the node G are not as high as those which are achieved in the head of the pilot tower. In fact, the maximum displacement u_x, which has been reached in the case in which there are not piles under the concrete block, when it is run a dynamic analysis, is approximately equal to 0,95 meters. Otherwise, the value of u_x which has been achieved at the end of the simulation time is very similar to that obtained by means of the static analysis. It is approximately 0,84 meters.

Figure 6-42 Comparison of the displacements in the node G when there are not piles under the block.

In the node H, which is located in the head of the pilot control tower, are reached the highest displacements that are approximately equal to 1,60 meters. As it can be noticed in the variation of the displacements corresponding to the dynamic analysis (figure 6-43), the maximum value of u_x is achieved at 2,61 seconds within the simulation time. Between the eight nodes whose displacements are being compared, this is the last maximum displacement in being reached. This is due to the fact that, since the instant when the impact is produced, the deformations must flow through the elements of the model until reach the node H, which is the node located at the longest distance from the impact zone between the nodes studied.

Another aspect that must be mentioned in this case is that, there is a big difference between the results obtained by means of the static analysis and those obtained with the dynamic analysis. One the one hand, it can be appreciated that the maximum displacement in the head of the pilot tower, when it is run a static analysis, is equal to 0,97 meters. On the other hand, if it is studied the evolution of the displacements in the node H in the case of the dynamic analysis, the maximum displacement achieved is equal to 1,60 meters, while the displacement in this node at the end of the simulation time is 1,40 meters.
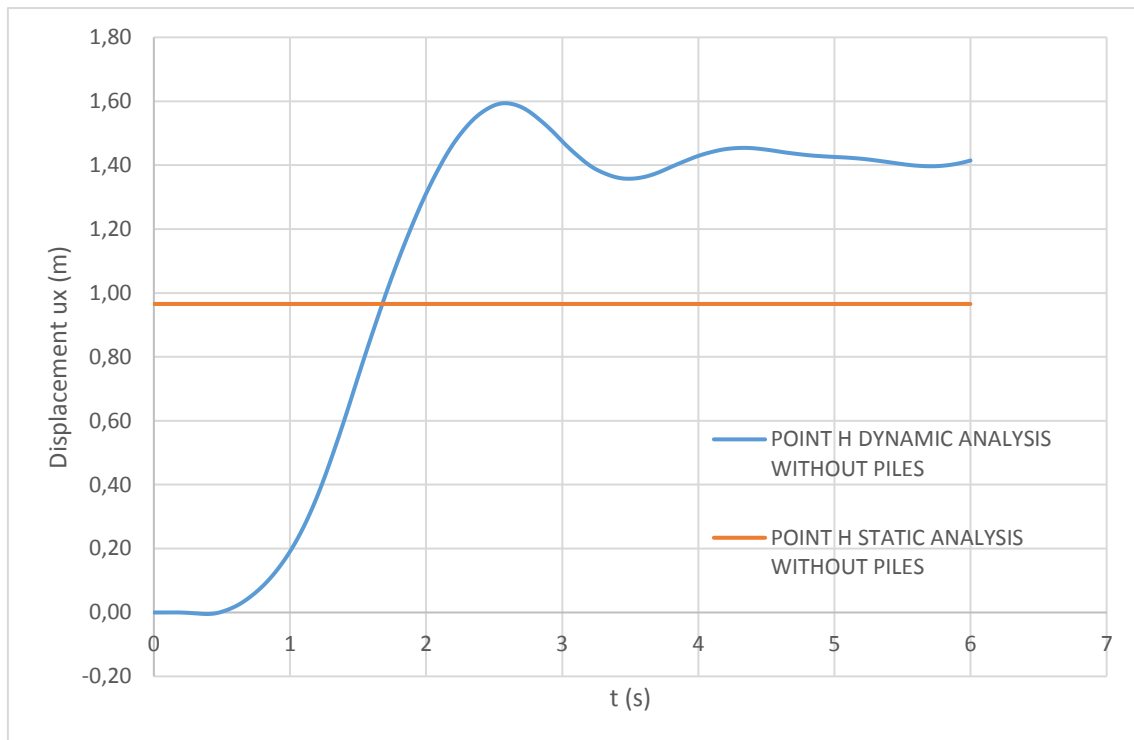
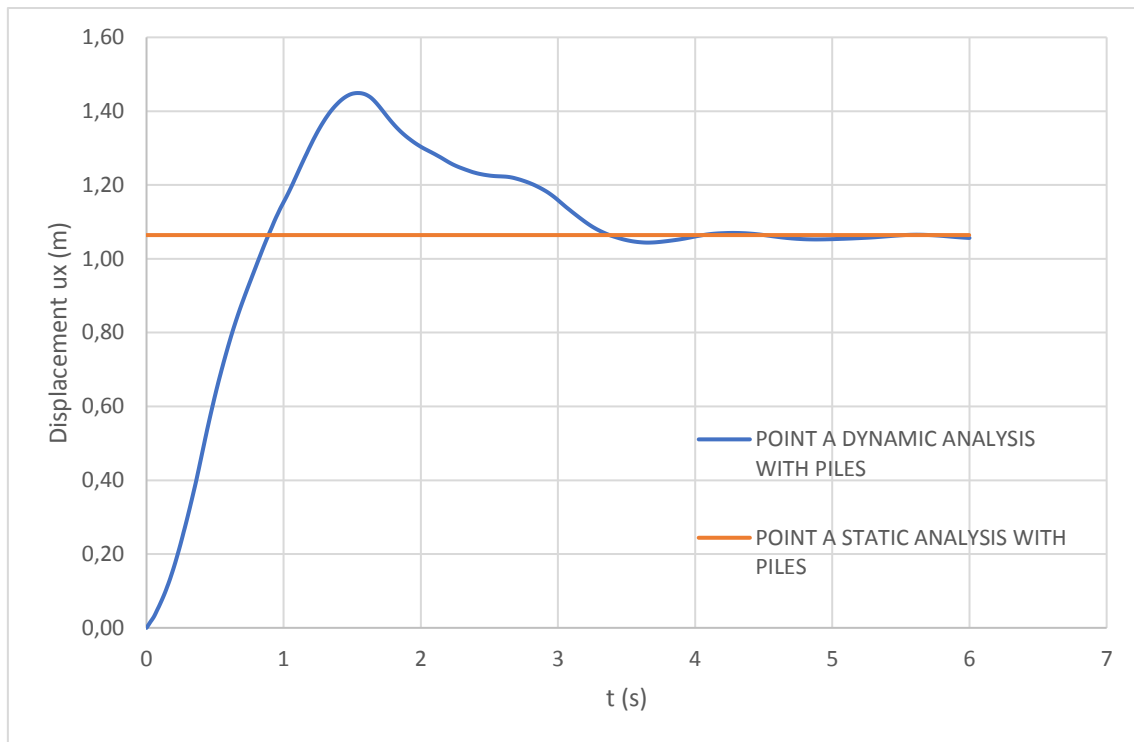*Figure 6-43 Comparison of the displacements in the node H when there are not piles under the block.*

CASE B. CONCRETE BLOCK WITH A PILE'S FOUNDATION.

Subsequently, are going to be compared the displacements obtained by means of the static and the dynamic analysis run in the second model developed with the software *PLAXIS*, in which it has been included a pile's foundations (4 x 4) under the concrete block with the aim of reducing its displacements through the soil. In this point, are going to be analyzed the displacements in the nodes A, B, C, D, E, F, G and H respectively (figure 6-5).

The first node whose displacements are going to be discussed is the node A. As it was mentioned in the previously, it is located in the breakwater of the dock of Genova. Concretely, in the impact area where the cargo ship hit the mole. In this second model, the maximum displacements reached in the dynamic analysis are approximately equal to 1,45 meters, while the displacements at the end of the simulation time tend to converge with the maximum value obtained according to the static analysis. It is equal to 1,07 meters.

With regards to the displacements produced in the real case, where the concrete block was not restrained by a pile's foundation, the displacements of the concrete block have been reduced in approximately 0,20 meters. It must be pointed that, the reduction observed in the displacements of the node A, after having added the piles to its bottom surface, is not very notable.
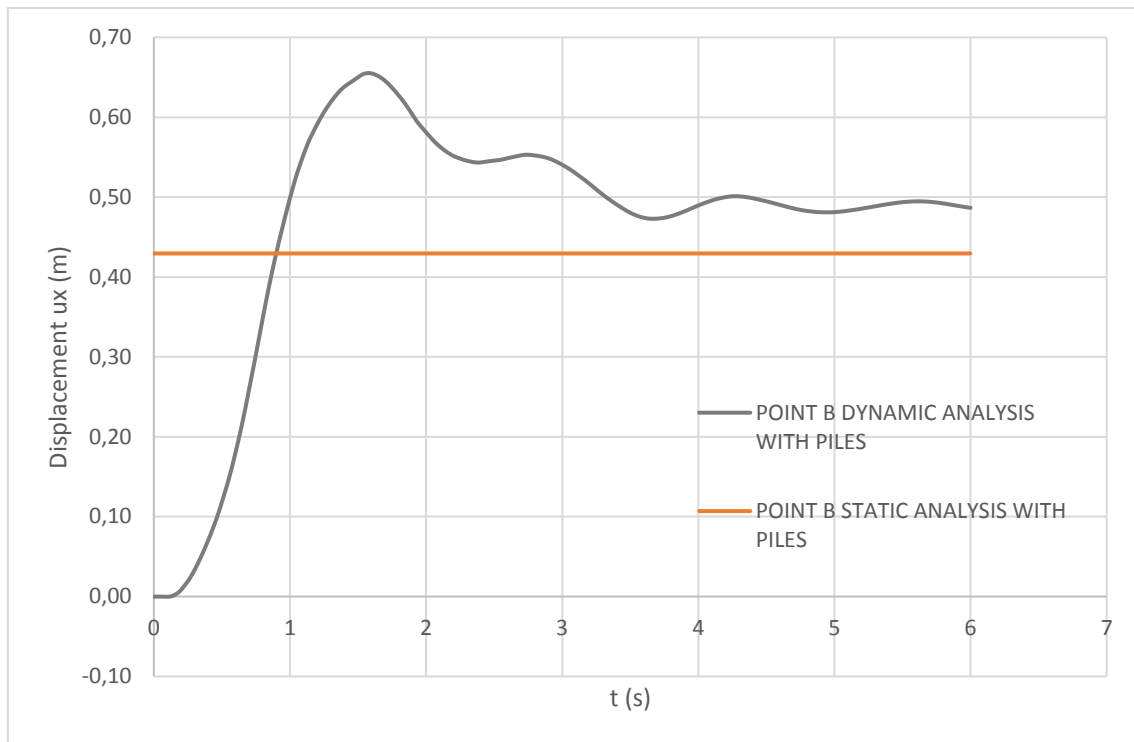
Figure 6-44 Comparison of the displacements in the node A when there are piles under the block.

The next node which has been analyzed is that placed on the top half of the concrete block. The displacements observed in the node B achieve a maximum value equal to 0,65 meters, according to the dynamic analysis. At the end of the simulation time, the displacements reached are equal to 0,48 meters. In this node, the values of u_x obtained with regards to the dynamic analysis are higher than those achieved by means of the static calculation process. In fact, the maximum displacement obtained with the static analysis for the node B, is equal to 0,43 meters.

Otherwise, it has been also observed a reduction in the displacements of the node B, by adding the piles under the concrete block. In fact, the maximum displacements reached in the static analysis have been halved. The same behavior with regards to the displacements can be appreciated in the results obtained from the dynamic analysis. Although, in this second case, the reduction is not as important as in the case of the static analysis.

Figure 6-45 Comparison of the displacements in the node B when there are piles under the block.

Afterwards, are going to be analyzed the displacements in the nodes C, D, E and F, which are placed on the head of the piles pertaining to the front, second, third and back row of piles of the foundation which has been added to the concrete block in this second case of study.

According to the figures 6-46, 6-47, 6-48 and 6-49, it can be concluded that the displacements achieved in the head of the piles pertaining to the front row of the group are higher than those reached in the second row. The displacements achieved in the second row of the group are higher than those reached in the third row, and the displacements achieved in the third row of the group are bigger than those reached in the piles pertaining to the back row of the group. These differences between the displacements in the heads of the piles pertaining to the rows of the foundation of the concrete block, which was justified in the Theoretical Base of this Master's Thesis, is due to the interaction phenomena between the piles of the group. In fact, the displacements in the heads of the piles pertaining to the first row of the group are the highest because the portion of soil which is placed before them is not disturbed by another rows of piles. However, the piles pertaining to the second, third and back rows are pushed by a disturbed soil due to its precedent row. This phenomenon of disturbance gives place to the shadowing and the edge effects, which are related to the different pile's efficiencies and consequently, with the different displacements on its heads depending on the row to which pertain within the group.

Otherwise, it must be told that the values obtained with regards to both kind of analysis (static and dynamic) are very similar. As it happened in the other nodes of the model, the maximum displacements u_x are achieved by means of the dynamic analysis. However, the values of the displacements in the nodes C, D, E and F at the end of the simulation time are lower than the maximum displacements obtained in the static analysis. It must be pointed that, the difference between the maximum displacement achieved in the static analysis and the final displacement

152

reached in the dynamic analysis becomes more significant with the row of the piles. In other words, this difference between both kind of displacements is more important in the second row than in the front row; more important in the third than in the second row and more important in the back than in the third row of the group.

For these nodes, there is no sense in comparing the displacements achieved in this second model with those obtained in the model corresponding to the real case, in which the concrete block does not contain the piles under its bottom surface.
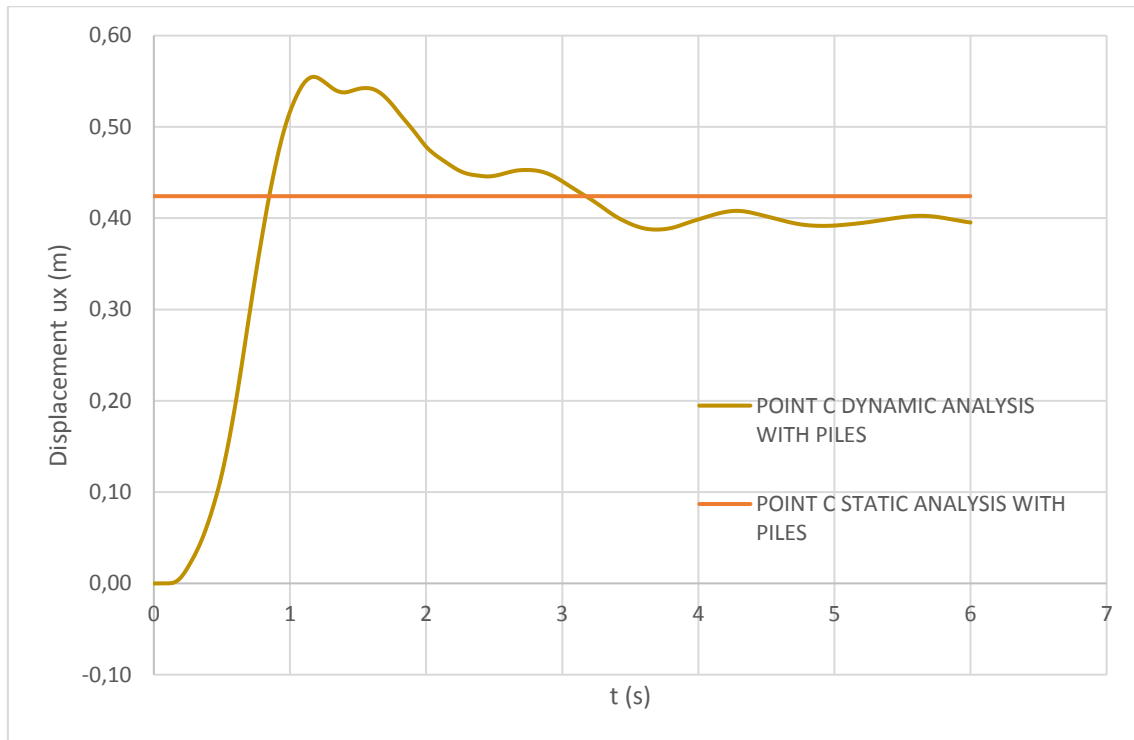
Figure 6-46 Comparison of the displacements in the node C when there are piles under the block.
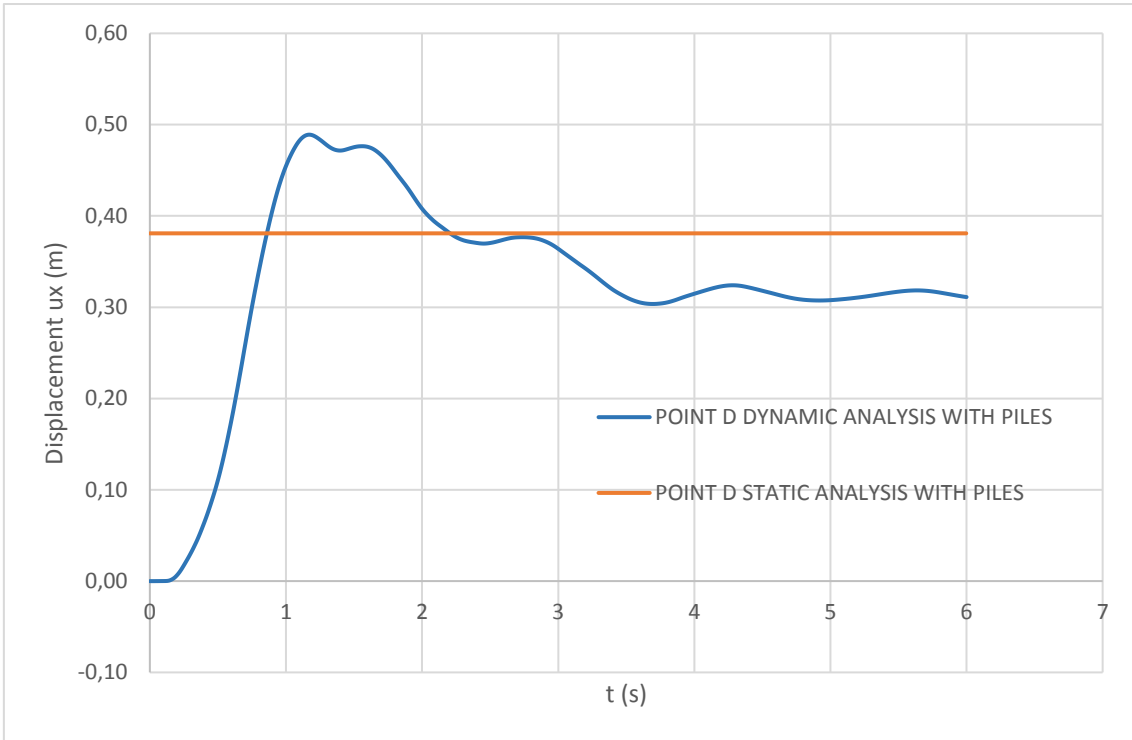
Figure 6-47 Comparison of the displacements in the node D when there are piles under the block.
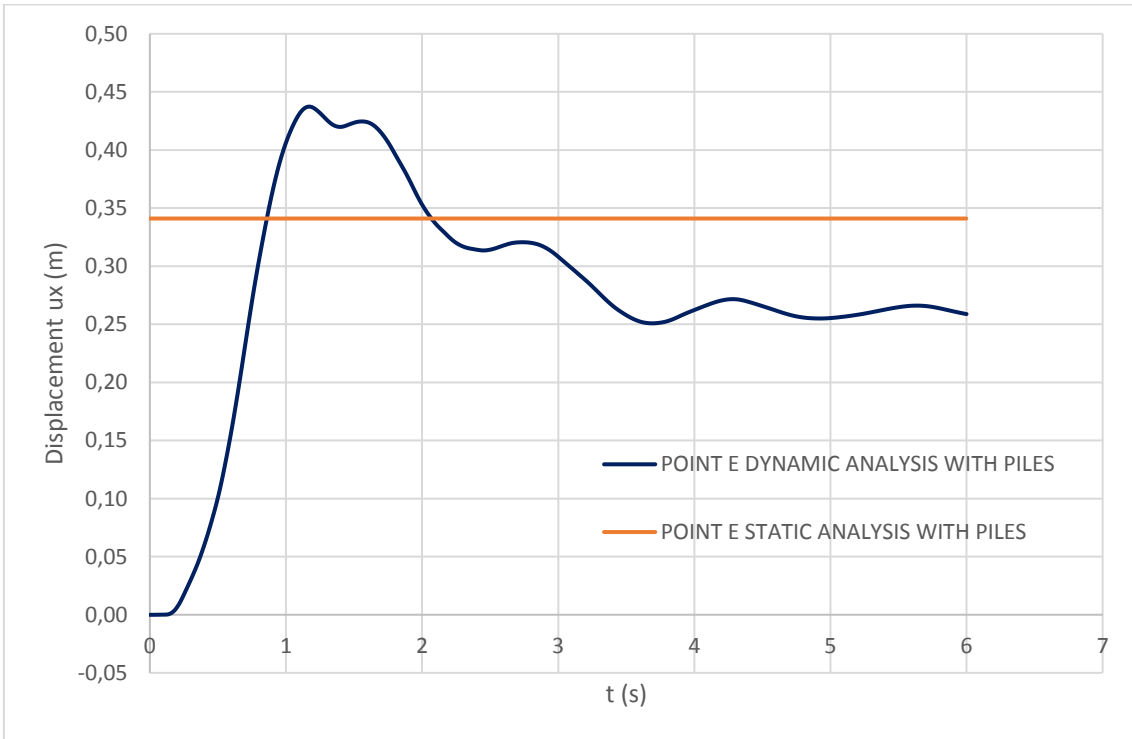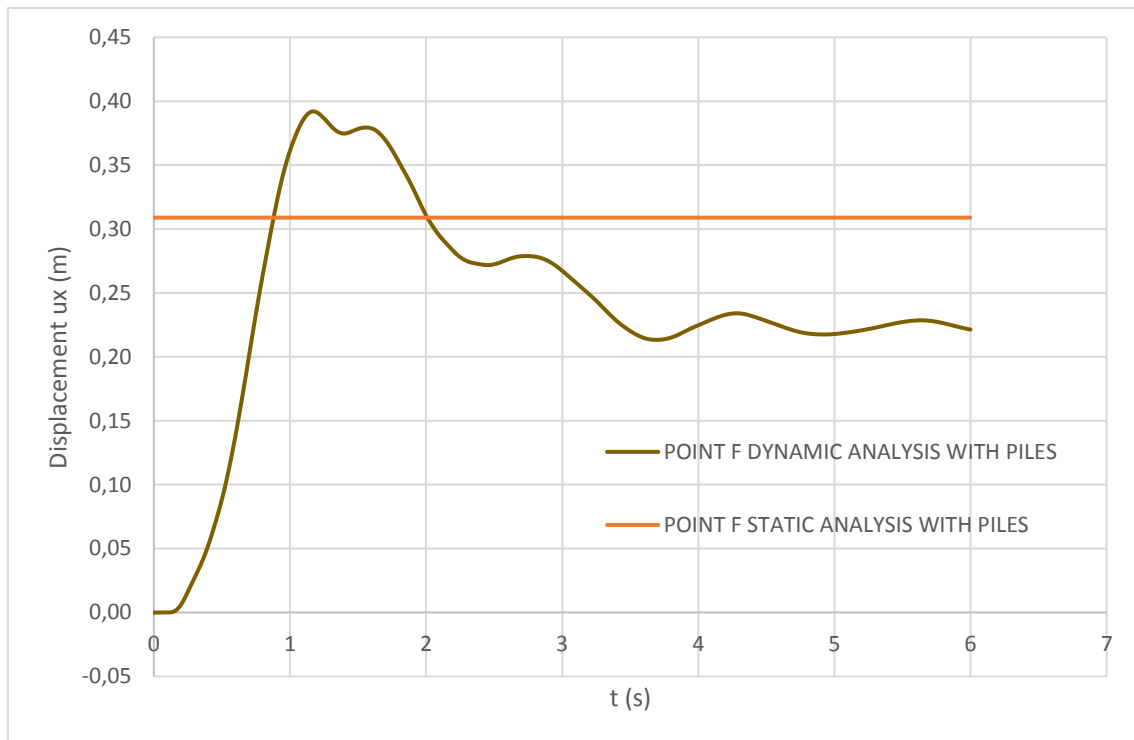

Figure 6-48 Comparison of the displacements in the node E when there are piles under the block.
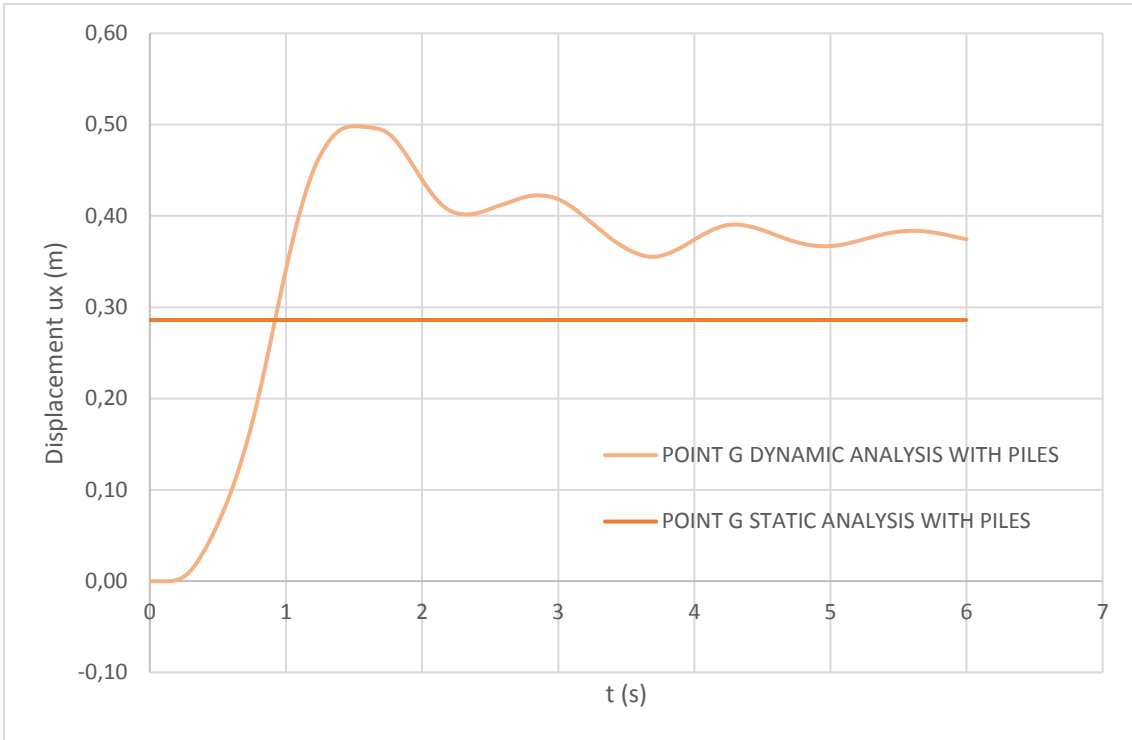
Figure 6-49 Comparison of the displacements in the node F when there are piles under the block.

Subsequently, are going to be compared the displacements obtained in the nodes G and H of the model, placed at the bottom and at the top of the pilot control tower respectively. In the node G, the maximum displacement, obtained according to the dynamic analysis, is equal to 0,50 meters. In addition to this, the value of the displacement u_x at the end of the simulation time, which has been obtained with regards to the dynamic analysis, is equal to 0,38 meters, which is higher than the maximum displacement that has been reached with the static analysis, equal to 0,28 meters.

As it was observed in the model of the real case, in the node H, placed on the head of the pilot tower, the differences between the displacements obtained according to the static and dynamic analysis are very different. In fact, in the dynamic analysis of this second case, the maximum displacement u_x is equal to 0,96 meters and the displacement at the end of the simulation time is equal to 0,71 meters, while the maximum displacement achieved in the static analysis is equal to 0,36 meters. It can be noticed that, it exists a high difference between both values.

Comparing the displacements obtained in the nodes G and H in this second model, in which the concrete block contains a pile's foundation, with those reached in the model of the real case, it can be concluded that the displacements have been reduced significantly due to the increasing of the system's stiffness which has been induced in the model by adding the pile's foundation under the bottom surface of the concrete block, restraining its displacements through the soil.

Figure 6-50 Comparison of the displacements in the node G when there are piles under the block.
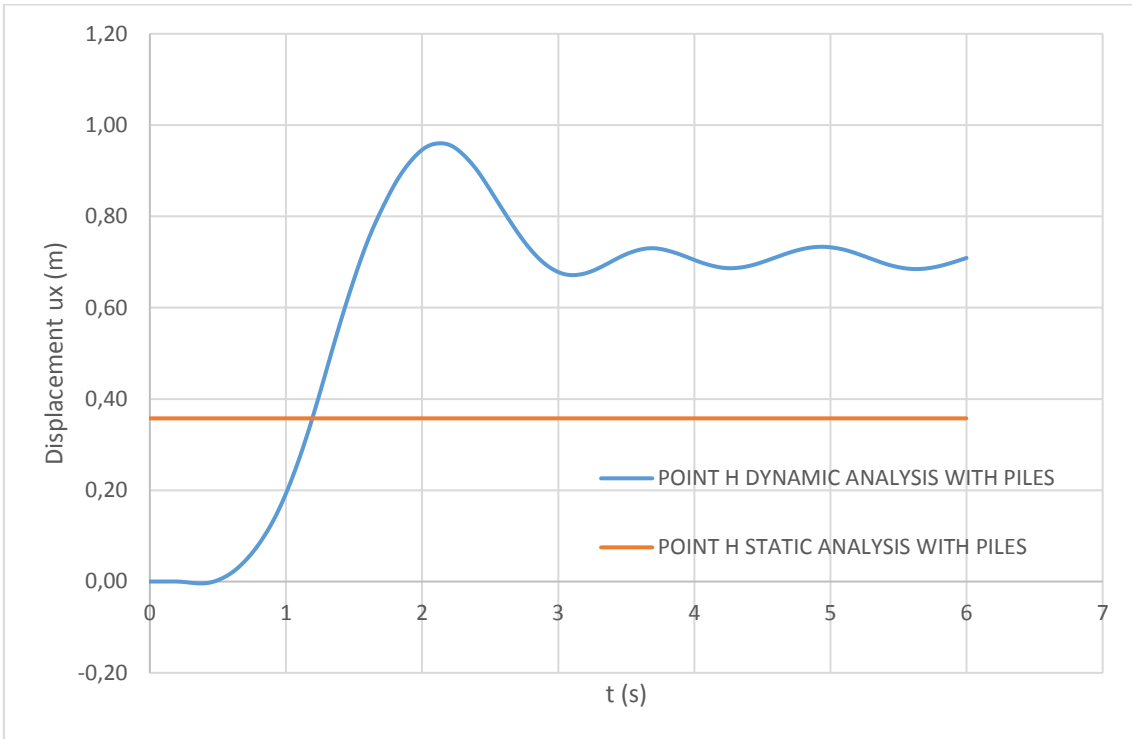
Figure 6-51 Comparison of the displacements in the node H when there are piles under the block.

6.5.6 Application of Brom's (1946b) and Barton's (1982) methods to the real scale case

The equations proposed by BROMS (1946b) for the failure mechanisms of the piles, as well as those particularized for the model of the soil's resistance suggested by BARTON (1982), which were obtained in the point 3.3. of this Master's Thesis as early as the equations of BROMS, have been applied to the second model developed by the FEM software *PLAXIS*, corresponding to that in which was added to the bottom surface of the concrete block a pile's foundation with the aim of restraining the displacements of the block through the soil. The first goal of this analysis is to obtain the limit values of the horizontal forces which will determine the behavior of the single pile, depending on the horizontal forces obtained from the calculation process developed by *PLAXIS*.

The mechanical properties of the soil which have been adopted in this calculation are:

- Friction angle: $\phi = 30^\circ$
- Passive earth pressure coefficient: $K_p = 3$
- Specific weight of the soil: $\gamma = 20 \, kN/m^3$

According to the mechanical properties of the soil listed above, have been calculated values of **H_{lim}** for several configurations of the steel reinforcement of the piles pertaining to the concrete block's foundation. The different number and diameter of the steel frames consisting on the reinforcement of the piles in analysis, determines the yielding moment **M_y** of the section. In the following table are showed the different configurations of the reinforcement with their yielding bending moments, as well as, the mechanic properties of the concrete used in the piles.

CONSTRUCTION MATERIALS		
CONFIGURATION OF THE STEEL REINFORCEMENT		**M_Y (kNm)**
ARMATURA 30 φ 30		3646
ARMATURA 30 + 10 φ 30		4609
ARMATURA 30 + 20 φ 30		5552
ARMATURA 30 + 30 φ 30		6473
CONCRETE	**f_{ck} (N/mm²)**	**R_{ck} (N/mm²)**
C 25/30	25	30

Another aspect which must be taken into account is that the values of **H_{lim}** calculated according to the equations of BROMS (1946b) and BARTON (1982) correspond to the characteristic resistances. To obtain the values of project, these horizontal limit forces must be reduced by the two coefficients established in the Italian Standard for the construction (*Norme Tecniche per le Costruzioni*). On the one hand, the **H_{lim}** must be reduced by the statistical coefficient ξ_3 that takes into account the number of surveys effected. This has been assumed equal to 1,4. On the other hand, the characteristic values of the resistance must be divided by a safety factor Υ_t, which according to the Italian Standard for the Construction, must be considered equal to 1,3. For this reason, the project values of the resistances have been calculated by means of the next expression:

$$H_{project} = \frac{H_{lim}}{\gamma_t \cdot \xi_3} = \frac{H_{lim}}{1,3 \cdot 1,4} \qquad (3.32.)$$

It must be pointed that, to calculate the limit horizontal forces in this case of application, have been considered the expressions corresponding to the restrained pile, referenced in previous points of this Thesis as (3.12.), (3.15.), (3.19.), (3.21.), (3.12.'), (3.15.'), (3.19.') and (3.21.') respectively.

Finally, in the following table are presented, for both models of the resistance of the soil (BROMS (1946b), BARTON (1982)), the characteristic values of the single pile's resistances, as well as the project resistances, obtained according to the expression (3.22.).

	H_{lim} BROMS RESTRAINED HEAD					
	H_{lim1} (3.12)	M_{max} (3.15.)	H_{lim2} (3.19.)	H_{lim3} (3.21.)	H_{lim}	R_d
	(kN)	(kNm)	(kN)	(kN)	(kN)	(kN)
REINFORCEMENT 30 φ 30	43200	576000	14582	2347	2347	1289,74
REINFORCEMENT 30 + 10 φ 30	43200	576000	14630	2744	2744	1507,86
REINFORCEMENT 30 + 20 φ 30	43200	576000	14678	3107	3107	1707,09
REINFORCEMENT 30 + 30 φ 30	43200	576000	14724	3442	3442	1891,01

	H_{lim} BARTON RESTRAINED HEAD					
	H_{lim1} (3.12')	M_{max} (3.15.')	H_{lim2} (3.19.')	H_{lim3} (3.21.')	H_{lim}	R_d
	(kN)	(kNm)	(kN)	(kN)	(kN)	(kN)
REINFORCEMENT 30 φ 30	43200	576000	14582	2993	2993	1644,66
REINFORCEMENT 30 + 10 φ 30	43200	576000	14630	3500	3500	1922,81
REINFORCEMENT 30 + 20 φ 30	43200	576000	14678	3962	3962	2176,86
REINFORCEMENT 30 + 30 φ 30	43200	576000	14724	4389	4389	2411,40

As it can be observed in the tables above, the horizontal forces obtained with regards to the model of BARTON (1982) are higher than those of the model of BROMS (1946b). This serves to reaffirm that the model proposed by BARTON is more accurate because does not underestimate the soil's resistance as much as the model of BROMS does.

From the analysis developed by *PLAXIS*, it has been obtained the equivalent shear force per unit of length acting on the concrete block (figure 6-52) . As it is known, the width of the block is equal to 13,5 meters. Consequently, can be calculated the resultant shear force acting on the concrete block as:

$$T_{total} = 1300 \, kN/m \, \cdot 13,5 \, m = 17550 \, kN$$
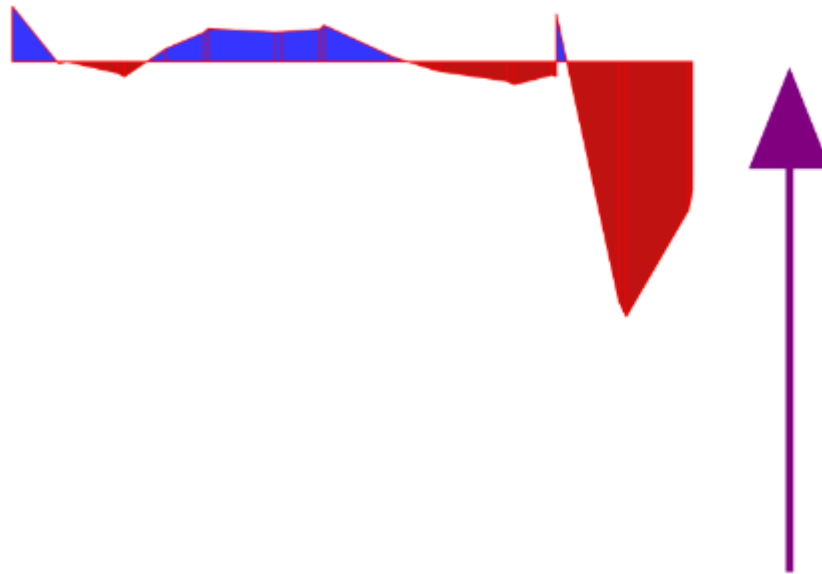
Shear stresses (cross section) τ_s (scaled up 0.0100 times)

Maximum value = 157.8 kN/m²

Minimum value = -725.0 kN/m²

Equivalent force is -1300 kN/m at position (40.773, -11.346) m

Figure 6-52 Equivalent shear force acting on the concrete block obtained by PLAXIS.

6.5.7   Analytical calculation of the displacements of the group.

The next step which has been carried out is to determine the displacements in the head of the 16 piles which conform the pile's foundation of the concrete block, following the same process and using the same equations as in the example case of the group 4 x 4 which was developed in the point 4.2 of this Master's Thesis.

The displacements in the heads of the piles are going to be calculated for two different forces, the Equivalent Shear Force obtained from the analysis run with PLAXIS, and a horizontal force equal to de 70 % of the Equivalent Shear Force.

In both cases have been taken into account the following features:

- Diameter of the piles: 1,20 meters.
- Length of the piles: 20 meters.
- Lateral soil's reaction coefficient: 1,5 N/cm³.

CASE A. TOTAL HORIZONTAL FORCE

As it has been mentioned above, the total force acting on the group of piles pertaining to the foundation of the concrete block, has been obtained from the equivalent shear force which has been provided as a result of the calculation process developed by *PLAXIS*. As the number of piles consisting on the group is equal to 16, the average load acting on each pile of the group will be equal to:

159

$$T_{total} = 17550 \, kN \quad \rightarrow \quad T_{pile} = \frac{17550}{16} = 1096{,}88 \, kN$$

Subsequently, have been calculated the efficiencies of the 16 piles conforming the group following the same process which was developed in the example case of the group 4 x 4. It must be pointed that the efficiencies of the piles pertaining to the same row of the group are the same, so that, in the next table can be found four different efficiencies. Each one of the corresponds to the piles of the front, second, third and back row, respectively.

EFFICIENCIES OF THE PILES			
Row 1	Row 2	Row 3	Row 4
0,67570	0,52314	0,52314	0,40502

According to the values of the efficiencies of the 16 piles of the group that are showed in the previous table, has been calculated the total efficiency of the group as:

$$e_{total} = \sum e_i = 4 \cdot (0{,}6757 + 0{,}52314 + 0{,}52314 + 0{,}40502) = 8{,}51$$

With regards to the total efficiency of the group and the total load acting on the foundation of the concrete block, it can be obtained the value of the horizontal force which would act on the single pile by means of the definition of efficiency:

$$T^* = \frac{17550}{8{,}51} = 2063 \, kN$$

With this value of the horizontal force, it can be obtained the medium displacement which would experience the single restrained pile when it is working under a force T*. The displacement **u** has been obtained by means of the Excel worksheet provided by *E & G SRL*. The average displacement which has been obtained is equal to:

$$u_{average-single \, pile} = 12{,}346 \, cm$$

In addition to this, can also be obtained the forces and the displacements in the heads of the piles pertaining to the front, second, third and back row of the group according to the efficiencies showed in the table above and the value of the total force provided by *PLAXIS*. In

the next table are presented the values of the forces acting on the piles of the four rows of the group, as well as the displacements reached on their heads as a consequence of these forces.

HORIZONTAL FORCES			
Trow 1 (kN)	Trow 2 (kN)	Trow 3 (kN)	Trow 4 (kN)
1623	2097	2097	2708
DISPLACEMENTS			
u row1 (cm)	u row2 (cm)	u row3 (cm)	u row4 (cm)
9,71448	12,54747	12,54747	16,20664

Based on the H_{lim} values obtained according to the expressions proposed by BROMS (1946b) and BARTON (1982) for the case of the restrained pile, it can be concluded that the behavior of the piles pertaining to the rows of the group, for the different configurations of the steel reinforcement are:

H lim BROMS RESTRAINED HEAD						
	Hlim	Rd	Pile row 1	Pile row 2	Pile row 3	Pile row 4
	(kN)	(kN)	-	-	-	-
REINFORCEMENT 30 φ 30	2347	1290	LONG PILE	LONG PILE	LONG PILE	LONG PILE
REINFORCEMENT 30 + 10 φ 30	2744	1508	LONG PILE	LONG PILE	LONG PILE	LONG PILE
REINFORCEMENT 30 + 20 φ 30	3107	1707	NO DAMAGE	LONG PILE	LONG PILE	LONG PILE
REINFORCEMENT 30 + 30 φ 30	3442	1891	NO DAMAGE	LONG PILE	LONG PILE	LONG PILE

H lim BARTON RESTRAINED HEAD						
	Hlim	Rd	Pile row 1	Pile row 2	Pile row 3	Pile row 4
	(kN)	(kN)	-	-	-	-
REINFORCEMENT 30 φ 30	2993	1645	NO DAMAGE	LONG PILE	LONG PILE	LONG PILE
REINFORCEMENT 30 + 10 φ 30	3500	1923	NO DAMAGE	LONG PILE	LONG PILE	LONG PILE
REINFORCEMENT 30 + 20 φ 30	3962	2177	NO DAMAGE	NO DAMAGE	NO DAMAGE	LONG PILE
REINFORCEMENT 30 + 30 φ 30	4389	2411	NO DAMAGE	NO DAMAGE	NO DAMAGE	LONG PILE

In this second case, are going to be calculated the displacements in the heads of the piles pertaining to the group, as well as the average displacement of the group caused by a horizontal force equal to the 70 % of the total force, obtained from the equivalent shear force which has been provided as a result of the calculation process developed by *PLAXIS*. As the number of piles consisting on the group is equal to 16, the average load acting on each pile of the group will be equal to:

$$T_{70 \% \, of \, the \, total} = 12285 \, kN \quad \rightarrow \quad T_{pile} = \frac{12285}{16} = 767,81 \, kN$$

The efficiencies of the 16 piles conforming the group are the same as those calculated in the previous case. These are presented in the following table:

EFFICIENCIES OF THE PILES			
Row 1	**Row 2**	**Row 3**	**Row 4**
0,67570	0,52314	0,52314	0,40502

According to the values of the efficiencies of the 16 piles of the group that are showed in the previous table, has been calculated the total efficiency of the group as:

$$e_{total} = \sum e_i = 4 \cdot (0,6757 + 0,52314 + 0,52314 + 0,40502) = 8,51$$

With regards to the total efficiency of the group and the 70 % of the total load acting on the foundation of the concrete block, it can be obtained the value of the horizontal force which would act on the single pile by means of the definition of efficiency:

$$T^* = \frac{12285}{8,51} = 1444 \, kN$$

With this value of the horizontal force, it can be obtained the medium displacement which would experience the single restrained pile when it is working under a force T*. The displacement **u** has been obtained by means of the Excel worksheet provided by *E & G SRL*. The average displacement which has been obtained is equal to:

$$u_{average-single \, pile} = 8,641 \, cm$$

In addition to this, can also be obtained the forces and the displacements in the heads of the piles pertaining to the front, second, third and back row of the group according to the efficiencies showed in the table above and the value of the force considered in this analysis. In the next table are presented the values of the forces acting on the piles of the four rows of the group, as well as the displacements reached on their heads as a consequence of these forces.

HORIZONTAL FORCES			
Trow 1 (kN)	Trow 2 (kN)	Trow 3 (kN)	Trow 4 (kN)
1136	1468	1468	1896
DISPLACEMENTS			
u row1 (cm)	u row2 (cm)	u row3 (cm)	u row4 (cm)
6,80013	8,78323	8,78323	11,34465

Based on the H_{lim} values obtained according to the expressions proposed by BROMS (1946b) and BARTON (1982) for the case of the restrained pile, it can be concluded that the behavior of the piles pertaining to the rows of the group, for the different configurations of the steel reinforcement are:

H lim BROMS RESTRAINED HEAD						
	Hlim	Rd	Pile row 1	Pile row 2	Pile row 3	Pile row 4
	(kN)	(kN)	-	-	-	-
REINFORCEMENT 30 φ 30	2347	1290	NO DAMAGE	LONG PILE	LONG PILE	LONG PILE
REINFORCEMENT 30 + 10 φ 30	2744	1508	NO DAMAGE	NO DAMAGE	NO DAMAGE	LONG PILE
REINFORCEMENT 30 + 20 φ 30	3107	1707	NO DAMAGE	NO DAMAGE	NO DAMAGE	LONG PILE
REINFORCEMENT 30 + 30 φ 30	3442	1891	NO DAMAGE	NO DAMAGE	NO DAMAGE	LONG PILE

H lim BARTON RESTRAINED HEAD						
	Hlim	Rd	Pile row 1	Pile row 2	Pile row 3	Pile row 4
	(kN)	(kN)	-	-	-	-
REINFORCEMENT 30 φ 30	2993	1645	NO DAMAGE	NO DAMAGE	NO DAMAGE	LONG PILE
REINFORCEMENT 30 + 10 φ 30	3500	1923	NO DAMAGE	NO DAMAGE	NO DAMAGE	NO DAMAGE
REINFORCEMENT 30 + 20 φ 30	3962	2177	NO DAMAGE	NO DAMAGE	NO DAMAGE	NO DAMAGE
REINFORCEMENT 30 + 30 φ 30	4389	2411	NO DAMAGE	NO DAMAGE	NO DAMAGE	NO DAMAGE

In conclusion, the displacements in the heads of the piles conforming the foundation of the concrete block, which have been calculated in this analysis for the total load and for the 70 % of the total load, are much lower than those obtained in the analysis carried out with *PLAXIS*.

7 Conclusions

In this chapter, are presented the conclusions drawn according to the analysis and discussions which have been developed in this Master's Thesis.

In general, the methods used to determine the horizontal limit loads for piles placed on granular soils are very precautionary. It must be underlined that, when are reached values of the friction angle of the soil higher than 36 º, these methods become quite precautionary.

The consideration of the interaction phenomena between the piles pertaining to a group, which are due to the shadowing and the edge effects as it has been explained in the Thesis, leads to conclude that, the displacements observed in the heads of the piles pertaining to the group are higher than those achieved in the case of the single isolated pile. Sometimes, the displacements in the heads of the piles within a group can be twice the size of those reached in the head of the single pile. As it has been observed in the analysis, the phenomena of interaction tend to be more significant, the lower the distance between the piles is. For this reason, it is very important to evaluate the efficiency of the group in the case of deep foundations composed by piles placed quite close between them. In other words, for a group of piles, the phenomena of interaction become important when the ratio among the distance between the piles and their diameters is comprised between 2 – 3, being unusual the adoption of distances between the piles lower than twice their diameters.

The considerations about the limit loads and the interaction phenomena between the piles pertaining to a group, have been applied to a real scale case. Afterwards, these have been confronted with the results derived from numerical analysis carried out by means of the software *PLAXIS*. It must be underlined that, have been developed both kind of analysis: static and dynamic. Particularly, it has been analyzed the consequences of the impact of a cargo ship against a mole's dock, like it happened in the dock of Genova. In the developed model, it has been considered a breakwater constituted by a reinforced concrete block covered by a coat of tetrapod concrete boulders. The pilot control tower has been placed at the back of the mole.

It has been noticed that, generally, the closed methods provide valuations reasonably precautionary of the displacements reached in the heads of the piles. In addition to this, it can be concluded that the values of the displacements obtained by means of the dynamic analysis are higher than those calculated in static conditions (applying the maximum force of the load's history). This is because of the overlapping of the effects of the deformations, in the different elements composing the model, along the simulation time.

In the case of study, the inclusion of the pile's foundation under the concrete block has resulted in a high reduction of the displacements in the head of the pilot tower. However, this reduction of the displacements has not been enough to avoid collapse of the structures placed at the back of the concrete block under which the pile's foundation has been added. As a consequence of this, it would be necessary to make a reprojection of the whole mole of the dock, specially, paying attention to the geometrical and structural points of view.

8 Bibliography

The bibliography consulted, which has been taken as the basis of the studies and discussions carried out in this Master's Thesis is listed below:

- Ph.D. Thesis: *"Pali soggetti a carichi orizzontali: indagini sperimentali ed analisi"* (GENNARO LANDI, 2005).
- *FONDAZIONI* (CARLO VIGGIANI, 1993).
- *PRINCIPLES OF FOUNDATION ENGINEERING* (BRAJA M. DAS, 1984).